
# THÈSE

**En vue de l'obtention du**

## DOCTORAT DE L'UNIVERSITÉ DE TOULOUSE

**Délivré par :**
Institut National Polytechnique de Toulouse (INP Toulouse)

**Discipline ou spécialité :** Génie des Procédés et de l'Environnement

---

**Présentée et soutenue par**
**Claudia COTE COY**

**le 7 Juin 2013**

**Titre :** Biocorrosion de l'acier au carbone dans les systèmes d'injection d'eau de l'industrie du pétrole et du gaz: nouveaux modèles expérimentaux issus du terrain

---

**Ecole doctorale : Mécanique Energétique Génie Civil et Procédés**

**Unité de recherche : Laboratoire de Génie Chimique**

**Directeur(s) de Thèse :**

**Régine BASSEGUY (Directrice de thèse)**

**Mathieu BERGE (Co-directeur de thèse)**

**Rapporteurs :**
Marie LIBERT
Bernard TRIBOLLET

---

**Membres du jury**

**Mme Régine BASSEGUY, Directeur de thèse**
**Mme Marie LIBERT, Rapporteur**
**M. Bernard TRIBOLLET, Rapporteur**
**Mme Nadine PEBERE, Membre**
**M. Mathieu BERGE, Membre**
**M. Damien FERON, Membre**
**M. Florin TURCU, Membre**

**Biocorrosion of carbon steel in water injection systems of the oil and gas industry: new experimental models from the field**

**Abstract**

The oil and gas industry is impacted by important economic losses due to corrosion problem. As part of this problem, microbially influenced corrosion (MIC) is still a subject of research. The most often evoked and well acknowledge MIC mechanism is linked to sulphate reducing bacteria (SRB). However, some studies have shown that MIC can occur even when SRB is not present in the corroding environment; in this framework, the main objective of the thesis is to provide new insights on corrosion of carbon steel caused by other mechanisms different to those described with SRB.

First, the influence of an electroactive strain, *G. sulfurreducens* (an iron reducing bacteria, IRB) on the corrosion/protection of steel C1145 was studied. When phosphate species are present in the medium, bacteria promote the formation of an iron phosphate layer (vivianite) that afterwards protects the material. In presence of $NH_4^+$, corrosion rates are higher but bacteria decrease the dissolution of the material.

In the second part, field samples from pigging operations performed in water injection pipelines were analysed from microbiological and electrochemical corrosion points of view. Molecular analysis and identification of the biofilm community show the presence of s*ulfidogenic species besides SRB*. These bacteria can stimulate metal corrosion through production of organic acids, $CO_2$ and different sulphur species such as $H_2S$. Moreover, it was proved that the consortium contained in field samples accelerated corrosion of carbon steel mainly by production of sulphide species.

Key-words: Biocorrosion, carbon steel, MIC, anaerobic, *Geobacter sulfurreducens*

---

**Biocorrosion de l'acier au carbone dans les systèmes d'injection d'eau de l'industrie du pétrole et du gaz: nouveaux modèles expérimentaux issus du terrain**

**Résumé**

L'industrie pétrolière et gazière subie d'importantes pertes économiques en raison de problèmes liés à la corrosion. Parmi ces problèmes, la corrosion induite par les micro-organismes (biocorrosion) fait toujours l'objet de recherche, le mécanisme le plus souvent évoqué et documenté étant lié aux bactéries sulfato-réductrices (BSR). Cependant certaines études ont montré que la biocorrosion pouvait se produire même en absence de BSR dans l'environnement corrosif ; le principal objectif de la thèse était donc de fournir un nouvel éclairage sur la corrosion anaérobie de l'acier au carbone en proposant des mécanismes différents de ceux impliquant les BSR.

En premier lieu, l'influence d'une souche électro-active, *G. sulfurreducens*, sur la protection/corrosion de l'acier C1145 a été étudiée. Lorsque des espèces phosphate sont présentes dans le milieu, la bactérie favorise la formation d'une couche de Fer/Phosphate qui ensuite protège le matériau. En présence d'ammonium, les vitesses de corrosion sont plus élevées mais les bactéries réduisent la dissolution du métal.

En deuxième partie, des échantillons de terrain issus des opérations de nettoyage des pipelines des systèmes d'injection ont été analysés d'un point de vue microbiologique et électrochimique. L'analyse moléculaire et l'identification de la communauté bactérienne montre la présence d'espèces sulfurogènes autre que les BSR. Ces bactéries peuvent stimuler la corrosion des métaux par la production d'acides organiques, de $CO_2$ et de différentes espèces soufrées telles que $H_2S$. De surcroît, il a été prouvé que le consortium contenu dans les échantillons de terrain accélérait la corrosion de l'acier au carbone, principalement par la production d'espèces sulfures.

Mots-clés: biocorrosion, acier au carbone, CIM, anaérobie, *Geobacter sulfurreducens*

**Acknowledgments**

Thanks to the financial support of the Centre National de la Recherche Scientific (CNRS), I was awarded a scholarship funded by the EU 7 frame work-Marie Curie program (FP7/2007-2013) allowing me to participate in the BIOCOR project. The project was under the grant agreement n° 238579. This work was performed in the Laboratory of Chemical Engineering (LGC) of the Institut National Polytechnique de Toulouse (INPT).

I would like to thank all the BIOCOR network team for their scientific support and constant suggestions during our meetings. Special thanks to all the people in LGC who since I arrived in France made me feel welcome and like at home, specially to my thesis director, Regine Basseguy, and the post-doc working in the LGC for the project, Omar Rosas, for their constant guidance and help teaching me electrochemistry. To the AXE 5 team and their enriching comments and great sense of humor which made a great environment for me during these three years.

Finally, massive thanks to all my family and friends who supported me and encourage me to do this PhD thesis and cheer me all along these years: To my mom, dad and sisters (Kate and Caro) who are my reasons for always wanting to be better. To my "adoptive" parents (Danny and Roger) who made me always feel that I have an extended family in France and to my love and soon to be husband, Olivier, who made of the long writing hours happy moments.

# *Table of contents*

# *General introduction*

Any material in contact with water or moisture is rapidly colonised by the microbial species that grow in assemblages referred to as biofilms. This microbial development, which occurs in almost all natural and man-made environments, is responsible for microbial influenced corrosion (MIC), also known as biocorrosion.
The main factors necessary to develop MIC on metal surfaces besides the microorganisms are the presence of water, temperatures between -12 to +112 °C and a carbon source. Biocorrosion can be defined as the enhancement or acceleration of corrosion by the presence of bacteria [Beech and Gaylarde, 1999; Coester and Cloete, 2005; Beech *et al.*, 2005]. However, MIC is not a new corrosion mechanism but it integrates the role of microorganisms in corrosion processes by, for example, affecting the electrochemistry of the system.

Corrosion and within its classifications MIC, is one of the main problems affecting different industries such as the oil & gas and power supply industries; costing them billions of Euros per year in costs and production losses. In the case of the oil & gas industry, nearly all the systems are prone to MIC. The main systems involved are: Oil separation train, produced water systems, water injection systems and oil export systems. In general, the corrosion of metals has a significant impact on the worldwide economy. Different studies have shown that the economic losses due to corrosion represent at least 4% of the gross national product (GNP) [Duncan *et al.*, 2009]. For example, the French Centre of Corrosion CEFRACOR, estimated at € 28 billion the economic losses generated by corrosion in France, every year; in the United States, a report published by the NACE (National Association of Corrosion Engineers) in 2002 estimated the direct cost of corrosion, meaning costs by direct damage such as pipelines replacement, the use of inhibitors and services facility maintenance, etc., to 276 billion U.S. dollars per year, 3.1% of the country's GNP. The indirect costs of corrosion, such as losses by stopping facilities and production losses, the delivery time extended, among others, are more difficult to determine, but an optimistic estimate would imply that they can be considered equal to the direct costs. This means that total corrosion costs could reach 6% of GNP in the United States [Koch et al. 2001]. Moreover, Fleming [Fleming, 1996] estimate that 20% of corrosion problems are linked to the presence of microorganisms and more over Jack *et al.* (1992) estimated that 34% of the corrosion damage experienced by oil companies was related to MIC.

In spite of these important losses figures, corrosion in different industries, including the oil and gas industry is still not considered an important and recognised problem. For instance, the U.S. possesses a network of over 2.3 million miles of pipelines that transmit about 75% of the nation’s crude oil and 60% of refined products. Despite this importance, pipelines are not regularly considered in assessment of societal infrastructure needs, but there is little doubt that these facilities are vulnerable and can deteriorate over time [Duncan *et al.*, 2009]. Through-wall breaches due to corrosion are expensive problems in the oil industry that can result in explosions, product interruptions, hazardous chemical releases and environmental damage. For this, corrosion and biocorrosion need to be studied and the knowledge concerning these topics needs to be continuously updated.

Since the involvement of microorganisms was recognised to have a key role in corrosion, sulphate reducing bacteria (SRB) has mainly been the only group of

bacteria studied and linked to anaerobic corrosion. Nowadays, more and more studies have presented evidence of different metabolic activities of microorganisms that have been implicated in incidents of corrosion and more precisely, of pipelines failures. For example, researchers found that the dominant metabolic activities of microorganisms found in a pipeline of Alaska's North Pole was fermentative, $H_2$ and $CO_2$ producers, methanogens, iron reducers, sulphur/thiosulfate-reducing bacteria and sulphate-reducing microorganisms [Duncan *et al.*, 2009]. In contrast, Rajasekar's team, in a study performed in corroding pipelines located in India did not find any sulphate reducing bacteria and found, as dominant species, *B. cereus* and *S. marcescens*.

All these examples show the complexity of the involvement of microorganisms in the deterioration of metals, which is why it is necessary to identify the microorganisms involved to understand the phenomena of this biocorrosion in order to elucidate the mechanisms to find effective and radical solutions.

**Presentation of the plan of chapters**

The work presented along this manuscript has been framed within a multidisciplinary approach with focus on electrochemistry and microbiology. The electrochemical studies has been performed in the Laboratoire de Genie Chimique in Toulouse (UMR 5503) in the context of the Marie Curie European research network, BIOCOR which has been financed by the EU 7 frame work "people programme". The research has been performed in intense collaboration with the network, especially with:

- Laboratory of microbiology of the University of Portsmouth, UK where the molecular biology studies were performed.
- Laboratoire Physico-Chimie des Surface of the Ecole National Superieure de Chimie de Paris, France, where the XPS surface analyses were performed.

This thesis work consisted on studying the anaerobic biocorrosion of carbon steel in water injection systems of the oil and gas industry.

Chapter I is a literature review with the state of the art in the areas of electrochemical corrosion and biocorrosion. This chapter ends presenting the scope of the study. Chapter II describes the materials and methods and also the theoretical fundaments of the techniques used. Chapters III and IV present the results and are organized around three articles that were or will be soon submitted.

# ***Chapter I-*** *STATE OF ART: Corrosion & Biocorrosion*

## I.1. Introduction

Corrosion of metals is an electrochemical process characterised by the metal dissolution. The electrochemical reaction involved is an oxidation reaction where the metal losses electrons. For corrosion to occur there must be a reduction reaction which must occur simultaneously with the oxidation reaction. Biocorrosion is a type of corrosion which involves the mediation of microorganisms.

Electrochemically, corrosion can be measured or detected by different techniques. One of the techniques which could provide some information about corrosion is the measurement of potential values ($E_{corr}$) along a period of time. For instance, in a biotic system, ennoblement of corrosion potential might be a consequence of a microbiologically mediated process which may indicate the increase on the corrosion risk. Ennoblement is a global phenomenon which has been studied intensely since the 1980s. This technique has dominated the literature on microbially influenced corrosion in natural marine environments.

This chapter introduces this thesis with insights in electrochemical corrosion and biocorrosion providing a brief description on the different types of corrosion, corrosion detection techniques used, biofilms influence on corrosion, the mechanisms and metabolic pathways of the microorganisms involved, and finally it gives an introduction of biocorrosion in the oil and gas industry. Furthermore, at the end of this chapter it is presented the scope of this study displaying the main objectives together with the research plan developed along this research study.

## I.2.Electrochemical corrosion

Corrosion is the destructive attack of a metal by chemical or electrochemical reactions with the environment [Uhlig *et al.*, 2008]. In other words, corrosion is an electrochemical process in which electrons from the metal are released at the anode (oxidation) and transferred to the cathode were the electrons are consumed (reduction) [Sparr and Linder, 2010].

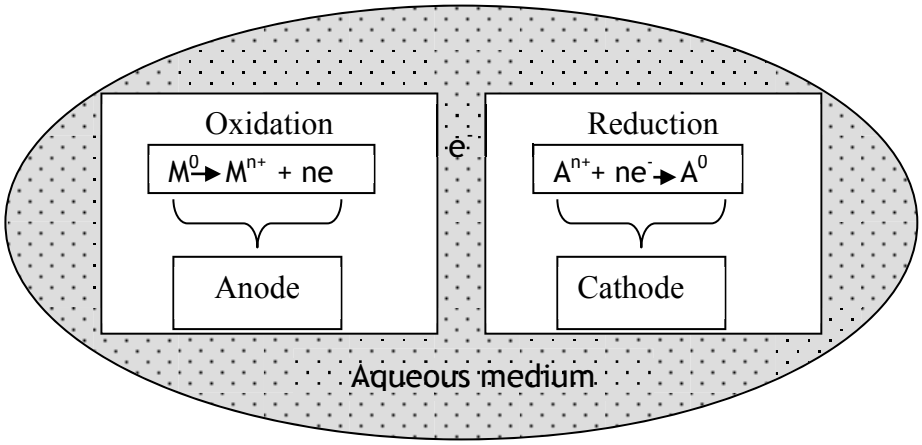


Fig. I.1 Graphic representation of the corrosion process of a metal surface immersed in an aqueous medium. In the corrosion process, both, cathodic and anodic sites are present at the surface of the metal which, also works as the electric connector. Even water droplet is considered to be the electrolyte.

In order to have the oxidation reaction, it is mandatory to have a simultaneous reduction reaction (Fig. I.1): the electrons transferred during the oxidation process are consumed in the cathode or cathodic sites to transform the species present in the medium. The main oxidation reaction will be the dissolution of the metal and the reduction reaction will depend upon the components in the aqueous medium.

In the literature of electrochemistry, reduction and oxidation reactions are defined as when metals lose electrons (i.e., oxidation) or gain electrons (reduction) [Javaherdashti, 2008]:

$$Fe \longrightarrow Fe^{2+} + 2e^- \quad (I.1)$$

Reaction (I.1) is an example of an oxidation reaction, the oxidation of iron. As it is seen, this reaction gives off electron to the interface. Such reactions are also called anodic reactions. The corrosion rate of iron in de-aerated neutral water at room temperature, for example, is less than 5 μm/year [Roberge, 2000].

$$2H^+ + 2e^- \longrightarrow H_2 \quad (I.2)$$

$$O_2 + 2H_2O + 4e^- \longrightarrow 4OH^- \quad (I.3)$$

Reaction (I.2) is an example of reduction reaction occurring in oxygen-free or acid environments. The rate of hydrogen evolution at a specific pH depends on the presence or absence of low-hydrogen overvoltage impurities in the metal. For pure

iron, the metal surface itself provides sites for $H_2$ evolution; hence, high-purity iron continues to corrode in acids, but at a measurably lower rate than does commercial iron [Roberge, 2000]. Reaction (I.3) is an example of reduction of oxygen in aerated neutral/alkaline solutions. Reduction reactions are also called cathodic reactions. Dissolved oxygen reacts with hydrogen atoms adsorbed at random on the iron surface, independent of the presence or absence of impurities in the metal. The oxidation reaction proceeds as rapidly as oxygen reaches the metal surface [Roberge, 2000]. So, alternatively, one can define corrosion as different reactions that are occurring at the anode, the cathode, and the solution and end up in the metal dissolution.

Reaction (I.4) is the overall reaction in aerated media for the case corrosion of iron:

$$Fe + 1/2O_2 + H_2O \longrightarrow Fe^{2+} + 2OH^- \quad (I.4)$$

Reaction (I.5) is the overall reaction in de-aerated media for the case of corrosion of iron:

$$Fe + 2H^+ + 2H_2O \longrightarrow Fe^{2+} + 2OH^- + 2H_2 \quad (I.5)$$

The factors that encourage corrosion are those which will overcome the atomic bonding of the metal and encourage metal ions to leave the surface. The greatest of these factors is the presence of water or some other ionic (conductive) solution (often referred to as an electrolyte) [Videla, 1997]. For corrosion to happen, two factors must be available: the material which may content the anode and the cathode and the electrolyte [Javaherdashti, 2008].

The sites hosting the previously described reactions can be located on a single piece of metal surface or far apart in two different metal surfaces (galvanic cell). However, each of the sites where the anodic and/or the cathodic reactions are occurring is known as half-cell and the reactions happening in each of the sites are known as half-cell reactions. Thermodynamically, each half-cell reaction has an electrical potential, known as the half-cell electrode potential (for $M/M^{n+}$ systems). The anodic reaction potential, $E_a$, subtracted from the cathodic reaction potential, $E_c$, result in $E^\circ$, the standard cell potential $E^\circ = E^\circ_c - E^\circ_a$. In electrochemical systems, if the overall cell potential is positive, the reaction will proceed spontaneously [Campaignolle, 1996; Stoecker, 2001; Bard and Faulkner, 2001; Jones and Amy, 2002]. The larger is the potential difference, the greater the driving force of the reaction. Still, other factors will determine if corrosion takes place and at what rate.

The electrode potential E is relative to the standard electrode potential $E^\circ$ of the redox couple or, equivalently, of each half cell, and is given by the Nernst equation:

$$E = E^\circ - \frac{RT}{n_e F} \ln Q_r \quad (I.6)$$

Where R is the gas constant, T the temperature in Kelvins, Qr the thermodynamic reaction quotient, F the Faraday's constant and $n_e$ the number of electrons transferred. The electrochemical potential depends on the diverse electrochemical

reactions taking place at the metal surface, and it can be measured with a high impedance voltmeter, as the potential difference between the metallic sample of interest and a reference electrode [Dominguez, 2007; Campaignolle, 1996].

The rate of a corrosion reaction can be measured by the anodic current, *i.e.*, by the current due to metal ions leaving the metal. Since the electrons flow must migrate from anodic sites of the metal through the interface and then arrive to cathodic sites of the metal, the cathodic current must be equal to the anodic current (I.6) [Videla, 1997]:

$$I_a + I_c = 0 \qquad (I.7)$$

where $I_a$ is counted (+) and $I_c$ is counted (-)

The tendency of a metal to corrode can be assessed using the concept of an electrochemical cell such as a galvanic cell. If the external resistance of this cell is short-circuited (R=0) and the internal solution resistance is small enough to be neglected, the current that flows through the cell would be current corresponding to the corrosion process $I_{corr}$ and the common mixed potential reached by the anode and the cathode, would be the corrosion potential $E_{corr}$ that can be measured experimentally. Fig. I.2 shows the relationship between the polarization reactions in an electrochemical system. The intersection of the two polarization curves closely approximates the corrosion current and the combined potentials of the freely corroding situation.

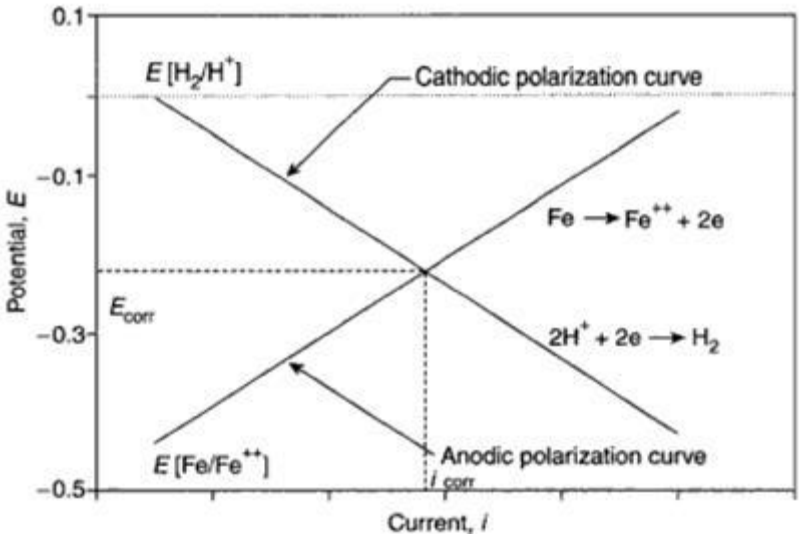


Fig. I.2 Mixed potential plot for the couple of iron and hydrogen [Dominguez, 2007]. The diagram explains the corrosion potential $E_{corr}$ and the corrosion current $I_{corr}$.

### I.2.1 Types of corrosion

Depending upon the different environments we can define different types of corrosion; for example, atmospheric corrosion when metals are attacked when exposed to the atmosphere, corrosion erosion in the transportation pipelines, high temperature corrosion in the heat exchangers and furnaces, and biocorrosion when the corrosion is enhanced by microorganisms [Videla, 1997]. The effect of corrosion on a metallic surface can take many forms. Identifying these forms can assist in

understanding the corrosion process and offer insight into its control. Different classifications of types of corrosion or corrosion forms have been found in the literature. A general description of some corrosion forms can be depicted as follow [Schweitzer, 1996]:

i. *General or uniform corrosion:* The reaction starts at the surface and proceeds uniformly. On iron alloyed metals, it occurs as a result of rust. When metal, specifically steel, is exposed to water, the surface is oxidized and a thin layer of rust appears. It is one of the most easily measured and predictable forms of corrosion [Mars, 1987]. Many references exist which report average or typical rates of corrosion for various metals in common media.

   Since the corrosion is so uniform, corrosion rates for materials are often expressed in terms of metal thickness loss per unit of time; often the expression is mm/year (mpy). Because of its predictability, low rates of corrosion are often tolerated and catastrophic failures are rare if planned inspection and monitoring is implemented. For most chemical process and structures, general corrosion rates of less than 3 mpy are considered acceptable.

ii. *Localised corrosion:* The consequences of localised corrosion can be a great deal more severe than uniform corrosion generally because the failure occurs without warning and after surprisingly short period of use or exposure. Different types of localized corrosion can be found in the literature; some of them can be described as follows:

*ii.i. Galvanic corrosion:* Galvanic corrosion occurs generally when dissimilar metallic materials are brought into contact in the presence of an electrolyte. Such damage can occur between metals and alloys and other conductive materials such as carbon or graphite [Roberge, 2000]. When the two materials are electrically connected and placed in a conductive solution, an electrical potential exist. This potential difference will provide a stronger driving force for the dissolution of the less noble (more electrically negative) material. It will also reduce the tendency for the more noble material to dissolve [Scheweitzer, 1996]. In other words, the material with the more nobel corrosion potential then becomes the cathode of the corrosion cell, whereas the less noble material is consumed by anodic dissolution [Roberge, 2000]. The area ratio of the two dissimilar materials is extremely important. If the anode to cathode surface is ratio is small, the galvanic current can be concentrated on a small anodic area. The corrosion rate, visible as thickness loss over time, can then become very high for the anode [Campaignolle, 1996] and then lead to pits or holes on the surface.

*ii.ii. Crevice corrosion:* is a localised type of corrosion which occurs within a confined zone where the water has limited exchange with the bulk environment. There is often an incubation period before corrosion starts in passivated metals in a crevice. This period corresponds to the time necessary to establish a crevice environment which is sufficiently aggressive to dissolve the oxide passive layer [Sparr and Linder, 2010].

*ii.iii. Pitting corrosion:* Is also a localised type of corrosion. The major characteristic of this mode of corrosion is a large ratio of cathode area (areas in full contact with the bulk environment) to anode area (occlude region). As a consequence, the current density and hence the corrosion rate over the occluded area is very large. Exceptions to this generalisation are those metals and alloys that form oxides that are poor electron conductors and, therefore, provide poor support for cathodic (reduction) reactions (e.g. aluminium oxides, titanium and tantalum) [Sparr and Linder, 2010; Stansbury and Buchanan, 2000]. The more conventional explanation of deep pits after pitting initiation is that the acidity inside the pit is maintained by the spatial separation of the cathodic and anodic half-reactions, which creates a potential gradient and electromigration of aggressive anions into the pit [Korb, 1987].

For instance, chloride ions facilitate the breakdown of the passive layer, especially if there are imperfections in the metal surface. The bare metal becomes the anode while the surrounded passivated area becomes the cathode. The unfavourable anode to cathode surface ratio will increase the attack at the anode. Once a pit is formed, the solution inside will become increasingly corrosive with time [Sparr and Linder, 2010].

*ii.iv. Erosion corrosion:* An increase rate of corrosion attack which is attributable to the movement of a corrodent over a surface is recognised as erosion corrosion. The movement of the corrodent can be associated with mechanical wear. The increase in localized corrosion due to the erosion process is usually related to the removal or damage of the protective surface film. The mechanism is usually identified by localized corrosion which exhibits a pattern that follows a flow of the corrodent [Scheweitzer, 1996].

*ii.v. Stress corrosion cracking (SCC):* The mechanism of SCC is specific of certain alloys (or alloy system) in specific environments. It is characterised by one or more crack fronts which have developed as a result of a combination of the particular corrodent and tensile stresses. Depending on the alloy system and corrodent combination, the cracking can be intergranular or transgranular. The rate of crack propagation can vary greatly and is affected by stress levels, temperature, and concentration of corrodent.

*ii.vi. Under deposit corrosion:* Is a generic description of wastage beneath deposits and not a single corrosion mechanism. The indirect attack occurs as a consequence of surface shielding provided by the deposit and involves concentration cell corrosion. Oxygen diffusion is retarded by the deposit and an oxygen cell is established. The corrosion attack always occurs beneath a deposit, which can be generated internally as or brought into the system from an external source [Sparr and Linder, 2010].

The easiest example to explain this form of corrosion is the droplet of water over a metal surface: Near its boundary with air oxygen concentration is higher. This part will provide the cathodic reaction of oxygen reduction (reaction I.3). In the region away from oxygen, the anodic reaction of iron oxidation takes place and there electrons are transfer through the metal from anode to cathode. The reaction depends on the electrolyte continuity between the anode and the cathode. This

can also be observed in cases where microorganisms are involved through biofilm formation. In cases where there is no electrolyte continuity under the deposit then a crevice effect maybe caused, resulting in a ring of corrosion around the edge of the deposit [Videla, 1997].

### I.2.2 Corrosion detection techniques

Electrochemical techniques have been shown to be very useful for mechanistic studies in laboratory investigations and for monitoring purposes in field studies. As with all studies of corrosion phenomena more detailed and reliable information can be obtained when a number of different electrochemical techniques are combined. Among the main electrochemical techniques used for the scope of corrosion studies and particularly used during this project are: Polarisation resistance, corrosion potential vs. time and electrochemical impedance spectroscopy (EIS).

In the special case of MIC it is of course necessary to use microbiological in addition to surface analytical techniques such as X-ray photoelectron spectroscopy (XPS) and scanning electron microscopy (SEM) with energy dispersive X-ray analysis (EDAX). These considerations lead to the conclusion that real advances in the understanding of the mechanisms of MIC can only be expected from the work of teams which consist of experts in the various techniques discussed above [Mansfeld and Little, 1991].

Moreover, corrosion can be directly quantified experimentally by means of weight loss measurements that provide the rate at which the thickness of a material is lost. This corrosion technique is widely used in the industry due to its simplicity, fast and *in situ* results. All these mentioned techniques will be wider explained in the materials and methods section.

## I.3. Biocorrosion or Microbiologically influenced corrosion

Corrosion associated with microorganisms has been recognized for over 50 years, and yet the study of microbiologically influenced corrosion (MIC) is a relatively new, multidisciplinary field in which there has been a continuum of innovations and contributions [Stoecker, 2001].

Microbial development occurs in almost all environments throughout biofilm formation and may be responsible for MIC, also known as microbial corrosion or biocorrosion which can be defined as the enhancement or acceleration of corrosion by the presence of bacteria [Beech and Gaylarde, 1999; Coester and Cloete, 2005; Beech *et al.*, 2005]. MIC is not a new corrosion mechanism but it integrates the role of microorganisms in corrosion processes. Thus, an inherently abiotic process can be influenced by biological effects [Beech *et al.*, 2000]; more precisely by affecting the electrochemistry of the system with changes on oxido-reduction reactions by the presence of microbial activities, especially when the microorganisms are in close contact with the metal surface forming a biofilm [Beech and Gaylarde, 1999].

MIC is caused by the biological production of substances that actively or passively cause corrosion. The distinction between active and passive attack is often vague.

According to Herro & Port, (1993) active biological corrosion may be defined as the direct chemical interaction of organisms with materials to produce new corrosion processes and/or the marked acceleration of pre-existing corrosion processes, whereas in passive biological corrosion, the biological material is a chemically inert deposit providing a concentration cell which increases the risk of under-deposit corrosion.

In spite of the last years advances, in the literature there are not many descriptions of active biological corrosion or more precisely descriptions of biocorrosion caused by the direct interaction of microorganisms with metal surfaces, inducing corrosion of the material by a direct electron exchange. For instance, this has been mentioned by Mehanna, (2009) when demonstrating an ennoblement of the open circuit potential 3 hours after the inoculation of *Geobacter sulfurreducens* in metals such as carbon steel and stainless steel and attributed to reduction catalysed by bacteria.

Moreover, a unifying electron-transfer hypothesis of biocorrosion using MIC of ferrous metals as a model system has been formulated by Hamilton *et al.,* (2003) for the study of metal-microbe interactions [Beech *et al.,* 2005; Hamilton, 2003]. According to this hypothesis, biocorrosion is a process in which metabolic activities of microorganisms supply insoluble products (e.g. manganic oxides/hydroxides MnOOH, $MnO_2$ produced by manganese oxidation bacteria) that can accept electrons from the base metal. This sequence of biotic and abiotic reactions produces a kinetically favoured pathway of electron flow from the metal anode to the universal electron acceptor, oxygen. Although convincing and based on sound scientific evidence, this theory does not take into account the involvement of ultimate electron acceptors other than oxygen. Indeed, the theory has recently been challenged based on a study of marine biocorrosion of carbon steel under anoxic conditions [Lee *et al.,* 2004]. The role that the organic component, i.e. the biofilm matrix, plays in the electron transfer processes has not been considered in the unified electron transfer hypothesis, despite evidence that enzymes active within the biofilm matrix, and metal ions bound by extracellular polymeric substances (EPS) can catalyse cathodic reactions [Beech *et al.,* 1998]. For instance, Mehanna *et al.,* (2008) and Da Silva *et al., (*2002), studied the influence of the hydrogenases on the corrosion of carbon steel finding that the sole presence of this enzyme without the presence of bacteria cells enhances the corrosion of carbon steel.

On the other hand, when the influence of microorganisms on corrosion started to be acknowledged, all the studies were directed into the study of Sulfate Reducing Bacteria (SRB) and their influence in anaerobic corrosion enhancement by the production of hydrogen sulphide ($H_2S$) and consequently iron sulphide (FeS) which is recognised to be a very corrosive agent [Beech, 2004; Hamilton, 1985; Malard *et al.,* 2008]. One of the first attempts to explain SRB's mechanisms involved in corrosion was made by Von Wolzogen Kur *et al.,* [Wolzogen-Kuehr, 1923] by applying the cathodic depolarisation theory arguing that consumption of hydrogen by SRB could accelerate the dissolution of iron at the anode. Today, this old mechanism where it was assumed that the consumption of molecular hydrogen (issued from the proton or water reduction) by SRB was the rate-limiting step, is now considered to be wrong because hydrogen evolution on steel is an irreversible

reaction [Da Silva, 2007]. On the other hand, nowadays, there is not vast literature about other bacterial groups such as iron oxidizers, iron reducers, acid producers among others, involved in corrosion.

### I.3.1. Biofilms and corrosion

Biofilms consist of micro-colonies separated by interstitial voids and are heterogeneous in many respects *e.g.* structurally, chemically and physiologically. The popular term biofilm structure means, more often implicitly than explicitly, spatial distribution of biomass density in biofilms, or, sometimes, the complementary distribution of biofilm porosity [Evans, 2000].

Bacterial biofilms can be developed in a wide range of environmental conditions. They have been found in environments with temperature ranges from -12 to 115 °C, in pH ranges from 0 to 13, in aqueous media with no salinity percentage to saturation, under pressures from 0.01 bar to 1400 bars, on the surface of all type of materials even in presence of biocides, on the surface of ultraviolet lamps and different radioactive sources [Flemming, 1996].

Microbial growth associated to surfaces or interfaces is the predominant lifestyle of these creatures: approximately 95% of the microorganisms build up biofilms as long as there is at least a minimum amount of water, containing the essential nutrients for their growth, adjacent to the surface or interface on which they establish [Evans, 2000].

Biofilms affect the interaction between metal surfaces and the environment, not only in biodeterioration processes such as corrosion, but also in several biological processes applied to material recovery and handling [Flemming *et al.,* 2000]. Gradual formation of biofilms can change chemical concentrations at the surface of the metal substrate significantly because the physical presence of the biofilm exerts a barrier effect on oxygen and nutrient diffusion to the metal surface [Javaherdashti, 2008]. In aquatic environments, microbial cells attach to solids. Immobilised cells, grow, reproduce and produce extracellular polymer substances (EPS) which frequently extend from the cell forming a tangled matrix of fibres which provide structure to the biofilm [Stoecker, 2001].

Biofilm formation may take minutes to hours –according to the aqueous environment where the metal is immersed. Fig. 3 shows the steps of biofilm formation. The different stages can be resumed as follows [Javaherdashti, 2008]:

Stage 1: conditioning film accumulates on submerged surface; this first stage is due to electrostatic arrangement of a wide variety of proteins and other organic compounds combined with the water's chemistry to be followed by the attachment of the bacteria through the EPS to minimize energy demand from a redundant appendage.

Stage 2: Planktonic bacteria from the bulk water form colonies on the surface and become sessile by excreting EPS that anchors the cell to the surface. At this stage, the bacteria are referred as "sessile bacteria" as opposed to their floating around or "planktonic" state before attachment to the conditioning film.

Stage 3: Different species of sessile bacteria replicate on the metal surface: In this stage, the outer cells will start to consume the nutrients available to them more rapidly than the cells located deeper within the biofilm, so that the activity and growth rate of the latter are considerably reduced.

Stage 4: Micro-colonies of different species continue to grow and eventually establish close relationship with each other on the surface. The biofilm increases in thickness and the electrochemical conditions beneath the biofilm begin to vary in comparison to the bulk of the environment.

Stage 5: Portions of the biofilm slough away from the surface.

Stage 6: the surface areas expose to bacteria are colonised by planktonic bacteria or sessile bacteria adjacent to the surface.

The microorganisms embedded in a biofilm can belong to one or different species, being the EPS which keeps the cohesion and the interaction possibilities among them [Harrison *et al.,* 2005]. Thus, microorganisms can coexist in naturally occurring biofilms with a wide bacterial community including fermentative bacteria, often forming synergistic communities (consortia) that are capable of affecting electrochemical processes through co-operative metabolisms [Beech and Gaylarde, 1999; Gonzalez-Rodriguez *et al.,* 2008].

Furthermore, the development of a microbial biofilm offers several advantages in contrast to planktonic growth. The proximity of different cells favours synergic interactions: complex microbial consortia can be formed, cells distribute naturally in the biofilm according to their specific requirements (strict aerobes, facultative anaerobes, strict anaerobes, acidophiles, etc.). As a consequence, inside a biofilm the creation of differential zones and gradients can be magnified e.g. differential aeration, differential acidification, ion concentration regions, etc. These zones enhance the establishment of these complex symbiotic communities [Harrison *et al.,* 2005]. For instance, while a biofilm with a thickness of 100μm may prevent the diffusion of nutrients to the base of a biofilm, a thickness of just 12 μm can make a local spot anaerobic enough for SRB activity in an aerobic system [Al-Hashem *et al.,* 2004].

The role of biofilms in enhancing corrosion in a biologically conditioned metal-solution interface can be diverse, and may proceed through simultaneous or successive mechanisms including [Videla and Herrera, 2005]: (a) Alteration of the transport of chemical species from or towards the metal surface. The biofilm accumulates and forms a significant diffusion barrier for certain chemical species. (b) Facilitating the removal of protective films when the biofilm detaches. (c) Inducing differential aeration effects as a consequence of a patchy distribution of the biofilm. (d) Changing oxidation–reduction conditions at the metal–solution interface. (e) Altering the structure of inorganic passive layers and increasing their dissolution and removal from the metal surface.

In parallel, biofilms role is not only the enhancement of corrosion rates but also is the protection of bacteria from biocides [38]. It also may aid to the entrapment of corrosion inhibitors such as aliphatic amines and nitrites to be later degraded by

microorganisms. Biofilms also reduce the effectiveness of corrosion inhibitors by creating a diffusion barrier between the metal surface and the inhibitor in the bulk solution [Beech and Sunner, 2004; Little *et al.*, 1991; Pope, 1987; Kirkpatrick *et al.*, 1980; Korenblum *et al.*, 2008].

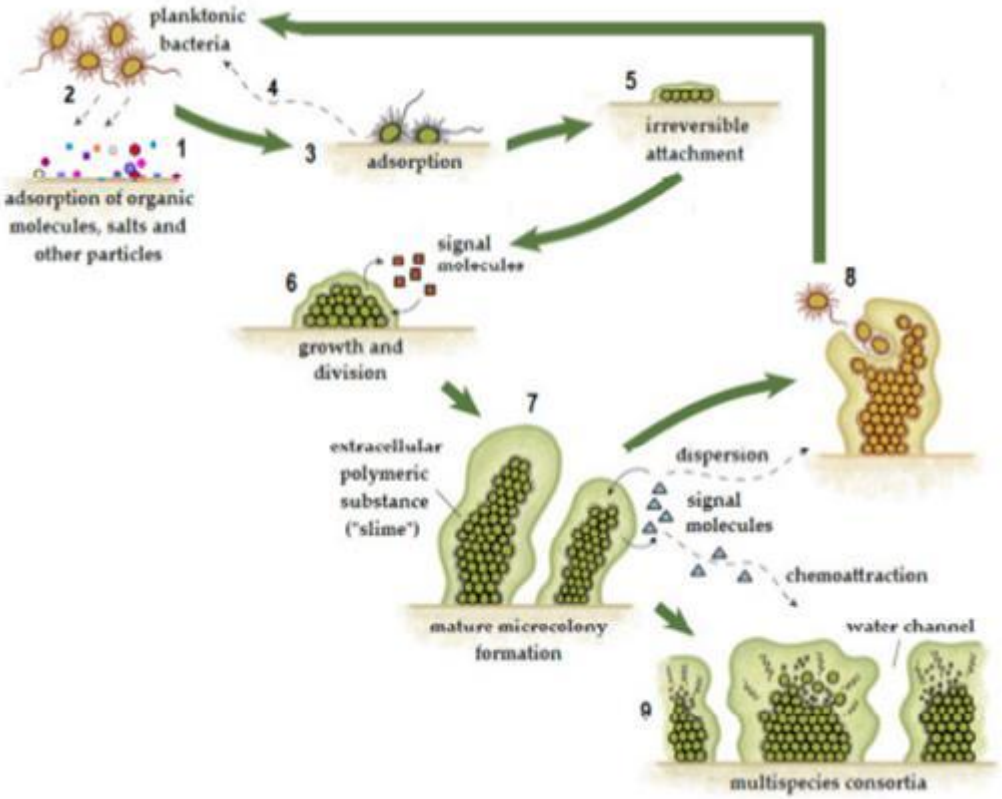


Fig. I.3. Diagram of biofilm formation [Harrison *et al.*, 2005].

In contrast, the importance of EPS to biocorrosion has rarely been addressed, and data available on corrosion rates due to EPS are scarce, in spite of the evidence that EPS alone can accelerate corrosion reactions [Beech *et al.*, 2000; Busalmen *et al.*, 2002]. Biofilm adhesion processes are mediated by EPS. Chemically EPS consist of biopolymers of polysaccharides and proteins, but other macromolecules such as DNA, lipids and humic substances have also been found to made part of it [Christensen and Characklis, 1990; Neu, 1992]; EPS is produced by natural or industrial microbial contaminants able to grow with low levels of nutrient in the medium [Videla, 1997; Evans, 2000]. In general, the proportion of EPS in biofilms can vary between 50 and 90% of the total organic matter [Evans, 2000].

### I.3.2. Role of bacteria on the anaerobic corrosion of carbon steel

Iron and iron alloys can corrode severely in oxygen free environments. Pipelines, offshore oil platforms and underground structures have been reported to be quite vulnerable to biological corrosion which is assumed to be mediated by different groups of microorganisms respiring with oxidized compounds such as sulphate, nitrate, ferric iron or carbon dioxide [Miller, 1981; Hang, 2003]. Obligate anaerobic bacteria are, however, routinely isolated from oxygenated environments associated with particles, crevices, and most importantly, in association with other bacteria

that effectively remove oxygen from the immediate vicinity of the anaerobe [Little *et al.,* 1991].

On the other hand, most of the research on anaerobic microbially influenced corrosion has focused on SRB primarily for the hydrogen sulphide generation and the fact that there is injection of sulphate-containing seawater into the reservoirs during the secondary recovery of oil which favours the proliferation of these bacteria [Rajasekar *et al.,* 2007; Jan-Roblero *et al.,* 2004]. However, recent studies suggest that SRB need not to be present in abundance in the microbial communities responsible for MIC [Zhu *et al.,* 2003] and that other types of bacteria could be involved, such as metal reducing-bacteria and methanogens [Beech and Gaylarde, 1999; Jan-Roblero *et al.,* 2004; Cote *et al,* 2013; Javaherdashti, 1996]. Thus, studies with other bacterial groups or consortia must be enhanced.

### I.3.3. Bacteria groups involved in corrosion

One of the "myths" of MIC, as Little *et al.,* (1991) call it, is the importance of sulphate-reducing bacteria. This is indeed a misleading issue to reduce all MIC problems to SRB by saying "in oil and gas production, the primary source of problems is *Desulfovibrio desulfuricans*, commonly known as SRB" [Javaherdashti, 1996; Byars, 1999]. Indeed, the main result highlighted by Lopez *et al.,* (2006) when performed phylogenetic analysis on bacterial population isolated from a water pipeline in the gulf of Mexico was the total absence of SRB detection on the samples analysed by microbiological isolation and PCR-based methods [Lopez *et al.,* 2006]. However, among the main bacterial types that are associated to metals deterioration —specifically carbon steel— under anaerobic conditions, there are found the sulphate-reducing bacteria (SRB), nitrate-reducing bacteria, thiosulphate-reducing bacteria (TSRB), iron or manganese oxidizing or reducing bacteria and those who secrete organic acids or important viscous masses of exopolymers. All these microorganisms cohabitate in natural biofilms (Figure 4), forming frequently symbiotic communities that affect the electrochemical processes of corrosion, through an integral cooperative metabolism [Beech and Gaylarde, 1999].

Some of the ways in which microorganisms can initiate or enhance corrosion are [Videla, 1997; Monfort, 2001]: a) production of acid metabolites (e.g. hydrogen sulphide) that regulate the local pH, b) production of metabolites that work against protective inorganic films (e.g. biogenic sulphides), c) enhancement of corrosion conditions by increasing the redox potential, d) promotion of differential aeration gradients, e) selective damage of bacteria to welded areas of the metal, f) facilitation of localized corrosion or pitting phenomena due to the heterogeneities caused by biofilm formation, g) microbial degradation of corrosion inhibitors, h) microbial degradation of protective coatings, i) dissolution of protective films on the metal surface, j) modification of the conductivity due to the EPS, k) metallic ions chelation in the EPS and l) interactions of corrosion products with the biofilm.

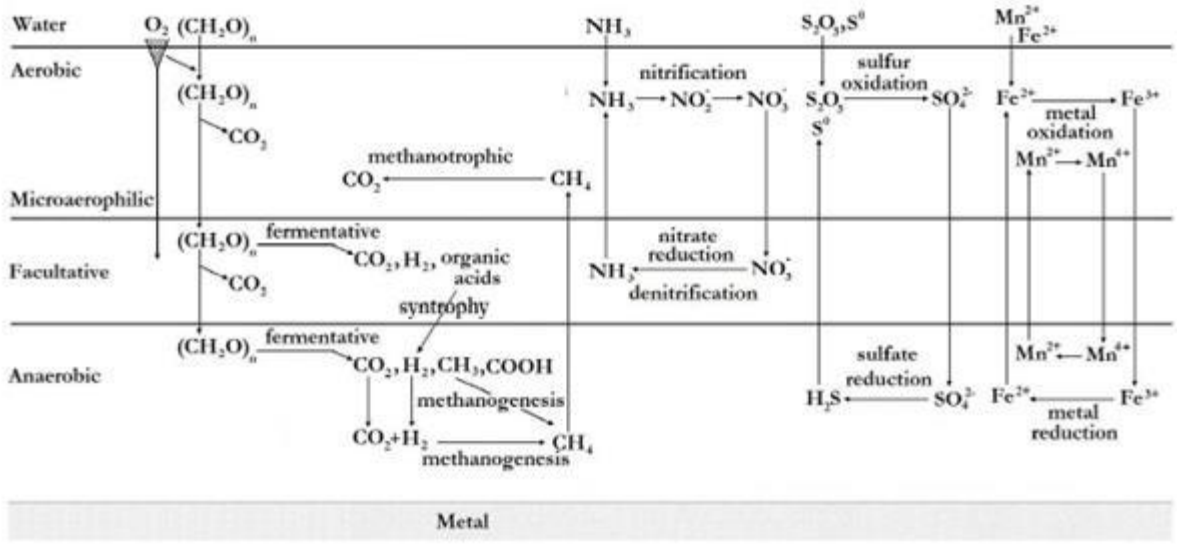


Fig. I.4. Bacterial interaction within the biofilm strata [Dominguez, 2007; Javaherdashti, 2008; Little *et al.*, 1991]

Chamritski *et al.*, [Chamritski *et al .*, 2004] found that MIC of stainless steel AISI 304 in low-chloride (less than 100 ppm) waters could be caused by bacteria such as iron-oxidising bacteria (reduction of the pitting potential), manganese-oxidising bacteria (ennoblement impact), and sulphate-reducing bacteria (pit stabilisation effects). Critchley and Javaherdashti [Critchley and Javaherdashti, 2005], Beech et al. [Beech *et al.*, 2000] and, more completely, Jones and Amy [Jones and Amy, 2002] give a detailed list of the bacteria that could be involved in corrosion where SRB are just one of these bacterial groups. In fact, in nature there is no such a thing as a pure culture of this or that bacteria [Javaherdashti, 2008], and it is quite possible to have a rather complex picture of all possible microbial reactions that may happen simultaneously or in sequence.

These cases as well as others prove the involvement of different groups of bacteria influencing corrosion processes. As follows, there is a short description of the communities studied during this project that may be inducing or accelerating corrosion processes.

### *I.3.3.1. Sulphate reducing bacteria (SRB)*

SRB are a group of diverse anaerobes which carry out dissimilatory reduction of sulfur compounds such as sulfate, sulfite, thiosulfate and even sulfur itself to sulfide [Beech and Gaylarde, 1999; Back and Cypionka, 1987]. Although SRB are often considered to be strictly anaerobic, some genera tolerate oxygen [Beech and Gaylarde, 1999; Abdollahi and Wimpenny 1990] and at low dissolved oxygen concentrations certain SRB are able to respire with Fe(III) or even oxygen with hydrogen acting as electron donor [Roden and Lovely, 1993].

*Influences in Corrosion:* Widely studied for its capability to reduce sulphates producing sulphides which are known to be very corrosive metabolites. SRB are supposed to act upon iron primarily by produced hydrogen sulphide as a corrosive agent and by consumption of ‘cathodic hydrogen’ formed on iron in contact with

water [Lee *et al.*, 1995; Von Wolzogen, 1923]. $H_2S$ in presence of iron will precipitate as FeS which next catalyzes proton reduction into molecular hydrogen and acts as a cathode in a galvanic couple with metallic iron [Barton *et al.*, 2007; Rajagopal and LeGall, 1989; Da Silva *et al.*, 2007]. Among SRB, *Desulfovibrio* species—with their capacity to consume hydrogen effectively—are conventionally regarded as the main culprits of anaerobic corrosion [Din *et al.*, 2004]. Recent reviews clearly state that one predominant mechanism may not exist in SRB-influenced corrosion and that a number of factors are involved [Lovely and Phillips, 1987]. Beech *et al.*, [Beech and Gaylarde, 1999] has resumed the main mechanisms for iron corrosion found in the literature that can be attributed to SRB:

| Corrosive process/substance | Reference(s) |
|---|---|
| Cathodic depolarization* by hydrogenase | von Wolzogen Kühr and van der Vlugt, 1923; Bryant *et al.*, 1991. |
| Anodic depolarization* | Salvarezza and Videla, 1984; Daumas *et al.*, 1988; Crolet, 1992. |
| Sulfide | Little *et al.*, 1998. |
| Iron sulphides | King and Wakerley, 1973. |
| A volatile phosphorus compound | Iverson and Ohlson, 1985. |
| Fe-binding exopolymers | Beech and Cheung, 1995; Beech *et al.*, 1996, 1998, 1999. |
| Sulfide-induced stress corrosion cracking | Edyvean *et al.*, 1998. |
| Hydrogen-induced cracking | Edyvean *et al.*, 1998. |

*depolarization is an acceleration of the corrosion reaction and may involve removal of cathodic or anodic reactants.

Table 1. Suggested mechanisms of metal corrosion by SRB [Beech and Gaylarde, 1999]

### *I.3.3.2. Iron oxidizing bacteria (IOB) and Manganese oxidizing bacteria (MOB): Metal depositing Bacteria (MDB)*

The manganese oxidizing group is characterised by the ability to catalyse the oxidation of divalent, soluble Mn (II) to insoluble manganese oxides of the general formula $MnO_x$ [Nealson, 2006]. The IOB group have the common feature of oxidizing Fe (II) to Fe (III), which generally precipitates as iron hydroxide [Videla, 1997]: the bacteria get energy by oxidizing Fe (II) and can performed this process either in aerobic or anaerobic conditions [Straubk and Buchholz-Cleven, 1998; Emerson *et al.*, 1999].

In the literature [Beech and Gaylarde, 1999; Little *et al.*, 1991], these two groups of bacteria are joint together in the scope of corrosion and classified as metal depositing bacteria. Both of these bacteria groups are involved with the formation of tubercles or deposits on the surface of the metal. The iron oxidising genera that are usually cited as causing MIC are *Gallionella*, *Sphaerotilus*, *Crenothrix*, and

*Leptothrix*. These organisms oxidise ferrous ions to ferric ions or manganous ions to manganic ions to obtain energy [Little *et al.,* 1991]. Moreover, Abdollahi's and Roden's teams have found a sheathed filamentous bacterium detected by microscopy in naturally formed corrosion deposits which have a role in the corrosion of steels [Kobrin, 1976; Tatnal, 1981]. These bacteria have been typically associated with formation of tubercles (macroscopic deposits containing microorganisms, inorganic and organic materials) and consequent under-deposit pitting attack on stainless steel.

Dense accumulations of MDB on the metal surface may thus promote corrosion reactions by the deposition of cathodically-reactive ferric and manganic oxides and the local consumption of oxygen by bacterial respiration in the deposit [Beech and Gaylarde, 1999]. However, care must be taken when detecting these microorganisms in corrosion products; they may not always have to be the causal agent of corrosion. Some bacteria are known to adhere preferentially to corrosion products and thus will be present in high numbers even when playing no role in the primary corrosion process [Beech and Gaylarde, 1999].

#### *I.3.3.3. Iron reducing bacteria (IRB)*

Dissimilatory Fe (III) reduction is the process in which microorganisms transfer electron to external ferric iron (Fe (III)), reducing it to ferrous iron (Fe (II)) without assimilating iron. A wide phylogenetic diversity of microorganisms, including archaea as well as bacteria, are capable of dissimilatory Fe (III) reduction [Lovely, 2006]; of these, a wide variety that have been examined by 16S rRNA phylogenies can oxidize hydrogen coupled with the reduction of Fe(III). Several that have been examined in more detail can conserve energy to support growth from this metabolism. Saying this, it is expected the results obtained by Lovely and Phillips which conclude that dissimilatory Fe (III) reduction has been shown to compete successfully for $H_2$ not only with methanogenesis but also with sulfate reduction in natural habitats [Lovely and Phillips; 1987]. Fe (III)-reducing bacteria have a higher affinity for $H_2$, and the change in free energy of Fe (III) reduction with $H_2$ is larger than that of sulfate reduction or methanogenesis [Lovely *et al.,* 1994]. Moreover, it was proven that the IRB *Shewanella putrefaciens,* which possesses hydrogenase, utilized $H_2$ for reduction of Fe (III) (in form of citrate salt) and simultaneously induced corrosion by inducing anodic polarisation observed only in presence of bacteria [Obuekwe *et al.,* 1981; Esnault *et al.,* 2010; Libert *et al.,* 2011].

In general, IRB are known to promote corrosion of iron and its alloys through reactions leading to the dissolution of corrosion-resistant oxide films that are formed on the metal surface. This results in the protective passive layers on *e.g.* stainless steel surfaces being lost or replaced by less stable reduced metal films that allow further corrosion to occur [Beech and Gaylarde, 1999]. Despite its widespread occurrence in nature and likely importance to industrial corrosion, bacterial metal reduction has not been seriously considered in corrosion reactions until recently.

Javaherdashti, (2008) has resumed some possible reasons why iron reduction by bacteria is important:

1. Availability of iron: Iron is not very soluble, but if it is reduced to ferrous iron (which is soluble) so that the organic compounds can stabilise iron by chelation where, later on, that iron can "liberate" itself from the organic matter and precipitate as iron.

2. IRB are a very important part of the soil microbial community, as most of the IRB are facultative anaerobes, and thus if oxygen is available, they will prefer it for their growth while also maintaining their capability of growth under anaerobic conditions too. It is estimated that in the surface layer of soil, on the average, the number of IRB could be as high as $10^6$ cells per gram of soil.
It must be kept in mind that as IRB are both chemoheterotrophic (organic compounds are the source of energy for them) and facultative anaerobes, their number within the soil's surface layer is higher than at deeper levels, especially if the soil is rich in organic matter at the surface level. As a result, in cases in which their number in soil is reported, the depth of sampling for the organic carbon content must also be recorded.

3. IRB are capable of making the environment suitable for SRB. In a mixed population of micro-organisms in a biofilm, as oxygen is consumed, the redox potential starts to decrease so that nitrate, then manganic and ferric ion and the sulphate is reduced.

On the other hand, one of the most studied genera of this bacterial group is *Geobacter sp.* being the species *G. sulfurreducens* tested in this study. Due to this, a small description of these bacterium genera is given below:

*Geobacter*

Geobacter was first isolated from fresh water sediments from the Potomac River, Maryland by D. R. Lovely's team. Enrichment cultures with acetate and yeast extract as potential electron donors and amorphic Fe (III) oxide and Fe (III) citrate as the electron acceptor, were performed in order to demonstrate for the first time the complete oxidation of organic matter compounds such as acetate coupled to dissimilatory Fe (III) reduction by these microorganisms. It was also demonstrated that there was not Fe(III) reduction if physical contact between the denominated GS-15 strain, and the amorphic Fe (III) oxide was prevented by placing the amorphic Fe(III)oxide within dialysis tubing [Lovely and Phillips, 1988; Lovely and Phillips, 1986].

GS-15 is not magnetotactic, but reduces amorphic ferric oxide to extracellular magnetite during the reduction of ferric iron as the terminal electron acceptor for organic matter oxidation [Lovely *et al.,* 1987]. Magnetite ($Fe_3O_4$) is a mixed ferric-ferrous mineral (F III Fe III Fe II). GS-15 could not reduce the Fe (III) contained in magnetite (Lovely and Phillips, 1986, Lovely *et al.,* 1987).

Moreover, *Geobacter sulfurreducens* is one of the most widely studied anodophilic species -especially in the domain of microbial fuel cell-, which has been shown able to completely oxidize organic electron donors, generally acetate, to carbon dioxide by using only an electrode as electron acceptor [Bond and Lovely, 2003, Dumas *et al.,* 2008a; Dumas *et al.,* 2008b]. Its genome contains a large number

(>100) of cytochromes C that function in metal reduction pathways; more specifically, cytochromes $C_7$ which are the ones involved in the reduction of Fe III [Londer *et al.,* 2007]; this quantity of cytochromes implies a significantly higher number of cytochrome genes than reported in any other organism whose sequence is available [Ding *et al.,* 2006]. Direct electron transfer to solid electrodes, without the need for soluble electron mediator, is then claimed to be achieved through periplasmic and outer membrane c-type cytochromes.

*G. sulfurreducens* has rarely been studied in the domain of biocorrosion. However, recent studies with *G. sulfurreducens* have shown that these bacteria can exert two antagonists effects on 304L stainless steel: Just after inoculating, *G. sulfurreducens* cells create a cathodic reaction on the material, which leads to a fast increase in its open circuit potential increasing the corrosion risk; in contrast, after a few days, well established biofilms shift the pitting potential towards positive values, which might be interpreted as a protective effect [Mehanna *et al.,* 2010].

#### *I.3.3.4. Acid Producing bacteria (APB*)

There are two types of acid producing bacteria; those that produce organic acids such as lactic acid and those that produce inorganic acids such as sulphuric acid. For the first, most of them are heterotrophic bacteria that secrete organic acids during fermentation of organic substrates. The kinds and amounts of acids produced depend on the type of microorganisms and the available substrate molecules [Little *et al.,* 1991]. For the latter, most of them are gram negative bacteria, aerobic rods that grow well at 20-30 °C [Harrison, 1984]. These lasts are generally autotrophic and acidophilic; obtain the energy needed by $CO_2$ fixation or by degrading organic substrates from the oxidation of the sulphur and the hydrogen sulphide.

*Influence in Corrosion:* Fermentative bacteria secreting organic acids may force a shift in the local pH provoking a tendency for corrosion to occur. The impact of acidic metabolites is intensified when they are trapped at the biofilm/metal interface. Acetic acid from *Clostridium aceticum* is an obvious contributor to corrosion. For instants, organic acid-producing bacteria were suggested as the primary cause in case of carbon steel corrosion in an electric power station; they were the only group of culturable microorganisms whose abundance was correlated positively with corrosion [Beech and Gaylarde, 1999]. Acetic, formic and lactic acids are common metabolic by-products of APB. Furthermore, *Thiobacillus lieni* (thermophilic) ferments certain aminoacids, proteinaceus substrates and organic acids, producing ethanol, acetate, propionate, isovalente/ 2-meylbutyrate, $H_2$ and $CO_2$. It can also reduce cystine and elemental "S" to $H_2S$ [Duncan *et al.,* 2009].

On the other hand, several of the inorganic APB bacteria that related to corrosion have a common function: to form part of the sulphur cycle in the nature [Videla, 1997] and acquire their energy for growth through the oxidation of inorganic sulphur [Harrison, 1984]. *Thiobacillus* is one of the better known genuses which are corrosive agents due to the sulphuric acid generation. For instance, sulphuric acid is produced by sulphur oxidising bacteria (SOB), such as *Thiobacillus thioxidans*. They are aerobic microorganisms using carbon dioxide as the main carbon source.

These bacteria sulpho-oxidants may have the following metabolic reactions [Vrignaud, 1988]:

$H_2S + 2\ O_2$ -----> $H_2SO_4$ (I.8)

$4\ S + 6\ O_2 + 4\ H_2O$ -----> $4\ H_2SO_4$ (I.9)

$2S + 3\ O_2 + 2\ H_2O$ -----> $2\ H_2SO_4$ (I.10)

Because of the metabolic characteristics of *Thiobacilli,* extreme conditions of acidity are produced in the environment. In the special case of *T. Thioxidans,* because of its ability to oxidize 31 g of sulphur per gram of carbon, pH values on the order of 0.5 are produced in the medium, attaining extremely aggressive conditions not only for metals, but also for concrete or stone structures [Videla, 1997].

#### *I.3.3.5. Methanogens*

The methanogenic bacteria are a large and diverse group that is united by three features: 1) They form large quantities of methane as the major product of their energy metabolism. 2) They are strict anaerobes. 3) They are members of the domain Archaea or archaebacteria. Methanogenic bacteria obtain their energy for growth from the conversion of a limited number of substrates to methane gas. The major substrates are $H_2 + CO_2$, formate, and acetate [Whitman *et al.,* 2006].

*Influence in Corrosion:* Methanogenic bacteria may use either pure elemental iron ($Fe^\circ$) or iron in mild steel as a source of electrons in the reduction of $CO_2$ to $CH_4$ [Daniels *et al.,* 1987]. These bacteria use $Fe^\circ$ oxidation for energy generation and growth. The mechanism of $Fe^\circ$ oxidation is cathodic depolarization, in which electrons from $Fe^\circ$ and $H^+$ from water produce $H_2$, which is then released for use by the methanogens; thermodynamic calculations show that significant $Fe^\circ$ oxidation will not occur in the absence of $H_2$ consumption by the methanogens. The data suggest that methanogens can be significant contributors to the corrosion of iron-containing materials in anaerobic environments [Daniels *et al.,* 1987].

## *I.4. Biofilms and microbiologically influenced corrosion inhibition (MICI)*

Corrosion inhibition is the slowdown of the corrosion reaction usually performed by substances (corrosion inhibitors) which, when added in small amounts to an environment, decrease the rate of attack by this environment on a metal [Videla and Herrera, 2009]. Some author have claimed that there are certain strains of bacteria that may induce corrosion inhibition [Dubiel *et al.,* 2002; Herrera and Videla, 2009; Mansfeld *et al.,* 2002; Mansfeld, 2007; Zuo, 2007]. For instance, different authors have debated about the harmfulness of biofilms on metal surfaces and even argued that some of them may reduce corrosion rates by different mechanisms [Mehanna *et al.,* 2010; Chongdar *et al.,* 2005; Volkland *et al.,* 2000; Volkland *et al.,* 2001a]. One of these mechanisms is a surface reaction leading to the formation of a corrosion inhibiting layer of phosphate such as the iron phosphate, vivianite.

Vivianite is an iron (II) phosphate, $Fe_3(PO_4)_2 * 8H_2O$ which may be used as a corrosion inhibiting agent of iron due to its low solubility properties forming a low soluble corrosion product film on the metal surface [Volkland *et al.,* 2000; Volkland *et al.,* 2001a; Gourbeyre *et al.,* 2003; Zuo, 2007]. A protection method against corrosion used by some industries is acid phosphating with phosphates of zinc, iron or manganese which leads to vivianite production [Volkland *et al.,* 2000]. This procedure is carried out at temperatures up to 95°C and pH values between 2 and 3.5.

One of the most studied mechanisms of corrosion inhibition promoted by microorganisms or microbially influenced corrosion inhibition (MICI) is the corrosion control using beneficial biofilms [Zuo, 2007; Videla and Herrera, 2009; Mansfeld, 2007; Mansfeld *et al.,* 2002]. These benefits can be linked to either physical characteristics of the biofilm or biochemical characteristics involving metabolites. A biofilm is a highly organised bacterial community with cells entrapped in a matrix formed by extracellular polymer substances (EPS). On one hand, biofilms may form a persistent film which adheres at the metal/solution interface reducing the corrosion rate by forming a transport barrier, which may prevent the penetration of corrosive agents (such as oxygen, chloride, etc.) and decreasing their contact with the metal surface, thus reducing corrosion [Din *et al.,* 2004; Beech and Gaylarde, 1999]. However, recent studies have shown that this protection is unreliable and that biofilms instead could also promote corrosion by a formation of a non-uniform patch which, in the presence of aerobic respiration, results in the formation of differential aeration cell accelerating the corrosion rate [Zuo, 2007; Videla and Herrera, 2009].

On the other hand, corrosion inhibition is sometimes explained by the biochemical characteristics of the microorganisms themselves and/or their enzymes. For instance, Da Silva *et al.,* (2004) and Mehanna *et al.,* (2008) observed a vivianite deposit on mild steel electrodes placed in a galvanic cell which had been catalysed by hydrogenase from *C. acetobutylicum*, consequently observing a delay on pitting corrosion or a reduced corrosion rate. Other authors [Dubiel *et al.,* 2002; Mansfeld, 2007; Mansfeld *et al.,* 2002; Duan *et al.,* 2008], have claimed that the bacteria induced the reduction of corrosion rates, the prevention of pitting corrosion and the reduction of both cathodic and anodic reactions in materials such as stainless steel [Little *et al.,* 2008], mild steel and aluminium brass [Mansfeld, 2007; Mansfeld *et al.,* 2002]. These observations were attributed to the presence of bacteria. Most of the bacteria reported to be involved in MICI are iron reducing bacteria (IRB). For instance, Little *et al,* 2008 and Eashwar *et al.,* 1995 have claimed that corrosion inhibition on stainless steel was due to a mechanism in which siderophores (iron chelators) produced by microorganisms within biofilms at neutral pH act as inhibitors and enhance passivity of stainless steel by reducing $i_{p.}$ Other mechanisms most frequently cited for the inhibition are formation of a diffusion barrier to corrosion products that stifle metal dissolution, consumption of oxygen by respiring aerobic microorganisms within the biofilm causing a diminution of that reactant at the metal surface, production of metabolic products that act as corrosion inhibitors (e.g., siderophores, vivianite), specific antibiotics that prevent proliferation of corrosion-causing organisms (e.g., sulfate-reducing bacteria), formation of passive layers that are unique to the presence of microorganisms [Little and Ray, 2002], reduction of ferric ions to ferrous ions (in presence of IRB)

and increase consumption of oxygen [Dubiel *et al.,* 2001]. Moreover, Herrera and Videla, 2009 claim that the introduction of IRB to industrial water systems which contain SRB and other corrosion-inducing bacteria causes not only the exfoliation of corrosion products but also the protection of the metal surfaces from further corrosion. In general, the main mechanism of corrosion inhibition by bacteria are always linked to a marked modification of the environmental conditions at the metal/solution interface by biological activity [Herrera and Videla, 2009]

Moreover, IRB have been reported to biologically produced vivianite at laboratory scale under aerobic conditions with few bacteria strains such as *Pseudomonas sp.* [Chongdar, 2006] and *Rhodococcus sp*. using a metal coupon and 20 mM of phosphate buffer [Volkland *et al.,* 2000; Volkland *et al.,* 2001a; Volkland *et al.,* 2001b]. Islam et. al., (2005) reported vivianite formation under anaerobic conditions by *Geobacter sulfurreducens* using soluble Fe (III) (iron citrate) as electron acceptor. When the organism was grown using insoluble crystalline Fe (III) and oxy-hydroxide as electron acceptor, Fe (III) reduction resulted in the formation of magnetite instead of vivianite. These same results were also observed by Lovley and Phillips, (1998).

However, it is still uncertain the role of *G. sulfurreducens* in corrosion. Recent studies with these bacteria have shown that it can exert two different effects on 304L stainless steel: just after inoculating, *G. sulfurreducens* cells create a cathodic reaction on the material, which leads to a fast increase in its open circuit potential increasing the corrosion risk; in contrast, after a few days, well established biofilms shift the pitting potential towards positive values, which may be interpreted as a protective effect [Mehanna *et al.,* 2010]. This research concluded that *G. sulfurreducens* plays a role in corrosion behaviour of 304L which depends on medium composition. In the absence of acetate (lack of electron donor), *G. sulfurreducens* biofilms promote the propagation of pitting whereas in the absence of fumarate (lack of electron acceptor), *G. sulfurreducens* cells were able to delay pit occurrence protecting the metal.

The controversy about enhancement of corrosion and/or protection against corrosion promoted by microorganisms is still unclear regarding this bacterial group. According to some reports, IRB are able to induce protection of carbon steel [Mehanna *et al.,* 2010; Herrera and Videla, 2009; Dubiel *et al.,* 2002] while others suggest an important enhancement of corrosion through the reduction and removal of passive films of ferric compounds on the metal surface [Mehanna *et al.,* 2010; Herrera and Videla, 2009; Esnault *et al.,* 2010; Libert *et al.,* 2011].

### *I.5. Biocorrosion in the Oil and Gas Industry*

Corrosion represents a considerable economic stake projected between 1 and 4% of the gross national product (GNP) of developed countries [Duncan *et al.,* 2009]. One of the most susceptible industries for biofilm formation and their detrimental consequences is the petroleum industry. Fleming *et al.* [Sparr and Linder, 2010] estimate that 20% of corrosion problems are linked to the presence of microorganisms and more over Jack *et al.* (1992) in [Mehanna, 2009] estimated that 34% of the corrosion damage experienced by oil companies was related to MIC.

Moreover, it has been estimated that in the petroleum-related, shipping and geothermic industries as well as in those that use certain amounts of water in their processes, many of the losses in metallic materials can be attributed to microbial presence or activity and might contribute between 10 % and 50% of the total corrosion damage [Dominguez, 2007; Sparr and Lindert, 2010; Mehanna, 2009; Beech and Gaylarde, 1999]. Just in the UK, studies have suggested that 50% of corrosion failures in pipelines involved MIC [Beech and Gaylarde, 1999].

However, there are no official figures for the cost of MIC, but some indication of its importance can be gained from individual companies or sectors of industry [Sparr and Linder, 2010]. For instance, Jana *et al.,* (1999) analysed crude oil pipelines at Mumbai offshore, India, and concluded that the combined effect of $CO_2$, SRB, and chloride in the low velocity area caused severe corrosion and failure of the pipelines [Rajasekar *et al.,* 2010].

On the other hand, it is well known that biodegradable materials, such as hydrocarbons, can provide a source of nutrients to microbial growth [Thomas, 2002]. Thus, it is possible that compounds that are inside the pipelines might be used as carbon and energy sources by the microbial flora that influence corrosion, as long as a water-hydrocarbon interface is present.

The largest potentially available source of carbon to support microbial activity is the oil itself. Since hydrocarbons are known to be suitable substrates for anaerobes, it is suspected that the more water-soluble oil components, like benzene, toluene, ethyl-benzene, and xylene isomers (BTEX) might be preferentially metabolized to support the diverse microbial communities detected at the facility. The subsequent metabolism of the fatty acids would eventually form acetate and $CO_2$, microbial products known to exacerbate corrosion of pipeline surfaces. Also, sea water can contribute sulphate and other nutrients that might stimulate increased corrosive microbial activity [Duncan *et al.,* 2009].

Nevertheless, oil and gas industries battles MIC problems and its potential damages in pipelines by different methods such as the use of biocides, coatings, corrosion inhibitors and different chemicals that could reduce or control bacterial growth and/or reduce corrosion rates but probably the best way to avoid microbial influenced corrosion is an appropriate design and operation to keep the systems clean combined with regular mechanical cleaning [Sparr and Linder, 2010].

Mechanical cleaning involves any method capable of the physical removal of deposits formed on the surface. It includes brushing, pigging and the use of cleaning spheres or water jet, etc., and is applied to remove sludge, scale, and encrustations as well as the biomass associated with these deposits [Videla, 2002]. Mechanical cleaning is mainly performed in water injection and production pipeline systems of oil and gas industries by the use of mechanical pigs (Fig. I.5).

Fig. I.5. Pig before (left) and after use (right)

Pipeline operators now describe any device made to pass through a pipeline for cleaning and other purposes with the word pig. The process of driving the pig through a pipeline by fluid is called a pigging operation [Guo *et al.*, 2005]. Operators need to run cleaning pigs to de-wax and descale the inside surface of the pipe and remove debris (corrosion products and biofilm), which help improve pipeline performance [Bubar, 2011]. This debris collected in the receivers of the pipelines (Fig. I.6) may be used to analyse not only corrosion products, organic matter, oil and water residues but also biofilm and bacterial presence.

Depending on the operating system, oil and gas companies combine different methods for the prevention and/or protection of corrosion of their pipelines. For instance, pigging operations are combined with biocide treatments and/or corrosion inhibitors treatments in order to reduce bacteria development. However, it is known that bacteria can adapt to drastic conditions posed by these treatments and resist rough environmental conditions still causing a threat for the materials. For example sulphate reducing bacteria (SRB) show considerable adaptability to extreme conditions making it possible to isolate active cultures from sites where bacteria are exposed to $O_2$ regardless the anaerobic nature of this group [Beech and Sunner, 2004; Hamilton, 1985; Marshall *et al.*, 1993].

Fig. I.6. Pigging debris collected in the receivers of a pipeline

## *I.6. Scope of the project*

Throughout the information given in the state of the art it can be seen that the study of biofilms and MIC involves multidisciplinary subjects. It is at the same time a concern for Microbiology as it is for Electrochemistry, for Molecular Biology and other specialists. In the present work, all these mentioned approaches have been used in this research project as tools for the study of corrosion of carbon steel in water injection systems of the oil and gas industry. The main objective of this study is to **develop new experimental models that will induce the reproduction of biocorrosion "in lab" on carbon steel using samples and environmental conditions found in pipelines of water injection systems in the oil and gas industry. Ideally this methodology will provide us new insights to understand corrosion mechanisms that could be extrapolated to the field mechanisms.** For this, the project was conducted in laboratory conditions but partnering up with a Norwegian oil and gas company concerned with problems of biocorrosion.

Information obtained from the field partners who provided us the samples (source of microorganisms) and information found in the literature drove us to comprehend that SRB are one of the most significant microorganisms involved in anaerobic corrosion of iron and steel having two mechanisms of prime importance already elucidated. One mechanism is the chemical acceleration by $H_2S$, the metabolic by-product of SRB. The other, more frequently discussed mechanism is the increased cathodic depolarization due to microbial scavenging of the reducing equivalents in a still unknown form. It is generally accepted that the deposition of iron sulfide induced by activity sulphate-reducing bacteria (SRB) and thiosulfate-reducing (TRB) plays a key role in anaerobic corrosion of steels. Despite this unanimity, laboratory manipulations struggle to reproduce the corrosion of low alloy steels observed in both industry and natural environments; it is not explain what is the element that triggers the corrosion since the SRB, present in almost all marine biofilms, do not induce systematically corrosion.

However, it is more and more recognised the involvement of other bacterial groups playing a key role in corrosion. Few studies, including this one, provide an insight on anaerobic corrosion of carbon steel caused by other mechanisms different to those described with SRB. The biodiversity found in biofilms is a key tool to attempt to elucidate the involvement of other bacterial groups in corrosion such as IRB, APB MDB, and methanogens. To prove this, two general approaches were applied: the first one was to study the influence of *G. sulfurreducens,* an IRB widely known for its electron exchange capabilities as a model bacterium, on the corrosion of carbon steel. These characteristics make these bacteria an excellent candidate to understand new biocorrosion mechanisms different to those widely studied such as the SRB mechanisms. The second approach was to use biofilm from the field to study its influence on the anaerobic corrosion of carbon steel under laboratory conditions but simulating some of those found in the field. Tools of the different disciplines previously mentioned were used (if appropriate) for both approaches in order to conduct the study. A schematic representation of the two approaches undertook during this project can be observed in Fig. I.7

The experimental section gives an overview of the experimental strategy and the techniques applied along this research work, which will be described in detail in

the following sections. However, specific details used for each section of the results will be further detailed if necessary for each specific case of study.

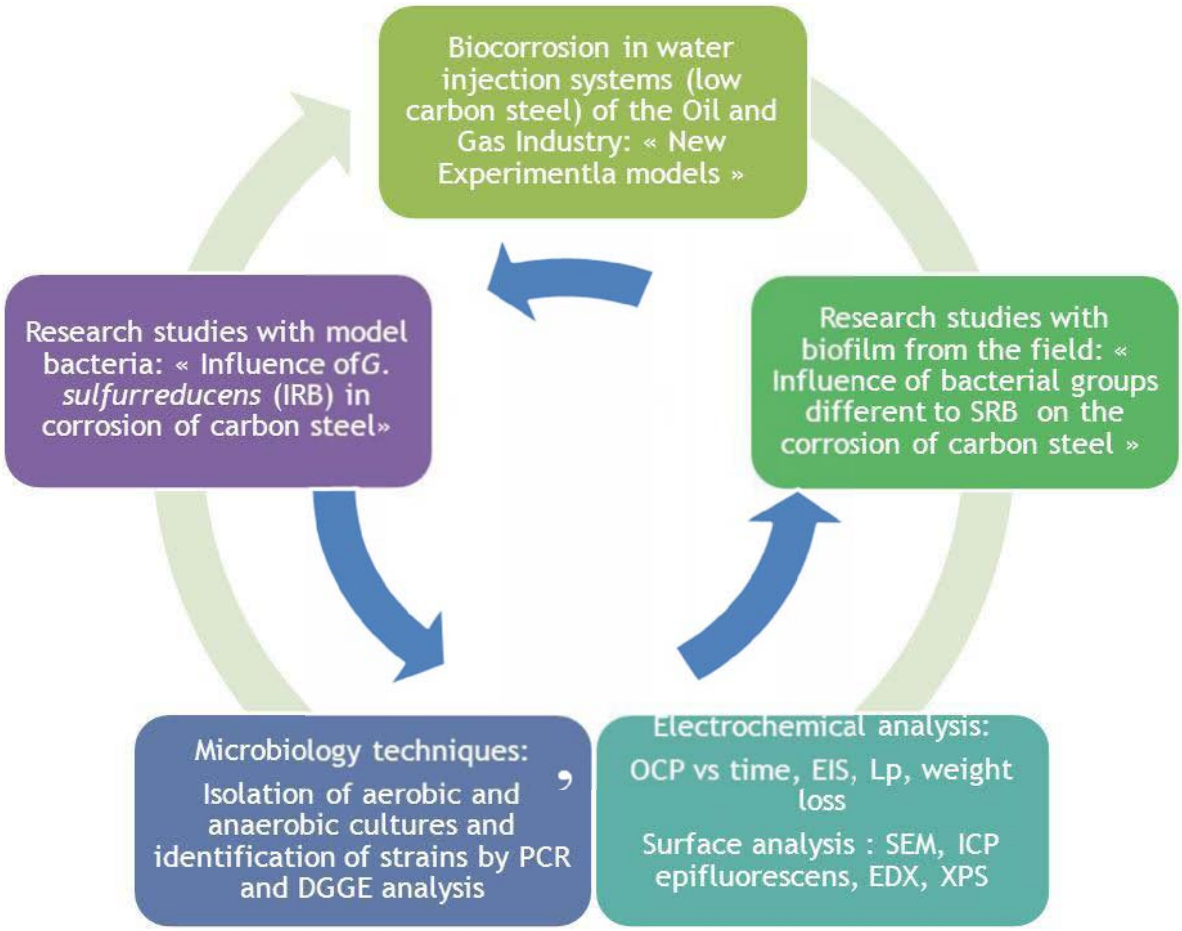


*Fig. I.7. Schematic layout of project approach*

# ***Chapter II-*** *Materials & methods*

This chapter describes the materials and methodology undertook all along this project which as previously explained, has been divided into two different approaches: the first approach centres on the electrochemical analysis of a system containing a pure culture of an electroactive strain of *Geobacter sulfurreducens* as a novel iron reducing bacteria in presence of carbon steel. The influence of these bacteria on the corrosion of carbon steel was assessed by mainly using electrochemical techniques such as: corrosion potential measurements, polarisation techniques and electrochemical impedance spectroscopy. Weight loss, surface analysis and analytical techniques were also used to complement the set of experiments based on this approach. All the electrochemical techniques were applied in the laboratoire de Genie Chimique of the INP-ENSIACET, Toulouse, France. X-ray photo electron spectroscopy (XPS) surface analysis technique was performed in the surface analysis laboratory of the university Pierre and Marie Curie, Paris, France.

The second approach aims to understand the influence of bacterial consortia extracted from a biofilm collected from a water injection system of an oil and gas company on the corrosion of carbon steel. For this approach, microbiological enrichments were performed aiming to isolate and identify the main bacterial groups that may have an influence on corrosion. The DNA separation was performed by Denaturing Gradient Gel Electrophoresis (DGGE) in the laboratory of Microbiology at the University of Portsmouth, UK, and then its sequencing was commanded to GATC Biotech (Germany), to the further identification by on-line blasting. The same electrochemical and analysis techniques used for the first approach were also applied for this approach using different types of bacteria source such as: the bacterial consortium pre-enriched in artificial sea water, pigging debris and enriched bacteria.

## II.1. Materials and Media

### II.1.1. The working electrodes

Two different types of carbon steel have been used as working electrodes (WE) during the experiments mentioned in this thesis: AISI 1145 and 1015. This denomination is according to the norm emitted by the American Iron and Steel Institute (AISI).

The steel coupons were cylinders which dimensions were: 1 cm height and 2 cm diameter. The WE was covered by a polymeric coating (thermo-contractible polyolefin, ATUM ®) leaving uncovered a flat disk surface with a total exposed area of 3.14 $cm^2$. A crystallography was performed in each of the clean metal coupons used during this project and the images are displayed in Fig. II.1. For both structures, the size of grains is quite small and boundaries are short indication compact structure. Note that ferrite is pure iron face and perlite is iron carbide.
Connections were made through titanium wire protected with the same polymeric coating. The WE was placed into the reactor in a way that was always facing the counter electrode and as far as physically possible from the $N_2/CO_2$ injection device (Fig II.2).

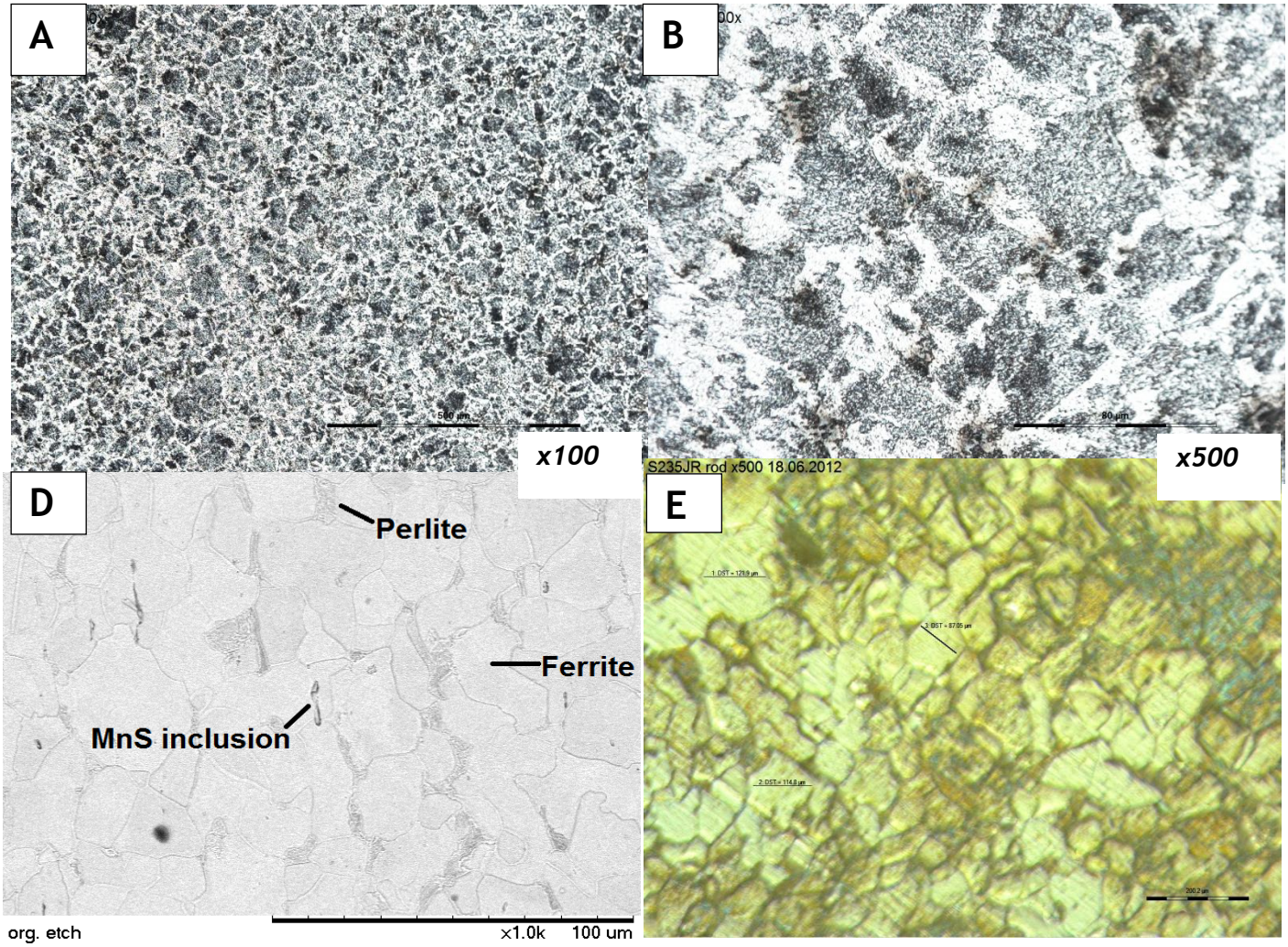


Fig. II.1. Crystallography and SEM characterisation performed to a clean ground coupon of carbon steel C1145: (A) Crystallography characterisation using the x100 amplification lens; (B) Crystallography characterisation using the x100 amplification lens; (C) SEM micrograph using the x7000 amplification lens. C1015: (D) Crystallography characterisation using the x100 amplification lens; (D) Crystallography characterisation using the x100 amplification lens

#### *II.1.1.1. Nomenclature*

In the AISI standard steels, names are composed by digits. First figure indicates the major class of steel, second figure indicates a sub-division of the major class and the percentage of the major alloying elements. The third and fourth figures are most important for welding because they indicate carbon in hundredths of a percentage. In this same order the AISI 1145 is classified within the carbon steels resulfurized and the AISI 1015 within the carbon steels.

Both of the steels are used in the oil and gas industries for general used and more specifically, the AISI 1015 is the analogue used for the industrial partner to construct their water injection pipelines.

Note that the AISI standard is not the only one to designate steels. In fact, according to each country, classifications differ. However, the European standard for these steels are: C45 for the AISI 1145 and S235 JR for the AISI 1015.

Table II.2 shows the mass compositions of the steels used in this work.

| *Alloy* | *Ni* | *C* | *Mn* | *Cu* | *Si* | *S* | *P* | *Mo* | *Cr* | *N* |
|---|---|---|---|---|---|---|---|---|---|---|
| AISI 1145 | 0.1 | 0.46 | 0.65 | 0.11 | 0.31 | 0.03 | 0.01 | 0.02 | 0.1 | -- |
| AISI 1015 | -- | 0.17 | 1.40 | 0.55 | -- | 0.03 | 0.03 | -- | -- | 0.01 |

Table II.1. Chemical composition of the steels used (wt %)

### *II.1.1.2. Surface treatment*

In order to obtain an identical surface state aiming to have reproducible results, all the steel samples were ground with SiC abrasive paper discs starting with P120, P180, P400 and finishing with P600 (Lam Plan) until achieving a 600 grit surface followed by a cleaning with ethanol (70%) and throughout rinsing with sterile deionised water. This treatment was performed the same day and minutes before launching each experiment. The cleaning with ethanol during 10 to 15 minutes was performed with the idea of conserving the sterile conditions of the systems.
A surface finishing of 600 grit was agreed aiming to work with a very similar surface roughness found in the pipelines. However, few experiments were performed with a mirror finishing in order to assess the influence of the surface state in the attachment of biofilm and its influence in corrosion. These changes in the surface treatment will be mentioned when pertinent.

## II.1.2. Reference and counter electrodes

An electrode of silver-silver chloride (Ag/AgCl) was used as a reference electrode (RE) for all the experiments. The electrode was prepared in the laboratory using silver wires (1.5 mm diameter). The wire was introduced in $NH_4OH$ for 5 hours, after rinsing with distilled water it was introduced in $HNO_3$ (concentrated) for 1 minute and then it was introduced to a solution of KCl (saturated) plus HCl 0.1 M. While the wire is in this solution, it was applied 6 mA/cm² during 10 minutes using a platinum counter electrode.

For the calculation of the theoretical potential of the Ag/AgCl electrodes, the following equation was considered:

$$AgCl + e^- = Ag^0 + Cl^- \qquad E^0_{vs\ SHE} = 0.2223\ V \tag{II.1}$$

Using Nernst equation (I.7), E= 0.2223 – 0.059 log [$Cl^-$]. Considering that the media used for electrochemical experiments from the first approach contained a chloride concentration of 0.03 M, E= 0.31 V vs. SHE and experiments from the second approach contained a chloride concentration of 0.5 M, E= 0.24 V vs. SHE.

Furthermore, platinum grid (Pt, Ir 10%) was used as counter electrode (CE) for all the experiments. Previous to each experiment, the CE were burned in the flame of a Bunsen burner until no coloration of the flame was observed (blue flame) indicating that all products on the electrode were burned, that the electrode is clean and that there is no more chemical pollution. After each experiment the CE were immersed in HCl (50% v/v) in order to remove any biofilm or rust attachment.

### II.1.3. Reactors

All of the experiments were performed in glass reactors of 0.5 L adjusting the liquid level to 350 mL of total volume (Fig. II.2). The reactor was hermetically closed using a metal clamp and the anaerobic conditions were obtained by bubbling $N_2/CO_2$ 80:20 into the reactors for at least 45 minutes before inserting the metal coupons. The flow of $N_2/CO_2$ was maintained during the whole experiment unless stated otherwise. Reactors were kept at 30 to 35°C in a thermal bath during experiments. pH was measured for all the experiments at initial time (h=0) and final time (h≥144 h).

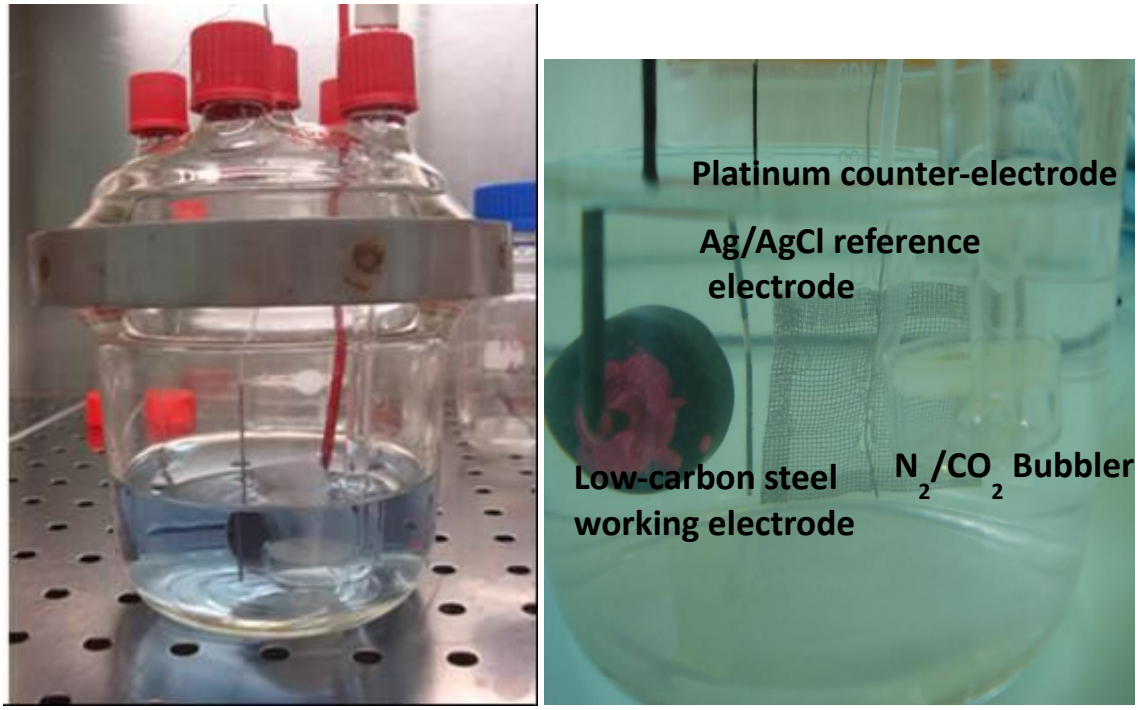


Fig. II.2 Photo of a 0.5 L reactor and its zoom up

## II.2. Bacteria samples

### II.2.1. *Geobacter sulfurreducens*

*Geobacter sulfurreducens* ATCC 51573 strain used during the first approach experiments of the project was obtained from DSMZ (Deutsche Sammlung von Mikroorganismen und Zellkulturen) as an actively growing culture suspended in liquid medium. The bacterial suspension received was re-suspended in the medium suggested by DSMZ and incubated during 5 days at 30 °C.

### II.2.2. Bacterial consortium from pigging debris

For the second approach of the project, biofilm from the field was used to assess its corrosion effects on carbon steel coupons. For this, pigging debris samples were collected from a water injection pipeline "A" located in the installation "A" of an Oil and gas company located in Norway between November 2010 and June 2011. The pipeline consists in 10-15 km long pipe made of low carbon steel with an average operating temperature of 35°C.

The pigging samples were received in schott sealed bottles that were flashed with inert gas right after the sample collection performed by the industrial partner (Fig. II.3) and stored at fridge temperature until 24 hours before the experiments were lunched. Five samples were received along the 3 years project. They were labelled pig 1, pig 2, pig 4, pig 5 and pig 9. Pig 1 corresponds to the first debris collected after the first pigging operation; pig 2 corresponds to the second debris collected after the second pigging operation and so on. Thus, it is consider that each of the pigging samples represents a different stratum of sample forming biofilm on the inner walls of the pipelines. Bacterial consortium living in the different strata of the pigging samples was cultured in different enrichment media aiming to separate bacteria regarding their different metabolic pathways.

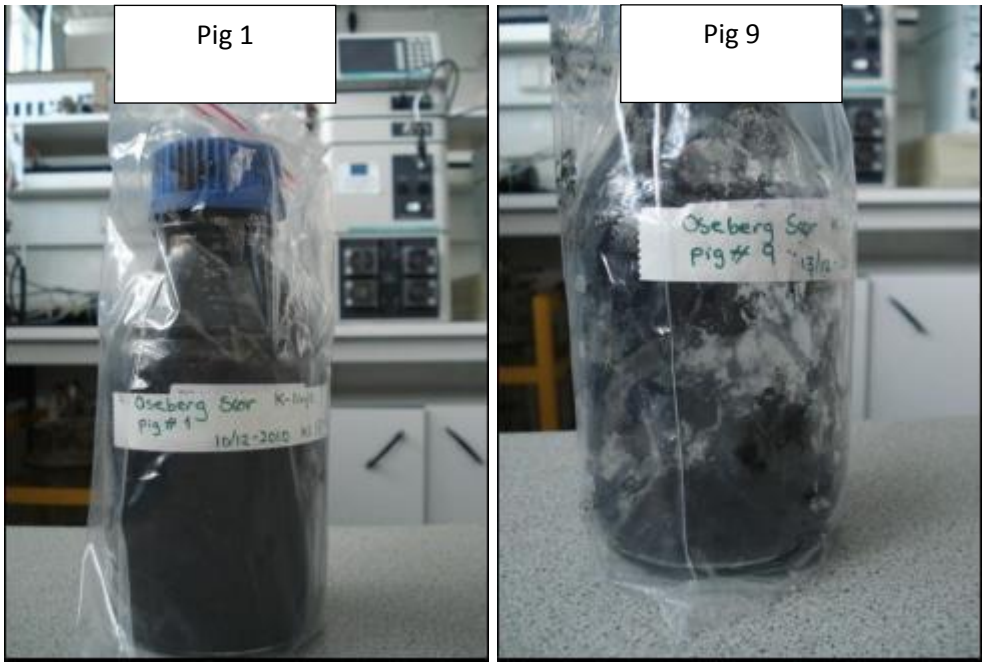


Fig. II.3. Example of pigging debris received

## II.3. Media

### II.3.1. *Geobacter sulfurreducens* growth medium

The media and solutions to grow *G. sulfurreducens* were prepared following the DSMZ protocol [DSMZ, 2007]. The culture growth medium contains 28 mM $NH_4Cl$, 5mM $NaH_2PO_4$, 1.3 mM KCl, 29.7 mM $NaHCO_3$, 2.0 g/L resazurin and 10 mM sodium acetate (electron donor). The medium was sterilised by autoclaving it at 121°C for

15 minutes. Once the medium cooled down it was added a sodium fumarate solution (electron acceptor) filtered with 0.2 µm pore filter, obtaining a final concentration of 50 mM of fumarate in the medium. 10 mL/L of vitamins (ATCC MD-VS) and 10 mL/L of minerals solution (ATCC MD-TMS) was also added.

The *G. sulfurreducens* culture was performed in glass anaerobic vials with 50 mL of growth medium. The vials were sealed with butyl rubber septums and they are de-aerated by injecting $N_2/CO_2$ (80:20, v/v) during at least 30 min before the injection of bacteria (10% of bacterial initial suspension). This first incubation lasted 3 to 5 days at 30 °C for optimum bacteria growth. Indeed, the culture was ready for inoculation in the electrochemical reactors once the absorbance of culture in the anaerobic vials measured around 0.3.

### II.3.2. *Geobacter sulfurreducens* reactors media

The anaerobic reactors used for the electrochemical measurements of the first approach were filled with medium containing all the chemical compounds found in the growth medium at the same concentrations for most of them, except for the electron donor and acceptor: their concentrations were adjusted to1 mM acetate and 10 or 25 mM fumarate. The criteria for choosing the compounds concentration will be clarified in chapter III.

### II.3.3. Pigging samples enrichments media

About 10 g of each of the 5 different pigging samples received were suspended in 90 mL of oxygen free sterile artificial sea water (ASW) and incubated during 1 hour before making the different enrichments. ASW consisted of: NaCl 408 mM, $Na_2SO_4$ 28 mM, KCl 9.3 mM, $NaHCO_3$ 24 mM, KBr 839 µM, $H_3Bo_3$ 36 µM, $MgCl_2*6H_2O$ 53 mM, $CaCl_2*2H_2O$ 10 mM. 10% of each of the 5 suspensions was inoculated into 37 mL of non-selective and selective enrichment media. The bacteria used for this study were cultivated and maintained in glass flasks kept in stagnant conditions (Fig. II.4). Positive grows of the selective and non-selective enrichment media were taken to the microbiology laboratory of the University of Portsmouth in the UK in order to perform DGGE analysis.

Fig. II.4. Glass vials for bacteria cultures

#### *II.3.3.1. Non-selective enrichment media*

Two non-selective enrichment media were used to grow heterotrophic bacteria in aerobic and anaerobic conditions by duplicate:
BD™ Tryptic Soy Broth TSB (g/L): Tryptone (pancreatic digest of casein) 17.0, soytone (peptic digest of soybean meal) 3.0, glucose 2.5, sodium chloride 5.0, dipotassium hydrogen phosphate 2.5 g (the medium was supplemented with 20 g/L of NaCl).

Difco™ marine broth 2216 (g/L): peptone 5.0, Yeast extract 1.0, ferric citrate 0.1, sodium chloride 19.45, magnesium chloride 5.9, magnesium sulphate 3.24, calcium chloride 1.8, potassium chloride 0.55, sodium bicarbonate 0.16, potassium bromide 0.08, strontium chloride 0.034, boric acid 0.022, sodium silicate 0.004sodium fluoride 0.0024, ammonium nitrate 0.0016, disodium phosphate 0.008.

Both media were boiled for 1 minute and then sterilised by autoclaving at 121°C for 15 minutes. The culture was performed in glass anaerobic vials with 50 mL of medium. The aerobic cultures were loosely closed whereas the anaerobic cultures were sealed with butyl rubber septums and de-aerated by injecting $N_2$ during at least 30 min before the injection of bacteria (10% of bacterial initial suspension). The vials were incubated at 30-35 °C during 5 days. Positive cultures were selected after turbidity was observed.

### *II.3.3.2. Selective enrichment media*

Six groups of bacteria were targeted according to 6 different metabolic pathways of microorganisms that could enhance the corrosion of carbon steel: acid producing bacteria, sulphate reducing bacteria, iron reducing bacteria, iron oxidizing bacteria, manganese oxidizing bacteria and methane producing bacteria. The bacterial groups targeted are justified in chapter IV.
10% of the initial bacterial suspension was used to inoculate the different media to then incubate in stagnant conditions at 30-35 °C for 5 to 20 days depending on the medium. The different media and positive growth criteria were as follows:

<u>Acid producing bacteria medium (APB):</u>

Sulfur amended Mackintosh medium by Mackintosh, (1978) (per L): $(NH_4)_2SO_4$ 2.6 mg, KH2PO4 0.5 mg, $MgCl_2$*6 $H_2O$ 0.5 mg, $CaCl_2$*2 $H_2O$ 2.9 mg, $MnCl_2$*4 $H_2O$ 2.4 µg, $ZnCl_2$ 1.4 µg, $CoCl_2$ 2.4 µg, $H_3BO_3$ 0.62 µg, $Na_2MoO_4$*2 $H_2O$ 0.24 µg, $CuCl_2$*2 $H_2O$ 1.7 µg, S° 5 g, Fe III (the tip of spatula), 0.01 mL $H_2SO_4$ concentrated. The medium was supplemented with 10 g/L of NaCl. Autoclave at 112 °C for 30 minutes. The incubation is performed in aerobic conditions. The assessment of bacterial growth is performed by measuring the pH. It is considered a positive growth once the pH gets reduced from 7 to 3.

<u>Sulphate reducing bacteria medium (SRB):</u>

API broth (g/L): yeast extract 1.0, ascorbic acid 0.1, $MgSO_4$*7$H_2O$ 0.2, $K_2HPO_4$ 0.01, NaCl 10, Fe $(NH_4)_2(SO_4)_2$*6$H_2$0 0.1 plus 4 mL sodium lactate. The incubation is performed in anaerobic conditions. Sulphate reduction is evident once the medium colour changes from clear to black which is an effect of SRB growth which reduced the sulphate and consequently there is FeS formation.

Iron reducing bacteria media (IRB):

FWA-Fe (III) medium by Lovley, (2006). Medium prepared with 1 litter of ASW (g/L): $NaHCO_3$ 2.5, KCl 0.1, $NH_4Cl$ 1.5, $NaH_2PO_4*H_20$ 0.6, 10 mM acetate, 20 mM iron citrate, 10 mL ATCC vitamins, 10 mL ATCC minerals. Incubation is performed in anaerobic conditions. Iron reduction is evident once the medium colour changes from yellow to green/black which is an effect of iron reduction induced by IRB.

Iron oxidizing bacteria medium (IOB):

9K medium for acidic oxidizing autotrophic bacteria [Rajasekar *et al.*, 2010] (g/L): Solution A: $(NH_4)_2SO_4$ 3.0, KCl 0.1, $MgSO_4*7H_20$ 0.5, $K_2HPO_4$ 0.5, $Ca(NO_3)_2$ 0.01, 700 mL H20. Solution B: $FeSO_4*7H_2O$ 3.0, 10 mL $H_2SO_4$ (1N), 290 mL $H_20$. (Solution A is autoclaved and solution B is filtrated, then they are mixed). Incubation is performed in aerobic conditions. Iron oxidation is evident when the medium colour changes from blue to brown which is an effect of iron oxidation induced by IOB.

Iron oxidizers nitrate reducers media (IOB/NRB) by Straubk *et al.*, (1998) supplemented with 20g/L of NaCl. Solution A (g/L): $NH_4Cl$ 0.3, $MgSO_4*7H_2O$ 0.05, $MgCl_2*6H_2O$ 0.4, $KH_2PO_4$ 0.6, $CaCl_2*H_2O$. Solution B (30 mL): 84 g/L $NaHCO_3$. Solution C: 10 mL vitamins (ATCC), 10 mL minerals (ATCC), 10 mL FeSO4 from anoxic stock 1M), 10 mL $NaNO_3$ from anoxic stock 0.4 M. Solutions A and B are autoclaved and cool under $N_2/CO_2$ atmosphere. pH is adjusted to 7 before adding solution C. Incubation is therefore performed in anaerobic conditions. Iron oxidation coupled to nitrate reduction is evident after observing a colour change on the medium from blue/green to dark yellow-green/black which is an effect of the presence of IOB/NRB.

Manganese oxidizing bacteria medium (MOB):

K medium by Krumbein and Altman, 1973 in [Nealson, 2006]. This is a rich medium that supports the growth of a variety of heterotrophic manganese oxidizers. Medium prepared in 1 litter of ASW (g/L): $FeSO_4*7H_2O$ 0.001, $MnSO_4*4H_2O$ 0.2, peptone 2.0, yeast extract 0.5, 10 mL hepes buffer added from 1M stock, pH 7.5. Incubation is performed in aerobic conditions. Manganese oxidation is evident when observing brown or dark precipitates in the medium.

Methane producing bacteria medium (MPB):

This is a enrichment medium for methanogens isolated from a marine environment modified from Romesser *et al.*, (1979) in [Whitman, 2006]: 500 mL solution A, 5 mL solution B, 10 mL phosphate solution (14 g/L $K_2HPO_4*3H_2O$), 10 mL trace elements solution, 10 mL sodium acetate solution (136 g/L acetate$*3H_2O$), 2 mL resazurin solution (0.5 g resazurin/L), 75 mL NaCl solution (293 g/L), 2 g yeast extract, 5 g $NaHCO_3$, 0.5 g cysteine hydrochloride, 20 mL solution C. Solution A (g/L): 0.28 $CaCl_2*2H_2O$, 0.67 KCl, 1.0 $NH_4Cl$, 5.5 $MgCl_2*6H_2O$, 6.9 $MgSO_4*7H_2O$. Solution B (iron stock solution): 0.2 $Fe(NH_4)_2(SO_4)_2*6H_2O$, 0.1 mL HCl concentrated, 100 mL distilled water. Solution C (sulphide solution): Prepared in anoxic water under $N_2$ gas. A 10 mM solution of NaOH, 110 mL, is boiled under $N_2$ gas until the volume is reduced to 100 mL. The solution is allowed to cool down under $N_2$ gas in

the fume hood. In parallel, a large crystal of $Na_2S*9H_2O$ (about 3 g) is washed in 50 mL of water for a few seconds and then it is dry on a paper towel and weight. About 2.5 g should remain and immediately added to the anaerobic solution of NaOH. After nearly 4 weeks of incubation, the media that showed turbidity were tested with a μ-gas chromatographer (μ-CPG) in order to detect the presence of methane in the anaerobic vial.

#### *II.3.3.3. Reactor media*

For the second approach, electrochemical experiments were performed in the reactors previously described. A comparison of the electrochemical signal using a microbial source from the field was performed between ASW and Mixed water from the field. Both media were supplemented with 10 mM of sodium acetate, 25 mM of sodium fumarate and 2 g/L of sodium bicarbonate. Anaerobic conditions were gained after injecting $N_2/CO_2$ (80:20) into the reactors for a minimum of 45 minutes.

Mixed Water from the field consisted on the water used to feed the water injection system and given by the industrial partner. This water is a mixture of 50% aquifer water plus 50% produced water recycled from the production pipelines. This water is re-injected into the oil-bearing formations to maintain pressure and facilitate oil recovery. Corrosion inhibitor KI-3804, imidazoline type, is added regularly in the production lines. Thus, 4 ppm of corrosion inhibitor is expected to be in the water injection pipelines according to the information provided by the partner company. The mixture of these waters will be called MIXED throughout this paper.

## II.4. Methods

### II.4.1. Electrochemical and corrosion experimental techniques

Following, there is a description of the experimental conditions and the different electrochemical and corrosion techniques used for both approaches undertook during this project. Before the experimental description a brief explanation of each technique has been provided. The electrochemical experiments were performed using a multipotentiostat (VMP1, VMP2 or VSP models of Bio-logic S.A., France)

#### *II.4.1.1. Corrosion potential measurement*

One of the simplest electrochemical techniques to monitor a material immersed in a medium is to measure the potential difference between the material itself and a reference electrode (*i.e.* saturated calomel electrode (SCE), standard hydrogen electrode (SHE), etc.). The magnitude and sign of the corrosion potential depend on the composition of the material, temperature and the hydrodynamic electrolyte [Iverson *et al.*, 1985; Monfort, 2001] among other factors.

Corrosion potential or open circuit potential (OCP) measurements can be obtained experimentally by using a potentiometric circuit or a high impedance voltmeter. The application of this technique is simple. It can be applied outside laboratory conditions, and it allows the differentiation between a passivation phenomenon

and a localized corrosion process, which occur under the presence of some types of biofilms.

The OCP or corrosion potential increase towards more positive values in a system may indicate that there is higher corrosion risk with an incremented probability for pitting and crevice corrosion [Little *et al.*, 2008; Javaherdashti, 2008; Mansfeld, 2007]. One of the disadvantages of OCP measurements is the possible over-interpretation of results. The technique does not provide mechanistic information and it is recommended to be used along with other electrochemical techniques to determine the cathodic and anodic influences of the electrochemical processes (since with OCP the separate contributions are monitored together) or with a pre-established corrosion mechanism [Monfort, 2001].

The OCP in function of time was measured for all the experiments once the $N_2/CO_2$ injection had been performed for at least 45 minutes.

#### *II.4.1.2. Polarisation techniques*

*Polarisation resistance ($R_p$), Linear Polarisation ($L_p$) and Cyclic voltammetry (CV)*
Most electrochemical methods consist of calculating the corrosion rate using what is called the polarization resistance. The polarization resistance ($R_p$) is usually the ratio of an applied small potential perturbation and the resulting current response, and it is expressed in Ohm·cm$^2$. The $R_p$ measurement is a direct measurement of the material resistance to the corrosion [Dominguez, 2007; Mehanna, 2009; Wallinder *et al.*, 2000; Elsener, 2005] and is a technique that gives an instantaneous measure of corrosion rate.

Moreover, $R_p$ is the inverse to the slope of the polarization curve in the vicinity of the corrosion potential. At any point of the polarization curve, the total current is the sum of the currents anodic ($i_\alpha$) and cathodic ($i_c$) partial responses. The complete equation following the Butler-Volmer model in the absence of mass transfer is:

$$i_s = i_a + i_c = i_{corr}\left\{\exp\left[\frac{\alpha_a F}{RT}(E - E_{corr})\right] - \exp\left[\frac{-\alpha_c F}{RT}(E - E_{corr})\right]\right\} \qquad \text{(II.2)}$$

With $\alpha_a$ and $\alpha_c$, the anodic and cathodic transfer coefficients, respectively; $i_{corr}$ corresponds to the current density of corrosion, and $E_{corr}$ to the corrosion potential. Getting away from the $E_{corr}$ region in the graphic data in order to have only one contribution anodic or cathodic of the total current, it is possible to simplify equation (II.2):

Anodic side: $i_s = i_{corr} \exp [ (E-E_{corr}) / \beta_\alpha]$ (II.3)

Cathodic side: $i_s = - i_{corr} \exp [- (E-E_{corr}) / \beta_c]$ (II.4)

$$\beta_a = \frac{\alpha_a F}{RT} \text{ et } \beta_c = \frac{\alpha_c F}{RT} \quad \text{(II.5)}$$

$\beta_a$ and $\beta_c$ are called Tafel constants and defined as the inverse of the slopes of the partial curves anodic and cathodic on a Tafel's representation of the polarization curve (log i = f (E)) in regions somewhat distant from $E_{corr}$ (Fig. II.5).

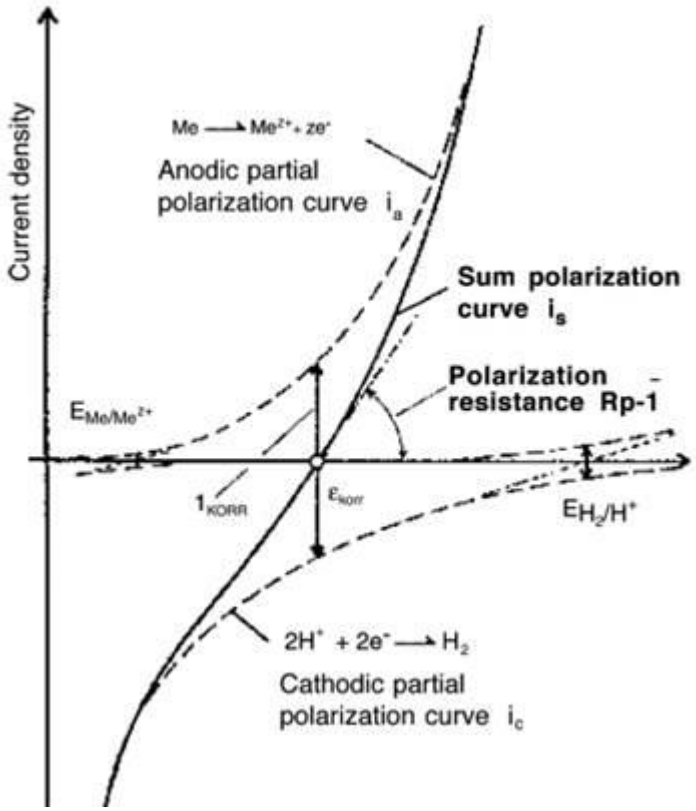


Fig. II.5 Polarization curves I = f (E) and partial overall a metal electrode [Elsener, 2005].

Adjacent to $E_{corr}$, the total current $i_s$ can be linearized and substituted in equation (II.2), the exponential function exp x (x→0) by 1+x, the Stern-Geary formula becomes:

$$i_s = i_a + i_c = i_{corr}\left[\left[1 + \frac{\alpha_a F}{RT}(E - Ecorr)\right] - \left[1 + \frac{-\alpha_c F}{RT}(E - Ecorr)\right]\right] \quad \text{(II.6)}$$

$$i_s = i_{corr}\,(E - E_{corr})\,(1/\beta_a + 1/\beta_c) \quad \text{(II.7)}$$

Equation (II.6) is that of a straight line of a slope and the relation is known as the Stearn- Geary relation:

$$i_{corr} = \frac{B}{R_p} \quad \text{(II.8)}$$

With B equal to,

$$B = \frac{\beta_a \beta_c}{2.303(\beta_a + \beta_c)} \quad \text{(II.9)}$$

Where $i_{corr}$ is the corrosion current in μA/cm$^2$, $R_p$ the polarization resistance in ohm.cm$^2$, $\beta_\alpha$ and $\beta_c$ are the anodic and cathodic slopes of the corresponding Tafel curves in mV/decade, and B is a proportionality factor dependant of the metal and the corrosive media.

On the other hand, the linear polarization (LP) technique is used in corrosion monitoring. This technique is especially designed for the determination of an $R_p$ of a material and $I_{corr}$ through potential steps around the corrosion potential. The LP application of the potentiostat software can be used for $R_p$ and $I_{corr}$ determination using the $R_p$ fit. In some cases, it can also be used to determine the corrosion rate with the tafel fit. Thus, tafel law can be used once getting away from the $E_{corr}$ region and Stern-Geary by contrary, can be used once around $E_{corr}$.

By contrast, in a cyclic voltammetry experiment the working electrode potential is ramped linearly versus time like linear sweep voltammetry. Cyclic voltammetry takes the experiment a step further than linear sweep voltammetry which ends when it reaches a set potential. When cyclic voltammetry reaches a set potential, the working electrode's potential ramp is inverted. This inversion can happen multiple times during a single experiment. The current at the working electrode is plotted versus the applied voltage to give the cyclic voltammogram trace. Cyclic voltammetry is generally used to study the electrochemical properties of an analyte in solution [Bard and Faulkner, 2001].

Some experiment along this project for both approaches consisted in applying the polarisation technique by applying ± 10 mV from ocp (for LP experiments), -400 to +300 mV vs. OCP (for CV experiments) and -100 to +1200 mV around OCP (for polarisation curves). Sweep rates used varied between 0.2 mV/s (for CV's and LP's) and 10 mV/s (for polarisation plots). Corrosion rates from polarisation techniques have been calculated using the tafel fit option available in the EC-lab software.

### *II.4.1.3. Chronoamperometry measurements*

This is a control potential technique which basis is the measurement of the current response to an applied potential step. Chronoamperometry involves stepping the potential of the working electrode from an initial potential; at which (generally) no faradic reaction occurs, to a potential Ei at which no reaction occurs (at the beginning of the experiment). The current-time response reflects the change in the concentration gradient in the vicinity of the surface. Chronoamperometry is often used for measuring the diffusion coefficient of electroactive species or the surface area of the working electrode [E-C Lab, 2007].

This technique was only used during electrochemical experiments for the first approach aiming to test the electroactivity of the strain used by applying either cathodic or anodic potential. For this, the following criteria (table II.2) were applied aiming to find whether the bacteria were able to catalyse the exchange of electrons between the WE and the acetate:

| Material (WE) | Operation | Potential applied |
|---|---|---|
| SS 254SMO | Reduction | [-0.6V ; -0.3V] |
| Graphite | Oxidation | [-0.2V ; 0.2V] |

Table II.2. Conditions and materials used for testing the electroactivity of *Geobacter sulfurreducens* previous to perform electrochemical/corrosion studies

These experiments were performed previous to the experiments (preliminary results) aiming to study the influence *G. sulfurreducens* on corrosion of carbon steel.

*II.4.1.4. Electrochemical Impedance Spectroscopy (EIS)*

Another way to approach electrochemical systems is applying perturbations to an electrochemical cell by means of an alternate electrical signal of low amplitude, which allows observing the behaviour of the system in a pseudo-steady state. The technique in which the frequency response of an electrochemical system to an alternate signal is analysed in a transfer function, between an input signal (e.g. voltage) and an output one (e.g. current), is known as electrochemical impedance spectroscopy (EIS) [Bard and Faulkner, 2001]. EIS is now a powerful tool for examining many chemical and physical processes happening at the interface. EIS finds lots of applications in corrosion, battery, fuel cell development, sensors and physical electrochemistry and can provide information on reaction parameters, corrosion rates, electrode surface porosity, coating, mass transport, interfacial capacitance measurements [E-C Lab, 2007].

In the EIS technique, the impedance data are recorded as a function of the frequency of the applied signal at a steady-state working point (E,i) of a polarization curve. In corrosion studies this working point often is the corrosion potential ($E = E_{corr}$, $i = 0$). Usually a very large frequency range has to be investigated to obtain the complete impedance spectrum. In most corrosion studies this frequency range extends from 65 kHz, which is the upper limit of a commonly used frequency response analyser (FRA), to 10 mHz [Mansfeld and Little, 1991]. A potentiostat is used to apply the potential at which the data are to be collected.

The measurement of the transfer function (input potential/output current) at different frequencies constitutes an impedance spectrum, which experimentally is obtained applying a low polarization to the electrochemical cell (usually 10 mV) without moving away from pseudo-steady state (Fig. II.6). This is made with the objective of obtaining the kinetic and mechanistic responses, transport phenomena and electrochemical phenomena distribution that occur in an electrical interface [Macdonald, 1997; Macdonald, 1991].

The objective of an impedance measurement is to obtain information on the electrochemical system studied. An impedance diagram can then be analysed quantitatively as a whole or only partially. The main objective of this method is not to fit an equivalent circuit even if this could equally provide a mean to obtain information [Orazem and Tribollet, 2008].

The frequency range that the technique uses, allows identifying the different elements comprising physic and electrochemical phenomena occurring at the interface. For example, at high frequencies (e.g. 10 kHz) the resistance of the electrolyte can be measured, while at low frequencies (e.g. 0.001 Hz) diffusional effects, adsorption phenomena and interfacial desorption can be identified [Dominguez, 2007; Gabrielli, 1998].

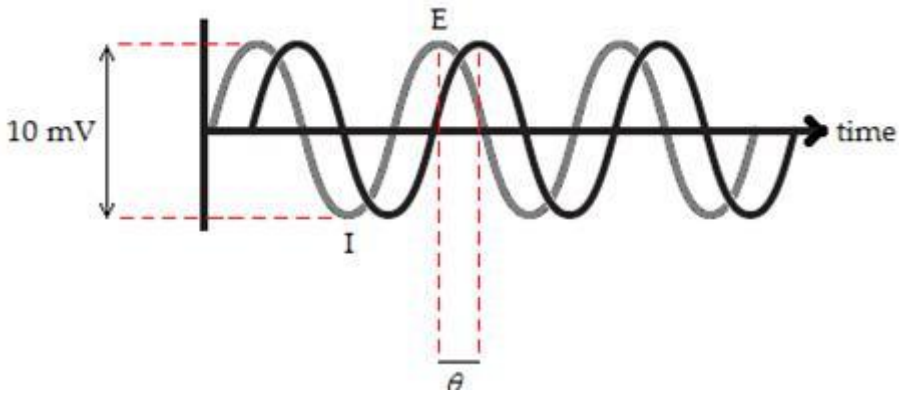


Fig. II.6. Sinusoidal AC potential of small-amplitude (10 mV) with its resulting current sinusoidal signal, phase shifted by an amount of θ radians.

In order to correctly analyse the impedance measurements, it is necessary to report the results using different types of coordinates in the graphical representations. There is not a good representation; the good representation is the one that for a given electrochemical system brings up information [Orazem and Tribollet, 2008]. Among the graphic representations, the Nyquist diagram is the most chosen in publications. In this kind of graph, the results are represented as an ensemble of points where each one of them corresponds to a frequency measurement (Fig. II.7).

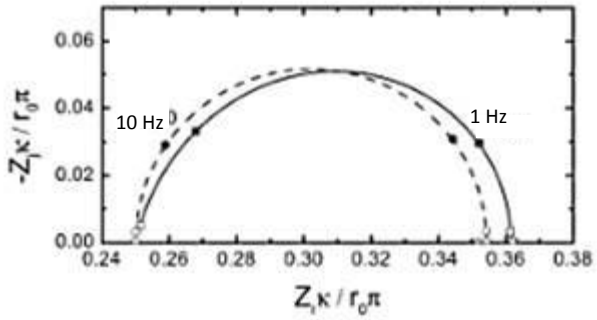


Fig. II.7 Nyquist diagram representation of the global impedance response from a disk electrode considering the influence of the electrode geometry (solid lines) and in the absence of geometry effect (dashed lines) [Orazem *et al.*, 2008]

A disadvantage for this kind of representation is that the frequency dependence is not always very clear. The high frequency (HF) limit corresponds to the resistance at high frequency which often corresponds to the electrolyte resistance, the low frequency limit (LF), if it can be obtained, it corresponds to the $R_p$ [Orazem and Tribollet, 2008].

In contrast, the Bode representation makes evident the dependence in function of the frequency. This representation comprises two diagrams: One is the impedance module in function of the frequency and the other is the phase in function of the frequency. The impedance amplitude tends towards the electrolyte resistance ($R_s$) whereas the frequency tends towards the infinity. This representation might help to limit the useful frequency domain. For electrochemical systems exhibiting an ohmic or electrolyte resistance, however, the Bode representation has serious drawbacks. The influence of electrolyte resistance confounds the use of phase angle plots to estimate characteristic frequencies. For this, Orazem *et al.*, have proposed logarithmic plots of the imaginary component of the impedance and effective capacitance plots which are useful for all the impedance data [Orazem *et al.,* 2006].

These graphical representations may help to spot phenomena occurring in the interface such as, for example, charge transfer. Charge transfer in an electrochemical interface occurs as a consequence of a succession of events that include: a) the transport of reactive species in the bulk electrolyte (frequently associated to homogeneous phase reactions), b) adsorption of reactive species in the electrode, and c) chemical reactions and interfacial reactions. Adsorption, as well as electrochemical reactions (even some chemical reactions), occurs over the surface of metallic materials, while transport phenomena occur in homogeneous phase [Macdonald, 1991].

Moreover, the impedance of electrochemical systems often reflects a time constants distribution which is normally represented using the equivalent circuits by constant phase element (CPE). The CPE behaviour is generally attributed to distributed surface reactivity, surface inhomogeneity, roughness or fractal geometry, electrode porosity, and to current and potential distributions associated with electrode geometry [Jorcin *et al.,* 2006]. The impedance of a CPE is given by:

$$Z_{CPE}(\omega) = \frac{1}{Q(j\omega)^{\alpha}} \qquad \text{(II.10)}$$

with $\omega=2\pi f$.

The CPE parameters α and *Q* can be graphically obtained. The parameter α is calculated from the slope of the log|Z*j*| *vs.* log *f* curve in the HF range (plateau value). The Nyquist representation of the CPE impedance described in (II.10) corresponds to a straight line passing by the origin and forming a 90 degrees angle with the axis. The module graph of the Bode is represented by a straight line which slope is equal to – α; its phase is constant and equal to -90α degrees. Otherwise, it can be obtained by the following equation (slope value):

$$\alpha = \left| \frac{d \log \left| Z_j(f) \right|}{d \log f} \right| \qquad \text{at HF} \qquad \text{(II.11)}$$

When α=1, *Q* have capacitance dimensions, *i.e.* $Fcm^{-2}$ and represents the capacity of the double layer; when 0< α<1, *Q* is expressed as $s^{\alpha}\Omega^{-1}cm^{-2}$ or even in $Fs^{(\alpha-1)}cm^{-2}$ and α has no dimensions. In the latter case, the system shows behaviour that has been attributed to surface heterogeneity or to continuously distributed time constants for charge-transfer reactions. A CPE impedance is equally described by:

$$Z_{CPE} = \frac{1}{Q(j\omega)^{\alpha}} \times \left[\cos\left(\frac{\alpha\pi}{2}\right) - j\sin\left(\frac{\alpha\pi}{2}\right)\right] \qquad \text{(II.12)}$$

This is the reason why if we plot the absolute value of the imaginary part of the impedance $|Z_j|$ in function of the frequency that we will obtain a straight line which slope will be equal to -α. This is the representation suggested by [Orazem *et al.*, 2006].

Once the α value has been calculated, the *Q* coefficient can be directly obtained from the imaginary part of the impedance by:

$$Q = -\frac{1}{Z_j(f)(2\pi f)^{\alpha}} \times \sin\left(\frac{\alpha\pi}{2}\right) \qquad \text{(II.13)}$$

*Q* corresponds to the average values forming the plateau. The coefficient *Q* is used to find capacitance values of systems that follow a CPE behaviour regardless of the type of time constants distribution found in the system that can be either surface or normal distribution. In the case of surface distribution, the 2D type of distribution can be due to heterogeneity of the surface (grain boundaries, crystal faces, among others) or to the non-uniform distribution of current and potential induced by the geometry of the electrode. In the case of the normal distribution, the 3D type of distribution can be generated by a roughness of the surface, fractal geometry, porosity or a conductivity variation in the oxide layer or in the organic coats.

Moreover, in the surface distribution of time constants, the global admittance of the electrode is the sum of individual admittances of each part of the electrode surface (Fig. II.8). For an appropriate time constant distribution, the impedance response can be expressed in CPE terms. In the absence of ohmic resistance, the surface distribution of time constants results in a behaviour R//C in which:

$$\frac{1}{R_{eff}} = \sum \frac{1}{R_i} \quad \text{and} \quad C_{eff} = \sum C_i \qquad \text{(II.14)}$$

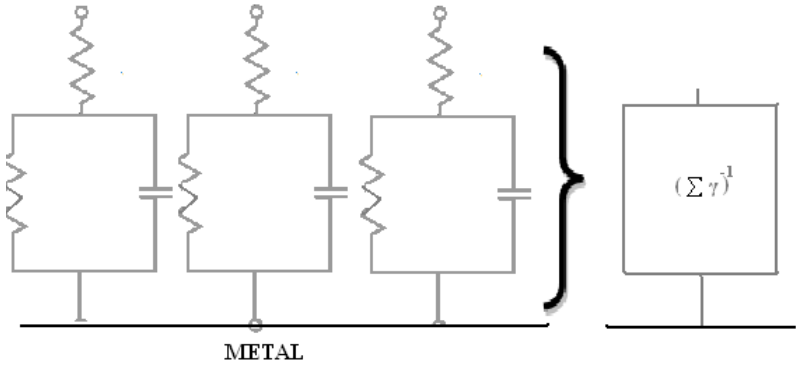


Fig. II.8 Representation of a surface distribution of time constants

Thus, the apparition of a CPE behaviour associated with a surface distribution of time constants needs the contribution of an ohmic resistance. One way to calculate the capacitance associated to a surface distribution of a CPE behaviour is express by the equation derived by Brug *et al.*, (1984) [Orazem and Tribollet, 2008; Orazem *et al.*, 2006; Brug *et al.*, 1984]:

$$C_{eff} = Q^{1/\alpha}\left(R_e^{-1} + R_t^{a\,-1}\right)^{(\alpha-1)/\alpha} \qquad \text{(II.15)}$$

with $R_e$ as the electrolyte resistance and $R_t$ as the transfer resistance.

In contrast, a normal distribution of time constants of a surface layer can be described by a serial of R//C elements (Fig. II.9). The global impedance of the electrode is the sum of the individual impedances of each part of the layer.

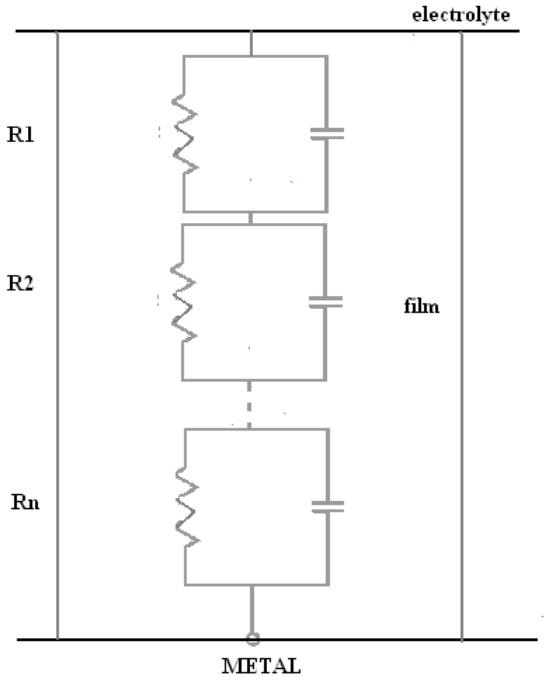


Fig. II.9. Representation of a normal distribution of time constants

For an appropriate distribution of time constants, the impedance response can be expressed in terms of CPE. In this case, the presence of a CPE behaviour does not need the contribution of an ohmic resistance. The presence of a CPE expressed with a serial R//C elements need, however, the contributions of resistive and capacitive elements. For this, two models are found in the literature that can help to elucidate the parameters of a normal distribution of time constants in the case of oxide layers covering metal surfaces: Young [Young, 1955; Young, 1961; Frateur *et al.*, 2012; Hansen *et al.*, 2010] and Power low model [Hirschom *et al.*, 2010; Frateur *et al.*, 2012].

**Young Model:**

This model assumes that the resistivity ρ(x) in the thickness of the film decreases exponentially due to a non-stoichiometry of the oxide layer according to:

$$\rho(x) = \rho_0 \exp(-x/\lambda) \tag{II.16}$$

where $\rho_0$ corresponds to the resistivity of the oxide at the oxide/solution interface (boundary value of resistivity), $x$ is the normal distance to the surface of the electrode and $\lambda$ is the characteristic length.
Assuming that the dielectric constant ε is uniform, the impedance of a film for a distribution of arbitrary resistivity can be written as follows:

$$Z_f(\omega) = \int_0^{\delta} \frac{\rho(x)}{1 + j\omega\varepsilon\varepsilon_0\rho(x)}\, dx \tag{II.17}$$

Where δ is the film thickness and $\varepsilon_0$the permittivity of vacuum.

An analytic expression for impedance resulting from the equation (II.17) can be found for an exponential distribution of resistivity to be:

$$Z_Y(\omega) = -\frac{\lambda}{j\omega\varepsilon\varepsilon_0} \ln\left[\frac{1 + j\omega\varepsilon\varepsilon_0\rho_0 e^{-\delta/\lambda}}{1 + j\omega\varepsilon\varepsilon_0\rho_0}\right] \tag{II.18}$$

Equation (II.18) as calculated by Göhr *et al.*,[Hirschom *et al.*, 2010; Hansen *et al.*, 2010] is known as the young impedance and is widely use to model impedance data arising from a film.

**Power-Law model:**

Another model applied to systems with normal distribution of time constants within a film is the power-law model [Hirschorn *et al.*, 2010, Frateur, *et al.*, 2012]:

$$\frac{\rho}{\rho_\delta} = \left(\frac{\rho_\delta}{\rho_0} + \left(1 - \frac{\rho_\delta}{\rho_0}\right)\xi^\gamma\right)^{-1} \tag{II.19}$$

where the parameters $\rho_0$ and $\rho\delta$ are the boundary values of resistivity at the interfaces, to show that, for $\omega<(\rho_\delta \varepsilon\varepsilon_0)^{-1}$, an analytic expression for the impedance could be obtained as:

$$Z_f(\omega) = g\frac{\delta\rho_\delta^{1/\gamma}}{(\rho_0^{-1} + j\omega\varepsilon\varepsilon_0)^{(\gamma-1)/\gamma}} \quad \text{(II.20)}$$

where

$$\alpha = \frac{\gamma - 1}{\gamma} \quad \text{(II.21)}$$

The function *g* was evaluated numerically and could be expressed as:

$$g = 1 + 2{,}88\gamma^{-2{,}375} \quad \text{(II.22)}$$

Equation (II.20) assumes that the dielectric constant is independent of position; a normal power-law distribution of local resistivity can be consistent with the CPE. For $(\rho_0\varepsilon\varepsilon_0)^{-1} < \omega < (\rho_\delta\varepsilon\varepsilon_0)^{-1}$, equation (II.20) takes the form of equation (II.10) with:

$$Q = \frac{(\varepsilon\varepsilon_0)^\alpha}{g\delta\rho_\delta^{1-\alpha}} \quad \text{(II.23)}$$

Equation (II.23) connects the CPE parameters to the physical properties of the film. Moreover, the equivalent capacitance of a film is linked to its thickness δ according to:

$$C_{eff} = \frac{\varepsilon\varepsilon_0}{\delta} \quad \text{(II.24)}$$

This last equation serves to calculate the effective capacitance using either Young model or power-law model.

ElS measurements were applied to experiments for the two approaches undertook during this project. EIS was used to obtain information on the interface, using a frequency from 100 kHz to 10 mHz or from 200 kHz to 20 mHz (depending on the experiment) and amplitude of 10 mV. Measurements were performed every 12 hours recording 7 points per decade.

#### *II.4.1.5. Weight loss*

Corrosion can be directly quantified experimentally by means of weight loss measurements that provide the rate at which the thickness of a material is lost. This technique is used to quantify the mass loss for cases of uniform corrosion. However, electrochemical measurements are sometimes preferred because they allow real-time monitoring and immediate calculations of the corrosion rates.

The technique consists in immersing steel sheets or coins into the medium studied for several months and determinate the mass loss by using the following formula:

$$\text{Corrosion rate (mmpy)}: \frac{0.465\ X}{tA} \qquad \text{(II.25)}$$

where,

0.465 is a factor accounting for the dimensional analysis and the density of the steel.

X is the difference between "initial weight" and "weight after cleaning" in milligrams

t is exposure time in days

A is total area of the coupon in $cm^2$.

Weight loss tests were performed for the both approaches undertook during this project. Weight loss tests were performed following the American Society for Testing and Materials (ASTM) standards D26811 during 3 weeks and 3 months for experiments with *Geobacter* and during 3 months for experiments from the second approach. Rectangular sheets with dimensions of 20 mm x 10 mm x 1 mm were used.

For experiments of the first approach, the metallic sheets were immersed in the *G. sulfurreducens* reactor media testing different concentrations of electron donor and acceptor, phosphate and ammonium chloride. For the experiments of the second approach, the sheets were immersed in ASW and MIXED water from the field both supplemented with 10 mM sodium acetate, 25 mM sodium fumarate and 2g/L of sodium bicarbonate as added buffer. Different types of bacteria inoculum were tested (pigging debris 1 and 5, pre-grown consortium, IOB and IRB enriched bacteria). Control abiotic systems were performed for each of the conditions tested. Control systems consisted on injecting a filtrate of the grown bacteria culture medium (5%) in the reactor for the cases of: *Geobacter sulfurreducens,* IOB/NRB and IRB. For the cases of systems with pigging debris, it consisted on the autoclaved debris (about 10 g). For the case of the consortium, they were compared to a blank system which is a system that does not have either bacteria or bacteria metabolites (it consists on the electrolyte plus the steel only). This is because we didn't want to add a source of sulphide found in the consortium cultures.

Fishing thread was used to suspend the coupons into the water mediums served in 150 mL glass anaerobic vials hermetically closed with butyl rubber septums. All the different media were flashed with $N_2/CO_2$ during 1 hour previous to the inoculation and 30 minutes after inoculation.

At the end of the experiment, coupons were cleaned introducing the coupon in a solution of 50% (vol) HCl concentrated and 2.5 g/L of EDTA ($C_{10}H_{16}N_2O_8$) during 30 seconds. This procedure was performed aiming to take off the corrosion products accumulated on the surface of the coupon. Weight loss was calculated after the cleaning procedure using equation (II.25).

## II.4.2. Microscopy and surface analysis techniques

### *II.4.2.1. Scanning Electron Microscopy (SEM)*

The principle of the SEM is based on electron-matter interactions. An electron beam scans the surface of the sample which in response retransmits certain particles. Different detectors allow analysing these particles in order to rebuild images of the surface. The resolution can reach 0.1 µm. The conducting steel sample is attached either by a conducting tape or by metal screws allowing to evacuate electrons bombarding the surface so that the electrons are reflected and do not disturb the quality of the image.

Scanning Electron Microscopy (SEM) pictures were taken using a TM3000 Hitachi Analytical Table Top Microscope at different magnifications working at 15 kV acceleration voltages. The coupons were washed with distilled water and dried with the gas mixture $N_2/CO_2$ 80:20 after 140 hours of immersion in the media described. Once the coupons were taken out of the electrochemical reactors, they were kept dry under $N_2$ atmosphere until the analysis was performed.

### *II.4.2.2. Energy-dispersive X-ray spectroscopy (EDX)*

Energy-dispersive X-ray spectroscopy (EDS, EDX, or XEDS) is an analytical technique used for the elemental analysis or chemical characterization of a sample. It relies on the investigation of an interaction of some source of X-ray excitation and a sample. Its characterization capabilities are due in large part to the fundamental principle that each element has a unique atomic structure allowing unique set of peaks on its X-ray spectrum. To stimulate the emission of characteristic X-rays from a specimen, a high-energy beam of charged particles such as electrons or protons, or a beam of X-rays, is focused into the sample being studied. At rest, an atom within the sample contains ground state (or unexcited) electrons in discrete energy levels or electron shells bound to the nucleus. The incident beam may excite an electron in an inner shell, ejecting it from the shell while creating an electron hole where the electron was. An electron from an outer, higher-energy shell then fills the hole, and the difference in energy between the higher-energy shell and the lower energy shell may be released in the form of an X-ray. The number and energy of the X-rays emitted from a specimen can be measured by an energy-dispersive spectrometer. As the energy of the X-rays is characteristic of the difference in energy between the two shells, and of the atomic structure of the element from which they were emitted, this allows the elemental composition of the specimen to be measured [Goldstein, 2003].
EDX was used for elemental analysis of the surface of the coupons generally after finalising the electrochemical tests. EDX was performed while obtaining SEM images with the TM3000 Hitachi Analytical table microscope.

### *II.4.2.3. X-ray photo electron spectroscopy (XPS)*

X-ray photoelectron spectroscopy (XPS) is a quantitative spectroscopic technique that allows to determine the elemental composition, empirical formula, chemical state and electronic state of the elements within a material. XPS spectra are obtained by irradiating a material with a beam of X-rays while simultaneously

measuring the kinetic energy and number of electrons that escape from the top 1 to 10 nm of the material being analysed. XPS requires ultra-high vacuum (UHV) conditions.

XPS is a surface chemical analysis technique that can be used to analyse the surface chemistry of a material in its "as received" state, or after some treatment, for example: fracturing, cutting or scraping in air or UHV exposure, ion beam etching to clean off some of the surface contamination, exposure to heat to study the changes due to heating, exposure to reactive gases or solutions, exposure to ion beam implant, exposure to ultraviolet light.

XPS analysis was performed on metal sheet coupons obtained from the weight loss tests from the second approach. The following core levels were analysed: Fe 2p, O 1s, C 1s, N 1s and S 1s. Coupons were analysed once the biofilm and corrosion products had been removed in order to observe the changes in the surface structure. A Thermo Electron Escalab 250 spectrometer with a monochromated Al K α radiation (1486.6 eV) was used. The analyser pass energy was 100 eV for survey spectra and 20 eV for high resolution spectra. The analysed area was  500 mm. The photoelectron take-off angle, between the surface and the direction in which the photoelectrons are analysed, was 90°. Curve fitting of the spectra was performed with the Thermo Electron software Avantage. For the calculation of the surface composition, the inelastic mean free paths calculated by Tanuma *et al.,* in [Tanuma *et al.,* 1994] and the photoemission cross sections determined by Scofield [Scofield, 1976] were used.

### II.4.3. Planktonic cells measurement techniques

The number of planktonic cells was determined by turbidity measurement for experiments from the first approach only. In contrast, other technique such as cell counting was used to determine the number of planktonic cells for experiments from the second approach due to many metabolites or corrosion products found on the media that impeded an absorbance measurement.

#### *II.4.3.1. Turbidity measurement by optic density (OD) technique*

The number of planktonic cells was evaluated by measuring the absorbance at 620 nm. The absorbance was correlated to cell forming units per millilitre ($CFU.mL^{-1}$) by the following calibration formula [Dumas *et al,* 2008b]

$$[CFU.mL^{-1}] = OD_{620nm} \times 472067 \qquad (II.26)$$

where OD is the optical density measured at 620 nm. Equation II.26 was established by measurements in petri dishes under $N_2/CO_2$ atmosphere. Bacteria were ready for inoculation after it reached an absorbance of 0.3 [Dumas, 2007].

#### *II.4.3.2. Direct cells counting by Thomas chamber*

Total biomass estimation was obtained for experiments from the second approach. For this, serial dilutions were performed in grown cultures obtained after each electrochemical test. Dilutions were made until it was possible to observe no more

than 100 cells in the chamber grid. Samples were observed with a light microscope using a Thomas chamber. Bacteria concentration was calculated in cells/mL using the following relation:

Concentration (cell/mL)= Number of cells/Volume (mL) (II.27)

where the volume was 0.00625 $mm^3$

### II.4.4. Total iron determination by inductively coupled plasma technique

Inductively coupled plasma optical emission spectrometry (ICP-OES), is an analytical technique used for the detection of trace metals. It is a type of emission spectroscopy that uses the inductively coupled plasma to produce excited atoms and ions that emit electromagnetic radiation at wavelengths characteristic of a particular element. The intensity of this emission is indicative of the concentration of the element within the sample [Stefansson et al., 2007].

Total iron in solution was determined by Inductively Coupled Plasma (ICP) analysis using an ICP-OES ULTIMA2, Horiba. 20 mL of the sample were used for total iron measurement. Different samples along the experiment were taken for experiments from the two approaches. For some cases when rust was observed as corrosion product it was added 50 mL of HCl (50 %) in order to dissolve the iron deposited on the reactor.

### II.4.5. DNA extraction and strains identification

Bacteria and archea identification was performed for the experiments from the second approach. Identification was performed in three types of samples: A) The pigging debris obtained from the water injection system "A" (identification performed by one of the project partners in University of Portsmouth). B) The culture reactor media obtained from the electrochemical test and C) Enriched bacteria obtained from the different enrichment cultures performed.
Identified bacteria population was compared in the three types of samples aiming to acknowledge the difference in bacteria diversity regarding the sample used and how this diversity can affect the corrosion of carbon steel.

#### *II.4.5.1. DNA extraction*

A) Pigging debris :

Total DNA was extracted from approximately 0.5 g of pigging debris with the MO BIO PowerBiofilmTM DNA isolation kit (Mo BIO Laboratories, UK) according to the manufacturer's instructions. The DNA was concentrated and quantified with PicoGreen® dsDNA quantification kit (Invitrogen, USA) performed on BMG LABTECH POLARstar OPTIMA Microplate Reader.

B) Culture reactor media:

DNA was extracted from the pellets obtained after multiple centrifugations of the grown liquid media using NucleoSpin® (Machery-Nagel) following the

manufacturer's instructions. A NanoDrop ND-1000 spectrophotometer (Thermo Scientific, USA) was used to establish the concentration of extracted and purified DNA.

C) Enrichment cultures:

The procedure was identical to the previous one described to sample type B.

### *II.4.5.2. Polymerase chain reaction amplification (PCR)*

PCR was performed on DNA extracted from all the samples in order to probe the presence of gene 16SrRNA.
The targeted gene was amplified using the primers 341F+GC: 5`-CGCC CGCCGCGCGCGGGCGGGGCGGGGGCACGGGGGGCCTACGGGAGGCAGCAG-3` and 907R: 5`-CCGTCA ATTCMTTTGAGTTT-3` [Muyzer *et al.*, 1993] (purchased from Life Technologies, UK). Reactions contained 10x GoTaq® Green Master Mix (12.5 µL, Promega); primers 341F+GC and 907R (each 1µL, 10 pmol/µL). Reactions were initially denatured at 94°C for 4 minutes, followed by a touchdown PCR: 20 cycles of 94°C for 1 minute, 63-54°C for 1 minute and 72°C for 1 minute followed by 15 cycles of 94 °C for 1 minute, 53°C for 1 minute and 72°C for 1 minute plus an additional 10 minutes cycle at 72°C. Reactions were performed in 25 µL reaction mixtures.

### *II.4.5.3. Denaturing gradient gel electrophoresis analysis (DGGE)*

Agarose gel electrophoresis was performed after PCR to determine the size of the PCR products by running beside a DNA marker (1kb Ladder, Promega). PCR products were run on 0.9% of agarose gel on 150V for 30 minutes to 1 hour to enable proper separation. Agarose gel was stained with SYBR® Safe DNA gel stain (Invitrogen Corp., USA) and viewed under UV transillumination (Alpha Innotech Corporation, USA) and Digital Camera (Olympus C-4000 Zoom) to ensure that the correct size fragment was amplified.
To separate the PCR-amplified products for bacterial 16S rRNA genes (550 bp), 40µL of PCR-amplified products was used in an Ingeny Gel Apparatus (Ingeny, Netherlands), at a constant voltage of 90 V for 18 hours and a constant temperature of 60°C, after an initial 15 minutes at 200V. The standard gradient was formed of 6% polyacrylamide in 0.5x TAE buffer with between 30% and 90% denaturant (7M urea and 40% formamide defined as 100% denaturant). After electrophoresis, the gel was stained with SYBR® Safe DNA gel stain (Invitrogen Corp.), viewed under UV transillumination, and a permanent image captured by the Alpha Innotech Gel Documentation System (Alpha Innotech Corporation, USA).
All visible bands were cut from the gel using a sterile scalpel blade and transferred into sterile 1.5 mL microcentrifuge tubes containing 30 µL of ultra-pure water to extract the DNA. Samples were then centrifuged at 13 000 x g for 1 minute (Heraeus Fresco 21, Thermo Scientific, UK) and 5 µL aliquots of supernatants were used for PCR re-amplification as described above. PCR products were purified using the NucleoSpin® Extract II PCR purification kit (Macherey-Nagel, UK) and sent to the GATC Biotech UK DNA sequencing service.

# *Chapter III- Role of Geobacter sulfurreducens in the anaerobic corrosion of carbon steel*

## III.1. Introduction

As previously mentioned in chapter I.6. (Scope of the project), experiments using an electroactive strain of G. sulfurreducens were performed in order to assess the influence of iron reducing bacteria on the corrosion of carbon steel. For this, weight loss tests, surface analysis and electrochemical experiments measuring free corrosion potential (OCP) along time, electrochemical impedance spectroscopy and linear polarisation were performed using carbon steel coupons immersed in a basic medium where the bacteria growth was favoured. All this experimental results fall into the frame of the first approach given to the project. The first approach aims to understand the influence of an iron reducing bacteria on the corrosion of carbon steel before attempting to work with a bacterial consortium extracted from a water injection system of an oil and gas company.

Understanding the influence of a pure culture of bacteria on corrosion is of vital importance in order to have a better insight of the different mechanisms that might be occurring in the normal environment, in this case in the water injection pipelines environment. Until today, it has been recognised the key involvement of SRB on the corrosion of carbon steel due to their act as catalysers on the production of the corrosive agent, sulphide. In contrast, the importance of IRB has rarely been addressed to corrosion, and even more rarely the importance of an electroactive bacterium such as *Geobacter sulfurreducens*. Thus, the first approach of this project displays different results that will provide insights on other mechanisms different to those widely explained with SRB. These results might be of help for the oil and gas industry when encountering microbially influenced corrosion problems that cannot be explained by the sole presence of SRB.

Initially, some preliminary results are given followed by the main results presented in form of two articles which one has been submitted to the scientific journal, corrosion science and the other one will be soon submitted. The first article titled ***"Geobacter sulfurreducens:* an iron reducing bacterium that can protect carbon steel against corrosion?"** consists on the influence of *Geobacter* on the corrosion or protection of carbon steel in a medium containing sodium phosphate. The second article where I figure as a second author titled **"Formation of Iron Phosphate from Carbon Steel Corrosion Products induced by *Geobacter sulfurreducens*: Thermodynamic Analysis"** consists on a thermodynamic analysis for the formation of iron (II) phosphate assisted by the presence of *Geobacter sulfurreducens*. Further results presented in this chapter as preliminary and/or complementary results highlight the different parameters of the electrochemical system such as the influence of the electrode surface finishing and the medium composition.

## III.2. Why to use *Geobacter sulfurreducens* for the corrosion studies

There are two physiologically distinct types of microbial Fe (III) reduction: assimilatory and dissimilatory. The purpose of assimilatory Fe (III) reduction is to incorporate reduced iron into proteins with important catalytic activities, while that of dissimilatory Fe (III) reduction, also named Fe (III); respiration is to generate energy to support cell growth. Dissimilatory Fe (III) reduction is the most significant Fe (III)-reducing process under anoxic conditions [White, 2000; Qian,

2009]. *Geobacter sulfurreducens* is a dissimilatory IRB that has been widely studied in the frame of microbial fuel cell due to its electroactivity. G. sulfurreducens is the most studied member of the *Geobacteraceae* family and it was isolated from the sediment of a hydrocarbon-contaminated site in Oklahoma [Caccavo, 1994].

On the other hand, electroactivity is the capacity of certain microbial genera and species to connect their metabolism to solid electrodes, directly exchanging electrons with them through different mechanisms [Mehanna et al., 2010]. One of the most widely studied of these bacteria, *G. sulfurreducens,* has been shown to be able to oxidize organic electron donors (acetate, benzoate, toluene, etc.) to carbon dioxide using graphite [Bond and Lovely, 2003], or stainless steel [Dumas et al., 2008a] anodes as electron acceptors. Thanks to these last characteristics, *G. sulfurreducens* has been used in the frame of electricity production studies but it has rarely been addressed to the studies of corrosion.

In this project, *G. sulfurreducens* is studied under the frame of anaerobic corrosion of carbon steel. The reasons of why this bacterium was chosen as a model bacterium for corrosion studies is precisely its electron exchange capabilities. Knowing that corrosion is an electrochemical phenomenon where the transport of electrons must take place for corrosion to occur, it is important to understand the involvement of a bacterium that can itself exchange electrons with solid compounds. The implication of direct electron transfer between material surfaces and microorganisms was first evoked in the framework of microbial corrosion with *Desulfobacterium*-like and *Methanobacterium*-like isolates extracted from natural biofilms [Dinh et al., 2004] and with *Geobacter sulfurreducens* [Mehanna et al., 2010]. Thus, the electron transfer between carbon steel and acetate mediated by *G. sulfurreducens* is considered of high interest in the influence of corrosion. Another of the important reasons of why this bacterium was chosen is precisely that it has been first isolated from sediments contaminated with hydrocarbon which falls perfectly into the frame of corrosion for water injection systems of oil and gas industry. Moreover, this bacterium is ubiquitous of soil and sediments thus it can have a high impact in the corrosion of buried metal equipment and pipelines.

Electrochemical experiments were performed in anaerobic conditions at 30 or 35 °C, considering that these are characteristics found in the field environment of water injection pipelines of the oil and gas company that partner up with this project. These conditions were also favourable for the growth of the bacteria studied.

## III.3. Preliminary experiments

In order to establish the best experimental conditions to find out the influence of *Geobacter sulfurreducens* on the corrosion of carbon steel, some preliminary experiments were performed modifying some parameters such as the surface roughness and the acetate concentration. Results found, helped us to determine the best electrochemical conditions that were adopted for the rest of the project.

### III.3.1. Influence of surface roughness

Preliminary tests consisted in testing different surface roughness of the WE (mirror finishing and 600 grit) in order to find the best experimental conditions where bacteria could attach on better. In the literature, mirror finishing has been used for the analysis of the immediate electroactive response between surface-bacteria; however, the presence of imperfections in the metallic surface may induce a better attachment of the colonies hence, a response due only to the bacterial activity [Arnold and Bailey, 2000]. Tests with mirror finishing and 600 grit were carried out in presence of bacteria (5% of total volume), OCP vs. time was measured in the anaerobic system ($N_2/CO_2$, 80:20 atmosphere) consisting of steel C1145 immersed in *Geobacter* standard reactor medium with 3 mM acetate and 25 mM fumarate (electron donor and acceptor, respectively). Results were compared to a mirror finished abiotic control. Once the experiment finished coupons were taken out to aerobic atmospheric conditions and microscopy was used to observe the corrosion products on the surface.

Figure III.1, shows the OCP vs. time for the different surface finishing in biotic systems and the control abiotic system. Results show that there was no change on OCP regardless the surface roughness and the presence of bacteria; however, macroscopic observations (Figure III.2) show clearly the difference of the surface finishing. In absence of bacteria, general corrosion is found, the yellow-reddish colour is proper of rust and it is covering homogeneously the surface. In presence of bacteria, there is a grey layer covering the surface and less presence of rust than in the former sample. On top of this grey layer, it can be observed a green layer covering unevenly the surface of the coupon. However, the green layer occupies a bigger surface on the 4000 grit finishing than in the 600 grit. These results are more evident in the observation to the microscope in Figures II.3, III.4, and III.5.

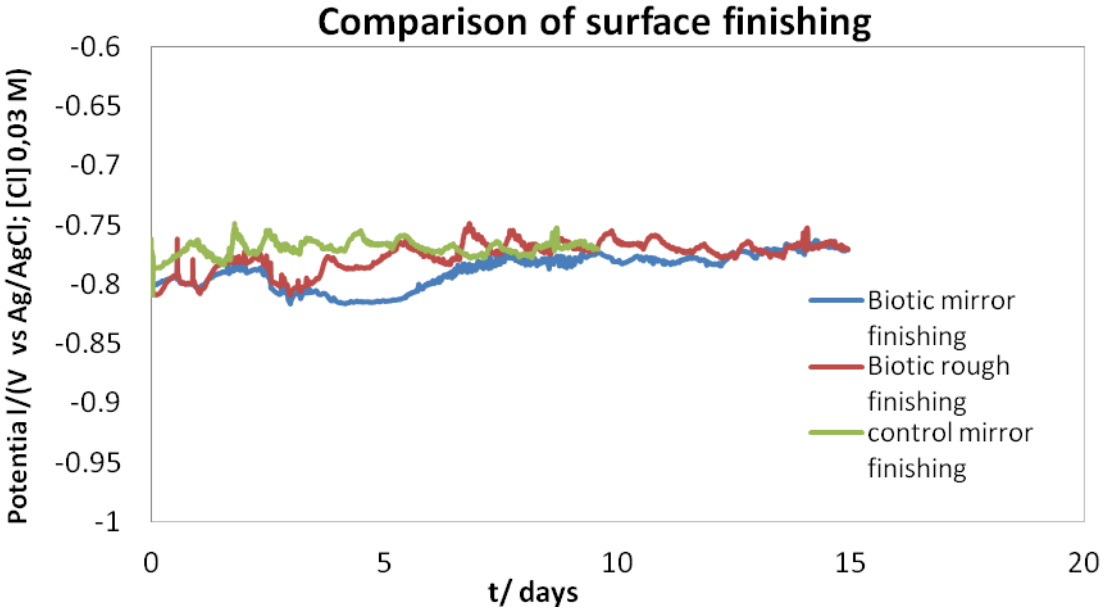


Figure III.1. OCP vs. time measurements for C1145 in presence of bacteria for different surface roughness. In the Figure, Mirror finishing corresponds to grit 4000 SiC and rough finishing to grit 600 SiC.

Figure III.2. Macroscopic observation of the inoculated and blank systems with different surface finishing. The sample on the top corresponds to the blank system with 4000 grit finishing, the bottom-left sample corresponds to the inoculated system with 600 grit finishing, and the bottom-right sample corresponds to the inoculated system with 4000 grit finishing.

Macroscopic results showed in Figures III.3 to III.5, lead to conclude that the bacteria is forming a surface layer on the metallic surface, this layer is not an iron oxide (rust) typically found in this environment. Microscopically results show than in absence of bacteria, the metal surface seems more homogenous than in presence of bacteria where some cavities or pits may be observed. These cavities or pits seem larger on the mirror finishing coupon than in the 600 grit finishing coupon. However, more tests were needed to find out the nature of the layer and the results of them can be found in article 1.

On the other hand, the surface finishing chosen for further experiments is 600-grit because even if no difference in electrochemical response was observed, it allows an influence of the bacteria on surface modification as well as the mirror finishing but simulating in a closer manner the field conditions. As the general frame of this project is biocorrosion in water injection systems of the oil and gas industry, it was chosen a surface roughness similar to that found in carbon steel pipelines, thus further results presented in this chapter are with a surface finishing of 600 grit.

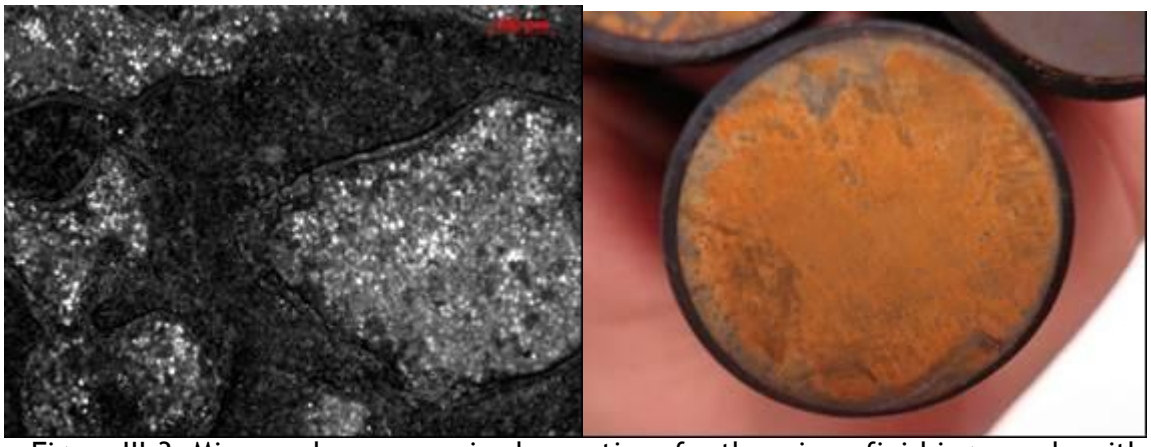

Figure III.3. Micro and macroscopic observations for the mirror finishing sample without bacteria.

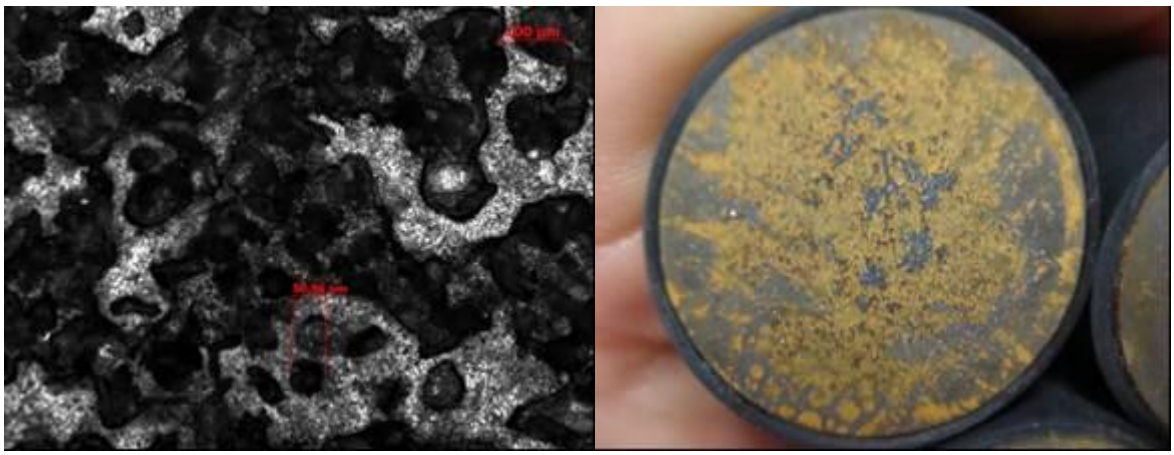

Figure III.4. Micro and macroscopic observations for the mirror finishing sample with bacteria.

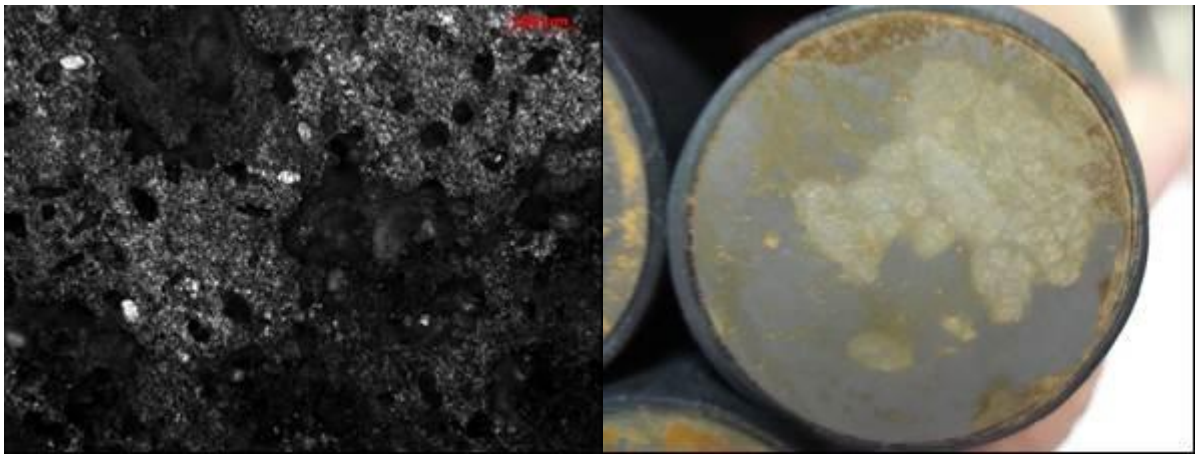

Figure III.5. Micro and macroscopic observations for the 600 grit finishing sample without bacteria.

### III.3.2. Influence of acetate concentration as electron donor

Once the surface roughness of the working electrode to be used in the electrochemical experiments was defined, it rested to be defined the acetate concentration to work with. For this, we started testing two different

concentrations of acetate (0 and 3 mM of acetate). OCP along time of carbon steel C1145 immersed in anaerobic reactor medium was measured in presence and absence of *Geobacter sulfurreducens* (Fig.III.6).

Results show that the corrosion potential remained stable along the whole experiment for each of the conditions tested, observing variation of potential of less 50 mV.

After not observing any difference on the corrosion potential, cyclic voltammetry (CV) tests were performed. For this, the same conditions previously described were used; this is: carbon steel C1145 immersed in anaerobic standard reactor medium with different concentrations of acetate and 25 mM fumarate, in presence and absence of bacteria.

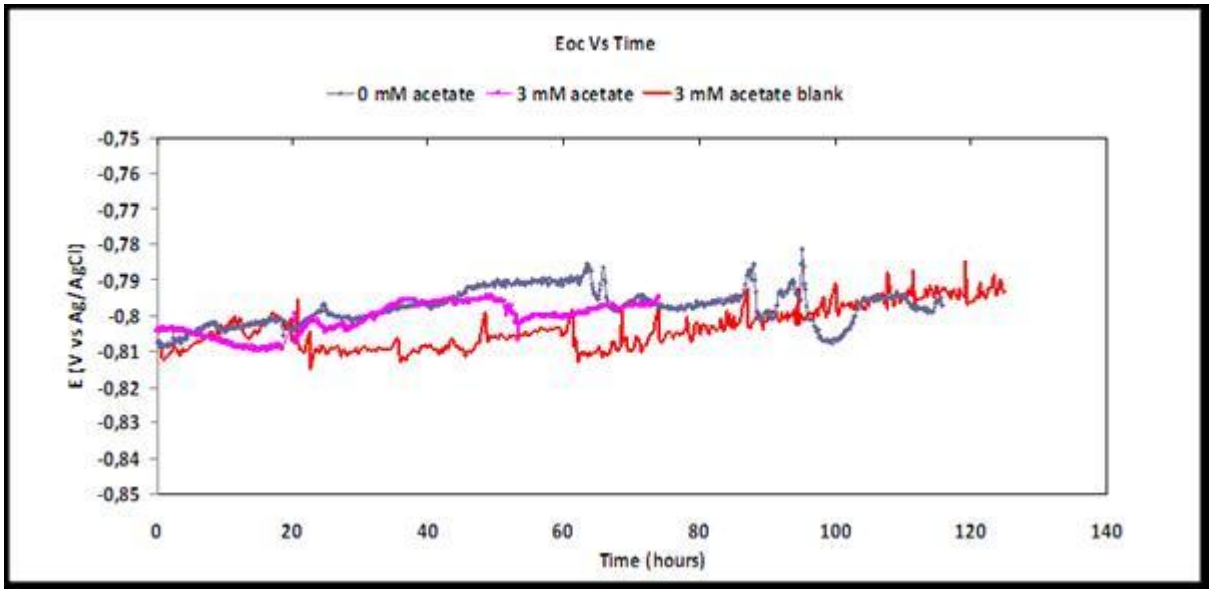


Figure III.6. OCP vs. time for carbon steel C1145 immersed in anaerobic reactor medium in presence of bacteria and absence of bacteria: blue line (biotic system with 0 mM acetate), pink line (biotic system with 3 mM acetate), and red line (abiotic control system with 3 mM acetate).

Fig. III.7 resumes the voltammetry results obtained: a first CV was performed in biotic and control abiotic system without acetate (0 mM acetate) after 80 hours of the WE immersion. At hour 102 of immersion, a second CV was performed to the systems (control abiotic and biotic) after injecting acetate from a sterile and anoxic stock solution obtaining a final concentration of 3 mM. At hour 110 of immersion, a third CV was performed to the systems (control abiotic and biotic) after injecting acetate from a sterile and anoxic stock solution obtaining a final concentration of 10 mM. At hour 118 of immersion, a final CV was performed to the systems (control abiotic and biotic) after injecting acetate from a sterile and anoxic stock solution obtaining a final concentration of 30 mM. A voltammetry curve (CV) was plotted after applying potential from -400 to +300 mV vs. OCP, at a sweep rate of 0.2 mV $s^{-1}$.

In Figure III.7, the effect of the acetate in the biotic and abiotic systems is observed when applying potential. Fig. A shows the biotic (blue) and abiotic (red)

systems without acetate. In the anodic branch, it is observed a wave in the control abiotic system and no wave is observed in the inoculated system. Anodic current (Ia) of the biotic system reaches 8 mA/cm² at -0.50 V vs Ag/AgCl whereas Ia of the control abiotic system reaches 1 mA/cm² around -0.53 V vs. Ag/AgCl. Fig. B shows the CV performed in the control abiotic system with 3 mM acetate (blue), 10 mM acetate (red) and 30 mM acetate (green). One anodic wave is observed in each of the curves between -0.7 and -0.5 V vs. Ag/AgCl. It should be noticed that in absence of bacteria, the acetate concentration is affecting the anodic reaction: the higher the acetate concentration the higher the Ia (from 1 to 3 mA/cm²). In contrast, in presence of bacteria (Fig. C) no oxidation or reduction waves are observed. However, the Ia is considerably higher (14 mA/cm²) than in the control abiotic for all the different acetate concentrations tested (around 3.5 times higher).

**A**

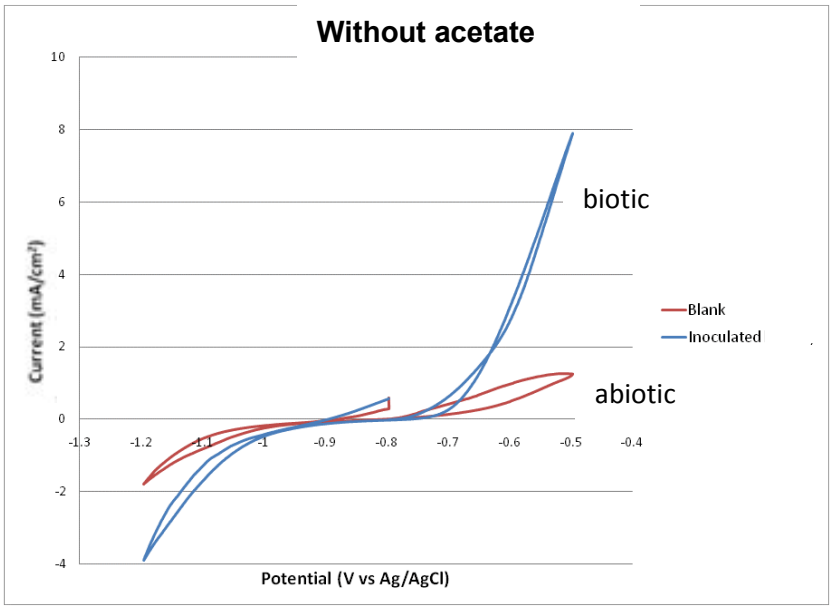


**B**

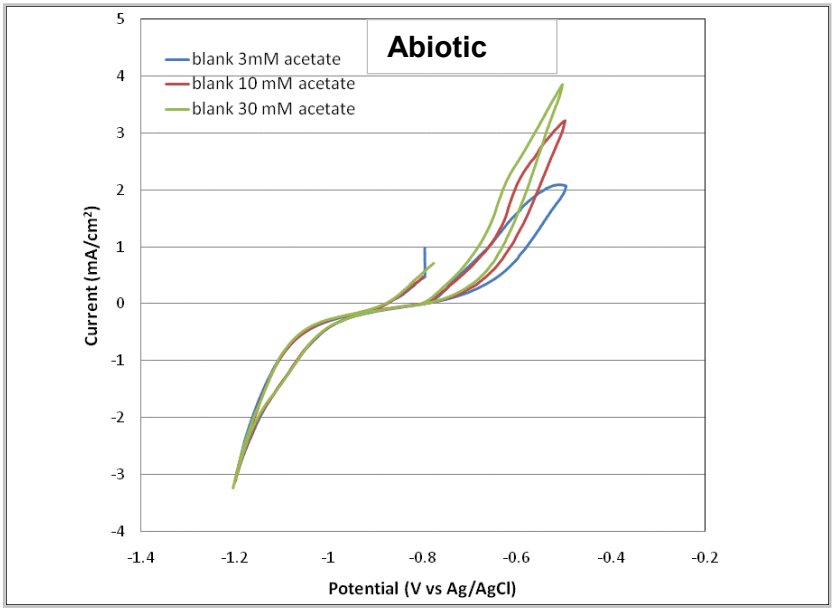

C

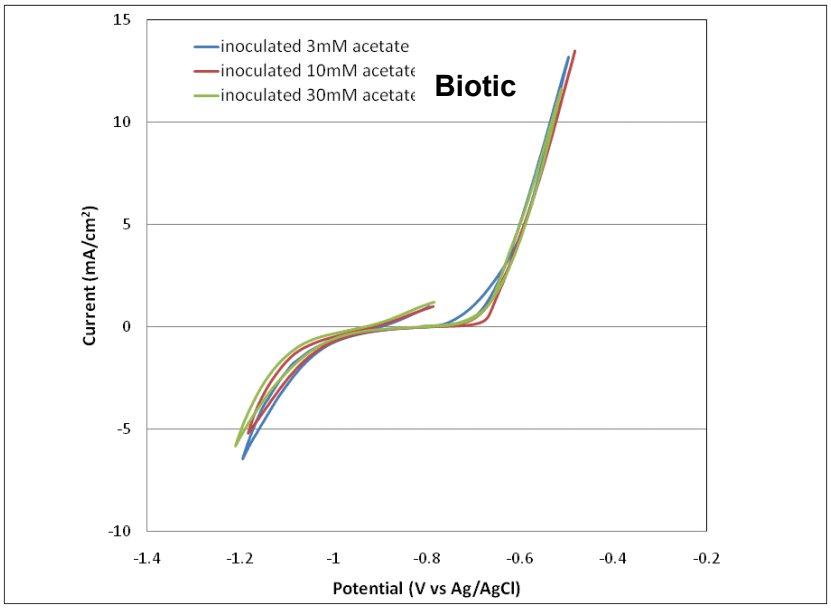


Figure III.7. Voltammetry for C1145 at different concentrations of acetate for control abiotic system. Fig A (without acetate control and inoculated), Fig. B (control with 3, 10 and 30 mM acetate), Fig. C (biotic system with 3, 10 and 30 mM acetate).

These results suggest that the acetate concentration influences the corrosion of carbon steel in both abiotic systems: the anodic current increases once increasing the acetate concentration. For biotic system there is no influence of the concentration of acetate in the potential range studied. So, it was concluded that 1 mM acetate would be used for the electrochemical experiments reducing as much as possible the influence of the acetate on the corrosion of the steel and aiming to reduce the likeliness of biofilm formation due to the scarce carbon source. Furthermore, lowering the acetate concentration (but providing sufficient for bacterial growth) would unbalance the redox state of the bacterial cells, forcing them to search for a new source of electrons on the material surface. This concentration chosen would allow us to see the response of the bacteria on carbon steel in conditions much closer to those of the environments where this type of bacteria may inhabit.

### III.3.3. Testing *G. sulfurreducens* electroactivity

In order to continue with the experimental plan, it was necessary to verify the efficiency of the bacteria inoculum which is characterised by its electroactivity. As it was previously mentioned, *G. sulfurreducens* was chosen as novel IRB bacteria thanks to its electron exchange capabilities. In order to test this requirement, the electrochemical technique called chrono-amperometry (CA) was used by polarising cathodically and/or anodically the WE, which allowed us to see the cathodic and/or anodic current produced thanks to the presence of an electroactive strain. Figure III.8 and III.9 show a CA of a strain of *Geobacter sulfurreducens* that had been stored in two different conditions: A) the strain was cryo-preserved at -80°C; B) the strain was stored at fridge temperature.
Results show that the strain A kept at -80°C had lost its electroactivity thus no current was detected in reduction conditions and very little current (< 0.005 mA) was detected in oxidation conditions. However, strain B kept at 4°C had kept its electroactivity and current was detected in both conditions: in reduction domain,

obtaining a maximum value of -2.5 mA and in oxidation one, obtaining a maximum value of 6 mA. Thus, this strain was chosen for performing further corrosion and electrochemical experiments. Electroactivity was checked from time to time during the experiments with *Geobacter sulfurreducens* to be sure that the inoculum used for the corrosion tests was still electroactive.

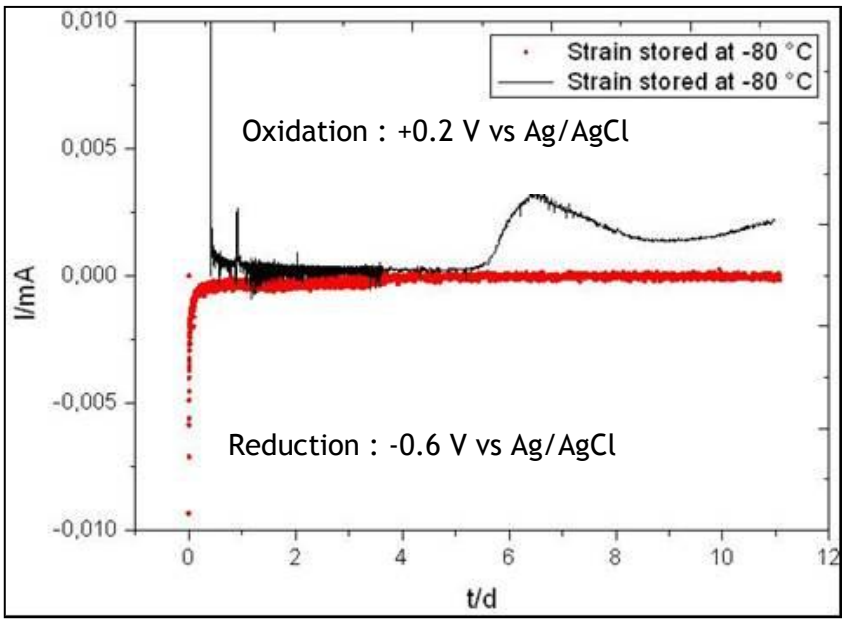


Fig. III.8. CA performed in a system with 245 SMO steel (reduction) and graphite (oxidation) immersed in reactor medium with 10 mM acetate in presence of G. sulfurreducens stored at -80°C

Oxidation : +0.2 V vs Ag/AgCl

Reduction : -0.6 V vs Ag/AgCl

Fig. III.9. CA performed in a system with 245 SMO steel (reduction) and graphite (oxidation) immersed in reactor medium with 10 mM acetate in presence of G. sulfurreducens stored at 4°C

## III.4. Results using standard reactor medium

### *III.4.1. Article 1*

*This article is titled "**Geobacter sulfurreducens:*** **an iron reducing bacterium that can protect carbon steel against corrosion?"** The main objective of this first paper with *Geobacter* was to find out whether *Geobacter sulfurreducens,* is able to protect carbon steel against corrosion and the mechanism of inhibition, if any. After some authors argued that Microbially Influence Corrosion Inhibition (MICI) was occurring in presence of IRB, we decided to test this hypothesis and to find out the possible mechanisms of corrosion inhibition. For this, an electroactive strain of *G. sulfurreducens* was electrochemically studied in an anaerobic system containing carbon steel C1145 immersed in an adjusted medium for the bacterial growth.

These first results highlight the influence of phosphate in presence of an IRB in corrosion of carbon steel. The presence of phosphate in the medium, reduce corrosion rate when bacteria is present due to the formation of an Fe (II) phosphate on the surface of the coupon, concluding that indeed the presence of bacteria exerts protection because it acts as catalyser for the formation of a protective and homogenous layer of iron (II) phosphate, which thanks to SEM and EDX analysis was found to likely be vivianite.

**"*Geobacter sulfurreducens:* An Iron Reducing Bacterium that Can Protect Carbon Steel Against Corrosion?"**

*Article submitted to Corrosion Sciences on June, 2013*

# *Geobacter sulfurreducens:* An Iron Reducing Bacterium that Can Protect Carbon Steel Against Corrosion?

Claudia Cote*, Omar Rosas, Régine Basseguy

*Laboratoire de Génie Chimique, CNRS, Université de Toulouse, 4 Allée Emile Monso, 31030, Toulouse, France*

---

**Abstract**

*Geobacter sulfurreducens* effect on the electrochemistry of carbon steel in anaerobic phosphate solution was studied. In nature, *G. sulfurreducens* is able to reduce Fe (III) to Fe (II) coupled with the oxidation of acetate. High availability of Fe (II) promoted the formation of an iron (II) phosphate layer on the steel; which was formed only when bacteria was present. It is assumed that the phosphate layer is responsible for maintaining the corrosion potential stable even after intrusion of air. In contrast, the corrosion potential of the abiotic experiments suffered an increment of 450 mV after few hours of exposure to air.

*Keywords:* A. Mild steel; B. EIS; C. Microbiological corrosion

*

* Corresponding author. Tel.: +33 5 34 32 36 17; fax: +33 5 34 32

E-mail address: regine.basseguy@ensiacet.fr (R. Basseguy).

## 1. Introduction

Microbial development occurs in almost all environments throughout biofilm formation and may be responsible for microbial influenced corrosion (MIC), also known as microbial corrosion or biocorrosion which can be defined as the enhancement or acceleration of corrosion by the presence of bacteria [1]. However, many authors have debated about the harmfulness of biofilms on metal surfaces and even argued that some of them may reduce corrosion rates by different mechanisms [2-5]. One of these mechanisms is a surface reaction leading to the formation of a corrosion inhibiting layer of phosphate such as the iron phosphate, vivianite.

Vivianite is an iron (II) phosphate, $Fe_3(PO_4)_2 * 8H_2O$ which may be used as a corrosion inhibiting agent of iron due to its low solubility properties forming a low soluble and non-oxidizing corrosion product film on the metal surface [4-7]. Corrosion inhibition is the slowdown of the corrosion reaction usually performed by substances (corrosion inhibitors) which, when added in small amounts to an environment, decrease the rate of attack by this environment on a metal [8]. A protection method against corrosion used by some industries is acid phosphating with phosphates of zinc, iron or manganese which leads to vivianite production [4]. This procedure is carried out at temperatures up to 95°C and pH values between 2 and 3.5.

One of the most studied mechanisms of corrosion inhibition promoted by microorganisms or microbially influenced corrosion inhibition (MICI) is the corrosion control using beneficial biofilms [7,8,30,31]. These benefits can be linked to either physical characteristics of the biofilm or biochemical characteristics involving metabolites. A biofilm is a highly organised bacterial community with cells entrapped in a matrix formed by extracellular polymer substances (EPS). On one hand, biofilms may form a persistent film which adheres at the metal/solution interface reducing the corrosion rate by forming a transport barrier, which may prevent the penetration of corrosive agents (such as oxygen, chloride, etc.) and decreasing their contact with the metal surface, thus reducing corrosion [7,8]. However, recent studies have shown that this protection is unreliable and that biofilms instead could also promote corrosion by a formation of a non-uniform patch which, in the presence of aerobic respiration, results in the formation of differential aeration cell accelerating the corrosion rate [7,9]. On the other hand, corrosion inhibition is sometimes explained by the biochemical characteristics of the microorganisms themselves and/or their enzymes. For instance, Da Silva *et.al* [10] and Mehanna *et.al* [11] observed a vivianite deposit on mild steel electrodes placed in a galvanic cell which had been catalysed by hydrogenase from *C. acetobutylicum,* consequently observing a delay on pitting corrosion or a reduced corrosion rate. Other authors [17,30-32], have claimed that the bacteria induced the reduction of corrosion rates, the prevention of pitting corrosion and the reduction of both cathodic and anodic reactions in materials such as stainless steel [33], mild steel and aluminium brass [30,31]. These observations were attributed to the presence of bacteria. Most of the bacteria reported to be involved in MICI are iron reducing bacteria (IRB). For instance, Little *et al,* [33] and Eashwar *et al.,* [35] have claimed that corrosion inhibition on stainless steel was due to a mechanism in which siderophores (iron chelators) produced by microorganisms within biofilms at neutral pH act as inhibitors and enhance passivity of stainless steel by reducing $i_p$. Other mechanisms most frequently cited for the inhibition are formation of a diffusion barrier to corrosion products that stifle metal dissolution, consumption of oxygen by respiring aerobic microorganisms within the biofilm causing a diminution of that reactant at the metal surface, production of metabolic products that act as corrosion inhibitors (e.g., siderophores, vivianite), specific antibiotics that prevent proliferation of corrosion-causing organisms (e.g., sulfate-reducing bacteria), formation of passive layers that are unique to the presence of microorganisms [36], reduction of ferric ions to ferrous ions (in presence of IRB) and increase consumption of oxygen [17]. Moreover, Herrera and Videla, [16] claim that the introduction of IRB to industrial water systems which contain SRB and other corrosion-inducing bacteria

causes not only the exfoliation of corrosion products but also the protection of the metal surfaces from further corrosion. In general, the main mechanism of corrosion inhibition by bacteria are always linked to a marked modification of the environmental conditions at the metal/solution interface by biological activity [16]

Moreover, IRB have been reported to biologically produced vivianite at laboratory scale under aerobic conditions with few bacteria strains such as *Pseudomonas* sp [2] and *Rhodococcus* sp. using a metal coupon and 20 mM of phosphate buffer [4,5,12]. Islam *et. al.,* [13] reported vivianite formation under anaerobic conditions by *Geobacter sulfurreducens* using soluble Fe (III) (iron citrate) as electron acceptor. When the organism was grown using insoluble crystalline Fe (III) and oxy-hydroxide as electron acceptor, Fe (III) reduction resulted in the formation of magnetite instead of vivianite. These same results were also observed by Lovley and Phillips [14].

*G. sulfurreducens* is a dissimilatory iron reducing bacteria (IRB) thanks to its electron exchange capabilities with solid substrate [15]. However, it is still uncertain its role in corrosion. Recent studies with *G. sulfurreducens* have shown that these bacteria can exert two different effects on 304L stainless steel: just after inoculating, G*. sulfurreducens* cells create a cathodic reaction on the material, which leads to a fast increase in its open circuit potential increasing the corrosion risk; in contrast, after a few days, well established biofilms shift the pitting potential towards positive values, which may be interpreted as a protective effect [3]. This research concluded that *G. sulfurreducens* plays a role in corrosion behaviour of 304L which depends on medium composition. In the absence of acetate (lack of electron donor), *G. sulfurreducens* biofilms promote the propagation of pitting whereas in the absence of fumarate (lack of electron acceptor), *G. sulfurreducens* cells were able to delay pit occurrence protecting the metal.

The controversy about enhancement of corrosion and/or protection against corrosion promoted by microorganisms is still unclear regarding this bacterial group. According to some reports, IRB are able to induce protection of carbon steel [3,16,17] while others suggest an important enhancement of corrosion through the reduction and removal of passive films of ferric compounds on the metal surface [3,16,45].

On the other hand, iron reducers can have a major effect on availability of iron ions through solubilisation of insoluble iron compounds consequently forming biominerals [18]. Biologically induced mineralisation is a process where bacteria produce biominerals commonly generated as secondary event from interactions between the activity of the microorganisms and their surrounding environments. The formation of phosphate minerals has frequently been observed in sedimentary environments under high biological productivity [19]. Since *Geobacter sulfurreducens* is ubiquitous species in sediments and soils, it can have a relevant effect on corrosion and in the corrosion protection of buried industrial equipment such as off-shore and harbour structures, oil and gas pipes and buried storage tanks [20]. Nevertheless, this bacteria genus has not been widely studied in the scope of corrosion but mainly in the scope of microbial fuel cell.

Although *Geobacter metallireducens* and *Shewanella oneidensis* have been equally studied concerning their role on biomineralisation and their use of Fe (III) as terminal electron acceptor in anaerobic respiration processes, only *Shewanella* has been studied in relation to corrosion processes [24,45,46].

Corrosion studies involving iron reducing bacteria such as *G. sulfurreducens* have been reported only by Mehana *et.al.* [3,11,20]. Other studies have reported only their behaviour in the environment: electroactivity, environmental role concerning the iron sources, bio-mineralisation and their metabolisms [13-15,25,26]. Moreover, little work has been done to examine which iron reducing microbial species are prevalent within corrosion bacterial

communities [16]. Based on the lack of knowledge about the influence of these bacteria in corrosion, the present study has as objective to find out whether *Geobacter sulfurreducens,* is able to protect carbon steel against corrosion and the mechanism of inhibition, if any.

The concentration of electron donor (acetate) and electron acceptor (fumarate) were considerably reduced for the electrochemical experiments with the objective of reducing the likeliness of biofilm formation due to the scarce carbon source conditions and therefore reducing the interference of EPS on the electrochemical behaviour and of the complex biofilm itself. Furthermore, lowering the acetate concentration would unbalance the redox state of the bacterial cells, forcing them to search for a new source of electrons on the material surface. All this altered conditions (electron acceptor and donor and phosphate concentration) would allow us to see the response of the bacteria on carbon steel in conditions much closer to those of the environments where this type of bacteria may inhabit. The final objective is to determine whether *G. sulfurreducens* enhances or inhibits corrosion of carbon steel in these conditions.

## 1. Experimental procedure

### *2.1. Bacteria and media*

*Geobacter sulfurreducens* ATCC 51573 strain used for the experiments was obtained from DSMZ (Deutsche Sammlung von Mikroorganismen und Zellkulturen). The media and solutions were prepared following the DSMZ protocol [21]. The culture growth medium contains 28 mM $NH_4Cl$, 5mM $NaH_2PO_4$, 1.3 mM KCl, 29.7 mM $NaHCO_3$ and 10 mM sodium acetate (electron donor). The medium was sterilised by autoclaving it at 121°C for 15 minutes. Once the medium cooled down it was added a sodium fumarate solution (electron acceptor) filtered with 0,2 µm pore filter, obtaining a final concentration of 50 mM of fumarate in the medium. 10 mL/L of vitamins (ATCC MD-VS) and 10 mL/L of minerals solution (ATCC MD-TMS) was also added.

The *G. sulfurreducens* culture was performed in glass anaerobic vials with 50 mL of growth medium. The vials were sealed with butyl rubber septums and they are de-aerated by injecting $N_2/CO_2$ (80:20, v/v) during at least 30 min before the injection of bacteria (10% of bacterial initial suspension). This first incubation lasted 3 to 5 days at 30 °C for optimum bacterial growth. Indeed, the culture was ready for inoculation in the electrochemical reactors once the absorbance of in the anaerobic vials measured around 0.3. The number of planktonic cells was evaluated by measuring the absorbance at 620 nm. The absorbance was correlated to cell forming units per millilitre ($CFU.mL^{-1}$) by the following calibration formula [22]:

$$[CFU.mL^{-1}] = OD_{620nm} \times 472067 \quad \text{(Eq.1)}$$

where OD is the optical density measured at 620 nm.

The anaerobic reactors used for the electrochemical measurements were filled with medium containing all the chemical compounds found in the growth medium at the same concentrations for most of them, except for the electron donor and acceptor: their concentrations were adjusted to1 mM acetate and 10 or 25 mM fumarate.

### *2.2. Electrochemical measurements*

Anaerobic reactors of 0.5 L for experiments with *Geobacter* were used adjusting the liquid level to 300 mL of total volume. The anaerobic conditions were obtained by bubbling $N_2/CO_2$ 80:20 into the reactors for at least 45 minutes before inserting the metal coupons. The flow of $N_2/CO_2$ was maintained during the whole experiment unless stated otherwise. Reactors were

kept at 30°C in a thermal bath during experiments. pH was measured for all the experiments at initial time (h=0) and final time (h≥144 h).

The working electrodes (WE) were 2 cm diameter cylinders of carbon steel AISI 1145. The nominal chemical composition for the steel 1145 is shown in table 1.
The WE was covered by a polymeric coating (thermo-contractible polyolefin, ATUM ®) leaving uncovered a flat disk surface with a total exposed area of 3.14 $cm^2$. Connections were made through titanium wire protected with the same polymeric coating. The electrodes were ground with SiC paper using P120-P600 until achieving a 600 grit surface followed by a cleaning with ethanol (70%) and throughout rinsing with sterile distilled water.

Table 1
Chemical composition of AISI C1145 (wt %)

| *Alloy* | *Ni* | *C* | *Mn* | *Cu* | *Si* | *S* | *P* | *Mo* | *Cr* |
|---|---|---|---|---|---|---|---|---|---|
| 1145 | 0.1 | 0.46 | 0.65 | 0.11 | 0.31 | 0.03 | 0.01 | 0.02 | 0.1 |

For all the experiments, electrochemical measurements were performed using a multipotentiostat (VMP-Bio-Logic) with a platinum grid (Pt, Ir 10%) used as counter electrode (CE) and a silver wire coated with silver chloride (Ag/AgCl) was used as reference electrode (RE); since the chloride concentration of the electrolyte was 0.03 M the potential of the reference was E= 0.223 – 0.059 log [Cl-]= 0.31V vs. SHE.

The Open circuit potential OCP in function of time was measured for all the experiments. Electrochemical Impedance Spectroscopy (EIS) was used to obtain information on the interface, using a frequency from 100 kHz to 10 mHz and amplitude of 10 mV. The previous described techniques were combined in order to obtain information on the electrochemical system formed by the metal coupon in the electrolyte and the influence of the electroactive bacteria *G. sulfurreducens* on the system. The combination of these 2 techniques together with surface analysis techniques is a good tool to studies applied to corrosion and electrochemical systems.

The carbon steel coupons were immersed in the de-aerated reactor medium containing 5 mM of $NaH_2PO_4$, 1 mM acetate as electron donor and 10 mM or 25 mM fumarate as electron acceptor. The concentration of electron donor and electron acceptor were considerably reduced for the electrochemical experiments compared with the growth medium aiming to reduce biofilm formation in order to reduce the interference of EPS and biofilm on the electrochemical behaviour. Furthermore, lowering the acetate concentration would unbalance the redox state of the bacterial cells, forcing them to search for a new source of electrons on the material surface. On the other hand, phosphorus is an essential constituent for bacterial development and it is added into the medium in form of sodium phosphate, expecting it to bind with the ferrous ions in order to form vivianite.

The electrochemical measurements were performed to abiotic control systems and biotic inoculated systems during at least 144 hours. The de-aerated conditions were maintained during at least the first 90 hours of measurements and from this time on, as stated in the results, air was allowed into the system regaining aerobic conditions. Note that the results of the experiments stated in this paper were carried out 6 times for the systems with bacteria (1 of them injecting compressed air) and 5 times for the control system (1 of them injecting compressed air) finding high reproducibility amongst them.

*2.3. Analytical techniques*

Total iron in solution was determined by Inductively Coupled Plasma (ICP) analysis using an ICP-OES ULTIMA2, Horiba. 20 mL of the sample were used for total iron measurement. Samples were taken 3 times until hour 98 when the conditions were kept anaerobic. The reason for taking samples only when oxygen is absent is because oxygen may interfere with the measurements by precipitating soluble iron, not allowing to measure real total iron dissolved into the medium.

*2.4. Surface analysis*

Scanning Electron Microscopy (SEM) pictures were taken using a TM3000 Hitachi Analytical Table Top Microscope at 7000x magnification working at 15 kV acceleration voltages. The coupons were washed with distilled water and dried with the gas mixture $N_2/CO_2$ 80:20 after 140 hours of immersion in the media described.
Energy dispersive x-ray spectroscopy (EDX) was used for elemental analysis of the surface of the coupons.

## 2. Results and Discussion

*3.1. Open circuit potential results*

Carbon steel coupons AISI 1145 were immersed in the electrochemical reactors filled with a medium containing 5 mM of $NaH_2PO_4$, 1 mM acetate as electron donor and 10 mM fumarate as electron acceptor, among other compounds. The metallic coupons were set up in the reactors 24 h before inoculation under anaerobic conditions: $N_2/CO_2$ (80:20) flow was maintained during the first 98 hours of the experiment. At hour 98 (t=98 h), the $N_2/CO_2$ was deliberately stopped and air was allowed to come into the system by opening one of the exits of the reactor in sterile conditions or by injecting sterile compressed air.

At hour 24, the reactors were inoculated with 5% (v/v) of cell culture that contained approximately $1.42 \times 10^5$ CFU $mL^{-1}$. In the cases of the control reactors, 5% inoculum was also injected but this time filtrated with 0.2 µm porous cellulose filter in order to remove the bacterial cells. In this way only the chemical composition of the injected solutions were identical, including the presence of metabolites; no bacterial cells entered into the control reactors. The electrochemical behaviour of the system was tested recording open circuit potential in function of time. A resume of electrochemical experiments and the main results are displayed in table 2. Fig. 1 describes the OCP behaviour of 4 different experiments running in parallel: two control systems (curves A and B) and two systems with bacteria (curves C and D). OCP remained stable along the time in the 4 reactors under anaerobic conditions.
When air entered into the reactors, an OCP jump was observed on the control systems, whereas none or very little increment was observed in the systems with bacteria if anaerobic conditions were maintained for at least 90 hours. Note that the results of all the experiments described in table 2 display high reproducibility regardless of the fumarate concentration.

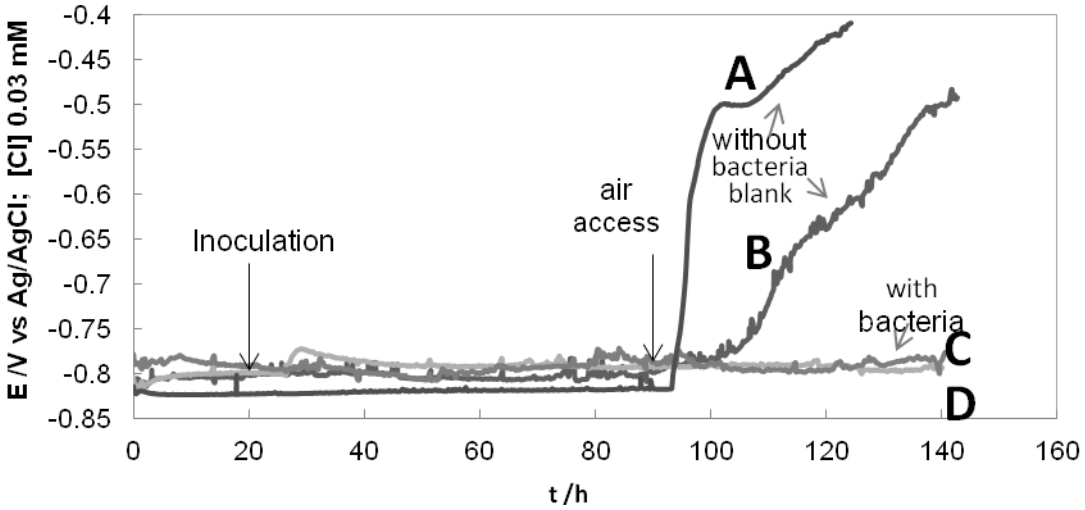


Fig. 1. Variation of OCP of mild carbon steel C1145 with 5% *G. sulfurreducens* and without bacteria. Medium containing 1 mM sodium acetate (electron donor), 10 mM of sodium fumarate (electron acceptor) and 5 mM phosphate. A and D: air entrance by air injection; B and C: air entrance by opening the reactors.

Table 2
Initial and final potential of C1145 steel at the start and the end of the experiments of systems with and without bacteria using 1 mM of electron donor, 10 and 25 mM of electron acceptor and 5 mM phosphate. (NA: Not Applicable because there was not observed an OCP jump; samples marked with (*) had injection of air instead of air entrance by opening the reactor)

| Type of experiment | [fumarate] (mM) | Initial OCP (V vs Ag/AgCl) | Final time (h) | Final ocp (V vs Ag/AgCl) | Anaerobic time (h) | OCP jump (V) at time (h) |
|---|---|---|---|---|---|---|
| Control Experiments | 25 | -0,80 | 149 | -0,55 | 95 | +0,25/100h |
| | 10 | -0,81 | 143 | -0,49 | 98 | +0,32/105h |
| | 10 | -0,82 | 140 | -0,56 | 90 | +0,26/120h |
| | 10 | -0,81 | 141 | -0,28 | 90 | +0,53/95h |
| | 10 | -0,81 | 135 | -0,45 | 90 | +0,36/90h(*) |
| Inoculated Experiments | 10 | -0,80 | 130 | -0,45 | 70 | +0,35/74h |
| | 10 | -0,81 | 144 | -0,79 | 90 | NA(*) |
| | 25 | -0,78 | 142 | -0,78 | 95 | NA |
| | 10 | -0,81 | 140 | -0,79 | 98 | NA |
| | 10 | -0,81 | 168 | -0,85 | 120 | NA |
| | 10 | -0,81 | 168 | -0,8 | 120 | NA |
| | 10 | -0,81 | 157 | -0,79 | 100 | NA |

*3.1.1. Open circuit potential results: Anaerobic system (hour 0 to hour 98)*

Generally, OCP results in anaerobic conditions show that the corrosion potential remained stable (Fig. 1). However, a small increment on the OCP (+15 mV) was observed few hours after inoculation in the systems where cells were inoculated (Fig 1, curve C,D).

This small increase of OCP was also found by Mehanna *et. al.,* [20] on experiments with *G. sulfurreducens* in a similar medium using the same type of electrode, C1145. They observed

a small OCP increase during the first 20 minutes after inoculation of bacteria, followed by a larger jump of OCP (+300 mV) on the next 3 hours. When observing the coupons surface, they stated that the presence of bacteria changed the corrosion pattern by grouping corrosion attack into large zones and setting up cathodic electron transfer in places where the cells grew, which protected the metal against corrosion.

Experiments reported here didn't reproduce the exact same results obtained by Mehana *et. al.,*[20] besides conditions were very similar. The large potential increase in presence of bacteria observed in [20] only 3 hours after inoculation and not observed here might be explained by comparing the initial OCP values; the initial potential reported in [20] was around -600 mV vs. Ag/AgCl, which is nearly 200 mV more positive than the one observed here. Having lower potential eases the conditions for bacteria to reduce Fe(III) to Fe(II). Fe (II) ions could then bind with phosphate, consequently producing iron phosphate that could protect the metal against a possible increase of OCP.

In conclusion, the small augmentation on OCP indicates an increment on the cathodic reaction due to the reduction of ions Fe (III) to Fe (II) which led to the formation of an iron (II) phosphate, likely to be vivianite. This slight increase in potential involves an initial activation of the interface therefore an initial acceleration of the corrosion rate that decreased after the vivianite formation.

Additionally, the quantity of total dissolved iron was measured by ICP at 3 times (24h-just before inoculation, 26h- after inoculation and 92h- before oxygen entrance). Results show that at hour 24 and hour 26 a very similar concentration of iron was found in both systems reassuring the reproducibility of the tests (table 3). The slight decrease of dissolved iron at hour 26 may be explained by a slight entrance of oxygen while inoculating: iron oxide may precipitate in presence of oxygen. At hour 92, an increase on the iron concentration is observed in the control abiotic system whereas there is a decrease in the biotic inoculated one. Moreover, the quantity of total dissolved iron at hour 92 is 6 times lower in the system with bacteria (1.37 mg/L) compared to the control system (8.46 mg/L). This can be explained by the precipitation of iron phosphate compound in presence of bacteria. Indeed, the Fe II, coming from iron III reduction catalysed by *G. sulfureduscens*, bound with the phosphate, that can form either the vivianite layer on the surface of the coupon or phosphate precipitates in solution.

Table 3
ICP results for total dissolved iron. (A) Control system (B) Inoculated system.

**A**

| TEST 1 (control) | |
|---|---|
| **Time (h)** | **Fe (mg/L)** |
| **24** | 5.22 |
| **26** | 4.68 |
| **92** | 8.46 |

**B**

| TEST 2 (inoculated) | |
|---|---|
| **Time (h)** | **Fe (mg/L)** |
| **24** | 5.11 |
| **26** | 4.37 |
| **92** | 1.37 |

*3.1.2. Open circuit potential results: Aerobic system (hour 98 to hour 140)*

Without stopping OCP measurements, the 4 reactors previously described (Fig. 1), were exposed to aerobic conditions at hour 98. Once the injection of $N_2/CO_2$ stopped and air was allowed to enter into the reactor, either by opening the reactor (curves B, C) or by injecting compressed air (curve A, D), it was observed a potential increase of over 300-400 mV in the control reactors (without bacteria, curves A, B) whereas the OCP of the reactors with bacteria remained stable (curves C, D). As it was expected, the increase of OCP of the control system was much faster when the compressed air was injected (curve A) compared to the experiment where air was allowed to enter into the system by only opening one of the

reactors closing capsules (curve B). When injecting the air, the potential increase was observed immediately whereas when opening the reactor, the increase on OCP was observed after 5 to 20 hours after opening it.

The OCP or corrosion potential increase observed in the control systems indicates that the system changed drastically switching the cathodic reaction from the water reduction to the oxygen reduction which induced higher corrosion rates [40].
In contrast, the stability of the OCP in the inoculated system tells us that the presence of bacteria prevented the acceleration of the cathodic reaction seen in the control system, due to the coating of iron (II) phosphate that was formed only when bacteria were inoculated. Therefore, *G. Sulfurreducens* catalysed the formation of a protective layer against corrosion that was able to prevent the increase of corrosion when oxygen was present into the system reducing its oxidant action on the metal.

Moreover, an OCP increase was observed when the anaerobic conditions were stop before 90 hours of immersion in the systems with bacteria (table 2, curve not shown). It is presumed it is needed a minimum of 90 hours of anaerobic conditions to create a homogenous vivianite layer that may protect the surface against corrosion. It is also known that *G. sulfurreducens* tolerates oxygen but does not reduce iron in presence of it [15]. Thus the presence of oxygen before 90 hours of experiment inactivates the bacterial metabolism impeding the homogenous formation of the iron (II) phosphate layer.

Furthermore, pH measurements were taken at the beginning and the end of the experiment (table 4) and it was observed that the pH in systems with bacteria were kept stable (around neutrality) even when the $N_2/CO_2$ injection stopped and oxygen was allowed into the system, whereas the pH in the control systems was less stable and slightly increased in a range of 7.5 to 8.0. This is in accordance with the oxygen reduction that occurs with higher rate in absence of bacteria.

Table 4
Comparison of initial and final pH measurements for systems with *G. sulfurreducens* in presence of a metal coupon C1145 and control systems (without bacteria).

| Type of experiment | [fumarate] (mM) | pH initial | pH final |
|---|---|---|---|
| Control Experiments | 25 | 6,9 | 7,5 |
| | 10 | 6,9 | 7,5 |
| | 10 | 6,9 | 7,6 |
| | 10 | 6,8 | 7,2 |
| | 10 | 6,8 | 8,4 |
| Inoculated Experiments | 10 | 6,8 | 7,1 |
| | 25 | 6,8 | 7,2 |
| | 10 | 6,8 | 7,4 |
| | 10 | 6,8 | 7,0 |
| | 10 | 6,8 | 6,9 |
| | 10 | 6,8 | 7,0 |

*3.2. Macro and microscopic results*

*3.2.1. Macroscopic observations*

Macroscopy observations (Fig. 2) performed on the coupons after 140 hours of immersion showed that on the surface of the coupon with bacteria there was formed a grey layer (Fig. 2A, right) whereas on the coupon without bacteria there was a yellowish layer which appeared to be an iron oxide usually seen on corrosion in presence of oxygen [23] (Fig. 2 A, left). To have an approximate determination of the conductivity of the deposited layers, a voltmeter was used touching the surface of the coupon keeping a distance of 1 cm: an insignificant current was obtained on the grey layer (poorly conductive) whereas some current was detected on the surface of the control coupon.

*3.2.2. Morphology and composition analysis*

Microscopy observations showed a needle- like layer distributed homogeneously on the surface of the coupon with bacteria (Fig 2: C1) and some deposits with a random distribution of what it seems to be a rhombohedral mineral (Fig 2: C2). In contrast, coupons coming from control experiments exhibited uniform corrosion features with a cracked flat layer (Fig 2: B2) covering what it seems to be pure iron (Fig. 3: B1).

These observations suggested that the grey layer of the coupon in presence of bacteria is an iron phosphate layer (Fig. 2: C1) and that indeed the surface layer of the control coupon was mainly iron oxide.

Surface analysis using energy dispersive x-ray spectroscopy (EDX) (Table 5) confirmed that the layer formed on the surface of the coupon with bacteria was an iron phosphate most likely to be $Fe_3(PO_4)_2 * 8H_2O$, vivianite (Table 5: C1) and that the rhombohedral deposit was iron carbonate ($FeCO_3$) (Table 5: C2), commonly known as siderite.

It is also important to highlight that the SEM pictures observed in Fig 3 (B and C) did not undergo a biofilm fixation procedure and therefore biofilm was not observed. The poor bacteria development in solution ($4.25 \times 10^4$ CFU $mL^{-1}$ at hour 90) was sufficient for the formation of the phosphate layer, vivianite and of a thin biofilm attached to the surface of the coupon. It was expected that the scarce carbon source conditions of the medium (1 mM of acetate) would unbalance the redox state of the bacterial cells, forcing them to search for a new source of electrons on the material surface. It is presumed that this thin biofilm layer was easily removed after the washing procedure.

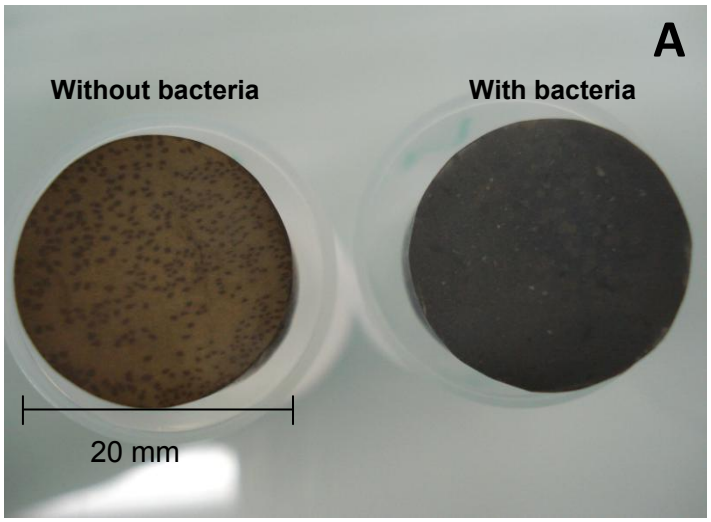


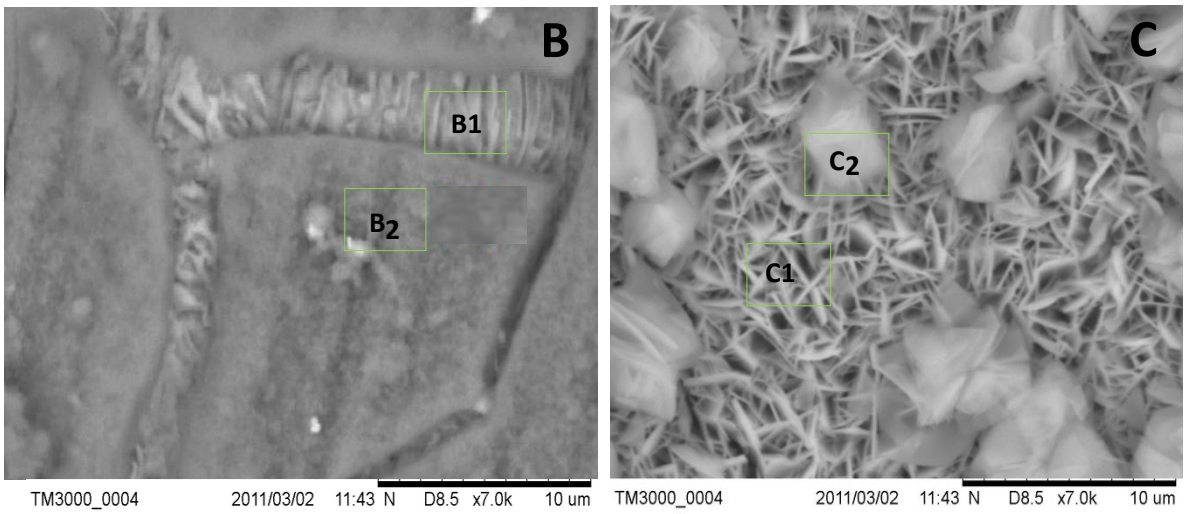


Fig.2. Macro and micro photographs of coupons after 140 hours of immersion: (A) Photographs of coupons with and without bacteria after oxygen entered the reactors; (B) SEM image of control coupon; (C) SEM image of coupon with bacteria

Table 5
EDX analysis of coupons surface after 140 hours of immersion. (A): clean coupon after grinding (no immersion); B1 and B2: control coupon (see Fig. 2B); C1 and C2 coupon in presence of bacteria (see Fig. 2C);

Clean coupon

**A**

| *Element* | *Weight %* | *Atomic %* |
|---|---|---|
| **Carbon** | 4.3 | 17.3 |
| **Iron** | 95.7 | 82.7 |

Control Coupon

**B1**

| *Element* | *Weight %* | *Atomic %* |
|---|---|---|
| **Carbon** | 15.0 | 38.3 |
| **Oxygen** | 10.2 | 19.6 |
| **Phosphorus** | 1.5 | 1.5 |
| **Iron** | 72.1 | 39.6 |

**B2**

| *Element* | *Weight %* | *Atomic %* |
|---|---|---|
| **Carbon** | 8.4 | 15.1 |
| **Sodium** | 2.5 | 2.3 |
| **Magnesium** | 0.6 | 0.5 |
| **Phosphorus** | 10.5 | 7.3 |
| **Manganese** | 1.4 | 0.6 |
| **Iron** | 29.3 | 11.3 |
| **Oxygene** | 46.3 | 62.3 |

Inoculated coupon

**C1**

| *Element* | *Weight %* | *Atomic %* |
|---|---|---|
| **Carbon** | 5.5 | 13.4 |
| **Oxygen** | 21.3 | 38.9 |
| **Sodium** | 1.4 | 1.8 |
| **Phosphorus** | 18.6 | 17.5 |
| **Manganese** | 3.7 | 1.9 |
| **Iron** | 48.0 | 25.1 |

**C2**

| *Element* | *Weight %* | *Atomic %* |
|---|---|---|
| **Carbon** | 22.2 | 34.0 |
| **Oxygene** | 45.4 | 52.1 |
| **Sodium** | 1.1 | 0.8 |
| **Phosphore** | 9.9 | 5.9 |
| **Manganese** | 0.9 | 0.3 |
| **Iron** | 20.0 | 6.6 |

*3.4. Electrochemical impedance measurements*

EIS measurements were performed every 24 hours on both systems, inoculated and control. Notice that these two experiments were running in parallel during 144 hours. The curve observed at hour 24 corresponds to the only measurement performed before inoculation. Curves shown until hour 96 are in anaerobic conditions. After, the aerobic conditions were achieved by opening the reactor allowing air to come into the systems in sterile conditions.

*3.4.1. Control system*

Fig. 4 shows the impedance response for carbon steel exposed in the control reactor (without bacteria). The Nyquist diagrams (global and zoom-up, Fig 4 A and B) display the presence of two depressed semi-circles at high and low frequencies respectively. The Bode and imaginary modulus versus frequency diagrams confirm the occurrence of these two time constants. As the two signals belong to two well-distinct frequency domains, they were analysed separately.
At high frequency (> 1kHz), the electrolyte resistance $R_s$ and the parameters corresponding to the depressed semi-circle were calculated using a R1 + Q2//R2 + Q3//R3 model (Fig 5) where Q corresponds to a CPE (constant phase element) which impedance can be described by (Eq. 2) [41,42]:

$$Z_{CPE} = 1/Q(\omega)^{\alpha} \times [\cos(\alpha\pi/2) - j \sin(\alpha\pi/2)] \quad \text{(Eq. 2)}$$

where $\alpha$ and Q are the CPE characteristic parameters
As it can be seen in table 6 (oxide HF), the electrolyte resistance little varied (around 40-61 Ω cm²) all along the test, the coefficient $\alpha$ was equal to 0.6, which expresses a heterogeneous distribution of the capacity and the resistance R (corresponding to the diameter of the semi-circle) was stable since the anaerobic conditions were maintained (around 20 Ω cm²) and then increased with the oxygen entrance: at the end of the test, R is 8 times higher than at the beginning. In order to determinate the phenomenon linked to this HF semi-circle, an evaluation of the capacity was performed thanks to the equation Eq. 3 using the frequency at the maximum of the circle as it will be done for a pure capacity:

$$C=1/(2\pi*f_{max}*R) \qquad \text{(Eq. 3)}$$

The capacitance values obtained (between 0.15-0.32 $\mu Fcm^{-2}$), can be related to an oxide layer (values are too small for attributing it to a double layer even if it can be thought that it was under-estimated by the way it was evaluated) which thickness (δ) was estimated by equation Eq. 4.

$$\delta = \varepsilon\varepsilon^{\circ}/C \qquad \text{(Eq. 4)}$$

with $\varepsilon^{\circ}$ the vacuum permittivity =8.85 $10^{-14}$ $Fcm^{-1}$ and ε the permittivity inside the oxide, taken equal to 12.

The thickness was evaluated to be 50-60 nm and tended to decrease in the presence of oxygen to around 30 nm (table 6). These values are in the range of those find on this kind of steel (4 nm < δ < 100 nm) [38,39,44] after immersion in different media in presence or absence of oxygen. The thickness of the oxide films is claimed to be affected more by the medium composition (for instance chloride exposure decreased it) than the immersion time. In the present work, the resistance of the layer increased with immersion time, was double after 96 hours in anaerobic conditions and was multiplied by 5 after 40 hours in the presence of oxygen.

At lower frequency (< 1kHz), linear parts were observed on the plot drawing the modulus of the imaginary component of the impedance versus the frequency in logarithmic coordinates (fig4D). The slope values of these linear parts were used for the calculation of alpha (α) values in order to determine whereas the system followed a constant phase element (CPE) behaviour or a pure capacitive behaviour [41,42]. For all the times, the α values found and displayed in table 6 were lower than 1 confirming a CPE behaviour, i.e. the system exposed a heterogeneous distribution of time constants. The Q and R values (table 6) were calculated thanks the R1 + Q2//R2 + Q3//R3 model presented figure 5. The effective capacitances associated to the CPE were calculated using the equation 5 derived by Brug et al. [43]:

$$C_{dl} = Q_{1/\alpha}\,(1/R_s + 1/R_{ct})^{(\alpha-1)/\alpha} \qquad \text{(Eq. 5)}$$

The values of capacitances varied from 82 to 90 $\mu Fcm^{-2}$. These values can be attributed to double layer capacitance values. Thus it can be assumed that the CPE behaviour was due to the surface distribution of time constants linked to the charge transfer. Consequently, the diameter of the depressed semi-circles can be attributed to a charge transfer resistance, $R_{ct}$ that increases as the duration of immersion increases. On a first approach, it can be said that this increase indicates a decrease on the corrosion rate since the electron transfer on the interface decreases. However, the $R_{ct}$ increase is more important in the presence of oxygen (from 6 to 12 kΩ cm² in 40 hours) than in anaerobic conditions (from 4 to 6 kΩ cm² in 96 hours).

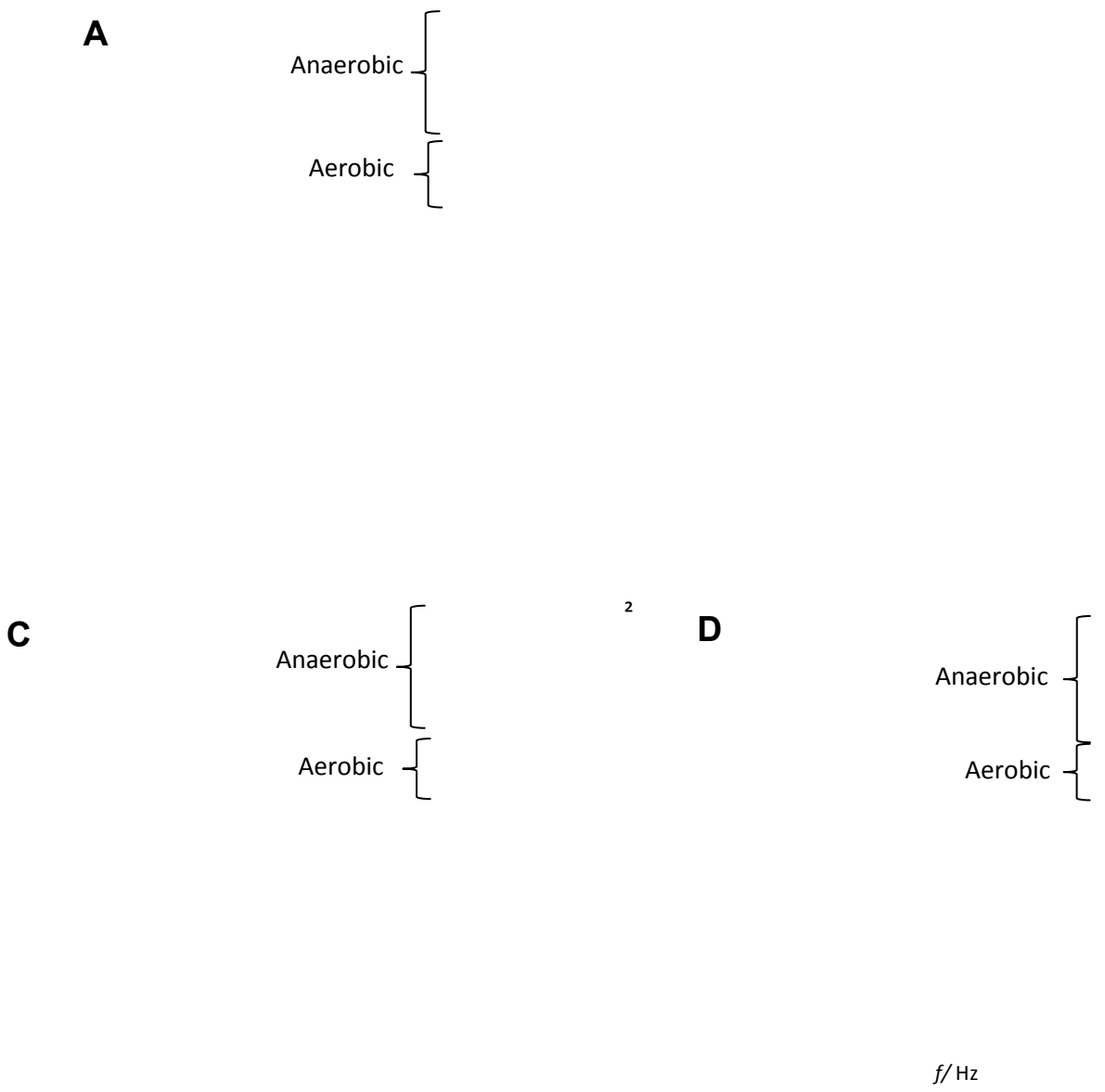


Fig.4 Impedance spectra of carbon steel C1145 during the 144 hours of immersion in the control reactor (without bacteria); medium containing 29 mM chloride, 1 mM acetate, 10 mM of fumarate and 5 mM of phosphate. System kept in anaerobic conditions until hour 96 as indicated in the graphs. (A) Nyquist, (B) Nyquist zoom-up (C) Bode phase angle and (D) Imaginary modulus versus frequency plots.

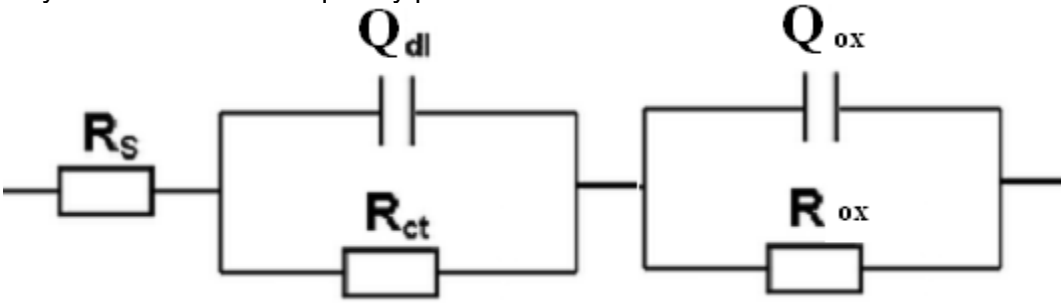


Fig 5. $R_s+Q_{dl}/R_{ct}+Q_{ox}/R_{ox}$ model to fit depressed semi-circles. $R_{ox}$ = HF resistance, Rct = resistance corresponding to the circle diameter and the CPE= constant phase element

Table 6.
Control system: evolution in time for $R_s$, $R_{ox}$, $C_{ox}$, δ, for values at HF, and α, $R_{ct}$, $Q_{eff}$, $C_{dl}$ for values at MF-LF of the control system in aerobic conditions in a medium containing 1 mM of acetate and 10 mM of fumarate in presence of a coupon of C1145.

| Oxide HF | | | | | | | Transfer LF | | | |
|---|---|---|---|---|---|---|---|---|---|---|
| Time (h) | $R_s$ (Ωcm²) | α | $R_{ox}$ (Ωcm²) | *f*(max) (Hz) | $C_{ox}$ µFcm$^{-2}$ | δ (nm) | α | $R_{ct}$ (Ωcm²) | $Q_{eff}$ ($\Omega^{-1}cm^{-2}s^{\alpha}$) | $C_{dl}$ µFcm$^{-2}$ |
| 24 | 41 | 0,6 | 17 | 45562 | 2.1E-07 | 52 | 0,80 | 3570 | 2,6E-04 | 83 |
| 48 | 40 | 0,6 | 18 | 45562 | 1,9E-07 | 56 | 0,80 | 4113 | 2,6E-04 | 82 |
| 72 | 39 | 0,6 | 22 | 45562 | 1,6E-07 | 68 | 0,81 | 4527 | 2,5E-04 | 84 |
| 96 | 61 | 0,6 | 33 | 30739 | 1,6E-07 | 67 | 0,84 | 6139 | 2,1E-04 | 90 |
| 120 | 61 | 0,6 | 50 | 14013 | 2,3E-07 | 46 | 0,85 | 9263 | 1,9E-04 | 86 |
| 144 | 59 | 0,6 | 166 | 2905 | 3,3E-07 | 32 | 0,87 | 12246 | 1,8E-04 | 88 |

Combining the analysis of these results with those of OCP and surface analysis, it is believed that a layer of magnetite is first formed (characterised by $C_{ox}$ and δ), which normally happens in abiotic anaerobic conditions [27]. This layer increasingly protects the material (augmentation of $R_{ct}$) but not enough to avoid the oxygen action: by modify the redox potential (strong oxidizing agent), the oxygen entrance may promote the formation of a new oxide layer due to a change on the oxidation state of the iron, probably from iron (II) oxides to iron (III) oxides. The growth of this oxide layer results in a protective effect on the surface against corrosion (Rct double in 40 hours). However, it must be keep in mind that an oxide layer on carbon steel is little resistant and unreliable against corrosion especially due to its porosity.

*3.4.2. Inoculated system*

In biotic conditions (5% of bacteria inoculum), on the Nyquist plots (Fig. 6 A & B), it can also be observed two depressed semi-circles as in abiotic conditions which diameter increased as the duration of immersion increased. The EIS results were analysed as for the control system and the calculated values of the different parameters are gathered in table 7.

At HF (oxide HF), the capacitance values are smaller than those found in control system (except before inoculation of course!), they can be attributed to the capacitance of an iron oxide layer certainly more reduced than the one found in control system due to the presence of bacteria. The thickness of this layer can be estimated at a first approximation using the equation 4 taken ε =12: δ increased when immersion time increased in anaerobic conditions and then it was maintained at around 300 nm thick in the presence of oxygen. The resistance linked to this layer also increased gradually from 23 to 53 Ω cm².

At LF, a linear part was found on the modulus diagram of the impedance where the imaginary component was plotted in function of the frequency (Fig. 6D) for each immersion time; the corresponding slopes had values lower than 1, confirming a CPE behaviour. The R and Q were calculated using the R1 + Q2//R2 + Q3//R3 model presented in figure 5 and the effective capacitances associated to Q using Brug's equation 5 (table 7). The values of $C_{dl}$, in the range of 59-93 µFcm$^{-2}$, can be attributed to the capacitance of double layer and consequently R corresponds to a charge transfer resistance. When the immersion time increased, $R_{ct}$ increased and even more after the entrance of oxygen. At the end, the interface was such as the charge transfer are very slowed down, Rct (22 k Ω cm² at t=144 h) was 3 time higher than that at the end of the anaerobic period. Since the oxygen presence has no impact on OCP value, it can be assumed that the iron phosphate layer (likely vivianite) that grew in the anaerobic conditions due to the presence of *G. sulfurreducens,* had a protective effect on the surface against corrosion even in aerobic conditions.

*3.4.3. Comparisons of the both systems (abiotic and inoculated)*

When comparing both systems, control and with bacteria, it can be observed similarities in the obtained plots untill hour 96, i.e. in anaerobic conditions. Then the differences were observed later once the oxygen entered the reactor. The system with bacteria showed larger $R_{ct}$ that can be translated to a lower corrosion rate in presence of bacteria. The stability of the OCP and the surface analysis coupled to EIS results confirmed that the Iron (II) phosphate layer (vivianite) formed on the surface in inoculated systems, was less conductive and stronger than oxide layer formed in the control system; therefore, it is a protective type of coating without being a passive layer. On the contrary, the iron (II,III) oxide layer (magnetite) found in abiotic systems varied depending on the oxygen presence, and although the charge transfers were reduced after a long immersion, the oxide layer was not so stable and protective than the vivianite one.

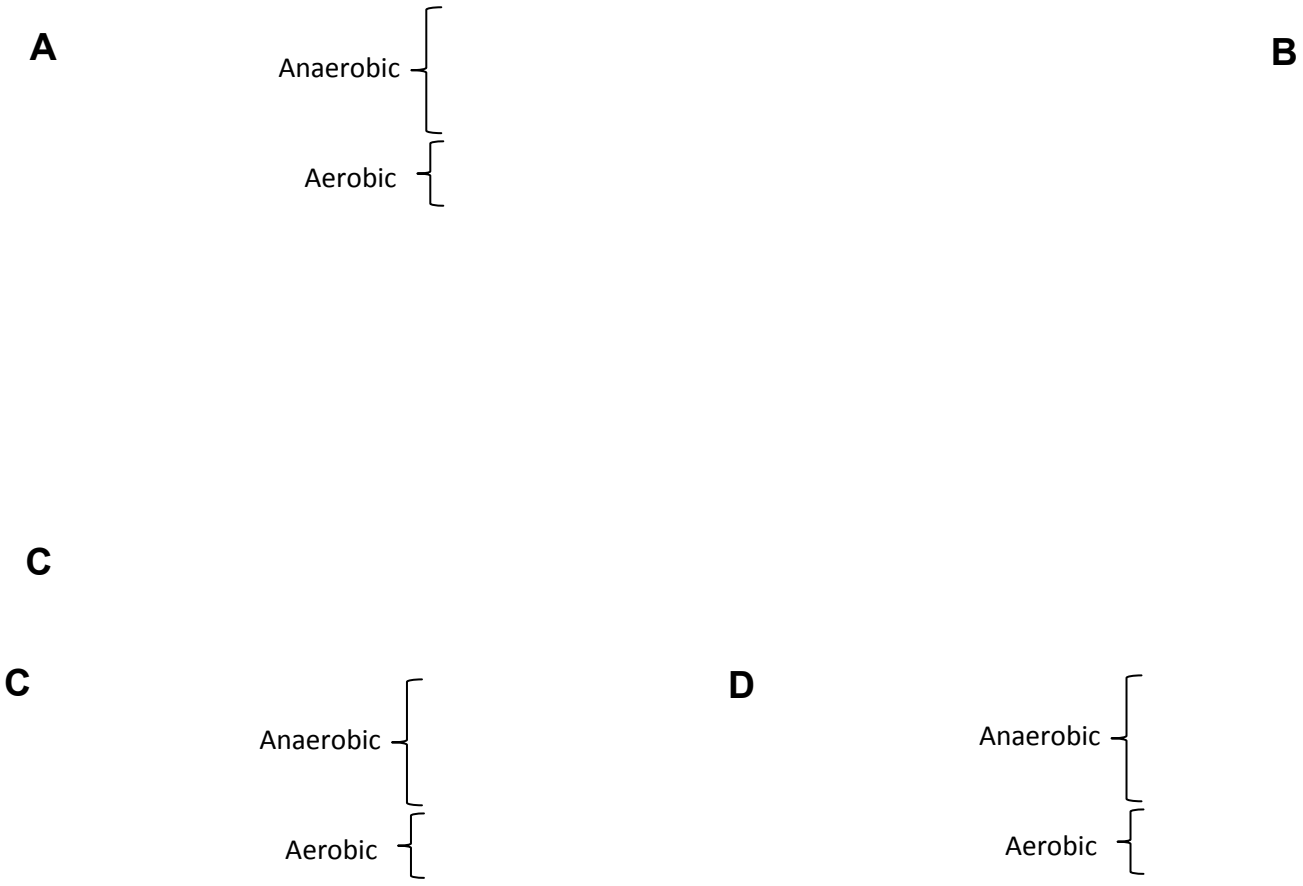


Fig. 6 Impedance of carbon steel C1145 during the 144 hours of immersion in reactor with *G. sulfurreducens* inoculated at hour 24 with; medium containing 29 mM chloride, 1 mM acetate, 10 mM of fumarate and 5 mM of phosphate. System kept in anaerobic conditions until hour 96 as indicated in the graphs. (A) Nyquist, (B) Nyquist zoom-up (C) Bode phase angle and (D) Imaginary modulus versus frequency plots

Table 7.
Biotic system: evolution in time for $R_s$, $R_{ox}$, $C_{ox}$, δ, for values at HF, and α, $R_{ct}$, $Q_{eff}$, $C_{dl}$ for values at MF-LF of the control system in aerobic conditions in a medium containing 1 mM of acetate and 10 mM of fumarate in presence of a coupon of C1145.

| Oxide HF | | | | | | | Transfer LF | | | |
|---|---|---|---|---|---|---|---|---|---|---|
| Time (h) | $R_s$ (Ωcm²) | α | $R_{ox}$ (Ω cm²) | $f_{(max)}$ (Hz) | $Q_{ox}$ μFcm$^{-2}$ | δ (nm) | α | $R_{ct}$ (Ω cm²) | $Q_{eff}$ (Ω$^{-1}$cm$^{-2}$s$^{α}$) | $Q_{dl}$ μFcm$^{-2}$ |
| 24 | 74 | 0,6 | 23 | 45562 | 1,5E-07 | 69 | 0,80 | 3542 | 2,3E-04 | 83 |
| 48 | 72 | 0,6 | 26 | 100000 | 6,1E-08 | 170 | 0,81 | 4238 | 2,2E-04 | 83 |
| 72 | 71 | 0,6 | 33 | 67500 | 7,1E-08 | 150 | 0,83 | 5140 | 2,2E-04 | 93 |
| 96 | 66 | 0,6 | 44 | 132500 | 2,7E-08 | 390 | 0,84 | 6770 | 2,1E-04 | 91 |
| 120 | 73 | 0,7 | 46 | 100000 | 3,5E-08 | 300 | 0,85 | 9860 | 1,8E-04 | 89 |
| 144 | 75 | 0,6 | 53 | 67500 | 4,5E-08 | 240 | 0,84 | 21917 | 1,4E-04 | 59 |

In the present work, the formation of vivianite by *G. sulfurreducens* using a carbon steel coupon as the electron acceptor is reported for the first time. Based on the electrochemical and surface analysis results, a hypothesis can be proposed for the mechanism of inhibitive layer formation by *G. sulfurreducens*. Initially when no oxide layers are present, dissolution of iron takes place at a low rate due to the absence of oxygen to finally forming an iron oxide layer of magnetite, $FeO*Fe_2O_3$ during the first 24 hours of immersion. An IRB such as *Geobacter* may switch from using an organic compound such as fumarate, as the sole electron acceptor to a more efficient source of electron acceptor such as Fe(III), to increase the limited amount of ATP [16]. Thus, once *G. sulfurreducens* is inoculated, it starts interacting with the iron oxide aiming to reduce Fe (III) to Fe (II) as it follows:

$$FeO*Fe_2O_3 + 3\ HPO_4^{2-} + 8H^+ + 2e^- \xrightarrow{\text{bacteria}} 3\ Fe(HPO_4) + 4\ H_2O \qquad \text{(Eq. 6)}$$

$$3\ Fe(HPO_4) \rightarrow Fe_3(PO_4)_2 + (HPO_4)^{2-} + 2H^+ \qquad \text{(Eq.7)}$$

The formation of insoluble iron phosphate depends on the metal ions present in solution at the interface, the concentration of phosphate ions in the solution, and the reactivity of metal surface.

## 3. Conclusions

The presence of *Geobacter sulfurreducens* in phosphate medium induces the formation of a compact layer of iron (II) phosphate on the surface of carbon steel C1145 immersed in a medium containing 1 mM of acetate 10 mM of fumarate and 5 mM of phosphate. Indeed, SEM and EDX analysis showed a formation of this iron (II) phosphate layer (allegedly vivianite) in the system where bacteria was inoculated whereas in the control system there was an iron oxide all over the coupon. The formation of the phosphate layer is assured only when the departing potential of the system is on the range 750 to 800 mV vs. Ag/AgCl. This layer maintains the stability of the open circuit potential even after air is allowed to enter into the system so that, it prevents from an acceleration of the cathodic reaction rate and then from an acceleration of corrosion. In contrast, the iron phosphate layer was not formed in the control systems in absence of bacteria which allowed an increment of the open circuit potential up-to 400-450 mV once oxygen entered.
EIS showed similarities in the behaviour of systems with and without bacteria. However, observations concluded that the iron (II) phosphate layer formed in presence of bacteria is fairly more protective than the iron oxide formed in absence of it without being a passive layer. ICP analysis for total iron proved that in absence of bacteria the quantity of iron dissolved into the medium is two-fold the amount of iron when bacteria is present.
Iron (II) phosphate layers such as vivianite $Fe_3(PO_4)_2*8H_2O$ are known to protect metals by forming a barrier between the surface and the surroundings. The layer could have been

formed due to an acceleration of Fe (III) reduction to Fe (II) which in contact with the phosphate in the medium forms this species.
In conclusion, *Geobacter sulfurreducens* indeed protected carbon steel AISI C1145 against corrosion in the conditions described, thanks to the formation of iron (II) phosphate layer which protected the metal against the oxidant action of oxygen.

**Acknowledgments**

The research leading to these results has received funding from the European Community's Seventh Framework Programme (FP7/2007-2013) under grant agreement n° 238579. Project website: www.biocor.eu/ip2
The author would like to thank Dr. Alain Bergel from the Laboratoire de Genie Chimique in Toulouse for the helpful discussions about this paper.

**References**

[1] I. Beech, C. C. Gaylarde, Recent advances in the study of biocorrosión: an overview, Revista de Microbiología, 30 (1999). 177-190, ISSN 0001-3714.
[2] S. Chongdar, G. Gunasekaran, P. Kummar, Corrosion inhibition of mild steel by aerobic biofilm, Electrochem. Acta. 50(2005) 4655-4665.

[3] M. Mehanna, R. Basseguy, M-L. Delia, A. Bergel, *Geobacter sulfurreducens* can protect 304L stainless steel against pitting in conditions of low electron acceptor concentrations, Electrochem. Commun. 12 (2010) 724-728

[4] H-P. Volkland, H. Harms, B. Müller, G. Repphun, O. Wanner, A. J. B. Zehnder, Bacterial phosphating of mild (unalloyed) steel, Appl. Environ. Microbiol 66 (2000) 4389-4395.

[5] H-P. Volkland, H. Harms, A. J. B. Zehnder, Corrosion protection by anaerobiosis, Water Sci. technolo. 44 (2001) 103-106.

[6] Y. Gourbeyre, E. Guilminot, F. Dalard, Study of the corrosion layer on iron obtained in solutions of water-polyethilene glycol (PEG400)- Sodium phosphate, J. Mater. Sci. 38 (2003)1307-1313

[7] R. Zuo, Biofilms: strategies for metal corrosion inhibition employing microorganisms, Appl. Environ. Microbiol. 76 (2007) 1245-1253

[8] H. Videla, L. K. Herrera, Understanding microbial inhibition of corrosion. A comprehensive overview, Intern. Biodeterior. Biodegrad. 63(2009) 869-900

[9] H. Videla, Manual of Biocorrosion, CRC-Press; first ed., USA, 1997

[10] S. Da Silva, R. Basseguy, A. Bergel, Hydrogenase-catalysed deposition of vivianite on mild steel, Electrochem. Acta. 49 (2004) 2097-2103

[11] M. Mehanna, R. Basseguy, M-L. Delia, L. Girbal, M. Demuez, A. Bergel, New hypothesis for hydrogenase implication in the corrosion of mild steel, Electrochem. Acta. 54 (2008) 140-147

[12] H-P. Volkland, H. Harms, K. Kauffman, O. Wanner, A. J. B. Zehnder, Repair of damaged vivianite coatings on mild steel using bacteria, Corr. Sci. 43 (2001) 2135-2146.

[13] F. S. Islam, R. L. Pederick, A. G. Gault, L. K. Adams, D. A. Polya, J. M. Charnock, J. R. Lloyd, Interactions between the Fe (III)-Reducing bacterium *Geobacter sulfurreduscens* and Arsenate, and capture of the metalloid by biogenic Fe(II), Appl. Environ. Microbio. 71 (2005) 8642-8648

[14] D. R. Lovley, E. J. P. Phillips, Novel mode of microbial energy metabolism: Organic carbon oxidation coupled to dissimilatory reduction of iron or manganese, Appl. Environ. Microbiol. 54 (1988) 1472-1480

[15] D. Bond, D. R. Lovley, Electricity production by *Geobacter sulfurreducens* attached to electrodes, Appl. Environ. Microbiol. 69 (2003) 1548-1555

[16] L. K. Herrera, H. Videla, Role of iron-reducing bacteria in corrosion and protection of carbon steel, Intern. Biodeterior. Biodegrad.63 (2009) 891-895

[17] M. Dubiel, C. H. Hsu, C. C. Chien, F. Mansfeld, D. K. Newman, Microbial iron respiration can protect steel from corrosion, Appl. Environ. Microbiol. 68(2002) 1440-1445

[18] B. Little, P. Wagner, K. Hart, R. Ray, D. Lavoie, K. Nealson, C. Aguilar, The role of metal-reducing bacteria in microbiologically influenced corrosion, Corr. Paper no. 215. NACE International, Houston, TX.

[19] K. Konhauser, Bacterial iron biomineralisation in nature, FEMS Microbiol. Rev. 20: (1997) 315-326

[20] M. Mehanna, R. Basseguy, M-L. Delia, A. Bergel, Effect of *Geobacter sulfurreducens* on the microbial corrosion of mild steel, ferritic and austenitic stainless steels, Corr. Sci. 51 (2009) 2596-2604

[21] Deutsche Sammlung von Mikroorganismen und Zellkulturen DSMZ GmbH, Microorganisms, 826. Geobacter medium, 2007

[22] C. Dumas, R. Basseguy, A. Bergel, Electrochemical activity of *Geobacter sulfurreducens* biofilms on stainless steel anodes, Electrochem. Acta. 53 (2008) 5235-5241

[23] D. Jones, Principles and Prevention of Corrosion, second ed., Prentice Hall, New York, 1995

[24] D. P.Lies, M. E. Hernandez, A. Kappler, R. E. Mielke, J. A. Gralnick, D. K. Newman, *Shewenella oneidensis* MR-1 uses overlapping pathways for iron reduction at a distance and by direct contact under conditions relevant for biofilms, Appl. Environ. Microbiol. 71(2005)4414-4426

[25] D. R. Loveley, Magnetite formation during microbial dissimilatory iron reduction, in: R.B. Frankel, and R. P. Blakemore (Eds.), Iron Biominerals, Plenum, New York, 1991, pp. 51-166

[26] D. Lovley, Dissimilatory Fe(III) and Mn(IV) reducing prokaryotes, in: M. Dworkin, S. Falkow, E. Rosenberg, K-H. Shleifer, E. Stackebrandt. Springer (Eds.) The Prokaryotes, a handbook on the biology of bacteria, N. Y., USA, 2(2006) 635-658

[27] O. Benali, M. Abdelmoula, P. Refait, and J-M. R. Genin, Effect of Orthophosphate on the oxidation products of Fe(II)-Fe(III) hydroxycarbonate : The transformation of green rust to ferryhydrite, Geochim. Cosmochim. Acta, 65 (2001) 1715-1726

[28] CS Hsu, F Mansfeld Concerning the Conversion of the Constant Phase Element Parameter Yo into a Capacitance, *Corrosion*, **57**(2001) 747.

[29] R. B. Frenkel and D. A. Bazylinski, In: Biomineralization (reviews in Mineralogy Vol. 54), P. M. Dove, J. J. De Yoreo, and S. Weiner (eds.), Mineralogical Society of America, Washington, D.C.; pp 217-247, 2003

[30] F. Mansfeld, The interaction of bacteria in metal surfaces, Electrochem. Acta 52 (2007) 7670-7680

[31] F. Mansfeld H. Hsu, D. Ornek, T. K. Wood, Corrosion control using regenerative biofilms on Aluminium 2024 Brass in different media, J. Electrochem. Soc. 149(2002) B130-B138

[32] J. Duan, S. Wu, X. Zhang, G. Huang, M. Du, B. Hou, Corrosion of carbon steel influenced by anaerobic biofilm in natural seawater, Electrochem. Acta, 54(2008) 22-28

[33] B. J. Little, J. S. Lee, R. I. Ray, The influence of marine biofilms on corrosion: A consice review, Electroch. Acta. 54(2008):2-7

[34] R. Javaherdashti, Microbially Influenced Corrosion – An Engineering insight-, Springer (Eds), (2008), London

[35] M. Eashwar, S. Maruthamuthu, S. Sathiyanarayanan, S. Balarkrishnan, The ennoblement of stainless alloys by marine biofilms –The neutral pH and passivity enhancement model-, Corr. Scienc. 37(1995):1169-1176

[36] J. B. Little, R. Ray, A perspective of corrosion inhibition by biofilms, *Corrosion*, 58(2002): 424-428

[38] P. Ghods, O. B. Isgor, J. R. Brown, F. Bensebaa, XPS depth profiling study on the passive oxide film of carbon steel in saturated calcium hydroxide solution and the effect of chloride on the film properties, App. Surf. Sci., 257, 10(2011):4669-4677

[39] O. Girčienė, R. Ramanauskas, L. Gudavičiūtė, A. Martušienė, Inhibition Effect of Sodium Nitrite and Silicate on Carbon Steel Corrosion in Chloride-Contaminated Alkaline Solutions, Corrosion: 67(2011):125001-1-125001-12.

[40] A. J. Bard, L. R. Faulkner, Electrochemical methods: Fundamentals and applications, John Wiley and Sons, Inc. Eds., second edition, In *Introduction and overview of electrode processes*, Chapter 1, (2001).

[41] M. E. Orazem, N. Pébère, B. Tribollet, Enhanced Graphical Representation of Electrochemical Impedance Data, J. Electrochem. Soc., 153(2006) B129-B136

[42] M. E. Orazem, B. Tribollet, Electrochemical Impedance Spectroscopy, John Wiley & Sons publications, NJ, USA

[43] G.J. Brug, A.L.G. van den Eeden, M. Sluyters-Rehbach, J.H. Sluyters, The analysis of electrode impedances complicated by the presence of a constant phase element, J. Electroanal. Chem. 176 (1984) 275–295

[44] M.F. Montemor, A.M.P. Simoes, M.G.S. Ferreira, Analytical characterization of the passive film formed on steel in solutions simulating the concrete interstitial electrolyte, Corrosion 54 (5) (1998): 347–354

### III.4.2. Article 2

The second article titled **"Formation of Iron Phosphate from Carbon Steel Corrosion Products induced by *Geobacter sulfurreducens*: Thermodynamic Analysis"** consists on a thermodynamic analysis for the formation of iron (II) phosphate assisted by the presence of *Geobacter sulfurreducens*.

The work carried out aimed to explain thermodynamically the formation of the protective layer (vivianite) in presence of *Geobacter sulfurreducens*. Experiments aim to explain how the bacterium is thermodynamically able to have a potential influence on the ratio FeII/FeIII by exerting an effect on the redox potential favouring conditions for the vivianite formation. For this, redox potential measurements were carried out to find the thermodynamic conditions for the reduction from ferric to ferrous ions, theoretical thermodynamic diagrams drawn from the experimental findings to investigate how microorganisms induce the formation of an iron reduced species. Thanks to the thermodynamic analysis, it was proved that the bacteria induce the reduction of ferric to ferrous ions on the surface of the coupon and on the corrosion products by changing the redox potential from -0.25 V to –0.6 V vs Ag/AgCl in a system which corrosion potential was around-0.8 V vs Ag/AgCl; vivianite formation was only possible in the ferrous ion containing medium which, is in agreement with the hypotheses formulated in this work.

"Formation of Iron Phosphate from Carbon Steel Production Products Induced by *Geobacter sulfurreducens*: Thermodynamic analysis"

Article to be submitted

**Formation of Iron Phosphate on Carbon Steel induced by *Geobacter sulfurreducens*: A Thermodynamic Analysis.**

Omar Rosas*, Claudia Cote and Régine Basseguy
*Laboratoire de Génie Chimique CNRS-INPT, 4 Allée Emile Monso, 31030, Toulouse, France*

**Abstract**

In the present work, a thermodynamic analysis for the formation of iron (II) phosphate in presence of *Geobacter sulfurreducens* is carried out. *G. sulfurreducens* is known to be an iron reducing bacteria able to reduce Fe(III) to Fe(II) ions coupled with the oxidation of acetate to carbon dioxide. The high availability of Fe(II) ions caused by the bacteria promotes the formation of an iron (II) phosphate layer. The phosphate layer is believed to be formed by the combination of decreasing the redox potential in the solution and the direct electron transfer bacteria/corrosion products. The phosphate layer was formed only when bacteria was present and not in the control experiments.

*Keywords:* Biocorrosion, carbon steel corrosion, vivianite, *Geobacter sulfurreducens*.

## 1. Introduction

Microbial development occurs in almost all environments and it can be responsible for the production of different compounds which formation is not possible in abiotic conditions. In biological mineralisation, the bacteria produce bio-minerals commonly generated as a secondary event from interactions between the microorganisms and their surroundings; when the conditions are propitious, biogenic iron minerals are particularly common products of biological mineralization because of their relatively high concentration in the earth"s crust [1]. In corrosion, the formation of certain compounds is crucial since they contribute to accelerate or to decrease the corrosion rate. The presence of bacteria changes the environmental conditions to induce the formation of species that are not found in abiotic conditions and affect the corrosion extent; it is therefore of prime importance to analyze the effect of microorganism in the formation of bio-compounds affecting the corrosion of metals.

Dissimilatory metal-reducing bacteria are well recognized for their ability to use a number of diverse oxidized metal ions as terminal electron acceptors [1]; this includes the oxides produced in the corrosion process. Dissimilatory iron reducing microorganisms respire with oxidized iron, Fe(III), usually in the form of amorphous Fe(III) oxyhydroxide [1,2] or crystalline iron oxides such as goethite, hematite, etc. Under anaerobic conditions, the Fe(II) ions produced in the Fe(III) reduction have subsequent interactions with other ions to form several minerals. Iron reducing bacteria are known to induce the precipitation of magnetite ($Fe_3O_4$), siderite ($FeCO_3$) and vivianite ($Fe_3(PO_4)_2*8H_2O$) depending on the environmental conditions [3].

Vivianite is an iron (II) phosphate that has been used as a corrosion inhibiting agent due to its low solubility properties [4, 5]; however, these processes are carried out in abiotic conditions. Biologically produced vivianite has been reported under anaerobic conditions; Islam *et. al*. [6], reported vivianite formation by *Geobacter sulfurreducens* using iron citrate as electron acceptor, Da Silva *et. al.* [7], and Mehanna [8] observed a vivianite deposite on mild steel electrodes placed in a galvanic cell which had been catalysed by hydrogenase from *C acetobutylicum* and also in presence of *Geobacter sufurreducens.* These findings represent corrosion processes induced by specific microorganisms and they are indeed of great consideration regarding the corrosion phenomenon.
Members of the Gebacteraceae family are the predominant dissimiliatory Fe(III) reducers in a diversity of environments in which Fe(III) reduction is coupled with the metabolism of organic compounds. The insolubility of Fe(III) oxide requires that electrons be transferred outside the cell; previous studies have demonstrated that Geobacter species have to establish direct

contact with insoluble Fe (III) iron for dissimilatory Fe(III) reduction [9, 10, 11]. Since *Geobacter sulfurreducens* is a ubiquitous species in sediments and soils, it can have a relevant effect where a high amount of corrosion products is present; e.g. from buried industrial equipment, off-shore and harbour structures, oil and gas pipelines, and buried storage tanks [12].

The present work is carried out to investigate under which conditions *Geobacter sulfurreducens* is able to produce iron (II) phosphate from corrosion products. Redox potential measurements are carried out to find the thermodynamic conditions for the reduction from ferric to ferrous ions; theoretical thermodynamic diagrams are use coupled to the experimental findings to investigate how the microorganism induces the formation of an iron reduced species.

## 2. Experimental procedure

### *2.1. Bacteria and media*

The *Geobacter sulfurreducens* ATCC 1745 strain used for the experiments was obtained from DSMZ. The media and solutions were prepared following the DSMZ protocol [13]. The growth of bacteria for electrochemical tests followed previous procedures found in the literature [8, 14, 15]. For all the tests, the inoculation was done after 24 hours of starting the experiments; the blank/control reactors were also inoculated with filtrated medium to maintain the bacterial metabolites in the medium but not the cells.

### *2.2. Electrochemical measurements and experimental system*

The anaerobic conditions in the 500 mL reactors were obtained by injecting $N_2/CO_2$ (80:20) for at least 60 min before inserting the metal coupons. The flow of $N_2/CO_2$ was maintained during the whole experiment unless stated otherwise. The temperature for all the tests was kept at 30°C during experiments.

The working electrodes (WE) were 2 cm diameter cylinders of carbon steel AISI C1145. The WE was covered by a polymeric coating (thermo-contractible polyolefin, ATUM ®) exposing one flat face to the electrolyte. Electrical connections were made through isolated titanium wire. The electrodes were polished with SiC paper with a 600 grit surface finishing followed by cleaning with ethanol (70%) and throughout rinsing with sterile distilled water. The nominal chemical composition for the steel C1145 is shown in Table 1.

Table1.
Alloying elements of AISI C1145 (wt %)

| *Alloy* | *Ni* | *C* | *Mn* | *Cu* | *Si* | *S* | *P* | *Mo* | *Cr* |
|---|---|---|---|---|---|---|---|---|---|
| 1145 | 0.1 | 0.46 | 0.65 | 0.11 | 0.31 | 0.03 | 0.01 | 0.02 | 0.1 |

A platinum (Pt) grid (Pt, Ir 10%) was used for redox measurements and a silver wire coated with silver chloride (Ag/AgCl) was used as reference electrode (RE). Electrochemical measurements were performed using a multipotentiostat (VMP-Bio-Logic), The Open circuit potential (OCP) in function of time was measured for all the experiments for the WE and redox potential was measured at the same time on the Pt wire.

### *2.3. Analytical techniques*

Iron in solution was determined using Inductively Coupled Plasma (ICP). 20 mL of the sample were used to determine the total iron content

*2.4. Surface analysis*

Scanning Electron Microscopy (SEM) pictures were taken using a TM3000 Hitachi Analytical Table Top Microscope at 7000x magnification working at 5 and 15 kV acceleration voltage. The coupons were washed with distilled water and dried and stored in a $N_2$ atmosphere. Energy dispersive x-ray spectroscopy (EDX) was used for elemental analysis on the surface of the coupons.

*2.5. Thermodynamic Data*

Table 2 shows the thermodynamic data used for the calculation of the speciation diagrams and the stability diagrams. The stability diagrams were used to determine the thermodynamic or redox conditions that are favourable for species to exist. Based on the analysis of these diagrams, a hypothesis on the formation of compounds was carried out. In addition, the diagrams were used to determine the likely pattern of formation of corrosion products.

## 3. Results and Discussion

*3.1. Open circuit potential and Redox potential*

During the first 24 hours, both systems, abiotic and bacterial, are identical and the OCP remained stable. When the inoculation was carried out after 24 hours, a small increment in potential was observed in the reactors containing bacteria, however, this small increment was no considerable and the potential remained stable until the end of the test (144 hours).

Both systems showed a stable potential during the first 96 hours; at this point, air was allowed to enter in the reactors. Figure 1 shows that the potential in the abiotic system increased about 300 mV when air entered in the reactor. On the contrary, for the system containing bacteria, the potential remained without any change even after air entered in the reactor. This test was repeated several times offering the same response.

Table 2.
Thermodynamic data for iron, phosphate, and carbonate species [16].

| *Species* | $\Delta G^0$*(KJ mol$^{-1}$)* |
|---|---|
| $H_2O$ | -236.96 |
| $H_3PO_4$ | -1111.69 |
| $H_2PO_4^-$ | -1130.30 |
| $HPO_4^{2-}$ | -1089.26 |
| $PO_4^{3-}$ | -1018.80 |
| $Fe^{2+}$ | -84.20 |
| $Fe^{3+}$ | -10.52 |
| $Fe_3O_4$ | -1014.2 |
| $Fe_2O_3$ | -742.24 |
| FeOOH | -490.40 |
| $FePO_4*2H_2O$ | -1657.5 |
| $Fe_3(PO_4)_2*8H_2O$ | -4375.3 |
| $CO_{2(aq)}$ | -386.02 |
| $H_2CO_3$ | -622.82 |
| $HCO_3^-$ | -586.85 |
| $CO_3^{2-}$ | -527.90 |
| $FeCO_3$ | -666.72 |

The small increment of OCP right after inoculation was also found by Mehanna *et., al.* [12], (32 mV) on experiments with *G. sulfurreducens* in a similar medium. In that work, a small increment in OCP three hours after inoculation of bacteria was observed, this increment was followed by a larger increment of 200 mV in the next few hours. When observing the surface of the metallic coupons, large zones with cell growth were found; the authors concluded that these zones were cathodic electron transfer regions protecting the metal against corrosion.

Opposite to the OCP results, the redox potential measurement showed a large variation during the experiment for the bacterial systems. The redox potential was measured on the platinum wire under the exact same conditions than the OCP for carbon steel; during the first 96 hours, anaerobic conditions were kept, then, air was allowed to enter to the reactor. At 120 hours, air flow was stopped and the reactor was sealed again until the end of the test at 144 hours. The results for the redox potential measurement can be observed in Figure 2

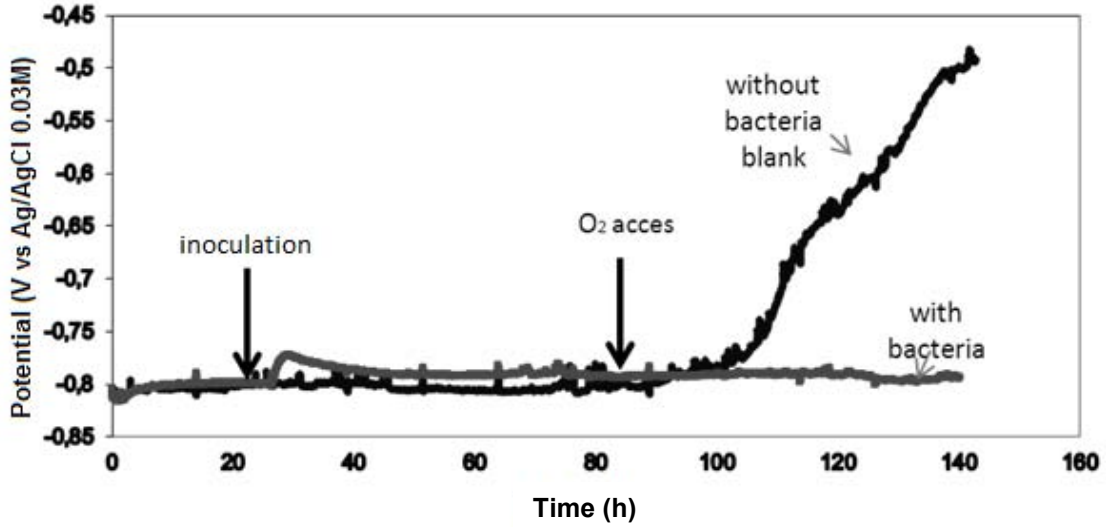


Figure 1. Variation of OCP of mild ca[illegible] C1145 with 5% *G. sulfurreducens* and without bacteria using different concentration of electron acceptor. Medium containing 1 mM sodium acetate (electron donor) and 25 mM of sodium fumarate (electron acceptor)

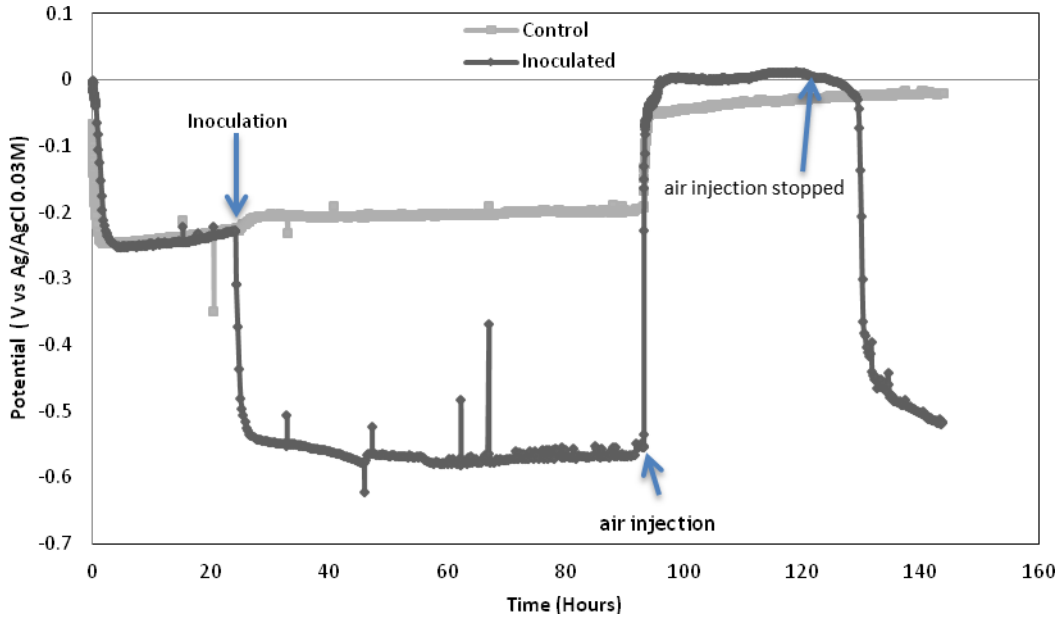


Figure. 2. Redox potential measured on a Platinum wire in a 5% *G. sulfurreducens* and without bacteria. Medium containing 1 mM sodium acetate (electron donor) and 10 mM of sodium fumarate (electron acceptor)

As it can be seen in Figure 2, the redox potential remained stable in both systems during the first 24 hours; immediately after the inoculation, the redox potential dropped 300 mV in the systems with bacteria and it remained around -0.55 V (vs Ag/AgCl 0.03M) until air is allowed to enter in the reactor. For the abiotic reactor there is no change in redox potential after inoculating the metabolites which indicated that bacterial attachment may cause the potential drop. After air is allowed to enter, both systems reach almost the same value of potential, which was expected since the main cathodic reaction will be the reduction of oxygen; however, after the bubbling was stopped and the reactors were sealed, the system with bacteria went back to the more negative values of potential, this means that even after the contact with oxygen for 36 hours, the biological system keeps the redox potential in low values.

According to equilibrium thermodynamics, as the redox potential decreases, the equilibrium Fe(III)/Fe(II) shifts in favour of Fe (II). In the redox model, as microbial metabolism lowers the redox potential, Fe(III) is non-enzymatically converted to Fe(II) in order to maintain the equilibrium. On the other hand, the experiments carried out with the bacterial metabolites did not change the redox potential in the solution; in the redox potential mechanism, this would be enough reason for dropping the redox potential. Instead, it was believed that the mechanism followed for the reduction of Fe(III) to Fe (II) is the direct reduction model, where the contact of the cells with insoluble Fe(III), is what produces the reduction from ferric to ferrous ions, which was also found in previous work [1, 2, 17].

An experiment was designed to test the direct reduction model; a dialysis membrane with a porosity of 6 kD was used to cover the electrodes, this size would be enough to avoid the pass of bacteria since it is equivalent to less than 0.1 μm; the main idea is to elucidate weather the redox potential drop is caused by the attachment of bacterial cells to the electrode or by the metabolic processes in the cells. The results are shown in Figures 3-5.

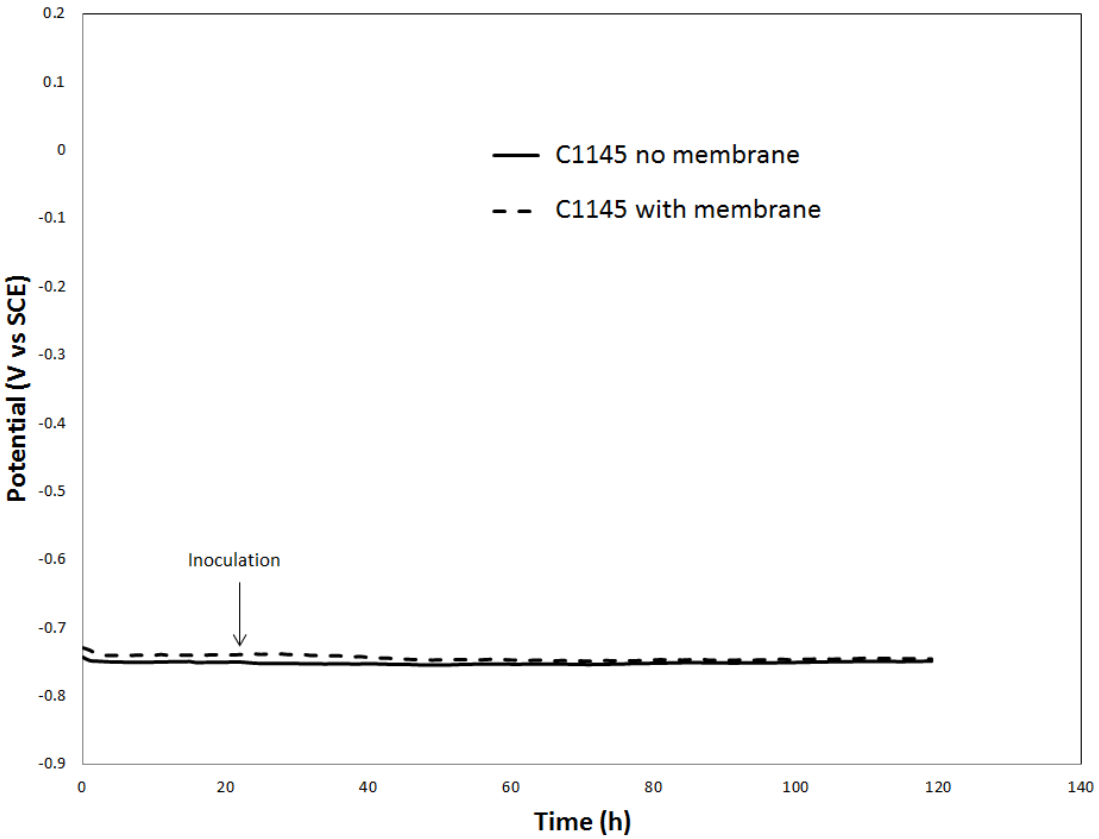


Figure 3. Comparison of OCP for carbon steel coupons with and without bacterial attachment.

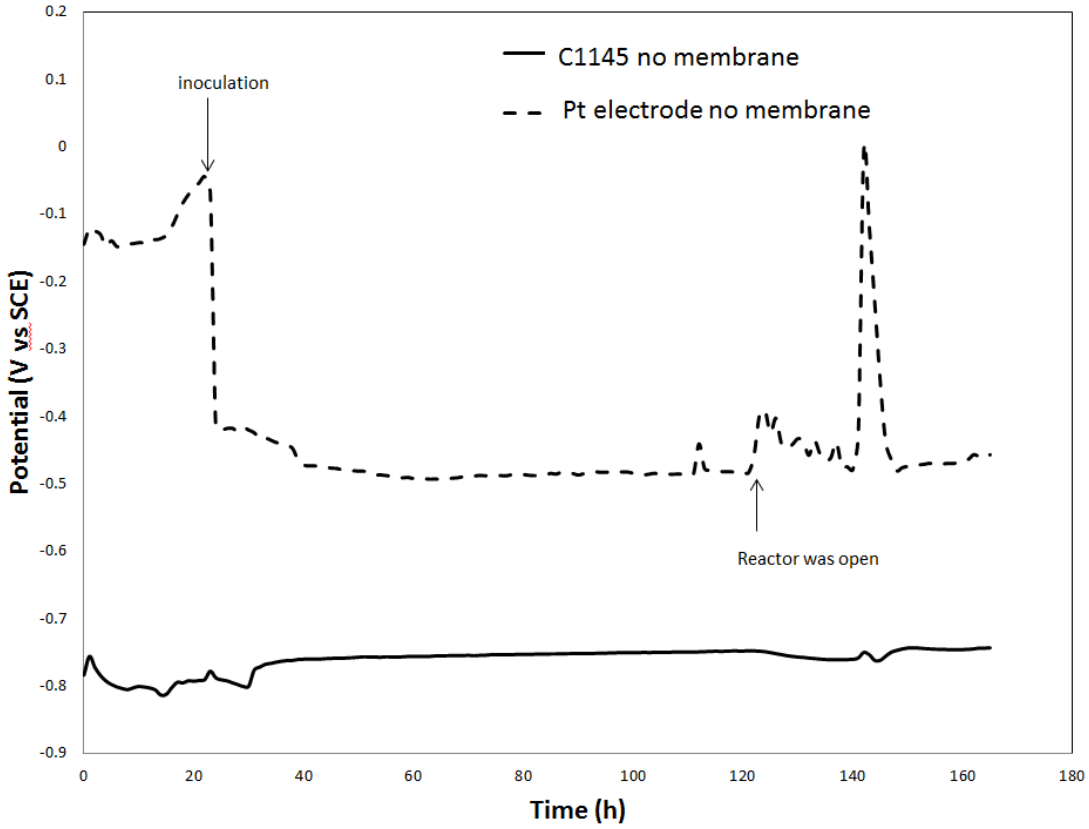


Figure 4. OCP for carbon steel C1145 without membrane and redox potential measurement with Pt electrode. Bacterial attachment was allowed in both surfaces.

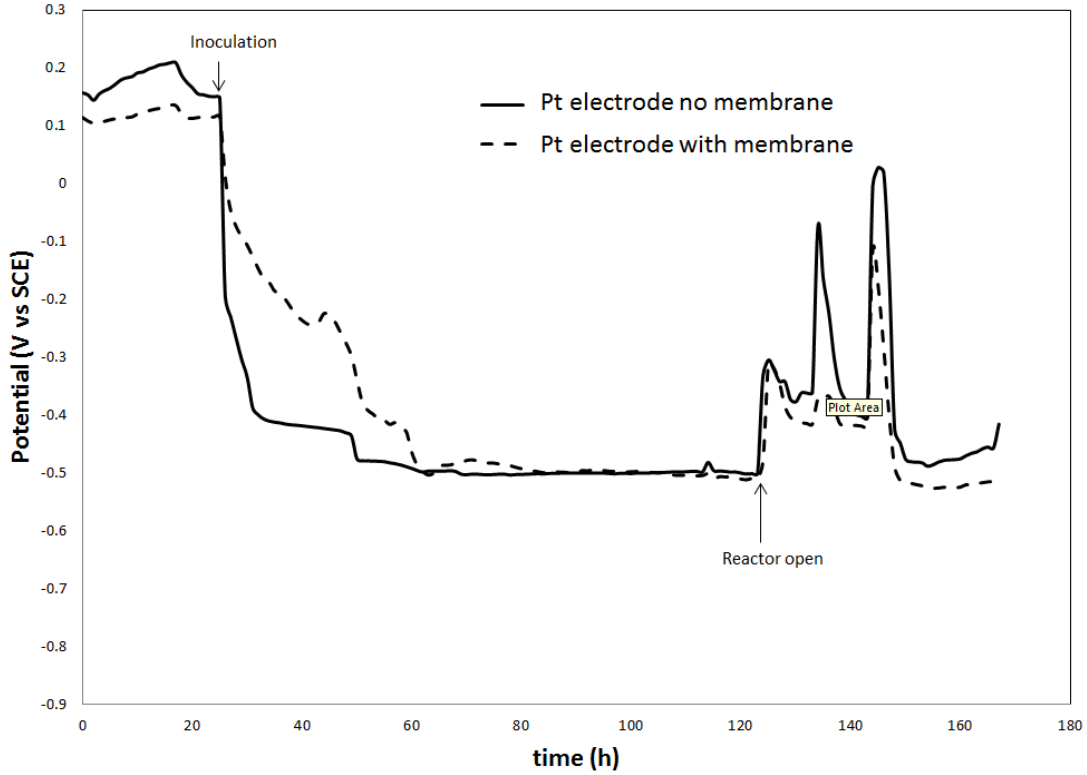


Figure 5. Comparison of redox potential measurement for Pt electrodes with and without bacterial attachment.

As it is shown in Figure 3, the bacterial attachment has no effect on the OCP for the carbon steel and this value is around -0.75 $V_{SCE}$ for both systems even after inoculation. It is important to point out that the electrode potential (corrosion potential) is not a measure of the potential of the environment, some changes produced on the electrode surface may not produce electric signals that is detectable by OCP measurements. The change in the redox potential without affecting the OCP is shown in Figure 4; here, it is clear how the inoculation changes the redox conditions, which is indicated by the Pt electrode, but the OCP for the carbon steel remains stable. After inoculation, the OCP value remains around -0.78 $V_{SCE}$ but the redox potential drops from -0.1 V to -0.5 $V_{SCE}$. In this experiment it was thought that perhaps the bacterial attachment to the Pt electrode was causing the change in redox conditions so that, different experiments placing two Pt electrodes, one with membrane and the other one without membrane were carried out; in Figure 5 it is observed the effect of bacterial attachment on the measurement of redox potential. The redox potential measurement is very similar in both electrodes however; it is clear from Figure 5 that the electrode with bacterial attachment registers an immediate potential drop while the electrode without bacterial settlement reaches the minimum of redox potential (-0.5 V vs SCE) nearly 40 hours after inoculation. This latter experiment shows that the bacteria exchange electrons with the substrate but also changes the environmental conditions by metabolic functions.

*3.2. Surface Analysis*

Macroscopy observations (Figure 6) performed to the coupons after 144 hours of immersion showed that on the surface of the coupon without bacteria there was a black layer which turned into yellow after several minutes in contact with air, typical of iron oxides in anaerobic to aerobic corrosion (Figure 6, upper left); whereas on the coupon with bacteria there was a poorly conductive grey layer (Figure 6 lower left) that maintained its physical characteristics even after the contact with atmospheric air. It is important to point out that the layer formed in

presence of bacteria kept its physical appearance even after several weeks of being stored in an open to the atmosphere container.

SEM observations showed that the surface of coupons coming from control experiments (no bacterial cells) exhibited uniform corrosion features; clusters of sponge-like structures exposing stripes of the metallic structure (Figure 6 upper right). In contrast, the coupons exposed to the bacterial cells showed a needle-like layer distributed homogeneously on the surface of the coupon with random distribution of what it seems to be a crystallographic well defined mineral (Figure 6 lower right). These observations suggested that the grey layer of the coupon in presence of bacteria was a phosphate layer, most likely the mineral vivianite as it was found in previous work [8], and that the surface layer of the control coupons was mainly iron oxide.

Surface analysis using energy dispersive x-ray spectroscopy (EDX) (Table 3) provided us stronger arguments to confirm that the grey layer formed on the surface of the coupon with bacteria is vivianite. Those results together with SEM observation also suggested that there was also presence of iron carbonate ($FeCO_3$) in presence of bacteria.

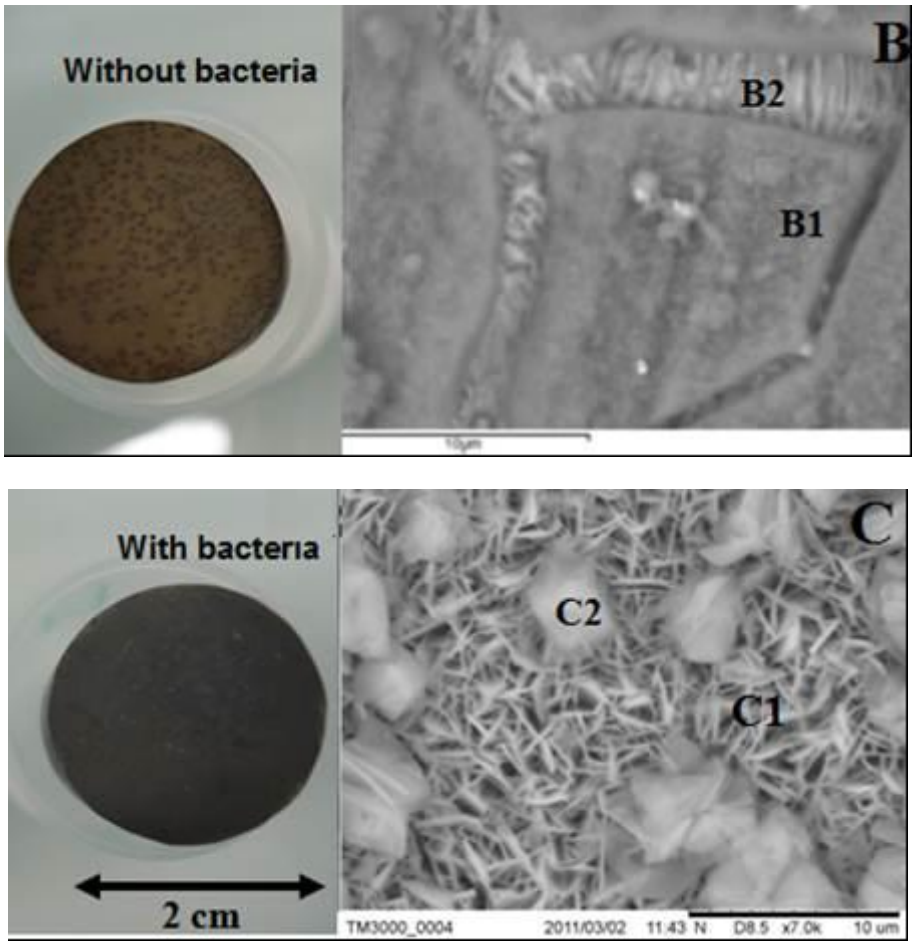


Figure 6 Macro and micro photographs of coupons after 144 hours of immersion without and with bacteria after; (B) SEM image (7000X) of blank"s coupon layer mainly iron oxide; (C) SEM image (7000X) of grey layer formed in the coupon with bacteria. B1, B2, C1, and C2 indicate the places where the composition analysis shown in Table 3 was performed.

Table 3.
EDX surface analysis of coupons after 144 hours of immersion, the number on the left of each column indicates %weight, the number in parenthesis indicates %atomic. Polished: clean coupon after polishing 600 grit (no immersion); (B1) and (B2): control coupon, (see Fig. 2B); (C1) and (C2): coupon in presence of bacteria, (see Fig. 2C). Traces of other elements are not shown in this table.

| | *As received* | *B1* | *B2* | *C1* | *C2* |
|---|---|---|---|---|---|
| **Carbon** | 4.3 (17.3) | 8.4 (15.1) | 15.0 (38.3) | 5.5 (13.4) | 22.2 (34.0) |
| **Oxygen** | 0.0 (0.0) | 46.3 (62.3) | 10.2 (19.6) | 21.3 (38.9) | 45.4 (52.1) |
| **Phosphorus** | 0.0 (0.0) | 10.5 (7.3) | 1.5 (1.5) | 18.6 (17.5) | 9.9 (5.9) |
| **Iron** | 95.7 (82.7) | 29.3 (11.3) | 72.1 (39.6) | 48.0 (25.1) | 20.0 (6.6) |

When using the membranes to avoid bacterial contact, the surface in the steel showed the same characteristics in both situations; when the bacteria attached on the substrate and when there was no attachment. As it is observed in Figure 7, both coupons showed the grey homogeneous layer on the surface however, the coupon with no bacterial contact showed also a yellow color, proper of an iron oxide. The SEM images in Figure 7 show the needle-like structure but this layer is poorly attached and not well formed in the case of no bacterial contact. These latter results indicate that the bacterial contact is not mandatory for the formation of an iron phosphate layer from corrosion products and the bacterial metabolism produce a change in redox conditions that make this phosphate species thermodynamically stable however, the formation of a homogeneous, well-formed iron phosphate layer needs the direct contact between the bacterial cells and the substrate. The composition of these layers is shown in Table 4.

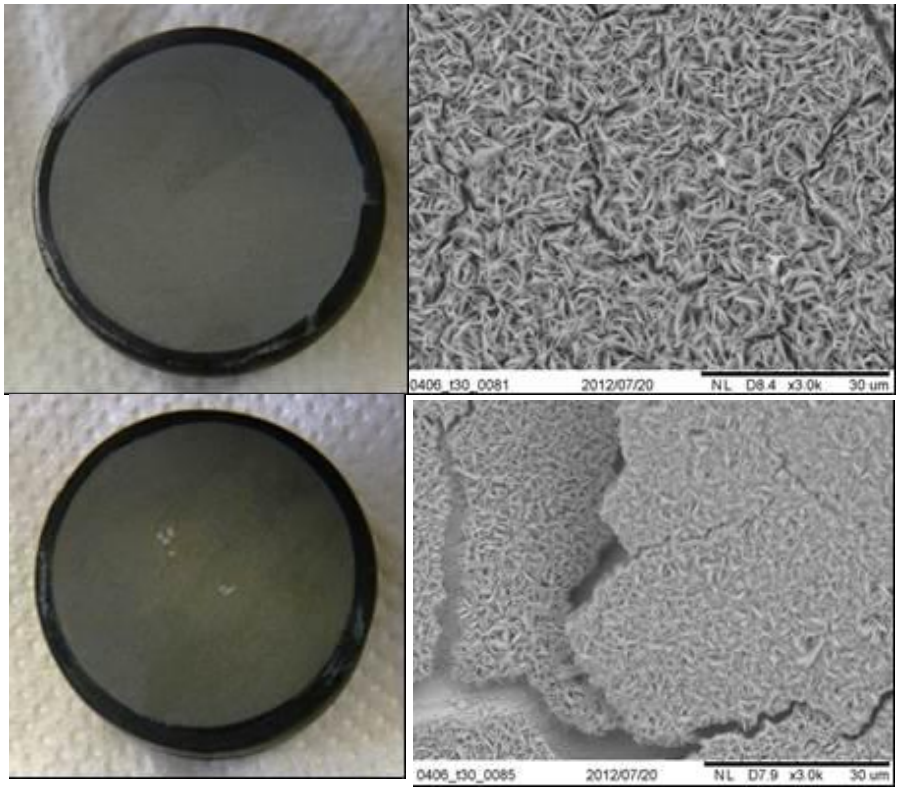


Figure 7. Macro and micro-graphs of coupons after 166 hours of immersion. Upper left; macrograph of coupon with direct bacterial contact (no membrane). Upper right; SEM image (3000X) of coupon with direct bacterial contact (no membrane). Lower left; macrograph of coupon with no bacterial contact (membrane). Lower right; SEM image (3000X) of coupon with no bacterial contact (membrane).

Table 4.
EDX general surface analysis of coupons after 166 hours of immersion, the number on the left of each column indicates %weight, the number in parenthesis indicates %atomic.

| | **No membrane** | **Membrane** |
|---|---|---|
| **Element** | % Weight (Atomic) | % Weight (Atomic) |
| **Oxygen** | 55.50 (75.54) | 53.10 (74.39) |
| **Phosphorous** | 22.72 (15.97) | 21.05 (15.97) |
| **Iron** | 21.78 (8.50) | 25.85 (10.37) |

*3.3. Thermodynamic Analysis for the formation of iron (II) phosphate*

The experimental findings of this work suggest a reduction process from ferric to ferrous ion in presence of bacteria; stability diagrams were built to analyze the likelihood of having an iron (II) phosphate layer as it is stated in this work. The first step was to determine the phosphate species that is stable in the range of pH where all the experiments took place. Since the initial and final pH in all tests was maintained between 6 and 7, $HPO_4^{2-}$ and $H_2PO_4^-$ are the most stable species. In Figure 8, the stability for $H_2PO_4^-$ in the range of pH between 6 and 7 is observed as well as the stability for a concentration of phosphate species of 0.005 M.

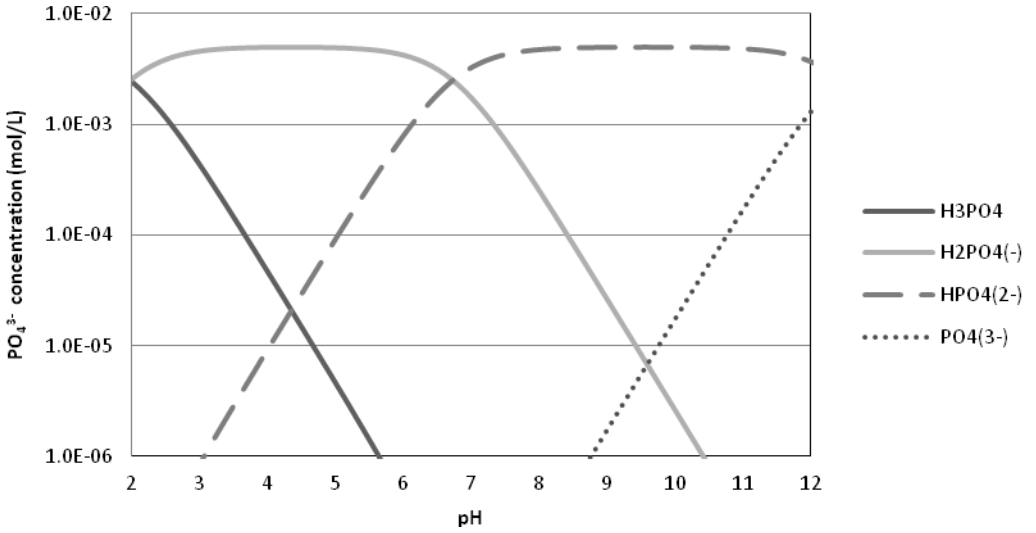


Figure 8. Stability diagram for phosphate species in function of pH. The concentration for the species is the same as the experimental concentration for the formation of the phosphate layer (0.005M) from corrosion products.

According to Frenkel [3], iron reducing bacteria can form vivianite from the reduction of ferric oxyhydroxide or goethite after several days. In the thermodynamic diagram shown in Figure 9, it is not clear at which values of potential and concentration of iron ions the conversion from goethite to vivianite is possible. If we observe the open circuit potential of Figure 1 before air entered into the system, this value corresponds to approximately -0.5 $V_{SHE}$. The formation of vivianite is dependent on the concentration of Fe(II) (dashed vertical line in Figure 9) increasing the likelihood of having vivianite when the concentration of iron ions increases. As it was mentioned before, if the bacteria attaches to corrosion precipitates to carry out the reduction of these products, it may not be registered by the OCP but for the redox potential which, represents the potential of the environment and it is much higher than the potential of the metallic coupon (Figure 2). If the bacteria induces the reduction of ferric to ferrous ions then it will also deplete the Fe(III) in the solution and there will be a much higher

availability of Fe(II). In order to find the reason how the bacteria induce the precipitation of a Fe(II) species, speciation diagrams varying the ratio Fe(II)/Fe(III) were calculated.

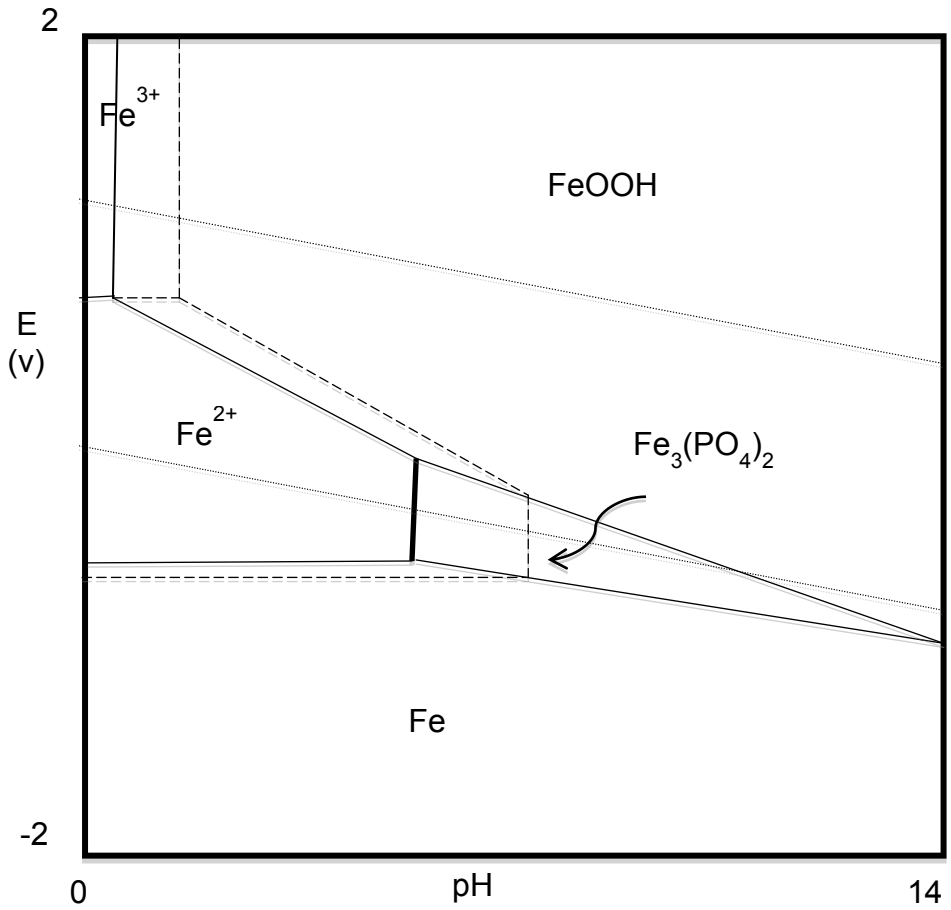


Figure 9. E vs pH diagram for goethite and vivianite. The solid lines correspond to [Fe(II)]=[Fe(III)]=$10^{-3}$M, dashed lines correspond to [Fe(II)]=[Fe(III)]=$10^{-6}$M. The concentration for the phosphate species is the experimental concentration, 0.005M

In the speciation diagrams shown in Figures 10-12, different ratio for Fe(III)/Fe(II) were used, the potentials at which these diagrams were built relies on the range of potentials shown in Figures 1-5. It is believed that at a potential of -0.2 $V_{SHE}$ and a relatively high concentration of Fe(II), the formation of vivianite is thermodynamically favorable.

As it is observed in Figure 10, if a low and equal concentration for Fe(III) and Fe(II) is used, $10^{-6}$ M, the stability of ferric species is higher than that one for ferrous species. In Figure 10 it is possible to observe Fe(III) species thermodynamically more stable than vivianite at all range of pH. Although $FePO_4*2H_2O$ is shown in the diagram, the more stable and likely species is the ferric oxyhydroxide. When increasing the concentration for both iron ions to $10^{-3}$ M, Figure 11, the same behavior is observed; this means that regardless the concentration used or the potential induced in the system, the ferric species will be more stable than the ferrous species and no Fe(II) precipitates will be found as long as both, Fe(III) and Fe(II), are in equal presence.

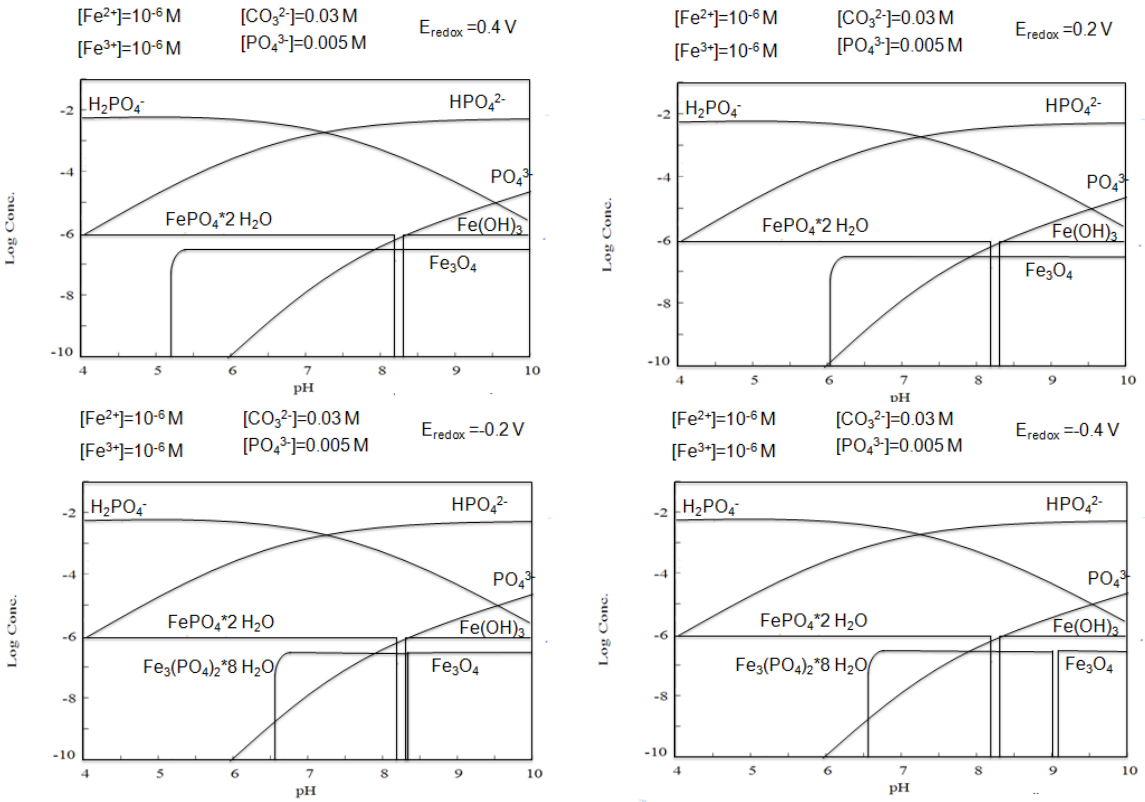


Figure 10 Log Concentration vs pH diagram for the species of Fe(II) and Fe(III) and phosphate. Top: left E=0.4 $V_{SHE}$, right E=0.2 $V_{SHE}$. Bottom: left E=-0.2 $V_{SHE}$, right E=-0.4 $V_{SHE}$. [Fe(II)]=[Fe(III)]=$10^{-6}$M; phosphate concentration is 0.005M

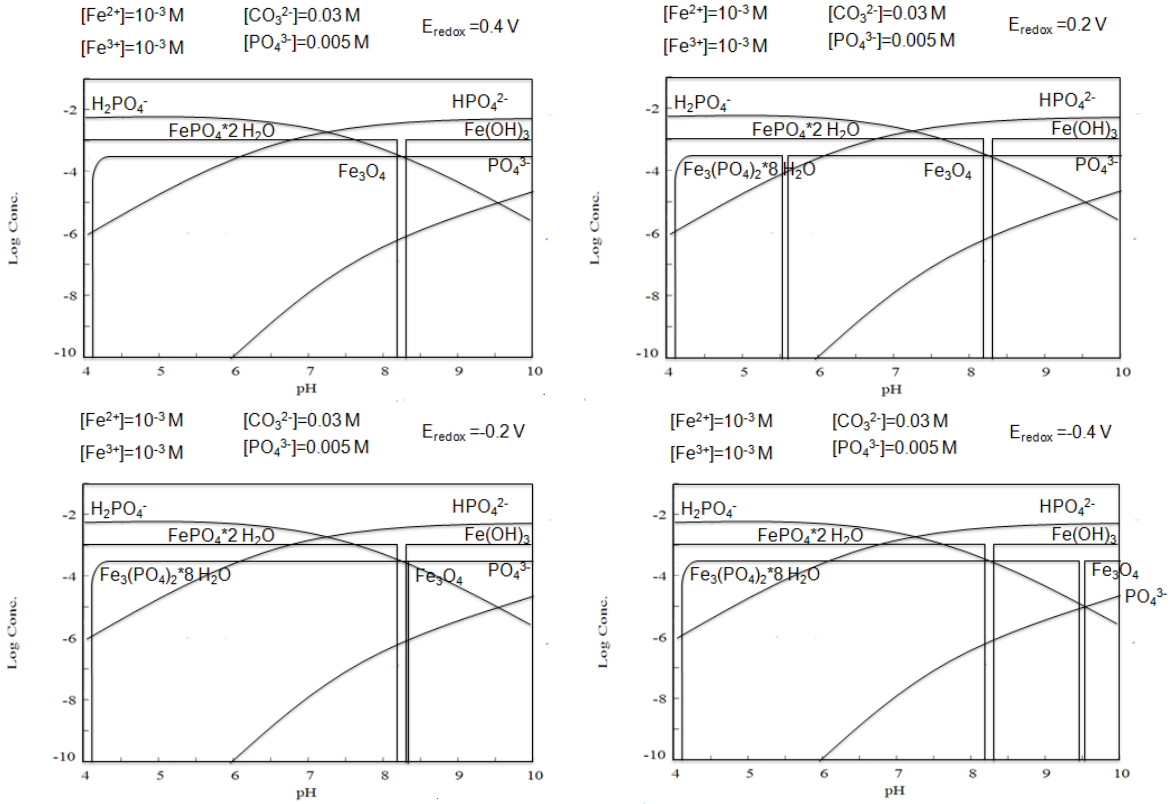


Figure 11 Log Concentration vs pH diagram for the species of Fe(II) and Fe(III) and phosphate. Top: left E=0.4 $V_{SHE}$, right E=0.2 $V_{SHE}$. Bottom: left E=-0.2 $V_{SHE}$, right E=-0.4 $V_{SHE}$. [Fe(II)]=[Fe(III)]=$10^{-3}$M; phosphate concentration is 0.005M

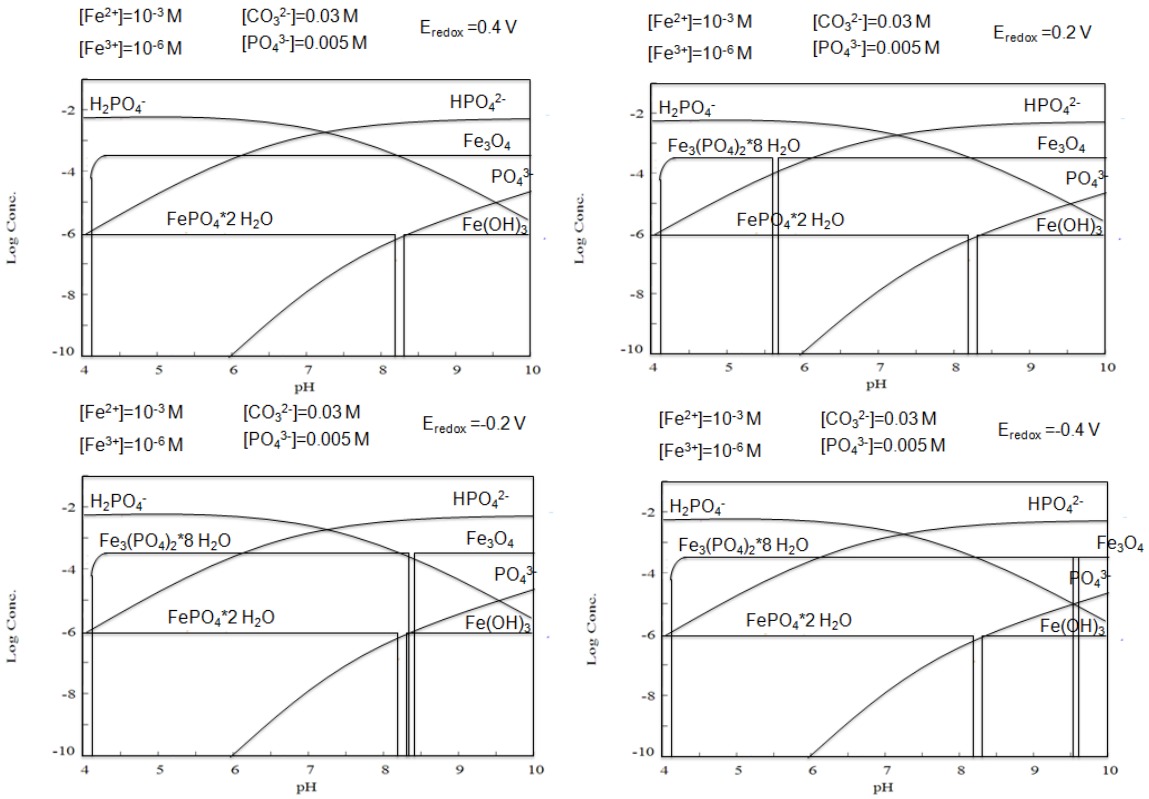


Figure 12 Log Concentration vs pH diagram for the species of Fe(II) and Fe(III) and phosphate. Top: left E=0.4 $V_{SHE}$, right E=0.2 $V_{SHE}$. Bottom: left E=-0.2 $V_{SHE}$, right E=-0.4 $V_{SHE}$. [Fe(II)]=$10^{-3}$M, [Fe(III)]=$10^{-6}$M; phosphate concentration is 0.005M

When the ferrous ions availability is higher than that one of ferric ions, an opposite effect to Figure 10 and 11 is observed. The stability of vivianite is much higher than any ferric species when the ratio Fe(II)/Fe(III) increases. Although at high potentials (0.4 $V_{SHE}$) vivianite is not observed, when the potential is lower than 0.2 $V_{SHE}$ it is the most stable compound. This analysis explains how the bacteria deplete the concentration of ferric ions and not only forms precipitates of Fe(II) (vivianite) in the surface of the carbon steel coupon, but also reduce the precipitated ferric species that are produced by the corrosion process. The thermodynamic analysis is in agreement with the experimental results and within agreement with the hypothesis presented by the authors; the bacteria reduce the ferric ions to ferrous ions which induces the formation of ferrous phosphate species.

## 4. Conclusions

Low carbon steel was exposed to a 0.005 M phosphate medium containing iron reducing bacteria (*Geobacter sulfurreducens*) to analyze the effect of the microorganism on the corrosion products.

A grey layer was found on the surface of the steel coupons in contact with the bacteria but not on those in the medium lacking of bacterial cells which, was a dark layer similar to the one normally found in anaerobic corrosion. SEM and EDX analysis showed that the grey layer found in presence of bacteria is most likely vivianite ($Fe_3PO_4*8H_2O$) while the one growth in the control experiments was an iron oxide. A thermodynamic analysis proved that the bacteria induce the reduction of ferric to ferrous ions on the surface of the coupon and on the corrosion products; vivianite formation was only possible when the ferrous ion concentration was higher than the ferric ion and the redox potential relied on a value around -0.5 $V_{SHE}$. The bacteria are reducing the corrosion products from ferric to ferrous ions, some of the reduced corrosion products are precipitated or converted to Fe(II) soluble species. The bacterial activity lowers the redox potential of the environment which produces the

spontaneous reduction of Fe(III) to Fe(II) however, the bacterial attachment onto the substrate facilitated and guaranteed the formation of a compact, homogeneous Fe(II) phosphate layer which, is in agreement with the model of the direct electron transfer from bacteria to insoluble iron species.

**Acknowledgments**

The research leading to these results has received funding from the European Community's Seventh Framework Programme (FP7/2007-2013) under grant agreement n° 238579. Project website: www.biocor.eu/ip2

**References**

[1] D. Lovley, Dissimilatory Fe(III) and Mn(IV) Reduction, Microbiological Reviews Vol. 55, No. 2, 1991

[2] D. R. Lovley, Magnetite formation during microbial dissimilatory iron reduction, In: Iron Biominerals, R.B. Frankel, and R. P. Blakemore (Eds.), Plenum, New York, pp. 151-166, 1990

[3] R. B. Frenkel and D. A. Bazylinski, In: Biomineralization (reviews in Mineralogy Vol. 54), P. M. Dove, J. J. De Yoreo, and S. Weiner (eds.), Mineralogical Society of America, Washington, D.C.; pp 217-247, 2003

[4] Y. Gourbeyre, E. Guilminot, F. Dalard, Study of the corrosion layer on iron obtained in solutions of water-polyethilene glycol (PEG400)- Sodium phosphate, J. Mater. Sci. 38 (2003)1307-1313

[5] H-P. Volkland, H. Harms, B. Müller, G. Repphun, O. Wanner, A. J. B. Zehnder, Bacterial phosphating of mild (unalloyed) steel, Appl. Environ. Microbiol 66 (2000) 4389-4395.

[6] F. S. Islam, R. L. Pederick, A. G. Gault, L. K. Adams, D. A. Polya, J. M. Charnock, J. R. Lloyd, Interactions between the Fe (III)-Reducing bacterium *Geobacter sulfurreduscens* and Arsenate, and capture of the metalloid by biogenic Fe(II), Appl. Environ. Microbio. 71 (2005) 8642-8648

[7] S. Da Silva, R. Basseguy, A. Bergel, Hydrogenase-catalysed deposition of vivianite on mild steel, Electrochem. Acta. 49 (2004) 2097-2103

[8] M. Mehana, Mécanismes de transfert direct en corrosion microbienne des acier: Application à *Geobacter sulfurreducens* et à l'hydrogénase de *Clostridium acetobutylicum*, PhD Thesis, Université de Toulouse, 2009.

[9] S. E. Childers, S. Ciufo, and D.R. Lovley, *Geobacter metallireducens* accesses insoluble Fe(III) oxide by chemotaxis, Nature 416 pp.767-769, 2002

[10] K.P. Nevin, and D.R. Lovley, Lack of production of electron-shuttling compounds or solubilization of Fe(III) during reduction of insoluble Fe(III) oxide by *Geobacter metallireducens*, Appl. Environ. Microbiol., 66, pp. 2248-2251, 2000

[11] K.P. Nevin, and D.R. Lovley, Mechanism for Fe(III) reduction in sedimentary environments, Geomicrobiol. J. 19, pp.141-149, 2002

[12] M. Mehanna, R. Basseguy, M-L. Delia, A. Bergel, Effect of *Geobacter sulfurreducens* on the microbial corrosion of mild steel, ferritic and austenitic stainless steels, Corr. Sci. 51 (2009) 2596-2604

[13] Deutsche Sammlung von Mikroorganismen und Zellkulturen DSMZ GmbH, Microorganisms, 826. Geobacter medium, 2007

[14] C. Dumas, R. Basseguy, A. Bergel, Electrochemical activity of *Geobacter sulfurreducens* biofilms on stainless steel anodes, Electrochem. Acta. 53 (2008) 5235-5241

[15] C. Cote, O.Rosas, and Regine Basseguy, *Geobacter sulfurreducens*: An Iron Reducing Bacteria that can protect carbon Steel aganst Anaerobic Corrosion?
*In press* 2012

[16] Lange"s Handbook of Chemistry 15th Edition, J.A. Dean, (Ed). McGraw-Hill, Princeton, 1999.

[17] D. Lovley, Microbial Fe (III) Reduction in subsurface Environments, FEMS Microbiology Reviews 20, p. 305-313, 1997

### III.4.3. Supplementary results

Supplementary results aim to complete and support the main results found and published in article 1 and 2. For this, a series of polarisation tests were performed intending to test the protection effect of the vivianite layer previously described. On the other hand, an introduction of the influence of fumarate is presented as part of this section aiming to better comprehend the role of this electron acceptor in a system that contains an iron reducing bacteria.

#### *III.4.3.1. Polarisation Results*

In order to electrochemically test the iron (II) phosphate layer formed on the system mentioned in articles 1 and 2, anodic polarisations (-100 to +1200 mV around OCP vs SCE) were performed at different times in parallel experiments, the coupon samples were then removed from the reactors for further surface analysis. This series of polarisations was also performed in an abiotic system as a control experiment. Experimental conditions are resumed in table III.1. $I_{corr}$ and corrosion rate ($V_{corr}$) were calculated for each of the conditions and the values can be found in table III.2. Calculations were made using the tafel fit option of EC-lab software, as explained in chapter II.

Fig. III.10 shows the polarisation curves obtained for anaerobic systems at hours 2 and 24 before any inoculation (abiotic conditions). At hour 2, it is observed a current plateau from -0.6 to -0.4 V vs SCE ($|j|$~ 0.035 mA.cm$^{-2}$) whereas no plateau is observed at hour 24.

Fig. III.11 shows the polarisation curves for: (A) abiotic systems and (B) biotic systems at hours 96 (anaerobic condition) and 120 (aerobic condition=24h after oxygen entrance). In the abiotic system, it is observed a current plateau from -0.2 to 0.2 V vs SCE ($|j|$~ 0.25 mA.cm$^{-2}$) at hour 96 and a pseudo-plateau from -0.2 to 0 V SCE at hour 120 with the same current density found at hour 96. This last curve shows how the $E_{corr}$ gets more positive in presence of oxygen, passing from -0.8 to -0.5 V due to the introduction of oxygen to the system, reproducing the potential ennoblement in the abiotic control system described in article 1.

In the biotic system (Fig. B), two plateaus are observed at hour 96: one current plateau between -0.25 to 0.15 V vs SCE ($|j|$~ 0.44 mA.cm$^{-2}$) and a pseudo-plateau between -0.65 to -0.5 V vs SCE ($|j|$~ 0.06 mA.cm$^{-2}$). In aerobic conditions (120 h), one peak at -0.6 V ($|j|$~ 0.25 mA.cm$^{-2}$) and one long plateau between -0.4 and 0.4 V vs SCE ($|j|$~ 0.14 mA.cm$^{-2}$) were observed. The first important remark out of these results is that $E_{corr}$ is slightly more negative (-0.06±0.03 V vs SCE) in aerobic conditions (120 h) than in anaerobic conditions (96 h), suggesting that the oxygen insertion into the system does not accelerate the cathodic reaction in the biotic system, contrary to what it was observed in the abiotic one.

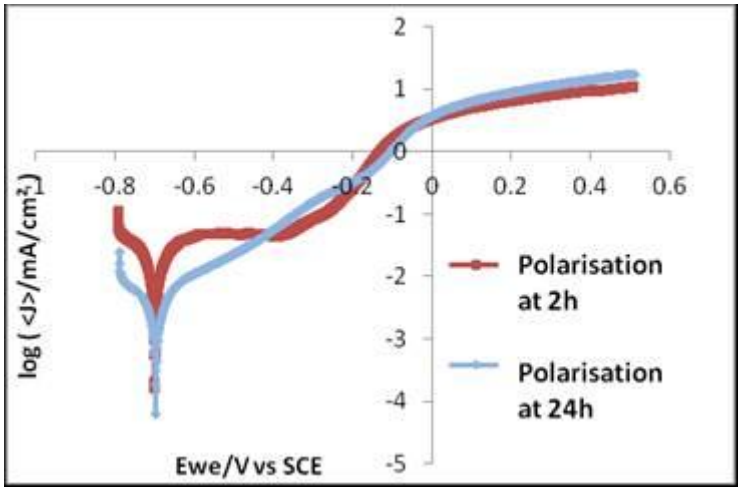


Fig. III.10. Polarisation curves performed in anaerobic systems at hour 2 and 24 (abiotic conditions). Polarisation: : -100<E<+1200 mV vs OCP ; sweep rate 10 mV/min

**A**

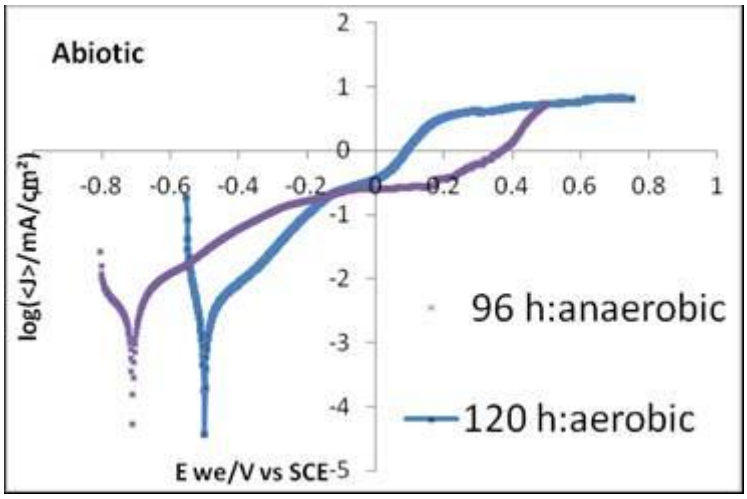


**B**

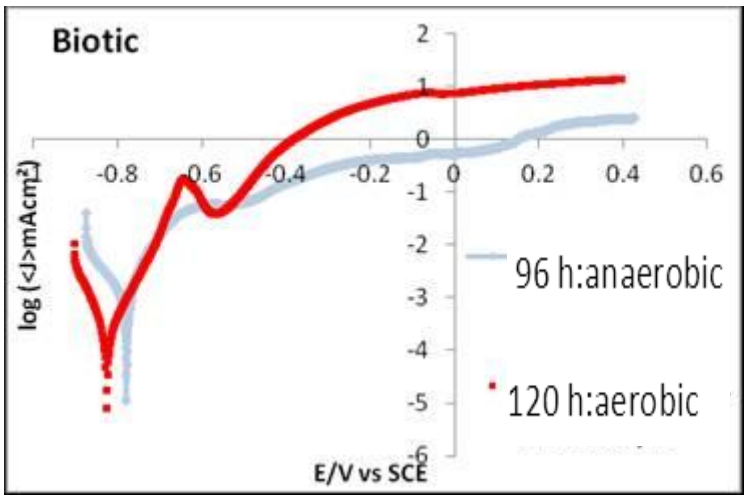


Fig. III.11. Polarisation curves performed: Fig (A) Control abiotic systems at hours 96 (blue line) and 120 (purple line); Fig (B): Biotic systems at hours 96 (red lines) and 120 (grey lines). Polarisation: -100<E<+1200 mV vs OCP ; sweep rate 10 mV/min

| Polarisation time (h) | Atmosphere conditions | System | Plot |
|---|---|---|---|
| 2 | Anaerobic ($N_2/CO_2$) | Abiotic | Fig. III.10, red line |
| 24 | Anaerobic ($N_2/CO_2$) | Abiotic | Fig.III.10, blue line |
| 96 | Anaerobic ($N_2/CO_2$) | Abiotic | Fig.III.11, blue line |
| 120 (24 h after $O_2$ entrance) | Aerobic | Abiotic | Fig.III.11, purple line |
| 96 (A and B) | Anaerobic ($N_2/CO_2$) | Biotic | Fig.III.11, grey line |
| 120 (24 h after $O_2$ entrance) (A and B) | Aerobic | Biotic | Fig.III.11, red line |

Table III.1. Experimental conditions for polarization experiments –parallel experiments: a reactor per a set of conditions-

| Polarisation time (h) | $I_{corr}$ ($mAcm^{-2}$) | $V_{corr}$ mmpy |
|---|---|---|
| 2 (abiotic) | 0.035 | 0.14 |
| 24 (abiotic) | 0.006 | 0.022 |
| 96 (abiotic) | 0.005 | 0.018 |
| 120 (abiotic) | 0.003 | 0.012 |
| 96 (biotic) | 0.003 | 0.012 |
| 120 (biotic) | 0.001 | 0.004 |

Table III.2. Calculation of $I_{corr}$ and $V_{corr}$ of the different polarisations performed in C1145 in presence and absence of bacteria immersed in standard reactor medium with 1 mM acetate and 10 mM of fumarate

Results show that the anodic reactions observed in the biotic system are many and very complex ones, that makes the system reactions very difficult to describe. Nevertheless, these results support the findings displayed in article 1 which describes the formation of a protective vivianite layer catalysed by the presence of *G. sulfurreducens*. Indeed, in average, lower $I_{corr}$ and therefore, lower corrosion rates are observed in biotic systems than in control abiotic systems, suggesting once again the protection of the iron (II) phosphate layer on the material: at hour 120, $I_{corr}$ and $V_{corr}$ are found 3 times lower in the biotic system than in the control abiotic one (table III.2).

On the other hand, it is important to highlight that in these experiments, the potential applied to the system with bacteria highly influenced the over development of the biofilm compared to biotic systems without polarisation presented in article 1. At the end of the anodic polarisation, in biotic systems, the biofilm could be observed by eye and planktonic bacterial counting was nearly 3 times higher than in no polarised system: $4.25 \times 10^4$ FCU $mL^{-1}$ at hour 98 under no polarisation compare to $1.51 \times 10^5$ FCU $mL^{-1}$ at hour 98 after polarisation. These

bacterial growth changes under polarisation were also observed by [Bulsalmen and Sanchez, 2005] with *Pseudomonas fluorescens* finding changes in cell morphology, size at cell division, time to division and biofilm structure. At an applied potential of 0.5 V, the doubling time of the population was 103 ± 8 minutes instead of 82 ± 7 minutes at -0.2 V.

Otherwise, SEM observations showed that after polarisation, the needle like structure shown in article 1 (which was attributed to vivianite), presented some morphological changes that can be observed in Fig. III.12. The original structure of the layer obtained at OCP (Fig. III.12A, article 1), exhibits smaller needles than the formed under polarisation (Fig.III.12B). In spite of the similarity on the images, it must be highlighted that the scale of the image in Fig. A (no polarised) is 3.5 times more amplified than in Fig. B (polarised). Fig.III.12C shows a second layer formed on top of the needle-like structure; this layer is presumed to be biofilm. These observations lead to conclude that due to the polarisation applied, a new or modified structure was formed in presence of bacteria.

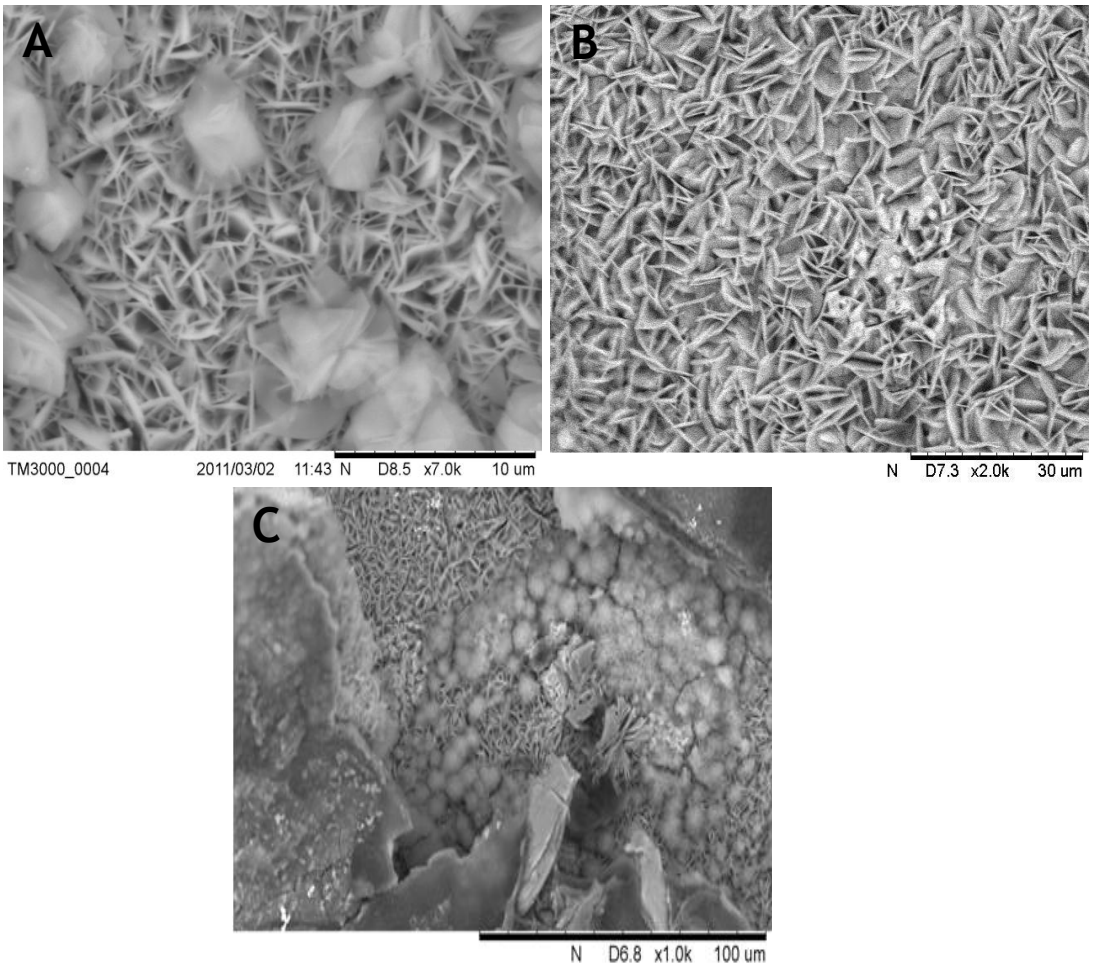


Fig. III.12. SEM pictures of coupon immersed in standard reactor medium (1 mM acetate, 10 mM fumarate and 5 mM of phosphate) in presence of *Geobacter sulfurreducens*. A) system no polarised (x7.0k amplification); B) system after polarisation (x2.0k amplification); C) system after polarisation (x1.0k amplification)

In order to have another evaluation of $I_{corr}$, linear polarisation (LP) was performed on the same previously described anaerobic inoculated systems with *Geobacter sulfurreducens* by applying ± 10 mV vs Ag/AgCl from OCP and using a sweep rate of 0.2 mV/s. This small potential applied does not accelerate corrosion process or bacterial growth as much as the potential applied in the previously described technique; thus, it will reproduce better the results described in article 1. If the electrodes are corroding at a high rate with the metal ions passing easily into solution, a small potential applied between the electrodes will produce a high current, and therefore a low polarization resistance which corresponds to a high corrosion rate. LP curves for different times obtained for the biotic system with different acetate concentrations (0, 1 and 3 mM) are presented in Fig. III.13. $R_p$ is the inverse to the slope of the polarization curve in the vicinity of the corrosion potential. The resistance measured is inversely related to the corrosion rate. Consequently, the bigger the slope the lower $R_p$ which indicates higher electron exchange and higher corrosion rate.

Fig III.12 A displays the polarisation curves and their evolution in time in a biotic system without acetate. According to Stern-Geary, the total current can be totally linearised only in the curve drawn one hour after inoculation; for further hours there is not such linearity on the whole potential range: a break on the line was found for the more cathodic part of the curve, indicating a fast cathodic reaction in presence of bacteria. However, the linear part was sufficiently large to calculate the slopes and then $R_p$ values (table III.3). It was observed that the slope decreases along the immersion time which suggests an increase on the resistance. Fig B and C displays the polarisation curves and their evolution in time in a biotic system with 1 and 3 mM of acetate, respectively. As for the previous cases, all the curves display a linear part but not on the whole potential range scan and an important current in the extreme cathodic part. Bigger slopes are observed as the concentration of acetate increases however the slopes evolution in time is less important than in the system without acetate (table III.3).

These results confirm what it was previously observed with the CV experiments (see preliminary results): lower resistances (bigger slopes) are observed when acetate concentration increases; the lower the resistance the higher the current ($I_{corr}$) thus, there is higher corrosion as acetate concentration increases. Nevertheless, the slope change along the time in a system without acetate seems faster than in systems with acetate. This might be due to acceleration of the cathodic reaction by hydrogen oxidation catalysed by the bacteria. Once acetate is no longer present in the medium, *G. sulfurreducens* can switch its metabolism to hydrogen oxidation, taking hydrogen as the sole electron donor for Fe (III) reduction [Caccavo *et al.,* 1994; Esnault, 2010; Libert *et al.,* 2011]. Moreover, due to the fast change of the slope on the extreme cathodic part of the curve it can be stated that the system is cathodically dominated in presence of bacteria.

A

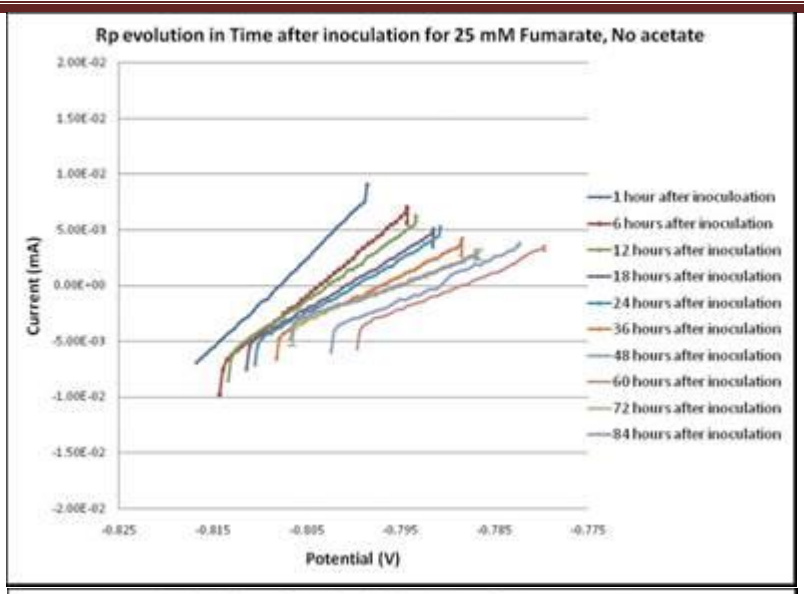


B

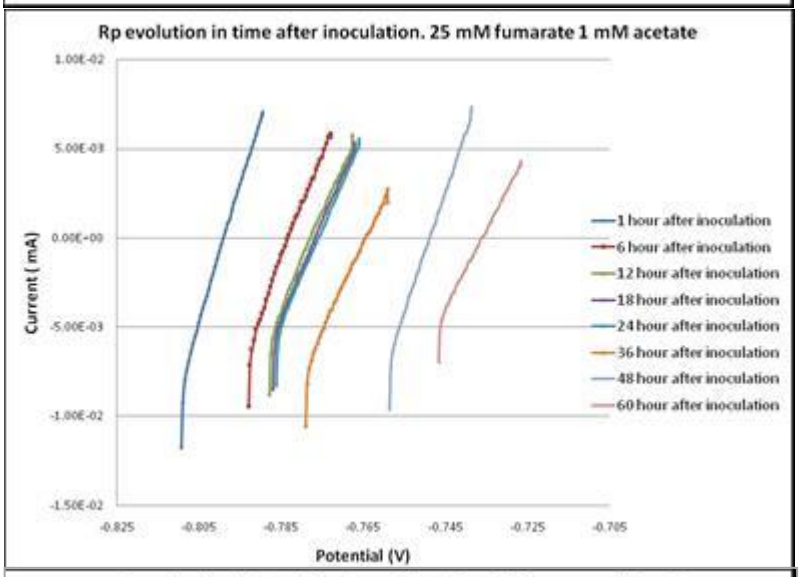


C

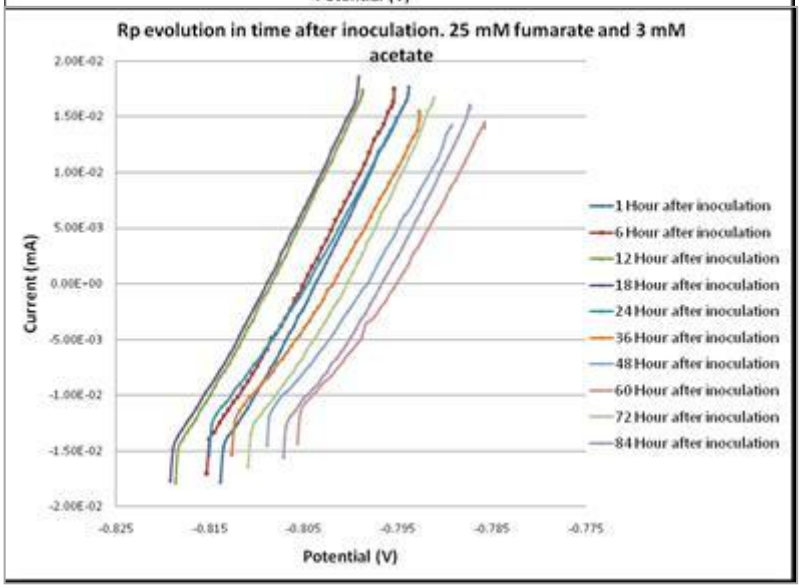


Fig.III.13. Linear polarisation performed on C1145 immersed in biotic anaerobic reactor medium with different acetate concentrations. A) 0 mM acetate; B)1 mM acetate and C) 3 mM acetate. Polarisation: ± 10 mV vs Ag/AgCl from OCP, sweep rate of 0.2 mV/s

| Time after inoculation | No acetate With bacteria (Ω cm²) | 1mM Acetate With bacteria (Ω cm²) | 3 mM acetate With bacteria (Ω cm²) |
|---|---|---|---|
| 1 h | 3925 | 3925 | 1962 |
| 6 h | 4484 | 5231 | 1963 |
| 12 h | 5231 | 5231 | 1963 |
| 18 h | 6280 | 5231 | 1963 |
| 24 h | 6280 | 5231 | 2242 |
| 36 h | 7850 | 6280 | 2242 |
| 48 h | 7850 | 4484 | 2415 |
| 60 h | 7850 | 6280 | 2415 |

Table III.3. Calculation of $R_P$ using the anodic branch for LP results presented in Fig. III.13. Notice that results correspond to data after inoculation which is performed at hour 24.

Moreover, $R_p$ values found for 1 mM acetate concentration were correlated to EIS results published in article 1. Values of $R_p$ and $R_{ct}$ for biotic systems are resumed in table III.4. Results show that LP results reproduce results published in article 1 in anaerobic biotic conditions. It shows that the longer the time of exposition to the bacteria in anaerobic conditions, the higher the protection; thus, the lower the iron dissolution.

| Time (h) | $R_p$ (Ω cm²) | $R_{ct}$ (Ω cm²) |
|---|---|---|
| **24** | 3925 | 3570 |
| **48** | 5231 | 4113 |
| **72** | 4484 | 4522 |
| **96** | 6280 | 6138 |

Table III.4. $R_p$ and $R_{ct}$ comparison for anaerobic systems in presence of *Geobacter sulfurreducens*. Carbon steel C1145 immersed in reactor medium containing 1 mM acetate, 10 mM fumarate and 5 mM phosphate.

### *III.4.3.2. Influence of fumarate concentration as electron acceptor*

Electrochemical tests such as OCP vs time and EIS in presence and absence of bacteria were also performed in reactor medium but this time in absence of fumarate, the electron acceptor. System conditions were identical to the previously described, this is: carbon steel C1145 (WE) immersed in reactor medium without fumarate and anaerobic conditions maintained by injection of $N_2/CO_2$.

IRB such as *Geobacter* may switch from using an organic compound such as fumarate, as the sole electron acceptor to a more efficient source of electron acceptor such as Fe (III), to increase the limited amount of ATP [Herrera and Videla, 2009]. Thus, the main objective of this part of the project was to find out the influence of *G. sulfurreducens* in a system where the sole source of electron acceptors is the iron (III) derived from the metal coupon. The hypothesis posed to this matter is: in conditions of fumarate absence, it is presumed that *Geobacter sulfurreducens* will use the corrosion products such as iron oxide as its sole source of electrons acceptor and as consequence it will solubilise the iron III to iron II, dissolving the oxide layer of the surface, previously formed. This will have a positive impact due to the production of a protective vivianite layer which may decrease corrosion rates.

OCP results (Fig. III.14) show a potential ennoblement of +500 mV in systems where bacteria is present. In contrast, a stable corrosion potential is observed in the control abiotic systems. Ennoblement of corrosion potential was observed in average at hour 125, meaning 101 hours after inoculation with bacteria. As it has been previously stated, ennoblement of corrosion potential represents an increase on the corrosion risk as $I_{corr}$ increases.

Furthermore, Fig.III.15 and III.16 shows the impedance diagrams in the complex plane plotted at OCP at different hours of immersion for the abiotic control and biotic system without fumarate, respectively. Three different representations have been chosen to plot the data. (A) Nyquist diagram with its zoom-up (B); (C) Bode modulus representation using the imaginary component of the impedance in function of the frequency in logarithmic coordinates, withdrawing the drawbacks of the influence of the electrolyte resistance on the estimation of the time constants [Orazem *et al.*, 2006] and (D) Bode phase angle diagram.

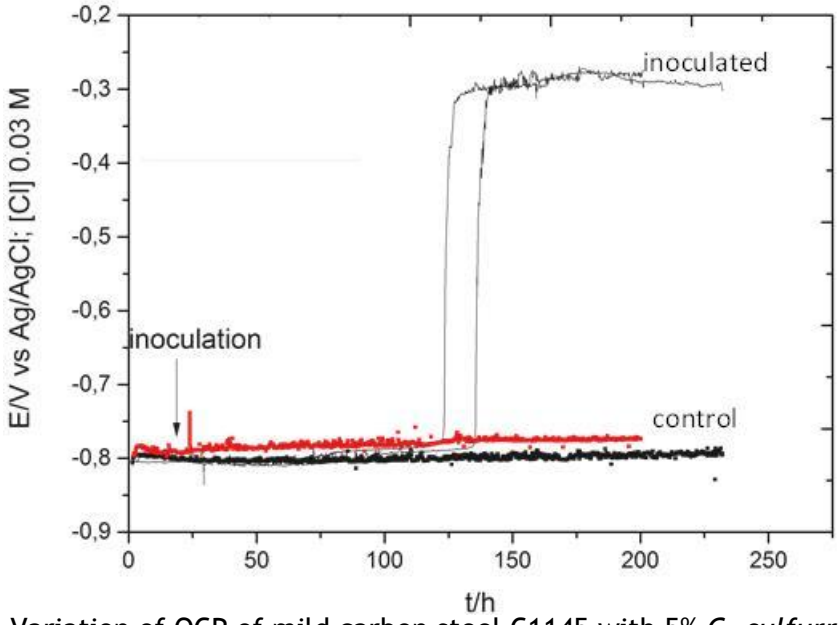


Fig. III.14. Variation of OCP of mild carbon steel C1145 with 5% *G. sulfurreducens* and without bacteria. Medium containing 1 mM sodium acetate (electron donor), no fumarate (electron acceptor) and 5 mM phosphate.

In Fig. III.15, the Nyquist diagram (A and B) displays three capacitive contributions at each of the times measured: two depressed semi-circles (one at HF and one at HF to middle frequencies (MF)) and one not well defined capacitive loop at LF. The HF semi-circles diameter increase in function of time as well as the HF to MF depressed semi-circles. The LF contributions are related to mass transport depicting diffusion phenomena. The three time constants observed in this system are more evident when observing the bode plots (C and D).

On the other hand, Fig.III.16 shows the impedance diagrams plotted at OCP at different hours of immersion for the biotic system without fumarate. The Nyquist diagram (A and B) displays also three capacitive contributions from hour 0 to 48: two depresed semi-circles at HF to MF, and one not well-defined loop at LF. From hour 72 only two capacitive loops are observed: at HF and HF/MF to LF. The HF semi-circles diameter increases in function of time as well as the HF/MF to LF depressed semi-circles.

Due to the complexity of both systems (control abiotic and biotic) a single equivalent circuit can not be proposed. However, the approach followed to analyse the experimental results is as follows: an estimation of capacitance values for the HF loops was obtained by using the pure capacitive system approach: the effective capacitance ($C_{eff}$) is estimated assuming that the system, at very HF, follows a purely capacitive behaviour (see chapter II.4.1.4). For this, the following relations are used:

$$Z_j = -1/C\omega \qquad \text{(III.1)}$$

$$C^{-1}_{eff} = (2\pi f_{RC} R) \qquad \text{(III.2)}$$

where $f_{RC}$ is the frequency which corresponds to the maximun imaginary impedance (Zim), R is the resistance of the electrochemical system. A first estimation of the capacitance at HF is calculated using (III.2). This value is used then to calculate the layer thickness (δ) in order to observe its evolution in time and verify if the values have a physic sense. δ is calculated by:

$$C_{eff} = \frac{\varepsilon \varepsilon_0}{\delta} \qquad \text{(III.3)}$$

where ε is the dielectric constant of the layer which value is taken equal to 12 (classic value for iron oxide), $\varepsilon_o$ is the permittivity of vacuum equal to $8.85 \times 10^{-14}$ F $cm^{-1}$, δ is the dielectric layer thickness and $C_{eff}$ is the equivalent capacity linked to a film expressed in F $cm^{-2}$.

Results show that HF capacitance values ranged between $1.5 \times 10^{-7}$ and $2.9 \times 10^{-7}$ F $cm^{-2}$ for the control abiotic system and $2.2 \times 10^{-7}$ and $7.0 \times 10^{-7}$ F $cm^{-2}$ for biotic system (table III.5). These small values of capacitance correspond to thicknesses of 18 to 70 nm that can be attributed to an oxide layer. Thus, the HF loops in both systems correspond to an oxide layer which thickness does not vary much among the different times of immersion.

For the analysis of the HF to MF loops (or in the case of biotic system from hour 72, the LF loop), the linear parts of the imaginary part of the impedance ($Z_j$) plotted as a function of the frequency ($f$) in logarithmic coordinates was used for the calculation of alpha. Alpha values found, ranged between 0.76 and 0.86 for both systems. These values are in agreement with a CPE behaviour (table III.5).

Once confirming that the HF/MF to low frequency loops (found in the systems with and without bacteria) follow a CPE behaviour. Following, it was applied the equation derived by Brug *et al.*, previously described, in order to calculate the effective capacitance associated with the CPE and to know whether the constant time are surface or radial distributed.
Capacitance values were extracted from the impedance diagrams displayed in Fig.III.15 and 16, taking as $R_{ct}$ the diameter of the middle to low frequency loop (depending of the system) (table III.5).

Capacitance values found ranged between 79 and 100 µF $cm^{-2}$ for the control abiotic system and between 91 and 100 µF $cm^{-2}$ for the biotic system. These values correspond to the upper limit for double layer capacitance ($C_{dl}$) values and have been associated to charge transfer reaction.

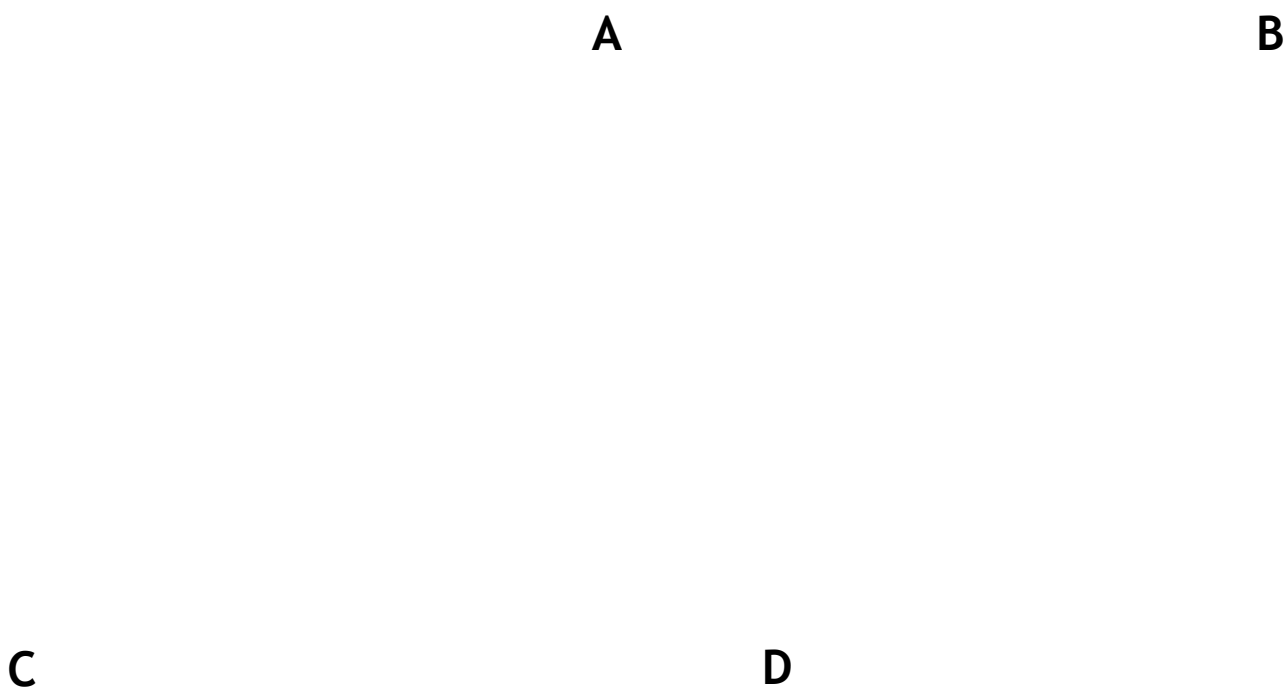


Fig.III.15. Control abiotic system impedance spectra of carbon steel C1145 during 168 hours of immersion in reactor medium without fumarate. System kept in anaerobic conditions. (A) Nyquist; (B) Nyquist zoom-up; (C) Bode plot of imaginary part of the impedance as function of frequency and (D) Bode plot phase angle vs. frequency.

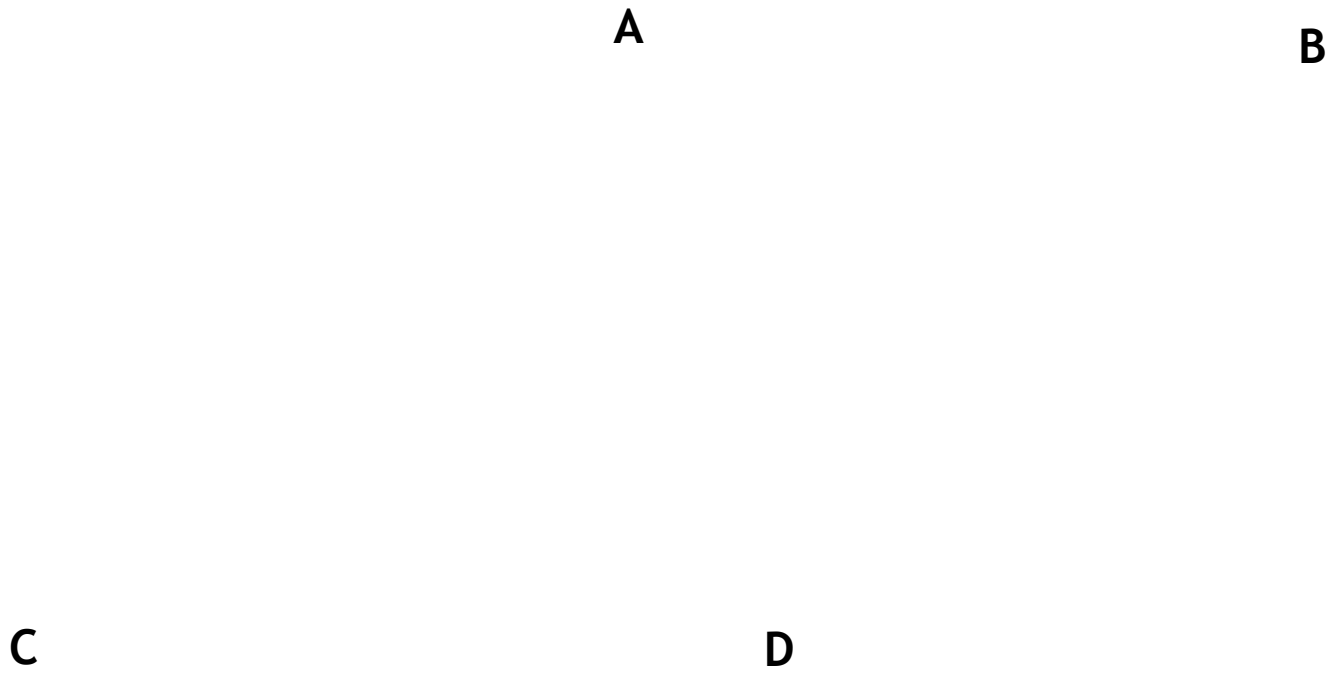


Fig.III.16. Inoculated (biotic) system impedance spectra of carbon steel C1145 during 168 hours of immersion in reactor medium without fumarate. System kept in anaerobic conditions. (A) Nyquist; (B) Nyquist zoom-up; (C) Bode plot of imaginary part of the impedance as function of frequency and (D) Bode plot phase angle vs. frequency.

**A**

| Oxide layer HF values | | | | | | Double layer MF values | | | |
|---|---|---|---|---|---|---|---|---|---|
| **Time (h)** | **$R_s$ (Ωcm²)** | **$R_{ox}$ (Ωcm²)** | ***F* (max) (Hz)** | **$C_{ox}$ Fcm$^{-2}$** | **δ (nm)** | **α** | **$R_{ct}$ (Ω cm²)** | **$Q_{eff}$ (Ω-1cm-²sα)** | **$C_{dl}$ µFcm$^{-2}$** |
| 0 | 82 | NA | NA | NA | NA | 0.76 | 1061 | 2.7x10$^{-04}$ | 81 |
| 24 | 64 | 25 | 28619 | 2.2x10$^{-07}$ | 48 | 0.81 | 3668 | 2.2 x10$^{-04}$ | 79 |
| 48 | 63 | 32 | 28619 | 1.7 x10$^{-07}$ | 61 | 0.82 | 4349 | 2.2 x10$^{-04}$ | 84 |
| 72 | 58 | 34 | 28619 | 1.6 x10$^{-07}$ | 66 | 0.83 | 4773 | 2.2 x10$^{-04}$ | 90 |
| 96 | 58 | 37 | 28619 | 1.5 x10$^{-07}$ | 71 | 0.84 | 4939 | 2.2 x10$^{-04}$ | 94 |
| 120 | 58 | 39 | 19048 | 2.2 x10$^{-07}$ | 49 | 0.84 | 5118 | 2.1 x10$^{-04}$ | 92 |
| 144 | 58 | 43 | 12874 | 2.9 x10$^{-07}$ | 37 | 0.85 | 5561 | 2.1 x10$^{-04}$ | 98 |
| 168 | 57 | 46 | 12874 | 2.8 x10$^{-07}$ | 38 | 0.86 | 5316 | 2.1 x10$^{-04}$ | 100 |

**B**

| Oxide layer HF values | | | | | | Double layer MF values | | | |
|---|---|---|---|---|---|---|---|---|---|
| **Time (h)** | **$R_s$ (Ω cm²)** | **$R_{ox}$ (Ω cm²)** | ***f* (max) (Hz)** | **$C_{ox}$ Fcm$^{-2}$** | **δ (nm)** | **α** | **$R_{ct}$ (Ω cm²)** | **$Q_{eff}$ (Ω$^{-1}$cm$^{-2}$s$^{α}$)** | **$C_{dl}$ µFcm$^{-2}$** |
| 0 | 114 | NA | NA | NA | NA | 0.76 | 1588 | 2.8 x10$^{-04}$ | 91 |
| 24 | 98 | 6 | 41718 | 6.0 x10$^{-07}$ | 18 | 0.80 | 3288 | 2.6 x10$^{-04}$ | 101 |
| 48 | 100 | 11 | 41718 | 3.5 x10$^{-07}$ | 30 | 0.82 | 4905 | 2. x10$^{-04}$ | 90 |
| 72 | 98 | 15 | 41718 | 2.6 x10$^{-07}$ | 41 | 0.82 | 6016 | 2. x10$^{-04}$ | 84 |
| 96 | 101 | 17 | 41718 | 2.2 x10$^{-07}$ | 48 | 0.82 | 6421 | 2.0 x10$^{-04}$ | 83 |
| 120 | 106 | 19 | 28169 | 3.0 x10$^{-07}$ | 35 | 0.82 | 6685 | 2.0 x10$^{-04}$ | 84 |
| 144 | 106 | 23 | 28169 | 2.5 x10$^{-07}$ | 43 | 0.82 | 7564 | 1.9 x10$^{-04}$ | 81 |
| 168 | 106 | 25 | 19048 | 3.4 x10$^{-07}$ | 32 | 0.83 | 8186 | 1.8 x10$^{-04}$ | 82 |

Table III.5. Evolution in time of values extracted from experimental results: solution resistance ($R_s$), oxide resistance ($R_{ox}$), representative frequency at the maximum ($f_{max}$), oxide capacitance ($C_{ox}$), and the layer thickness (δ) of the HF oxide layer. Alpha (α), charge transfer resistance ($R_{ct}$), CPE value ($Q_{eff}$), and double layer capacitance ($C_{dl}$) of the MF to LF double layer. (A): control abiotic system; (B) inoculated biotic system in a medium containing 1 mM of acetate, 5 mM of phosphate and 0 mM of fumarate. NA: Values not calculated due to not well-defined loop.

In general, the data extracted from the experimental results displayed in table III.5 show important differences between the abiotic control and the biotic system:

1- The oxide resistance increases in both systems along the immersion time. However, $R_{ox}$ values are between 1.8 and 4.2 times higher in the control abiotic system.
2- The oxide layer thickness has the same order of magnitude in both systems. However, it remains more stable in the biotic system than in the abiotic system.
3- Resistance to the charge transfer ($R_{ct}$) increases for both systems along the time of immersion. However, the value at the end of the experiment (168h) is 1.5 times higher in presence of bacteria than in absence of it. This

suggests that in terms of polarization resistance, $R_p$ is higher in the biotic system than in the control abiotic. Therefore, $V_{corr}$ is lower in the biotic system.

4- Double layer capacitances are around the maximum limit for typical values of $C_{dl}$ in both systems.

On the other hand, metal coupons from both systems were observed after 168 hours of the immersion in reactor medium without fumarate (Fig. III.17). Some cracks can be observed in the surface layer covering the electrode in both systems, a niddle-like structure similar to the one observed in the biotic system with standard reactor medium (described in article 1), was observed in both systems (control abiotic and biotic) suggesting the presence of vivianite. Nonetheless, the structure size varies considerable regarding the system, observing a bigger and thicker structure in the biotic medium.

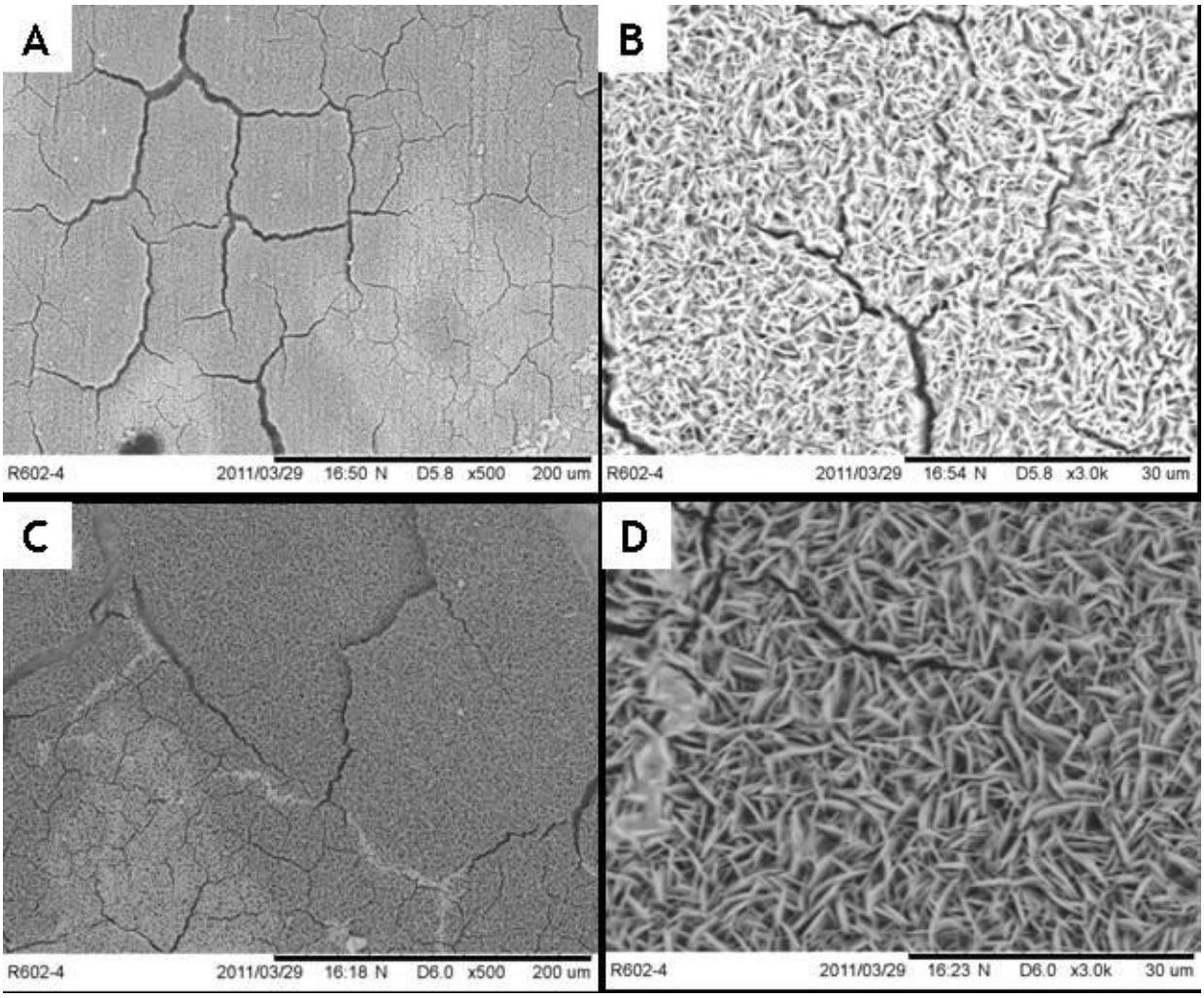


Fig. III.17. Micro photographs of coupons after 170 hours of immersion in reactor medium without fumarate: (A) SEM image of control abiotic coupon with x500 amplification; (B) SEM image of control abiotic coupon with x3000 amplification; (C) SEM image of coupon from system with bacteria with x500 amplification; (D) SEM image of coupon from system with bacteria with x3000 amplification

For instance, the micrographs A and B (control abiotic coupons) were compared with representations C and D (biotic coupons). The images show how, for example, the structure observed at x3.0k amplification is remarkably larger in the biotic system than in the abiotic control system. However, these structures cover unevenly the surface of the electrode (cracks). The presence of the cracks is certainly the reason why it was observed OCP ennoblement; the broken or damaged layers of vivianite may have induced a galvanic cell-like formation which is likely to induce a potential ennoblement and an increase on the corrosion rate. On the other hand, EDX analysis was performed in both parts of the observed layer (cracks or inner layer and needle-like structure or upper layer) to both systems. Results are resumed in table III.6.

**A**

| Element | Atomic % |
|---|---|
| **O** | 38.4 |
| **Fe** | 46.1 |
| **Mn** | 2.2 |
| **P** | 13.3 |

**B**

| Element | Atomic % |
|---|---|
| **C** | 12.6 |
| **O** | 61.6 |
| **Fe** | 17.1 |
| **Mn** | 0.9 |
| **P** | 7.1 |

**C**

| Element | Atomic % |
|---|---|
| **C** | 14.1 |
| **O** | 57.0 |
| **Fe** | 29.0 |

**D**

| Element | Atomic % |
|---|---|
| **C** | 14.0 |
| **Na** | 1.2 |
| **O** | 64.0 |
| **Fe** | 8.4 |
| **Mn** | 1.7 |
| **P** | 9.6 |

**E**

| Element | Atomic % |
|---|---|
| **C** | 17.1 |
| **Na** | 1.1 |
| **O** | 65.7 |
| **Fe** | 3.2 |
| **Mn** | 1.5 |
| **P** | 10.1 |

**F**

| Element | Atomic % |
|---|---|
| **O** | 51.3 |
| **Fe** | 46.9 |
| **P** | 1.8 |

Table III.6. EDX analysis performed in C1145 coupons immersed in reactor medium without fumarate. Control abiotic: (A) General spectra analysis; (B) upper layer (needle-like structure); (C) inner layer (inside crack). Biotic system: (D) General spectra analysis; (E) upper layer (needle-like structure); (F) inner layer (inside crack)

Results show that more than structure similarities, the atomic percentage composition of the layers formed in the two systems, with and without bacteria, is very similar. For instance, the composition of the inner layer found below the vivianite structure (inside cracks) is mainly an oxide layer such as FeO, $Fe_3O_4$ or $Fe_2O_3$. Furthermore, the composition of the upper layer is very similar if we compare table B (abiotic) and table C (biotic): the quantity ration between the Fe, O and P is the appropriate for that one of vivianite.

In conclusion, the main difference between these layers and the one described in article 1 is that, in the system without fumarate the vivianite layer is thicker and damaged, possibly inducing a cell galvanic effect. This may be explained by the fact that in absence of fumarate, the bacteria start reducing the iron (III) sooner and with a higher reaction rate than when a soluble electron acceptor is present. On the other hand, the fact that we also find vivianite in the abiotic systems but after longer time of immersion in anaerobic conditions lead us to think that the

formation of vivianite is feasible in absence of bacteria but it only takes longer time than in presence of an IRB. IRB induces a faster and higher concentration of Fe (II) which bonds to phosphate consequently forming vivianite. In absence of bacteria, the dissolution of iron leads to the concomitant presence of Fe (II) and Fe (III) species, being Fe (II) in lower concentration than Fe (III). Thus, vivianite formation will take longer time.

## III.5. Influence of medium composition

Once these last results presented in article 1 and 2 were confirmed a new questions raised: 1) in absence of phosphate does the bacteria exerts protection of the metal or by contrary it would accelerate corrosion by accelerating the cathodic reaction of the system; In order to answer this question several more experiments including weight loss tests, EIS, OCP vs time, linear polarisation, analytical techniques and surface analysis were performed adjusting the concentrations of phosphate and ammonium chloride.

### III.5.1. Influence of *G. sulfurreducens* in a medium without phosphate: role of ammonium species

Experiments with *Geobacter sulfurreducens* were performed in absence of phosphate using the same experimental set up described in article 1. The sole differences were the absence of phosphate in the reactor medium and the conditions were kept anaerobic during the whole experiment. Fig. III.18 shows the corrosion potential measurements along time in anaerobic systems with and without bacteria. It can be observed a corrosion potential ennoblement of around +300 mV for biotic systems whereas no ennoblement is observed in abiotic control systems. Ennoblement occurred between 50 to 60 hours of experiment, this is around 1.5 days after inoculation of bacteria.

inoculated

control

Fig. III.18. Variation of OCP of mild carbon steel C1145 with 5% *G. sulfurreducens* (black lines) and without bacteria (black and red dots). Anaerobic medium containing 1 mM

sodium acetate (electron donor), 10 mM of sodium fumarate (electron acceptor) and 0 mM phosphate.

Fig.III.19 describes the redox potential measurement performed in the control abiotic and biotic systems, both without phosphate. Redox potential measurements were performed using the CE platinum grid (Pt/Ir, 90:10) and reading its potential instead of the WE potential. At hour 24, when the inoculation is performed, it is observed a drop of the redox potential in the biotic system (-400 mV) whereas no change was observed in the control abiotic system. A second jump towards more positive values of the redox potential (from -0.5 to 0 V vs Ag/AgCl) was observed at the same time when the corrosion potential ennoblement was observed. These redox potential observations coincide with the observations remarked in article 2: *Geobacter sulfurreducens* affects the redox potential of the system and OCP in this medium. Note that the little increase in potential observed in the control abiotic system between hour 120 and 160 was due only to some troubles with the $N_2/CO_2$ injection.

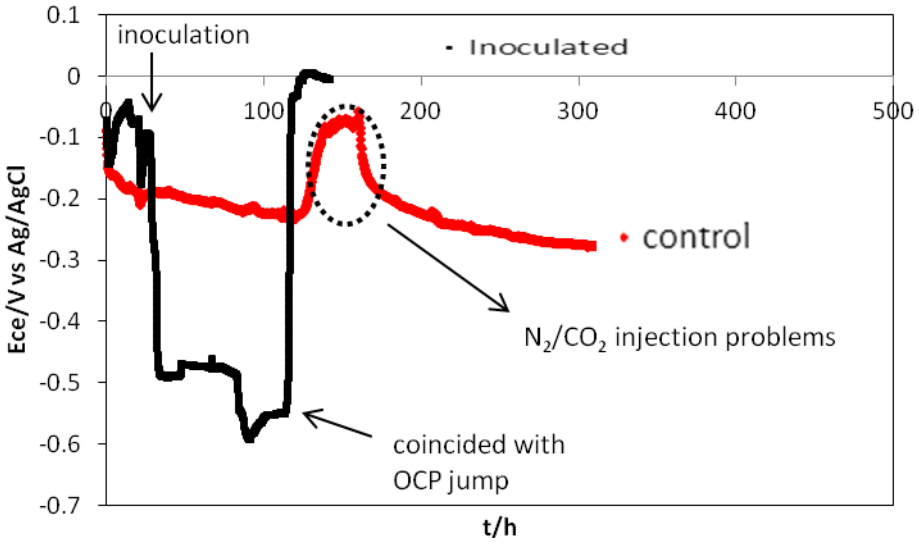


Fig. III.19. Variation of redox potential using a platinum grit: with 5% *G. sulfurreducens* (black line) and without bacteria (red line). Medium containing 1 mM sodium acetate (electron donor), 10 mM of sodium fumarate (electron acceptor) and 0 mM phosphate.

Furthermore, EIS measurements were performed in both biotic and control abiotic systems. Fig.III.20 and Fig.III.21 show the impedance diagrams in the complex plane plotted at OCP at different hours of immersion for the abiotic control and in presence of *Geobacter sulfurreducens* systems without phosphate. Three different representations have been chosen to plot the data. (A) Nyquist diagram; (B) Bode modulus representation using the imaginary component of the impedance in function of the frequency in logarithmic coordinates, (C) Bode phase angle diagram.

For both systems (control and biotic) and at each of the measured times, the Nyquist diagram (A) displays two main contributions: at HF one depressed semi-circle (capacitive loop) is observed and at LF there are observed points that overpass the real impedance axe (Re (Z)) which can be considered as one inductive loop. For the case of the biotic system, the inductive loop is not observed completely because the frequencies explored did not go as low as in the abiotic

system (100 KHz to 2 mHz for the control abiotic system and 200 KHz to 10 mHz for the biotic one). The phase angle diagram of both systems (plot C) displays two peaks at each time: the first ranging in frequencies around $10^{-3}$ and $10^{-2}$ Hz and the second around $10^{0}$ and $10^{1}$ Hz. It is also observed the increment of the maximum value of the phase angle from hour 0 to 24 (35 to 45 degrees, respectively) to then remain stable at further hours or to increase very little. It is also observed the displacement of the peak towards lower frequencies from hour 0 to 24 to then remain stable.

On the other hand, on representation B (log Im(Z) vs f/Hz) there are clearly displayed linear parts from $10^{0}$ and $10^{3}$ Hz; the slope allows to calculate alpha (α) values for determining whereas the system followed a constant phase element (CPE) behaviour or a pure capacitive behaviour [Orazem *et al.,* 2006]. For both systems (biotic and abiotic), the α values found and displayed in table III.7 were between 0.78 and 0.87 confirming a CPE behaviour. Then, in order to calculate the CPE parameters the equivalent circuit R1+R2//Q illustrated in Fig. III.22 was used. This model has been applied to simulate only the HF impedance response, making omission to phenomena occurring at LF in order to simplify the analysis. If this CPE behavior is assumed to be associated with surface distributed time constants for charge-transfer reactions (time-constant distribution along the electrode surface), then it is possible to apply the equation derived by Brug *et al*. [Brug *et.al.,* 1984; Hirshorn *et.al.,* 2010] to calculate the effective capacitance ($C_{eff}$) associated with the CPE as described in article 1. Capacitances values were calculated by fitting the Nyquist diagrams (minimized by simplex method) shown in Fig.III.20 and Fig.III.21 and are gathered in table III.7: (A) for abiotic control system and (B) for biotic system.

Although the calculated values of $C_{eff}$ are higher than the classic ones given for double layer capacitances (between 10 and 100 μF $cm^{-2}$), we can assume that the depressed semi-circles are linked to charge transfer phenomena due to an amplified effective surface. Consequently, the resistance given by the diameter of the semi-circle represents the charge transfer resistance ($R_{ct}$) in parallel with $C_{eff}$ corresponding to the double layer capacitance ($C_{dl}$). This suggestion is supported by the fact that at initial time (after only 2 hours of immersion) it is observed a low $R_{ct}$ values (<600 Ω $cm^2$). This leads to suggest that there is a high corrosion rate and an important attack on the surface, increasing the roughness of the material which augments the effective surface area and therefore the $C_{dl}$ values.

In abiotic system, $C_{dl}$ values double from hour initial to 24 to then increase by a factor of 4 until the end of the experiment. $R_{ct}$ values increase only 1.3 times from initial time to hour 24 and from there on resistances seem to fluctuate around the same values increasing only 1.1 times (less than 60 Ω $cm^2$) by the end of the experiment. This suggests that the growth and dissolution of the layer form occurs at the same rate.

In the biotic system, $C_{dl}$ values double by the end of the experiment and are in average I.3 times lower than those found in the control abiotic system. In terms of $R_{ct,}$ there is a bigger evolution observing the increase of the charge transfer resistance along time arriving to increase 4 times by the end of the experiment. By

the end of the experiment, $R_{ct}$ values are 2.2 times higher in the biotic system than in the control abiotic system making allusion to higher resistance to the charge transfer in the biotic system, thus lower corrosion rates. However, if we compare this values to the ones presented in article 1 (systems with phosphate) it seems that resistance to the charge transfer is around 9 times higher in the control abiotic system with phosphate than without phosphate and 4.2 times higher in the biotic system with phosphate than without phosphate. If we assume that the resistance to the charge transfer ($R_{ct}$) is inversely proportional to corrosion rates, we can conclude that corrosion rates are higher in systems without phosphate than with phosphate and in both cases corrosion rates are lower in presence of the IRB, *Geobacter sulfurreducens*.

Nevertheless, the effective surface ($S_{eff}$) must be taken into account. For this, $S_{eff}$ was estimated by calculating the ratio $C_{eff}/C_{dl}$ (upper limit) and a factor of 4 was found for the abiotic control system and a factor of 2 for the biotic one. The new surface values indeed affect the resistances values, obtaining 2200 Ω $cm^2$ by hour 84 for the abiotic system and 3200 Ω $cm^2$ for the biotic system. This confirms that even with the corrected surface values, $V_{corr}$ is 1.5 times higher in the abiotic control system than in the biotic one. When comparing the new calculated values to the ones presented in article 1 is then evident that still corrosion is lower in a system with phosphate obtaining Rct values 3 times higher for the control system and 2 times higher for the system with presence of the bacteria.

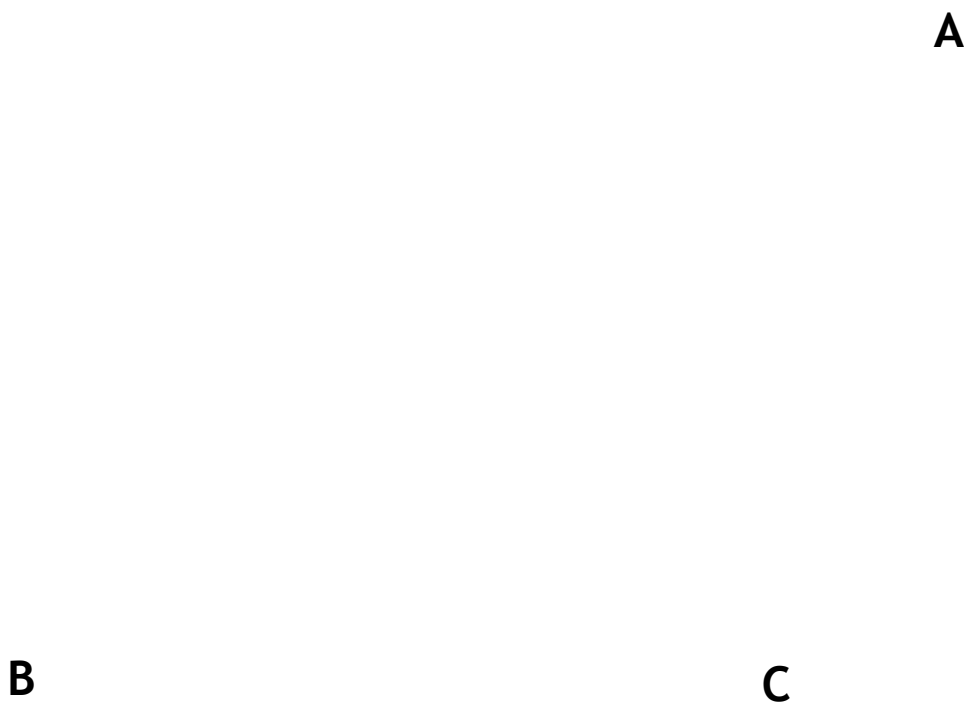


Fig.III.20. Control abiotic system: impedance of carbon steel C1145 after 84 hours of exposition in medium containing 1 mM acetate, 10 mM of fumarate and 0 mM of phosphate. System kept in anaerobic conditions during the whole experiment (A) Nyquist, (B) Bode modulus and (C) Bode phase angle plots

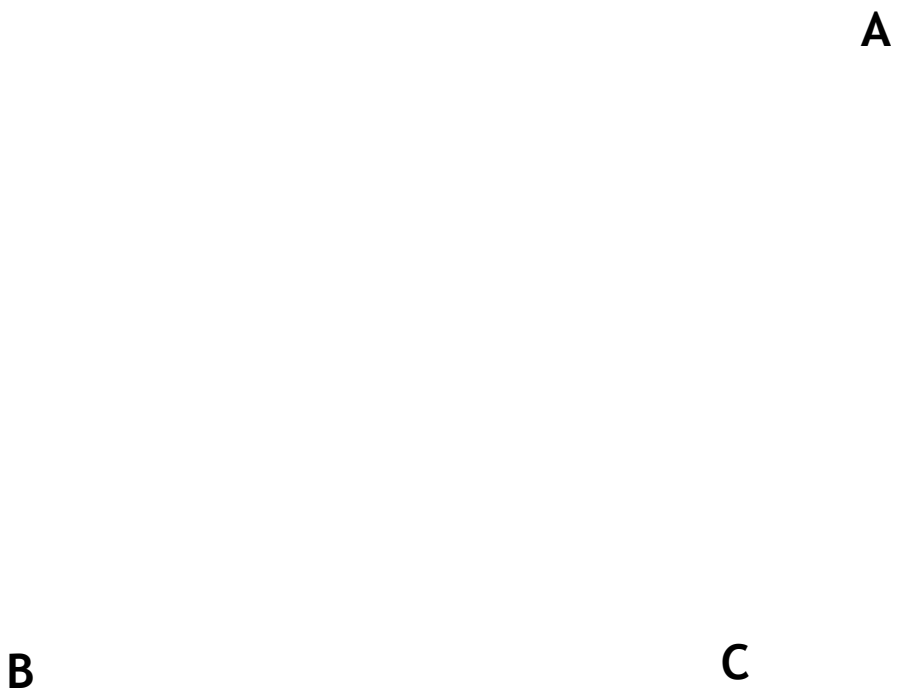


Fig.III.21. Impedance of carbon steel C1145 after 84 hours of exposition in medium containing 1 mM acetate, 10 mM of fumarate and 0 mM of phosphate. System kept in anaerobic conditions during the whole experiment (A) Nyquist, (B) Bode modulus and (C) Bode phase angle plots of reactor inoculated with *G. sulfurreducens*

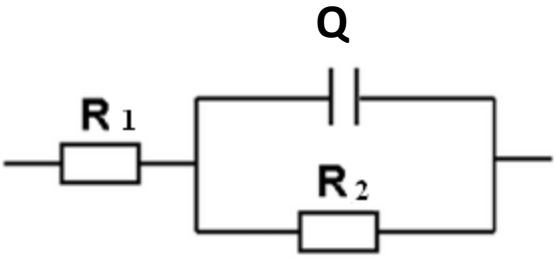


Fig. III.22. Equivalent circuit used to describe the electrochemical interface metal/solution and to obtain the values for solution resistance, R1 represents the solution resistance ($R_{s)}$, Q represents the CPE parameters (Q,α), and R2 represents the charge transfer resistance ($R_{ct)}$.

**A**

| TIME | $R_s$ (Ω cm²) | α | $R_{ct}$(Ω cm²) | Q($\Omega^{-1}cm^{-2}s^{\alpha}$) | $C_{eff}$ µFcm$^{-2}$ |
|---|---|---|---|---|---|
| initial | 86 | 0.74 | 557 | $3.1x10^{-04}$ | 113 |
| 24 | 78 | 0.79 | 665 | $5.0\ x10^{-04}$ | 288 |
| 48 | 79 | 0.79 | 652 | $6.1\ x10^{-04}$ | 365 |
| 72 | 80 | 0.79 | 743 | $6.3\ x10^{-04}$ | 395 |
| 96 | 80 | 0.80 | 719 | $6.6\ x10^{-04}$ | 416 |

**B**

| TIME | Rs (Ω cm²) | α | $R_{ct}$(Ω cm²) | Q($\Omega$-1cm-$^{2}s^{\alpha}$) | $C_{eff}$ µFcm$^{-2}$ |
|---|---|---|---|---|---|
| initial | 67 | 0.71 | 405 | $4.4\ x10^{-04}$ | 157 |
| 24 | 66 | 0.77 | 925 | $4.5\ x10^{-04}$ | 225 |
| 48 | 63 | 0.77 | 1026 | $4.8\ x10^{-04}$ | 257 |
| 72 | 62 | 0.78 | 1375 | $5.2\ x10^{-04}$ | 293 |
| 84 | 62 | 0.78 | 1611 | $5.2\ x10^{-04}$ | 298 |

Table III.7. Evolution in time for $R_s$,α, $R_{ct}$, Q, and $C_{eff}$ of the control abiotic system (A) and inoculated biotic system (B) in a medium containing 1 mM of acetate and 10 mM of fumarate and no phosphate in presence of a coupon of C1145

Moreover, macro and microscopic observations were performed in both systems (control abiotic and biotic). Fig. III.23 shows the photographs of the reactors after 84 hours of immersion in absence of bacteria (A) and presence of them (B). It can be observed how there is a rust corrosion deposit in the control abiotic systems whereas no deposits are observed in the inoculated biotic one.

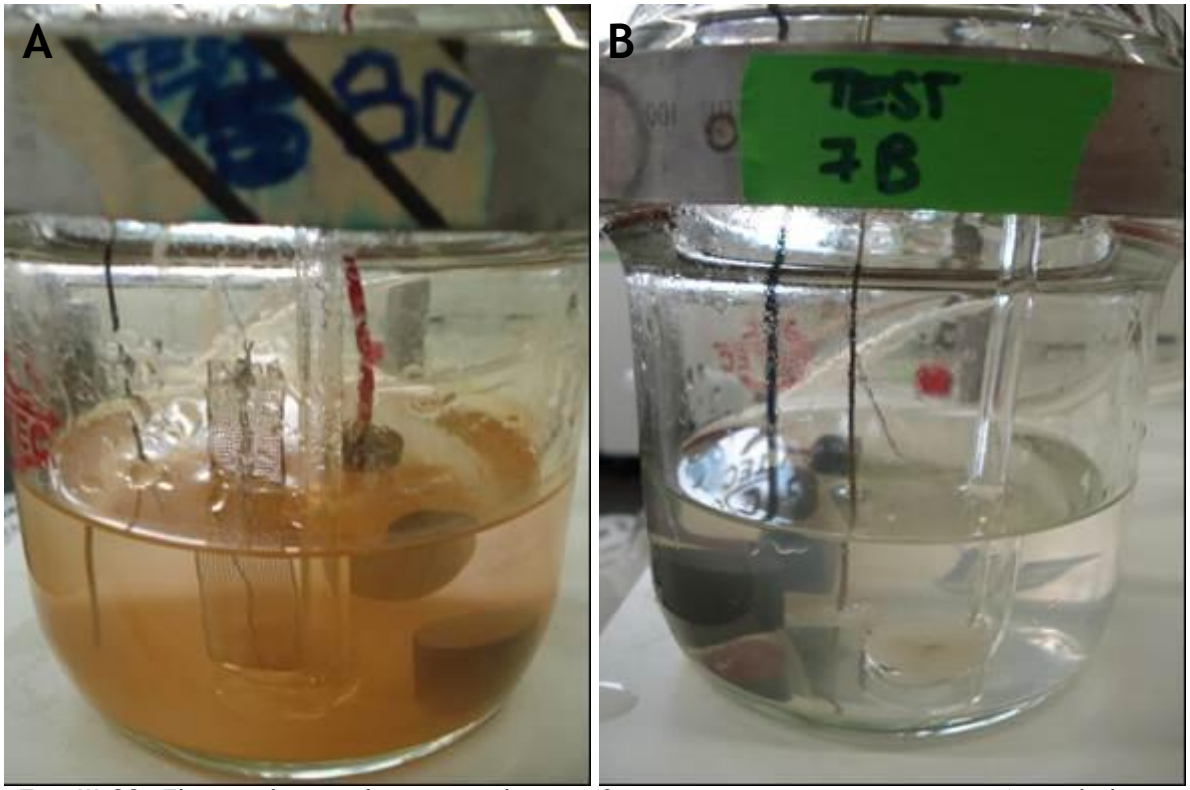


Fig. III.23. Electrochemical reactor photos after experiments in presence (A) and absence (B) of *G. sulfurreducens* in reactor medium without phosphate, 1 mM acetate and 10 mM fumarate.

Fig.III.24 shows the micrograph of the steel coupon immersed during 100 hours in abiotic (A) and biotic (B) reactor medium without phosphate. Table III.8 shows the EDX results for the general spectra performed for the abiotic coupon (A) and the biotic coupon (B): the element composition found on the surface of the coupons is based on the same elements, finding differences only in the proportion of carbon and oxygen: there is 2 times more elemental oxygen and 1.6 times less carbon in the abiotic system than in the biotic one. The higher oxygen quantity found in the control abiotic system suggests that there is a higher quantity of iron oxides which is in accordance with the calculated capacitances ($C_{dl}$) over 100 µF $cm^{-2}$ and the surface augmentation suggested. The higher quantity of carbon in the biotic system suggests bacteria/biofilm development.
Moreover, it has been detected some phosphorous on the surfaces of both coupons which source should be the sodium phosphate present in the growth medium used for inoculation (5% of bacterial culture for the inoculated biotic system and 5% of bacteria culture filtrate -no cells- for the control abiotic system). This means that there is a maximum of 0.03 g/L of sodium phosphate that was inoculated to both systems at hour 24 (without taking into account the phosphate already consumed for bacterial growth). Nevertheless, these traces of phosphate were not sufficient for the formation of the vivianite layer described in article 1. Finally, the analysed surface structure seems similar in both coupons, observing what it seems to be metal iron with some sponge-like oxide. However, the surface seems more affected by the corrosion attack in abiotic than biotic confirming EIS results.

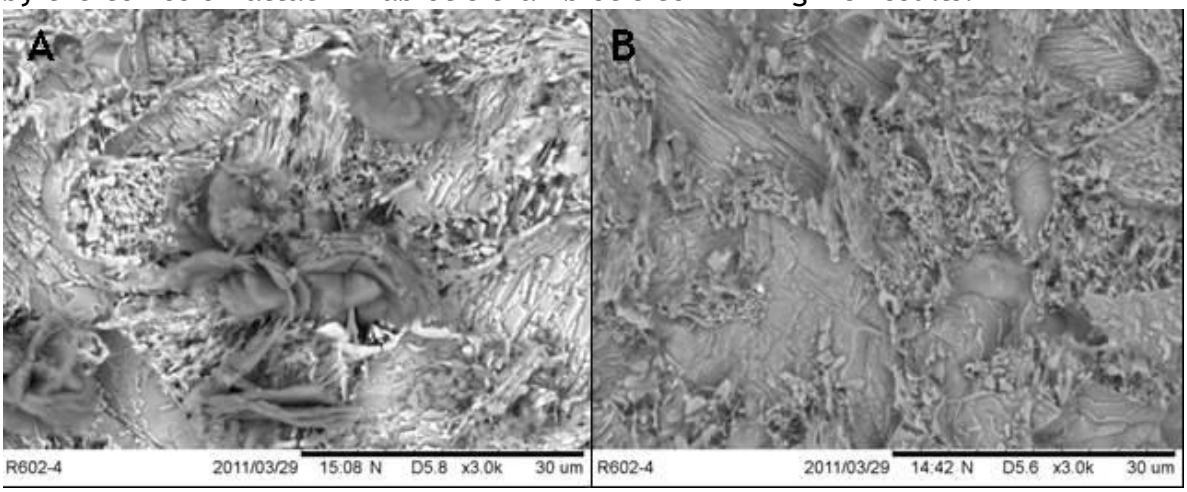


Fig.III.24. Micro photographs of coupons after 96 hours of immersion in reactor medium in absence of phosphate: (A) SEM image of control abiotic coupon; (B) SEM image of coupon from system with bacteria

**A**

| Element | Atomic % |
|---|---|
| C | 25.3 |
| O | 20.5 |
| Fe | 49.6 |
| Mn | 1.3 |
| P | 3.2 |

**B**

| Element | Atomic % |
|---|---|
| C | 39.8 |
| O | 9.8 |
| Fe | 48.9 |
| Mn | 1.0 |
| P | 0.5 |

Table III.8. EDX analysis of general spectra on coupons surface after 96 hours of immersion. (A): control abiotic coupon; (B): coupon in presence of bacteria

To complete these set of experiments using reactor medium without phosphate, total dissolved iron measurements were performed in both systems (control abiotic and biotic) by inductively couple plasma technique (ICP). For coupons immersed in reactor medium without phosphate during 84 hours it was obtained: 23.3 ± 0.7 mg/L for the abiotic control system and 6.34 ± 0.3 g/L for the inoculated biotic system. Dissolved iron was in average 4.6 times higher in absence of bacteria than in presence of it. These results together with the whole set of results suggest that the IRB *Geobacter sulfurreducens* reduces corrosion in medium without phosphate, even though a vivanite protective layer was not formed as shown in article 1. Nevertheless, instead of MICI, we could speak here of limitation of corrosion in a medium in which the corrosion rate is considerably high. However, the mechanisms linked to the corrosion limitation effects of the bacteria are still uncertain.
Concerning the high corrosion rates obtained in the medium without phosphate (for abiotic system, 8.8 times higher than with phosphate), a new question rose: what is the role of the weak acid $NH_4^+$ in the acceleration of corrosion once phosphate is not present in the medium?

In the domain of electro-analysis, some papers have shown that weak acids may catalyse the proton/water reduction [De Silva Munoz *et.al.*, 2010]. Hydrogen atoms of undissociated weak acids (HB) could be directly reduced without a dissociation step [De Silva Munoz *et.al.*, 2004]. The most widely weak acids studied are the protonated phosphate species. Weak acids can undergo an electrochemical deprotonation that strips their weakly bounded hydrogen atoms, which are more easily reduced than those linked to the water molecule. The cathodic deprotonation creates an equilibrated reaction that results in the production of molecular hydrogen and can be accelerated by hydrogen removal [L. De Silva Munoz *et.al.*, 2011]:

$$HB + e^- \rightleftarrows B^- + \tfrac{1}{2}H_2 \quad \text{(III.4)}$$

$$B^- + H^+ \rightleftarrows HB \quad \text{(III.5)}$$

De Silva *et al* [2007] showed that the electrochemical deprotonation of phosphate was possible on stainless steel and mild steel electrodes according to the following reaction mechanism: A two-step electrochemical reduction:

$$H_2PO_4 + e^- \rightleftarrows H_{ad} + HPO_4^{2-} \quad \text{(III.6)}$$

$$H_{ad} + H_2PO_4^- + e^- \rightleftarrows H_2 + HPO_4^{2-} \quad \text{(III.7)}$$

$$2H_{ad} \rightleftarrows H_2 \quad \text{(III.8)}$$

coupled with the acide-base equilibrium:

$$HPO_4^{2-} + H2O \rightleftarrows H2PO4 \quad \text{(III.9)}$$

In conclusion, LGC's team found that phosphate ions induced considerable anaerobic corrosion of mild steel, which was sensitive to hydrogen concentration in the solution; and that the corrosion potential of stainless steel in presence of

phosphate was shifted to more negative values as molecular hydrogen was added to the atmosphere in the reaction vessel. Phosphate species, and possibly other weak acids present in biofilms, are suggested to play an important role in the anaerobic corrosion of steels via a reversible mechanism of electrochemical deprotonation that may be accelerated by hydrogen removal.

In our case, the reactor medium contains two compounds that may behave as weak acids: $NaH_2PO_4$ and $NH_4Cl$. In article 1, the corrosion effect was not observed when these two compounds were present, thanks to the vivianite layer catalysed by the bacteria which protected the metal. At the same time, in absence of bacteria the presence of these two weak acids did not posed a mayor effect in the corrosion rates. Thus, it is presumed that there was a competitive effect between this two hydrogen donor species that restrained them from accelerating iron dissolution by their deprotonation. However, once taken away one of the two weak acids from the system, in this case taking out the phosphate species, there is left the $NH_4Cl$ that can be reduced as follows:

$$NH_4^+ + e^- \rightarrow NH_3 + \tfrac{1}{2}H_2 \qquad \text{(III.10)}$$

Therefore, this compound and its cathodic deprotonation results also in the production of molecular hydrogen which will end to accelerate corrosion by acceleration of the cathodic reaction, as observed in experiments by LGC team. The dissociation step for most weak acids is considered to be very rapid because, in most cases, no chemical limitation is found. Consequently, it may be observed acceleration of corrosion rate as it was observed in the control abiotic systems without phosphate.

## III.6. Weight loss results in these different media

In order to better conclude the whole set of electrochemical results previously presented in terms of corrosion rates, weight loss tests were performed simulating each of the previously presented experimental conditions. Weight loss tests were then performed in anaerobic conditions using reactor media with the different modifications already described; this is: standard reactor medium, reactor medium without phosphate, reactor medium without fumarate. Moreover, in this chapter's section, one more condition is presented in terms of weight loss test that was not presented in the electrochemical layout of experiments: reactor medium without $NH_4Cl$, aiming to test phosphate as a weak acid. Each of the conditions was tested with and without bacteria, immersing the coupons by duplicate in the different media.

These set of gravimetric experiments were performed using two types of metal coupons: C1145 (as presented in the electrochemical experiments) and C1015. This last, is the type of metal chosen to work with for the BIOCOR project and will be farther introduced in the next chapter. Two different immersion times were selected depending on the steel; 3 weeks for experiments with C1145 steel and 3 months for experiments with C1015. Table III. 9 resumes the experimental matrix designed for the mass loss experiments. For both types of metal coupons, conditions were kept anaerobic during the whole experiment by first taking out

dissolved oxygen after injection during 45 minutes with $N_2/CO_2$ (80:20) and then placing the weight loss hermetically closed vials into a $N_2$ chamber until the end of the experiment. Control systems where performed for each of the systems tested. They consisted in injecting a filtrate of a grown culture avoiding the presence of cells but injecting the bacteria metabolites.

| Test No. | Medium reference | Medium modifications | Bacteria source | Steel coupon | Time of immersion |
|---|---|---|---|---|---|
| 1 | G.S. reactor standard medium | Complete medium | *G. sulfurreducens* 5% | C1145 | 3 weeks |
| 2 | G.S. reactor standard medium | Complete medium | Control | C1145 | 3 weeks |
| 3 | $NH_4Cl$ as weak acid | Without $NaH_2PO_4$ | *G. sulfurreducens* 5% | C1145 | 3 weeks |
| 4 | $NH_4Cl$ as weak acid | Without $NaH_2PO4$ | Control | C1145 | 3 weeks |
| 5 | $NaH_2PO4$ as weak acid | without $NH_4Cl$ | *G. sulfurreducens* 5% | C1145 | 3 weeks |
| 6 | $NaH_2PO4$ as weak acid | without $NH_4Cl$ | Control | C1145 | 3 weeks |
| 7 | NaCl solution (30 mM) | NaCl | Blank | C1145 | 3 weeks |
| 8 | G.S.reactor medium | Complete medium | *G. sulfurreducens* 5% | C1015 | 3 months |
| 9 | G.S. reactor medium | Complete medium | Control | C1015 | 3 months |
| 10 | $NH_4Cl$ as weak acid | G.S medium without $NaHPO_4$ | *G. sulfurreducens* 5% | C1015 | 3 months |
| 11 | $NH_4Cl$ as weak acid | G.S medium without $NaH_2PO_4$ | Control | C1015 | 3 months |
| 12 | $NaH_2PO4$ as weak acid | G.S medium without $NH_4Cl$ | *G. sulfurreducens* 5% | C1015 | 3 months |
| 13 | $NaH_2PO4$ as weak acid | G.S medium without $NH_4Cl$ | Control | C1015 | 3 months |
| 14 | G.S reactor medium | G.S medium without fumarate | *G. sulfurreducens* 5% | C1015 | 3 months |
| 15 | G.S reactor medium | G.S medium without fumarate | Control | C1015 | 3 months |
| 16 | NaCl solution (30 mM) | NaCl | Blank | C1145 | 3 months |

Table III.9. Matrix of different conditions tested in weight loss tests in presence and absence of *Geobacter sulfurreducens* (G.S) using carbon steel C1145 and C1015 immersed in anaerobic G.S medium containing 1 mM acetate and 10 mM fumarate (except for tests 14 and 15) or NaCl solution

Fig. III.25 shows the results of weight loss in millimetres per year (mmpy) for carbon steel C1145 immersed in 3 different media (standard reactor medium, reactor medium without phosphate and reactor medium without ammonium

chloride) during 3 weeks. One blank system was also performed using this steel; this consisted in introducing the weight loss coupon into a NaCl solution (30 mM) which correspond to the chloride concentration used in all the sets of experiments. The figure displays the blue bars referring to the control abiotic systems and the red bars referring to the biotic systems.

Results show that in all the 3 conditions tested, it was found less mass loss when the bacterium was present into the systems than when it was not. For the cases of the control abiotic systems, the condition that presented the highest mass loss rate was the one using reactor medium without phosphate where the ammonium chloride was the only weak acid. It induced a corrosion rate of 2.2 times higher than when immersing the coupon in the standard reactor medium, 2.0 times higher than with medium without $NH_4Cl$ (only phosphate as weak acid) and 1.8 times higher than with the blank.
For the cases of the biotic systems, corrosion rates were very similar in all the three conditions tested; however, the conditions that presented higher mass loss rate were the one using standard reactor medium and the one using reactor medium without phosphate ($NH_4^+$ as weak acid). These conditions induced a corrosion rate of 1.5 times higher than when immersing the coupon in the reactor medium without ammonium (phosphate as weak acid).

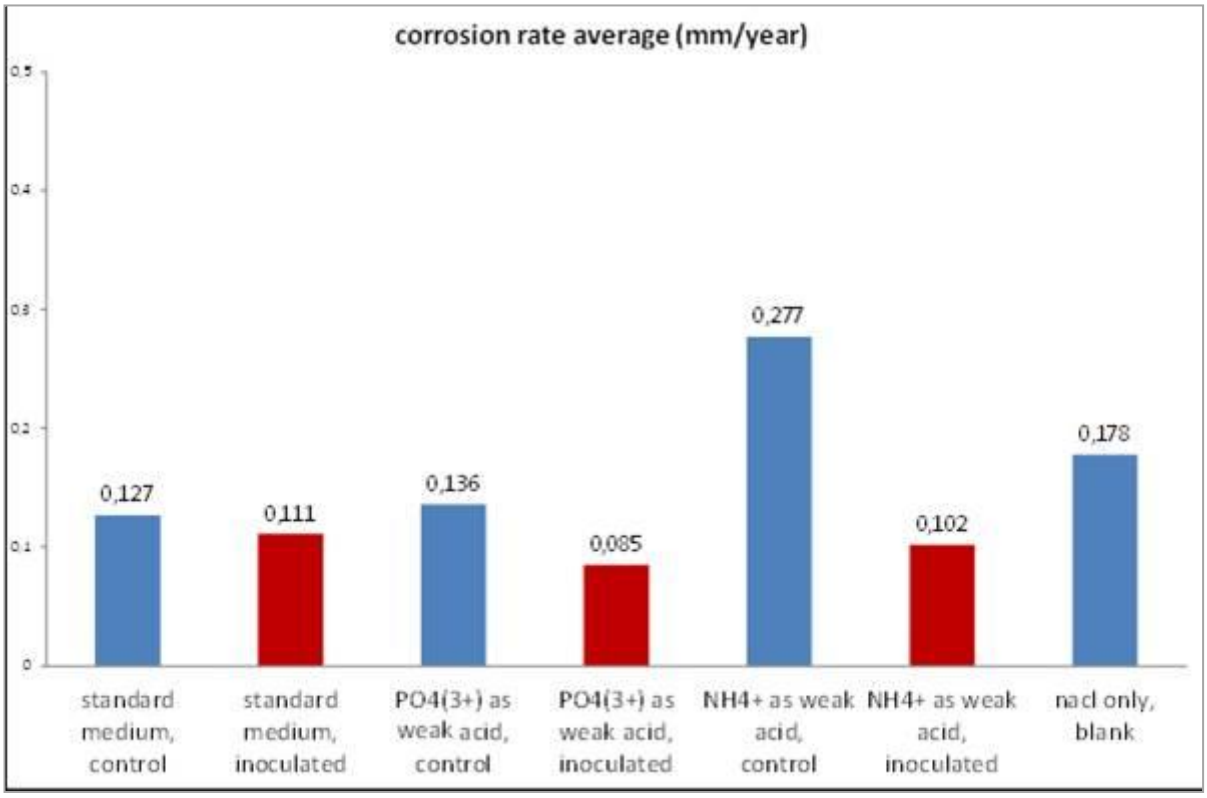


Fig. III.25. Weight loss diagram in mm/year for carbon steel C1145 after 3 weeks of immersion in reactor medium with 1 mM acetate, 25 mM fumarate. Experiments kept under anaerobic conditions by placing the reactors in an anaerobic container.

Finally, Fig. III.26 shows the results of weight loss in millimetres per year (mmpy) for carbon steel C1015 immersed in 4 different media (standard reactor medium,

reactor medium without phosphate, reactor medium without ammonium chloride, and reactor medium without fumarate) during 3 months. Results show that for 2 out of the 4 conditions tested, the control abiotic system depicted higher corrosion rates than on the biotic one in accordance with the previous electrochemical results; these are systems with standard reactor medium and reactor medium without phosphate. On the other hand, the system where it was found the most important difference of corrosion rate between the biotic and the abiotic system was the one with standard reactor medium finding 10.2 times more corrosion in the absence of bacteria than in presence of it.
The control reactor system that displays the highest corrosion rate is the one without phosphate, in accordance with results found with mild steel 1145. The corrosion rate found in this system is 1.6 times more important than with standard reactor medium, 16 times higher than with reactor medium without ammonium, 6.5 times higher than with reactor medium without fumarate and 1.4 times higher than the blank.

For the cases of the biotic systems, only two systems presented higher corrosion rates than in the control abiotic system: system without ammonium (phosphate as weak acid) and system without fumarate. This last was the biotic condition with the highest corrosion rate (0.47 mmpy), depicting 4.7 times higher rate than in the abiotic system and 11.8 times more corrosion than in the biotic system with fumarate, standard reactor medium. The fact of finding more corrosion in presence of bacteria is not in accordance with the $R_p$ results.

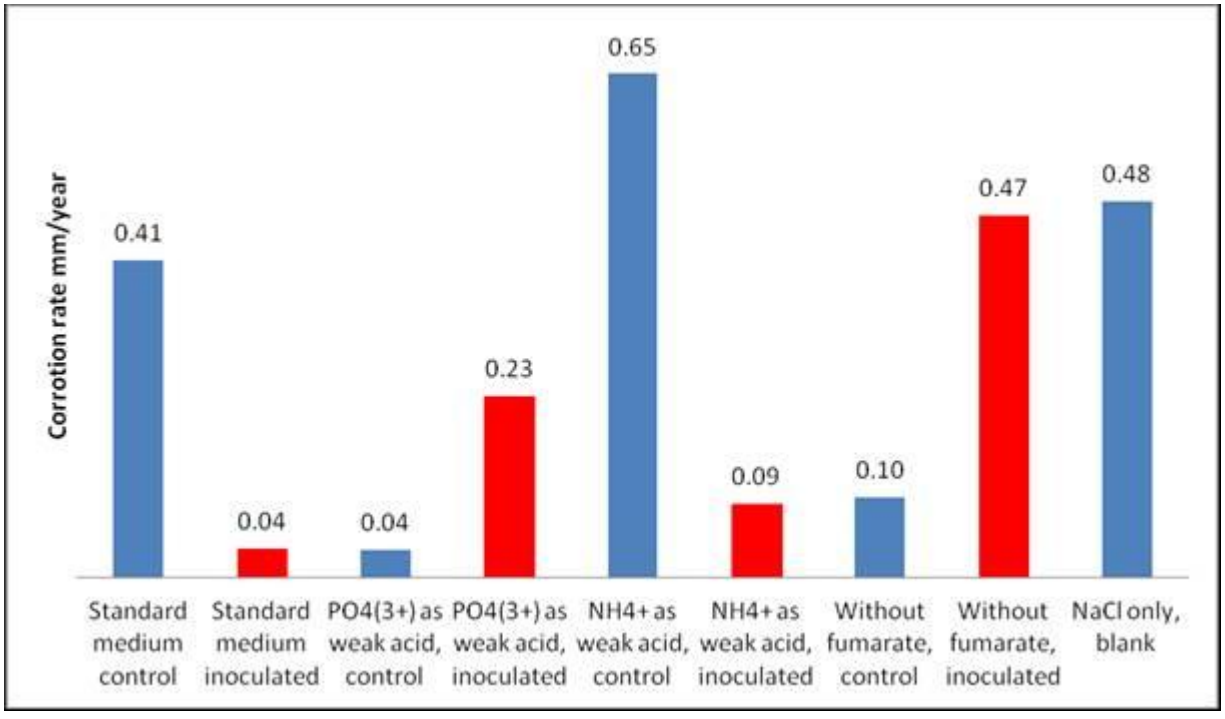


Fig. III.26. Weight loss diagram in mm/year for carbon steel C1015 after 3 months of immersion in reactor medium with 1 mM acetate, 25 mM fumarate. Reactor kept in anaerobic conditions by performing the experiment in anaerobic vials (no gas injection during the 3 months).

All the weight loss results support the main findings described under the frame of the electrochemical analysis. For instance, they support that in systems with phosphate, the presence of *Geobacter sulfurreducens* indeed protects the two types of steel tested depicting lower corrosion rates which can be correlated to lower Rp's found in the electrochemical results. The protection mechanisms proposed coincide with each of the outcomes from the different tests performed always suggesting that the presence of bacteria decreases corrosion rates. In absence of phosphate, it was also seen that after every test performed (EIS, weight loss, SEM, EDX and ICP) coincided with the suggestion of lower corrosion rates when bacteria is present. However, mechanisms are still uncertain and further analysis would be needed to elucidate them. Moreover, these results represent another evidence of the impact that in abiotic systems, the weak acids such as $NH_4^+$ can pose a threat on the corrosion of carbon steel. Surprisingly, results using phosphate as weak acid did not yield this same results then it is believed that a vivianite layer might have formed. Unfortunately, there are not SEM pictures that can support this hypothesis.

On the other hand, results in absence of fumarate remain inconclusive: weight loss results and corrosion potential monitoring suggest that the presence of bacteria accelerates corrosion which is represented by an ennoblement of the corrosion potential and higher mass loss than in the control system. In contrast, EIS results suggest that lower charge transfer reactions occur in presence of bacteria.

## III.7. Conclusions

The influence of *Geobacter sulfurreducens* on the anaerobic corrosion of carbon steel AISI C1145 and AISI C1015 was tested in different media conditions. For instance, the presence and/or absence of the electron donor and acceptor were tested as well as the presence and/or absence of phosphate and ammonium compounds acting as weak acids. For this, electrochemical, surface and weight loss analysis were performed.

The most important conclusion that can be obtained out of this work is that corrosion and the influence of the IRB *Geobacter sulfurreducens,* is highly dependent on the medium composition. However, it seems that for most of the different conditions tested, *G. sulfurreducens* tends to not accelerate the corrosion process by for example inducing the metal protection after the formation of a vivianite layer or by restraining corrosion rate in cases of accelerated corrosion as observed in the example of weak acids.

Weight loss results in their majority support the main findings described under the frame of the electrochemical analysis and microscopy observations. At the end of this study remained some questions that could not be answered: Mechanism of corrosion inhibition in absence of phosphate and the overall influence on corrosion that the absence of fumarate plays in a system with *G. sulfurreducens* in the All these remaining questions infer that biocorrosion processes are very complex and more multidisciplinary efforts need to be put in order to tackle it.

# *Chapter IV- Corrosion in the Oil and Gas Industry*

## IV.1. Introduction

After assessing the influence of a pure IRB strain in the corrosion of carbon steel, experiments using biofilm from the field, were performed. It is referred as biofilm from the field the microorganisms (consortia) and their EPS contained in the pigging debris which was extracted from a water injection system of the partner oil and gas company after a pigging operation. Water injection systems are widely used in the Oil industry, both on- shore and off-shore, in order to pressure up the hydrocarbon reservoirs and increase/maintain the oil production yield over a longer period of time. The injected fluid can be produced water (e.g. extracted from the hydrocarbon stream), sea water, aquifer water (e.g. extracted from water-bearing formations), river water or a mix of some of them. The water is pumped through carbon steel flow-lines and pipes.

The injections of these non-sterile waters induce the formation of biofilm which in some cases induce corrosion at high rates causing giant losses to the company. This part of the project aims to assess the corrosivity of this biofilm and to confirm whether only SRB bacteria are involved in the corrosion process or if by contrary, other bacterial groups such as IRB might be involved. For this, microbiological, surface analysis and electrochemical tests were performed such as: microbiological enrichments, DNA extraction and strains identification, SEM, EDX, XPS, weight loss tests and electrochemical experiments measuring free corrosion potential along time, electrochemical impedance spectroscopy and linear polarisation. Electrochemical and weight loss tests were performed using carbon steel coupons (AISI 1015) immersed in artificial sea water (ASW) and a mixture of produce water plus aquifer water from the field (50/50 v/v) (MIXED water). All these experimental results fall into the frame of the second approach given to the project.

Understanding the influence of a bacterial consortium on corrosion poses higher challenges than when working with a pure culture. This is due to the impossibility to perfectly reproduce the environmental conditions where the consortia from their micro-niche. Thus, a comparison of the results obtained with field natural water (MIXED) and an artificial medium (ASW) was performed and results are displayed in article 3 which is called: **Corrosion of Low Carbon Steel by Microorganisms from the 'Pigging' Operations Debris in Water Injection Pipelines**.

On the other hand, SRB have long time been considered to be the major hydrogen sulphide ($H_2S$) producers and, therefore, the core group of organisms associated within MIC of iron and ferrous alloys in oilfield environments [Orphan *et al.*, 2000]. However, in recent years, it has become evident that SRB are not the sole sulfidogenic microbial group in oil production systems. Thus, in order to understand and elucidate the microbial diversity found in a natural biofilm from an oil industry, DGGE analysis and DNA sequencing were performed intending to correlate the strains identified to corrosion tests, aiming to conclude whether SRB is or not the main responsible.

As with the first approach, these second approach results might be of help for the oil and gas industry when encountering microbially influenced corrosion problems. Having a better idea of the implication of a consortium of microorganisms in the

corrosion of water injection systems will be of help with the decision making process.

## IV.2. Corrosion in the oil and gas industry and its causes

One of the most susceptible industries for biofilm formation and their detrimental consequences is the oil and gas industry. Biofilms are present from the oil fields to the storage tanks where refined products are commercialized [Sanders and Sturman, 2005]. For instance, oil distribution systems and water injection pipelines host an ideal micro-environment for some potentially dangerous microorganisms in terms of corrosion. In Figure IV.1, a scheme provided by the industrial partner, displays some of the petroleum industry structures that are susceptible of being affected by biofilms. These structures are in direct contact with water or with fluids (oil) that have a certain percentage of water associated. The samples received from the industrial partner and used along this study were taken from the water injection sites appreciated in the scheme.

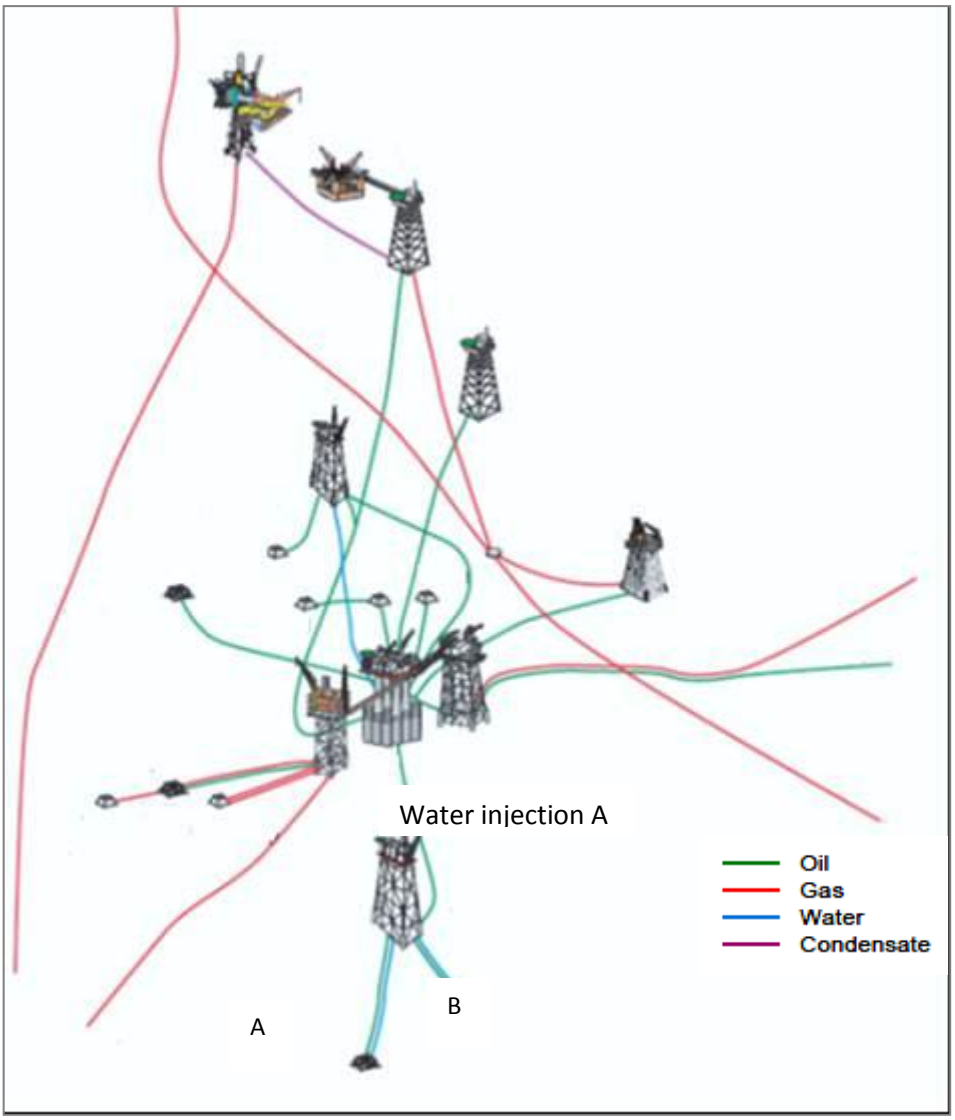


Fig. IV.1. Oil industry installation diagram including the water injection system A with installations A and B

Along the long chain of processes performed in the oil and gas industry, a large variety of bacteria such as SRB can produce $H_2S$ and influence corrosion. However, the presence of other bacterial groups has been underestimated or mistakenly stated that the presence of SRB are the sole sulphide producer causing corrosion. Thanks to recent molecular biology studies it has been found that for example, species which belong to phylum Firmicutes or Synergistetes are able to generate $H_2S$ using thiosulfate and organic sulphur-rich compounds under different temperature regimes [Crolet and Magot, 1996; Magot *et al.,* 1997]. Their presence and relatively high abundance has been confirmed in a number of oil field installations using techniques of molecular ecology [Duncan *et al.,* 2009. Kobayashi *et al.,* 2012].

Moreover, as it has been previously stated in this thesis, hydrogen sulfide is not the only causative agent of carbon steel corrosion. Other compounds such as sulphuric acid, ammonia, and hydrogen (which may be produced or catalysed by the presence of bacteria), can be responsible for corrosion processes. Furthermore, other bacterial groups such as IOB and IRB which are involved in the metal-oxidation and reduction are also important in MIC [Beech and Gaylard, 1999]. It is for these facts and based on the presence of metabolic pathways relevant to corrosion reactions that the bacterial groups previously presented in the previous chapters, have been targeted for purposes of this study. Thus, the main microorganisms involved in biocorrosion and targeted here, can be categorised into a few main groups: sulphate-reducing bacteria (SRB), acid-producing bacteria (APB), metal-oxidizing/reducing bacteria (IOB, IRB), nitrate reducing bacteria (NRB), manganese oxidising bacteria (MOB) and methane producing bacteria (MPB).

In these industries, the problems originated by microbial activity are particularly difficult to diagnose, evaluate and control. The characterization of the microbial communities in the oil and gas industry is important in order to establish their possible interactions, their multicellular strategies, their possible biocomplexity and their bioelectrochemical influence when they incorporate to the industrial metallic facilities [Dominguez, 2007].

## IV.3. Problems to be solved

The main problem that corrosion and biocorrosion pose in any industry is related to economic losses. For example, biocorrosion in offshore water injection systems results in extensive and costly damage to the equipment and additional production losses due to the shutting down of the production units for several weeks. It is important to better manage biocorrosion during the injection operations, in order to reduce costs, and for safety & environmental reasons. In order to achieve this, it is necessary to develop more knowledge about biocorrosion formation, monitoring and mitigation [Biocor, 2010].

This thesis has been framed under the European funded project BIOCOR. BIOCOR is an initial training network where scientists from around Europe joint their efforts to tackle biocorrosion related problems in different industries. The collaborative network expands through Europe with partners in Norway, Germany, France, Italy, Hungary, Portugal, Sweden and the UK.

The individual project (IP2) described in this thesis has centred its research studies using pigging samples from the oil and gas industry. The main objective of this IP is to identify new biocorrosion mechanisms (involving new microbial genera) for those cases where SRB theory is not relevant. For this, new experimental models able to reproduce biocorrosion cases observed in the field were developed in the laboratory.

## IV.4. Water injections systems and pigging samples

Biofilm from the field was used to assess its corrosion effects on carbon steel coupons. For this, pigging debris samples were collected from a water injection pipeline "A" located in the installation "A" of an Oil and gas company located in Norway between November 2010 and June 2011. The pipeline consists in 10-15 km long pipe made of low carbon steel with an average operating temperature of 35°C. Fig. IV.2 describes the layout of the water injection installation A of the oil and gas partner. It can be observed, as it has been previously stated, that the water injection system A is fed with around 50% of produced water (e.g. extracted from the hydrocarbon stream) and 50% of aquifer water (e.g. extracted from water-bearing formations). The mixture rate is not kept constant during the whole year but during the time of the study it averaged 50-50%. Furthermore, the figure also describes that a corrosion inhibitor is added at some level of the system and thanks to information provided, it is known that its concentration averages 4 ppm at the degasser level (previous to extracting the pigging samples).

Five samples were received along the 3 years project corresponding to two pigging operations performed in the same pipes. They were labelled pig 1, pig 4, pig 9 (first batch received in December 2010) and pig 2 and pig 5 (second batch, received in June 2011). Pig 1 corresponds to the first debris collected after the first pigging operation; pig 2 corresponds to the second debris collected after the second pigging operation and so on. Thus, it is considered that each of the pigging samples represents a different stratum of sample forming biofilm on the inner walls of the pipelines. Bacterial consortia living in the different strata of the pigging samples were cultured in different enrichment media aiming to separate bacteria regarding their different metabolic pathways. The pigging samples were used to perform the different enrichments already mentioned and to perform the corrosion and electrochemical tests.

On the other hand, table IV.1 resumes some surface and analytical analysis performed to the corrosion products extracted from the water injection system A. These analyses were performed and provided by the industrial partner. It can be observed the abundance of FeS as the main corrosion product. Thus, it is presumed the abundance of sulphide producer microorganisms.

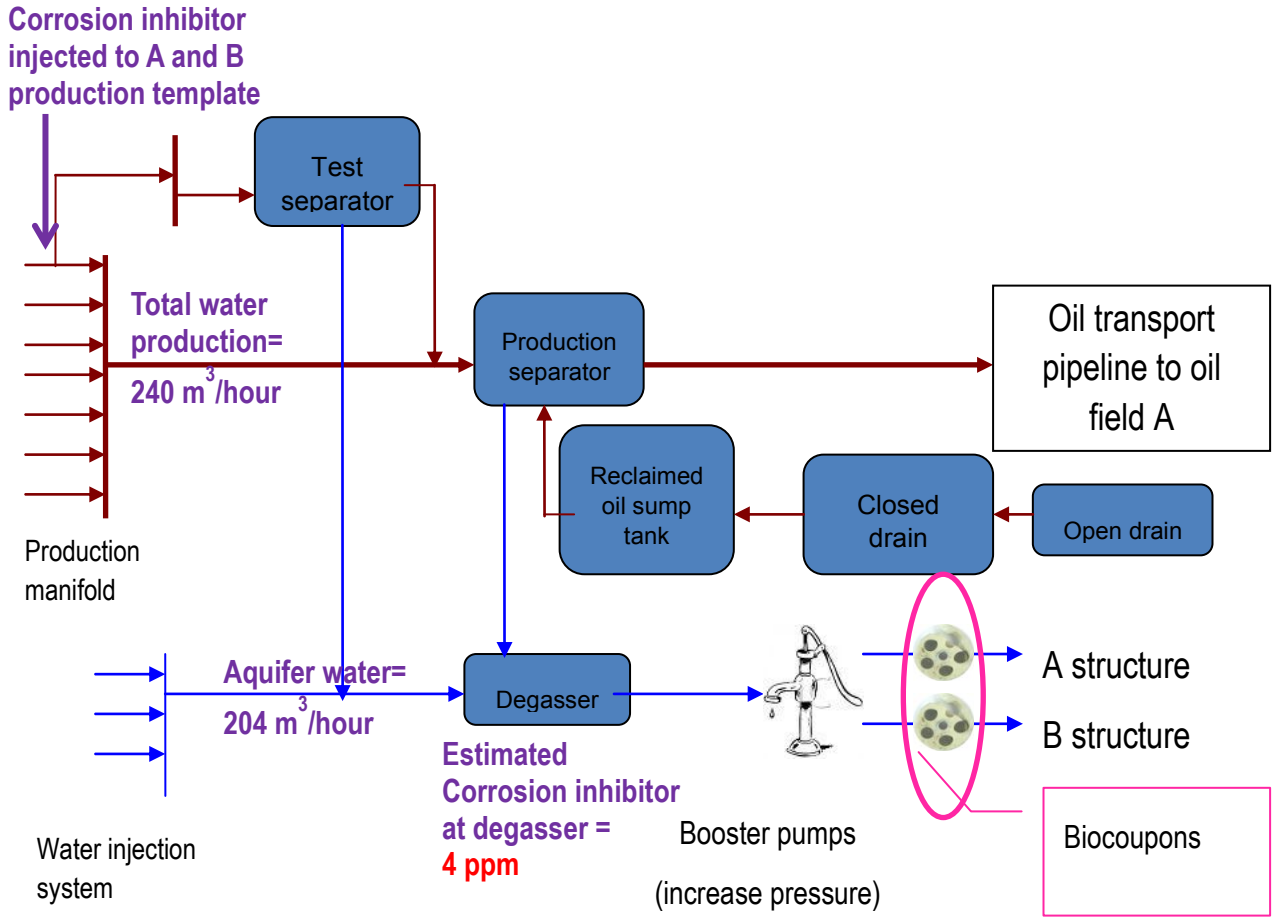


Fig. IV.2. Water injection A flow chart main process

| Sample | XRD | Ash content 800°C[1] (weight %) | Comments |
|---|---|---|---|
| A- structure, Pig 1 | In the fraction composed of black flakes:<br>Plenty FeS (mackinawite)<br>Little $FeCO_3$ (siderite)<br>Little $BaSO_4$ (barite) | Not analysed | The inorganic part of the sample was composed of two fractions that was separated by passing the sample through a sieve." Approximately 15 weight% of the inorganic material was composed of "black flakes",. The rest of the inorganic material was sand, quarts. |
| A - structure, Pig 4 | Plenty FeS (mackinawite)<br>Plenty $FeCO_3$ (siderite)<br>Little $SiO_2$ (quarts)<br>Little $BaSO_4$ (barite)<br>Little $CaCO_3$ (calcite) | 18 | |
| A – structure, Pig 9 | Plenty FeS (mackinawite)<br>Plenty $FeCO_3$ (siderite)<br>Little $BaSO_4$ (barite)<br>Little $CaCO_3$ (calcite)<br>Traes of $SiO_2$ (quarts) | 25 | |

Table IV.1. XRD and ash content analysis performed by the industrial partner to samples from the water injection installation A structure A.

## IV.5. The work performed

### IV.5.1 Microbiological results

The different pigging debris samples collected were used to perform several bacterial enrichments. 3 non selective enrichments presented in the table below (using pigs 1, 4 and 9) were done in order to favour the growth of a large group of heterotrophic bacteria in aerobic and anaerobic conditions. Furthermore, different selective enrichments were performed in order to target the following microorganisms' metabolic pathways. For anaerobic and/or facultative pathways: sulphate reduction, iron reduction, methane production, nitrate reduction coupled to iron oxidation. For aerobic and/or facultative pathways: iron and manganese oxidation and acid production.

After several weeks of incubation at 30 or 35 °C in stagnant conditions, bacterial growth was assessed. Table IV.2 resumes the growth observations noted for the non-selective media used. At the same time, table IV.3 resumes the growth results obtained in the selective media used.

| SAMPLE | MEDIUM | Atmosphere | TURBIDITY |
|---|---|---|---|
| PIG 1 | TSB+ NaCl | Aerobic | +++ |
| | | Anaerobic | +++ |
| | TSB + NaCl + Na- Lactate | Aerobic | +++ |
| | | Anaerobic | +++ |
| | Marine broth | Aerobic | +++ |
| | | Anaerobic | +++ |
| PIG 4 | TSB + NaCl | Aerobic | + |
| | | Anaerobic | + |
| | TSB + NaCl + Na- Lactate | Aerobic | -- |
| | | Anaerobic | -- |
| | Marine broth | Aerobic | + |
| | | Anaerobic | + |
| PIG 9 | TSB + NaCl | Aerobic | + |
| | | Anaerobic | + |
| | TSB + NaCl + Na- Lactate | Aerobic | + |
| | | Anaerobic | + |
| | Marine broth | Aerobic | +++ |
| | | Anaerobic | +++ |

Table IV.2. Non selective enrichments growth results. Growth is consider positive when turbidity is observed after one week of incubation: (+++): turbid, (+): little turbid (--): non-turbid

| SAMPLE | MEDIUM | Bacteria Group | GROWTH | Incubation time |
|---|---|---|---|---|
| PIG 1 | Sulfur amended Mackintosh | APB | - | < 2 week |
| | API broth | SRB | + | < 1week |
| | FWA-Fe(III) | IRB | + | <3 weeks |
| | 9 K | IOB | - | < 2 weeks |
| | Straubk | IOB/NRB | + | < 3 weeks |
| | K | MOB | + | < 2 weeks |
| | Romesser | MPB | + | < 5 weeks |
| PIG 4 | Sulfur amended Mackintosh | APB | - | < 2 week |
| | API broth | SRB | - | < 1week |
| | FWA-Fe(III) | IRB | + | <3 weeks |
| | 9 K | IOB | - | < 2 weeks |
| | Straubk | IOB/NRB | + | < 3 weeks |
| | K | MOB | - | < 2 weeks |
| | Romesser | MPB | + | < 5 weeks |
| PIG 9 | Sulfur amended Mackintosh | APB | - | < 2 week |
| | API broth | SRB | + | < 1week |
| | FWA-Fe(III) | IRB | - | <3 weeks |
| | 9 K | IOB | - | < 2 weeks |
| | Straubk | IOB/NRB | + | < 3 weeks |
| | K | MOB | - | < 2 weeks |
| | Romesser | MPB | - | < 5 weeks |
| PIG 2 | Sulfur amended Mackintosh | APB | - | < 2 week |
| | API broth | SRB | - | < 1week |
| | FWA-Fe(III) | IRB | + | <3 weeks |
| | 9 K | IOB | - | < 2 weeks |
| | Straubk | IOB/NRB | + | < 3 weeks |
| | K | MOB | + | < 2 weeks |
| | Romesser | MPB | - | < 5 weeks |
| PIG 5 | Sulfur amended Mackintosh | APB | - | < 2 week |
| | API broth | SRB | + | < 1week |
| | FWA-Fe(III) | IRB | + | <3 weeks |
| | 9 K | IOB | - | < 2 weeks |
| | Straubk | IOB/NRB | - | < 3 weeks |
| | K | MOB | - | < 2 weeks |
| | Romesser | MPB | + | < 5 weeks |

Table IV.3. Selective enrichments: growth results.

The criteria used for considering a positive growth in the case of the selective enrichments have been described in chapter II. This is, for most of the cases, a colour change of the medium induced or catalysed by the bacteria when it oxidize or reduce certain compounds which consequently changed the colour of the medium. For example, reduction of iron (III) citrate (yellow) by IRB produces iron (II) compounds (dark green). At the same time, sulphate reduction by SRB produce sulphide which in presence of iron compounds forms black deposits (FeS); thus it can be observed the colour change of the medium from clear to black, etc. (Fig.IV.3). On the other hand, detection of methane produced by methane producing bacteria (Romesser medium) was detected by a micro gas chromatographer (μ GC). Table IV.4 resumes the methane and hydrogen average concentration found in the different enrichments. Measurements were performed by triplicate. For instance, methane was detected in enrichment media inoculated with Pig 1, 4 and 5 and hydrogen was detected in enrichment media inoculated with Pig 1. An example of a chromatograph depicting methane detection is shown below in Fig. IV.4.

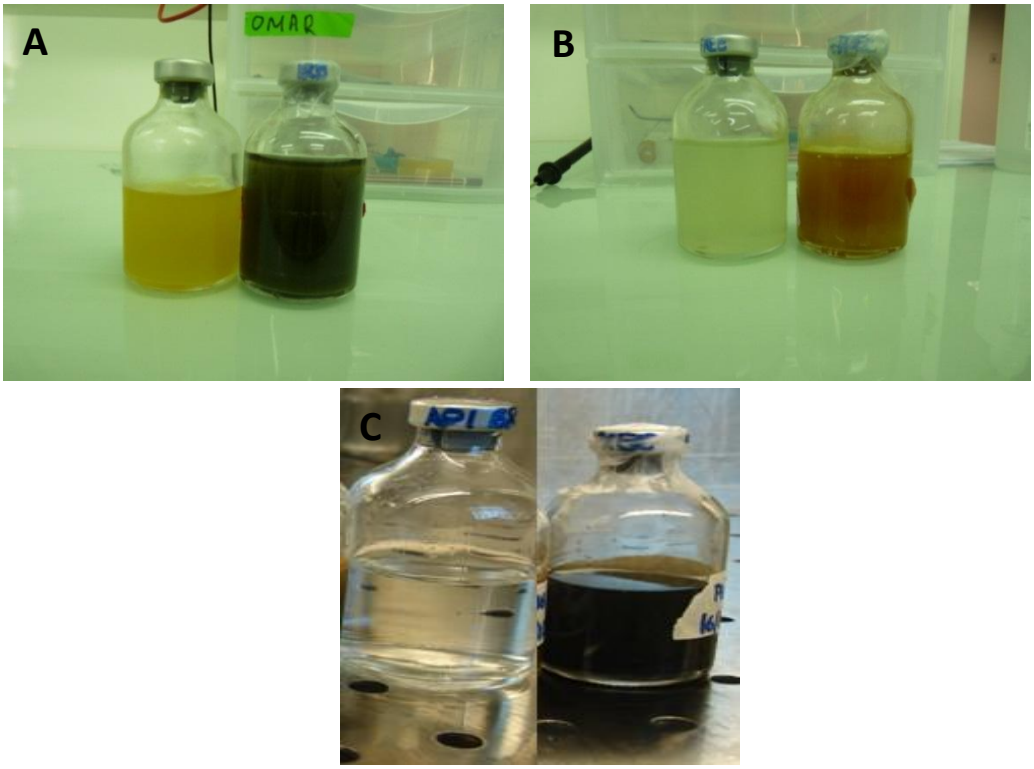


Fig.IV.3. Selective enrichment media before and after bacteria growth. (A): FWA-Fe medium for IRB; (B): Straubk medium for IOB/NRB; (C): Api broth for SRB

| Sample | Methane concentration | Hydrogen concentration |
|---|---|---|
| Pig 1 | 0.2 | 0.14 |
| Pig 2 | <0.001 | <0.001 |
| Pig 4 | 0.2 | <0.001 |
| Pig 5 | 5.8 | <0.01 |
| Pig 9 | <0.1 | <0.001 |

Table IV.4. Methane and hydrogen measurement using a μGC from Rossemer enrichment medium

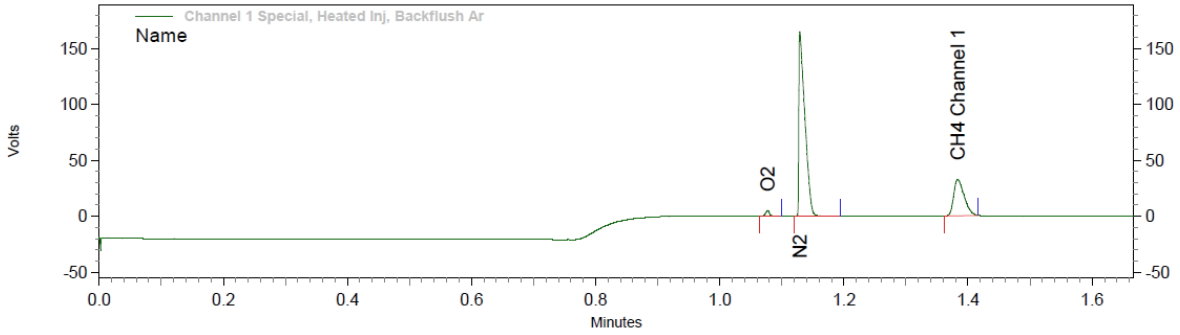


**Results**

| *Pk #* | *Name* | *Retention Time* | *Area* | *Concentration* |
|---|---|---|---|---|
| | H2 | | | **0.000 BDL** |
| 1 | O2 | 1.077 | 202998 | **1.019** |
| 2 | N2 | 1.129 | 11122981 | **70.084** |
| 3 | CH4 Channel 1 | 1.383 | 3824103 | **7.459** |
| Totals | | | 15150082 | **78.562** |

Fig.IV.4. GC chromatograph of enrichment medium inoculated with pig 5. Below there is a resume of the acquisition conditions (retention time and gases detected)

The first conclusion that can be highlighted from these results is that bacterial diversity decreases as the pig number increases. If the higher the number of the pig means that is closer to the pipeline walls, then it can be thought that closer to the pipelines there is a poorer diversity. It is possible that some compounds concentrations decrease also when they get closer to the pipeline walls or inner stratum. For example, fewer traces of oxygen and acetate might be found in the inner stratum than in the outer one. These differences could have affected the bacterial population. On the other hand, another explanation for these results is the physical consistency of the samples. The higher the pig number the less the quantity of water (liquids) contained in the sample (see chapter II, Fig.II.3). Thus, when the sampling was performed, oxygen could have diffused faster in those samples with less liquid [Ponnanperuma, 1972]. Some strict anaerobic strains might have died when in contact with the oxygen.

Once positive growths were confirmed, biomass pellets were extracted from the growing culture media. Pellets (in duplicate or triplicate) were sent to the laboratory of microbiology of the University of Portsmouth (UoP) for further analysis. However, in some cases where the criteria for positive growth was not fulfilled but turbidity was observed, biomass pellets were also extracted; this is the case for all the media used to target IOB and APB and media for MPB: pig 9. The samples were analysed using techniques which include DNA extraction from the samples, Polymerase Chain Reaction (PCR) for bacteria 16S rRNA (550 pb), agarose gel electrophoresis, Denaturing gradient Gel electrophoresis (DGGE), and examination through sequencing. Further results which include cloning and PCR targeting a wider group of genes such as *dsrAB*, *aprA*, and *Shewanella spp*. gene for PCR, are presented in annex I. This annex results were obtained thanks to the collaboration exerted with UoP.

Furthermore, in order to confirm the DNA extraction from the different enrichments pellets, the DNA concentration was checked on a NanoDrop ND-1000 spectrophotometer using a total volume of 2 µL (table IV.5).

| sample ID | sample name | ng/µl | 260/280 abs ratio | sample ID | Sample name | ng/µl | 260/280 abs ratio |
|---|---|---|---|---|---|---|---|
| 1 | IRB: pig 1 | 7.8 | 1.19 | 28 | MPB: pig 9 | 26.0 | 1.87 |
| 2 | IRB: pig 1 | 4.2 | 1.25 | 29 | APB: pig 9 | 3.7 | 1.27 |
| 3 | IOB: pig 4 | 4.9 | 1.34 | 30 | MOB: pig 9 | 4.8 | 1.52 |
| 4 | IOB/NRB: pig 1 | 3.6 | 1.62 | 31 | ASW: pig 9 | 17.2 | 1.95 |
| 5 | IOB/NRB: pig 1 | 5.2 | 1.35 | 32 | IOB: pig 9 | 2.2 | 1.36 |
| 6 | IRB: pig 1 | 7.4 | 0.97 | 33 | ASW: pig 2* | 13.1 | 2.05 |
| 7 | IRB: pig 1 | 11.8 | 1.17 | 34 | APB: pig 2 | 2.0 | 1.86 |
| 8 | SRB: pig 1 | 11.2 | 1.82 | 35 | MPB: pig 2 | 45.8 | 1.67 |
| 9 | ASW: pig 1* | 11.7 | 1.76 | 36 | IRB: pig 2 | 138 | 1.21 |
| 10 | MPB: pig 1 | 19.3 | 1.49 | 37 | MOB: pig 2 | 78.1 | 1.40 |
| 11 | MPB: pig 1 | 1.2 | 0.94 | 38 | MOB: pig 2 | 21.8 | 1.26 |
| 12 | APB: pig 1 | 4.5 | 1.30 | 39 | APB: pig 2 | 2.6 | 1.21 |
| 13 | MOB: pig 1 | 6.9 | 1.46 | 40 | IRB: pig 5 | 188 | 1.16 |
| 14 | IOB: pig 1 | 7.3 | 1.50 | 41 | MPB: pig 5 | 29.7 | 1.83 |
| 15 | MOB: pig 4 | 5.6 | 1.23 | 42 | APB: pig 5 | 2.3 | 1.20 |
| 16 | ASW: pig 2* | 13.9 | 1.63 | 43 | APB: pig 5 | 14.6 | 1.40 |
| 17 | SRB: pig 4 | 2.2 | 2.02 | 44 | IOB/NRB:pig9 | 78.3 | 1.16 |
| 18 | APB: pig 4 | 4.3 | 1.20 | 45 | IOB/NRB:pig1 | 52.2 | 1.25 |
| 19 | MPB: pig 4 | 18.9 | 1.76 | 46 | IRB: pig 1 | 1125 | 1.17 |
| 20 | IOB: pig 4 | 2.9 | 1.99 | 47 | IRB: pig 1 | 32.9 | 0.96 |
| 21 | SRB: pig 4 | 6.7 | 1.60 | 48 | IOB/NRB:pig 2 | 3.7 | 1.21 |
| 22 | IOB/NRB: pig 4 | 6.4 | 1.58 | 49 | MPB: pig 1 | 30.2 | 1.67 |
| 23 | IOB/NRB: pig 4 | 21.5 | 1.09 | 50 | MPB: pig 9 | 18.3 | 1.59 |
| 24 | IOB/NRB: pig 9 | 5.0 | 1.52 | 51 | MPB: pig 1 | 30.9 | 1.75 |
| 25 | SRB: pig 9 | 4.2 | 1.62 | 52 | MPB: pig 9 | 21.7 | 1.62 |
| 26 | IOB/NRB: pig 9 | 5.5 | 1.39 | 53 | MIXED: pig 1* | 27.2 | 1.81 |
| 27 | IOB: pig 9 | 1.7 | 1.13 | 54 | MIXED water* | 16.8 | 1.46 |

Table IV.5. DNA concentration extracted from the enrichments; *: results used for article 3

Absorbance measurements were performed at 260 nm wavelength which is the one where nucleic acids absorb light. Some other molecules such as nucleotides, RNA, ssDNA, and dsDNA, will absorb at 260 nm and contribute to the total absorbance. Moreover, the ratio of absorbance at 260 nm and 280 nm is used to assess the purity of DNA and RNA. A ratio of ~1.8 is generally accepted as “pure” for DNA; a ratio of ~2.0 is generally accepted as “pure” for RNA. If the ratio is appreciably lower in either case, it may indicate the presence of protein, phenol or other contaminants that absorb strongly at or near 280 nm. Thus, it can be said that regarding the enrichment samples, different DNA concentrations were found in all the samples tested. However, some of the samples contained some contaminants that were not discarded during the DNA extraction but amplification was still pursued. The highest DNA concentration was found in enrichment samples for IRB. Further DNA purification was attempted on these samples suspecting that were highly contaminated with compounds affecting the absorbance reading.

Once confirming the DNA presence in each of the samples, amplification of the DNA was attempted by performing PCR for bacteria 16SrRNA (550 pb) using the primers F3+GC and reverse [Muyzer, 1993] (Table IV.6).

Fig.IV.5. shows the electrophoresis gel run to evidence the presence or absence of DNA by the appearance of a band. The absence of a band in the agarose gel (which has been represented as (-) in table IV.6) led us to discard the sample due to the absence of DNA in the PCR product. It is important to remark that most of the enrichment revealed strong dark bands indicating a high concentration of amplified PCR products but just a few displayed low bands or weak bands. The weak bands observed might be due to one of the following cases: (i) a failure in cells concentration when preparing the biomass pellet which directly affected the DNA concentration; (ii) diversity decrease regarding the pig sample; (iii) a failure extracting DNA; (iv) a non-appropriate enrichment medium. For these cases of weak bands, a second attempt of amplification was pursued before taking the decision of discarding the sample. Samples that underwent a second PCR can be observed in Fig.IV.7.

Once the second PCR was performed, samples which showed a strong presence of a band, where then processed for DNA separation using a DGGE gel (table IV.6). DGGE was performed for 36 of the 48 enrichments chosen; this was as a consequence of little or no PCR product present in 12 samples numbered 2-5, 11, 23, 27, 32, 34, 43, 46 and 47. These last PCR products did not produce enough amplicons to be used on DGGE gel.

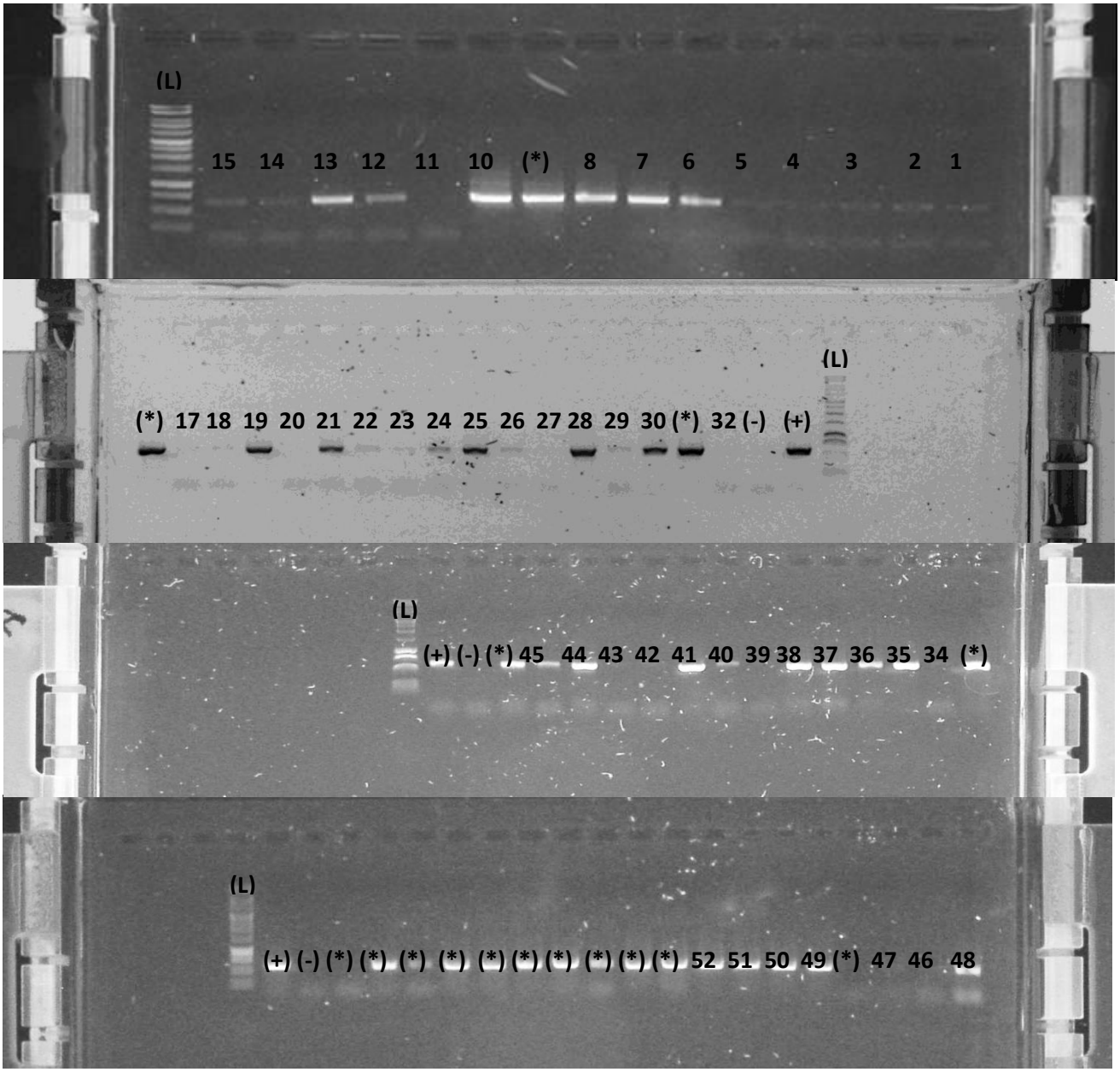


Fig. IV.5. Picture of 0.9% agarose gel showing result of Bacteria 16S rRNA from enrichments samples.(L): 1 kb DNA ladder; (-): negative control; (+): positive control; (*): samples used for article 3

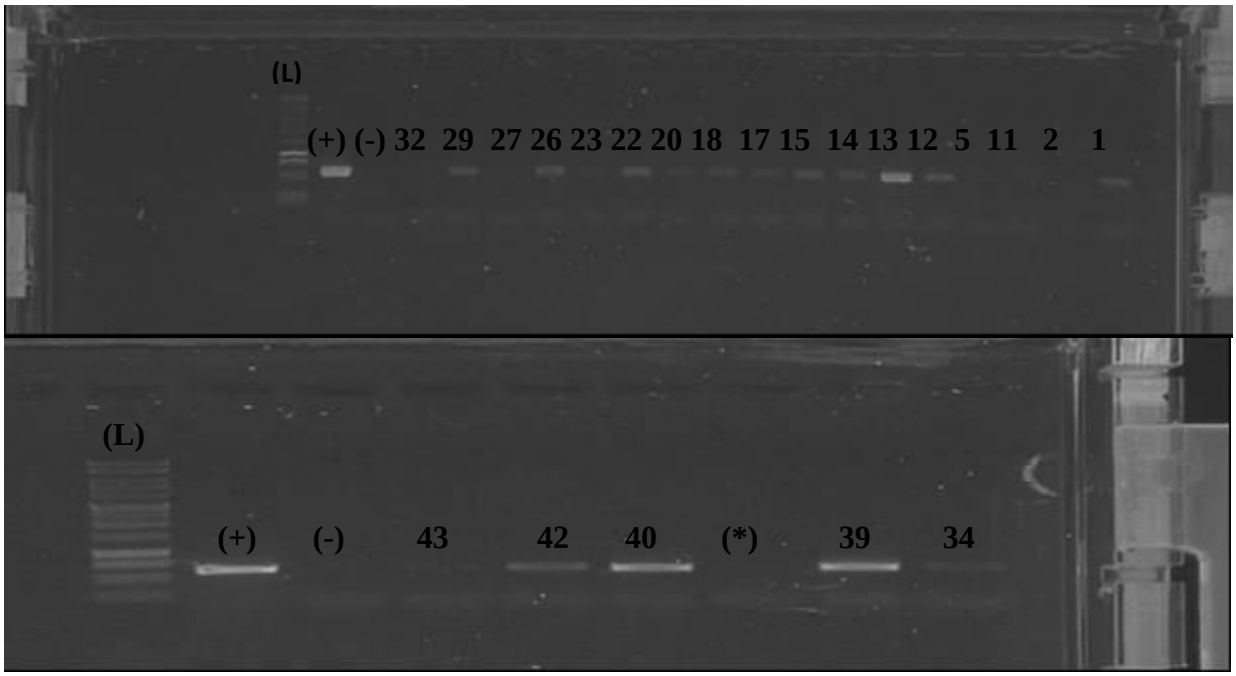


Fig. IV.6. Picture of 0.9% agarose gel showing result of Bacteria 16S rRNA from enrichments samples.(L): 1 kb DNA ladder; (-): negative control; (+): positive control; (*): samples used for article 3

| Sample ID | Sample name | Bacteria 16SrRNA | Sample ID | Sample name | Bacteria 16SrRNA |
|---|---|---|---|---|---|
| 1 | IRB: pig 1 | + | 29 | APB: pig 9 | + |
| 2 | IRB: pig 1 | - | 30 | MOB: pig 9 | + |
| 3 | IOB: pig 4 | - | 31 | ASW: pig 9 | + |
| 4 | IOB/NRB: pig 1 | - | 32 | IOB: pig 9 | - |
| 5 | IOB/NRB: pig 1 | - | 33 | ASW: pig 2* | + |
| 6 | IRB: pig 1 | + | 34 | APB: pig 2 | - |
| 7 | IRB: pig 1 | + | 35 | MPB: pig 2 | + |
| 8 | SRB: pig 1 | + | 36 | IRB: pig 2 | + |
| 9 | ASW:pig 1* | + | 37 | MOB: pig 2 | + |
| 10 | MPB: pig 1 | + | 38 | MOB: pig 2 | + |
| 11 | MPB: pig 1 | - | 39 | APB: pig 2 | + |
| 12 | APB: pig 1 | + | 40 | IRB: pig 5 | + |
| 13 | MOB: pig 1 | + | 41 | MPB: pig 5 | + |
| 14 | IOB: pig 1 | + | 42 | APB: pig 5 | + |
| 15 | MOB: pig 4 | + | 43 | APB: pig 5 | - |
| 16 | ASW: pig 2* | + | 44 | IOB/NRB: pig 9 | + |
| 17 | SRB: pig 4 | + | 45 | IOB/NRB: pig 1 | + |
| 18 | APB: pig 4 | + | 46 | IRB: pig 1 | - |
| 19 | MPB: pig 4 | + | 47 | IRB: pig 1 | - |
| 20 | IOB: pig 4 | + | 48 | IOB/NRB: pig 2 | + |
| 21 | SRB: pig 4 | + | 49 | MPB: pig 1 | + |
| 22 | IOB/NRB: pig 4 | + | 50 | MPB: pig 9 | + |
| 23 | IOB/NRB: pig 4 | - | 51 | MPB: pig 1 | + |
| 24 | IOB/NRB: pig 9 | + | 52 | MPB: pig 9 | + |
| 25 | SRB: pig 9 | + | 53 | MIXED: pig 1* | + |
| 26 | IOB/NRB: pig 9 | + | 54 | MIXED water* | + |
| 27 | IOB: pig 9 | - | | | |
| 28 | MPB: pig 9 | + | | | |

Table IV.6. PCR results of DNA extracted from selective enrichment media inoculated with pigging debris; *: results used for article 3

The totally of the enrichments samples previously described, have been divided into 3 gels (Fig. IV.7: A, B and C). Out of the 36 samples run in DGGE gel approximately 210 visible bands were observed but only 135 bands were cut. The bands that were visible but not cut were rule out because they were showing a similar pattern in other lines of the gel. Each line corresponds to a sample (refer to sample ID) and each band cut correspond to a letter; e.i.: line 1 corresponds to sample ID 1 (IRB pig 1) which has three bands that were cut (1: A, B and C). Furthermore, each band represents a DNA sequence characteristic of a single strain. Saying this, it can implied that DGGE results show that there is a large biodiversity of bacteria in the enrichments culture media, especially when results are compared to those of article 3: the biodiversity detected in the pigging debris and in the ASW and MIXED water inoculated with pigging debris is largely reduced when comparing it to the biodiversity found in the enrichment culture media.

On the other hand, out of the results observed in the 3 gels (A, B and C) there are certain bands that repeat a pattern in the different lanes. For instance, in gel A

lanes 14 to 22, it is observed a pattern of two bands that repeat in each of the lanes. This pattern is observed even though the enrichments media of these lines is not the same. This would lead us to think that the media used was not as selective as expected; however, it is important to remark that all the samples from this gel A, underwent a second amplification step because no band or a weak band was observed in the agarose gel. Thus, it can be said that indeed the DNA band detected after the second amplification corresponded to the DNA of strain which growth was not favoured in the respective medium.

In gel B it can be observed one band showing a pattern in lines 7 to 30 (line 7, band A). This band is mainly the only one which repeats in all these lanes. However, there are other bands observed in different regions of the gel within these lanes making us presume that there is a strain which prevails in several enrichment media and that this did not impede to observed other enriched bacteria in the different media.

Finally, gel C is the one gel showing less band positioning patterns. The only pattern observed is within lines 49 to 52 but this time this pattern was expected as these lines correspond to the same enrichment medium: Romesser medium for methane producing bacteria.

Once the bands detected and targeted were cut, they pursued a last DNA purification in order to send the DNA samples for sequencing. A total DNA solution volume of 20 µL at a concentration of 10-50 µg/µL were send to GATC sequencing services company. Identification was then pursued once the sequencing results were obtained, by blasting the sequence in the NCBI (national centre for biotechnology information) website.

Table IV.7 describes the identification results for each of the bands displayed in the DGGE gels. Unfortunately, not all the sequencing results were achieved. Out of the total bands cut, 38% of them did not yield ideal results due probably to errors made during the DNA preservation by problems in the freezing and unfreezing procedure. Moreover, some of the bands cut were not sent for sequencing due to not achieving to have enough DNA once the sample was purified. Whatever the reason for not obtaining the results, in the table has been marked as “did not yield good results” when results could not have been obtained due to either of the two reasons previously presented.

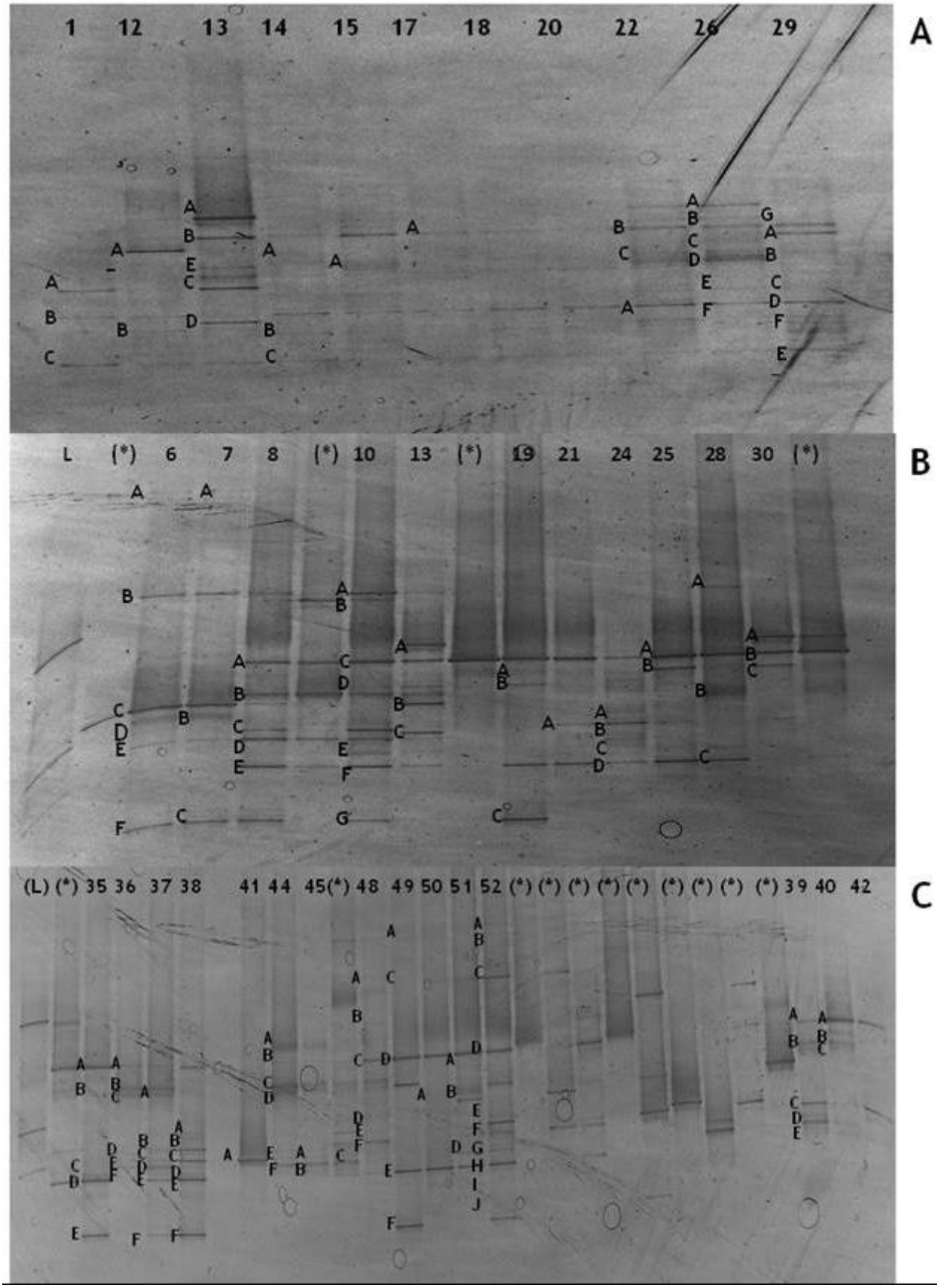


IV.7. Picture of 9% polyacrylamide DGGE gel showing biodiversity from enrichments. (L): Ladder; Lanes marked with: (*): results used for article 3; numbers 1 to 52 refer to ID number of table IV.6; letters A to I correspond to the bands cut in each lane

| Gel | Sample ID | From enrichment | Result | Identity |
|---|---|---|---|---|
| A | 1A | IRB | *Sinorhizobium americanum* strain CFNEI 156 | 96% |
| | 1B | IRB | *Thermoanaerobacter sp.* X514 strain | 99% |
| | 1C | IRB | *Dethiosulfovibrio marinus* strain sr12 | 99% |
| | 12A | APB | Did not yield good results | |
| | 13A | MOB | *Denitrovibrio acetiphilus* DSM 12809 | 100% |
| | 13B | MOB | *Desulfovibrio dechloracetivorans* strain SF3 | 98% |
| | 13C | MOB | *Sinorhizobium americanum* strain CFNEI 156 | 93% |
| | 13D | MOB | Did not yield good results | |
| | 13E | MOB | Did not yield good results | |
| | 14A | IOB | Did not yield good results | |
| | 14B | IOB | *Thermoanaerobacter sp.* X514 strain | 100% |
| | 14C | IOB | Did not yield good results | |
| | 15A | MOB | Did not yield good results | |
| | 17A | SRB | Did not yield good results | |
| | 22A | IOB/NRB | *Thermoanaerobacter sp.* X514 strain | 99% |
| | 22B | IOB/NRB | Did not yield good results | |
| | 22C | IOB/NRB | *Clostridium caminithermale* strain DVird3 | 96% |
| | 26A | IOB/NRB | *Paenibacillus tarimensis* strain SA-7-6 | 94% |
| | 26B | IOB/NRB | Did not yield good results | |
| | 26C | IOB/NRB | Did not yield good results | |
| | 26D | IOB/NRB | Did not yield good results | |
| | 26E | IOB/NRB | Did not yield good results | |
| | 26F | IOB/NRB | Did not yield good results | |
| | 29A | APB | *Clostridium sporosphaeroides* strain DSM 1294 | 95% |
| | 29B | APB | *Clostridium caminithermale* strain DVird3 | 97% |
| | 29C | APB | *Clostridium baratii* strain IP 2227 | 80% |
| | 29D | APB | Did not yield good results | |
| | 29E | APB | Did not yield good results | |
| | 29F | APB | *Thermovirga lienii* DSM 17291 strain | 99% |
| | 29G | APB | *Desulfovibrio dechloracetivorans* strain SF3 | 97% |
| | | | | |
| B | 6A | IRB | *Sinorhizobium americanum* strain CFNEI 156 | 93% |
| | 6B | IRB | Did not yield good results | |
| | 6C | IRB | *Sinorhizobium americanum* strain CFNEI 156 | 93% |
| | 6D | IRB | *Sinorhizobium americanum* strain CFNEI 156 | 93% |
| | 6E | IRB | *Sinorhizobium americanum* strain CFNEI 156 | 91% |
| | 6F | IRB | Did not yield good results | |
| | 7A | IRB | Did not yield good results | |
| | 7B | IRB | Did not yield good results | |
| | 7C | IRB | *Anaerobaculum thermoterrnum* strain RWcit | 99% |
| | 8A | SRB | *Desulfovibrio dechloracetivorans* strain SF3 | 98% |
| | 8B | SRB | *Desulfovibrio alkalitolerans* strain RT2 | 92% |
| | 8C | SRB | *Thermovirga lienii* DSM 17291 strain | 88% |
| | 8D | SRB | *Sphaerochaeta globus str.* Buddy strain | 96% |
| | 8E | SRB | *Dethiosulfovibrio acidaminovorans* strain sr15 | 99% |
| | 10A | MPB | *Geotoga spp* | 82% |
| | 10B | MPB | *Geotoga subterranea* strain CC-1 | 92% |
| | 10C | MPB | *Desulfovibrio dechloracetivorans* strain SF3 | 98% |
| | 10D | MPB | *Desulfovibrio sulfodismutans* strain ThAcO1 | 71% |
| | 10E | MPB | *Dethiosulfovibrio marinus* strain sr12 | 98% |
| | 10F | MPB | *Dethiosulfovibrio marinus* strain sr12 | 99% |
| | 10G | MPB | Did not yield good results | |
| | 13A | MOB | *Denitrovibrio acetiphilus DSM 12809* | 100% |
| | 13B | MOB | *Desulfovibrio dechloracetivorans* strain SF3 | 98% |
| | 13C | MOB | *Sinorhizobium americanum* strain CFNEI 156 | 93% |
| | 19A | MPB | Did not yield good results | |
| | 19B | MPB | Did not yield good results | |
| | 19C | MPB | *Anaerobaculum thermoterrnum* strain RWcit | 99% |
| | 21A | SRB | Did not yield good results | |
| | 24A | IOB/NRB | Did not yield good results | |
| | 24B | IOB/NRB | Did not yield good results | |
| | 24C | IOB/NRB | Did not yield good results | |

Table IV.7. Sequencing and identification results from selective enrichment media

Figure IV.8 resumes the bacteria identification results obtained from a general perspective and not classified regarding the pig number in order to simplify the analysis: 16S rRNA sequences related to 13 different genera of bacteria were detected and among them 20 different species. The most abundant 16S rRNA gene sequence detected in the enrichments analysed (20%) was that similar to *Thermovirga lienii* showing 93-100% identity. Coincidentally, the 16S rRNA sequence for *T. lienii* was also the most abundant sequence found in a similar study of an oil production pipeline in Alaska [Duncan, *et al.,* 2009]. After this last, sequences similar to those of bacteria from the genera *Clostridium* was the most frequently detected, finding it 16% of the times of the total bacteria identified. Moreover, sequences similar to the genera *Desulfovibrio* and the genera *Dethiosulfovibrio* were also abundantly detected, finding them both in around 30% of the total bacteria detected.

A resume of the main corrosion concerning bacteria related to the sequences found in the enrichments is displayed in table IV.8. Most of these bacteria have been isolated mainly from oil fields in different parts of the world such as the North Sea [Dahle and Birkeland, 2006], France [Cayol *et al.,* 1995], USA and Alaska [Stevenson *et al.,* 2011; Mauner and Tanner, 2012; Davey *et al.,* 2003] or from hot springs [Xue *et al.,* 2001; Surkov *et al.,* 2001. Abilgaard *et al.,* 2006].

As it can be seen in a description of table IV.8, the greater part of these bacteria does not belong to the widely studied SRB group. However, all of these bacteria can potentially cause corrosion due to their capability to produce hydrogen sulphide which has a key involvement in corrosion process. These findings suggest that SRB makes only a minor contribution to sulphide production at the facility, although careful studies of microbial sulphate reduction activity will be required to test this hypothesis. Nevertheless, the sole genus of SRB detected (*Desulfovibrio),* is however an important finding for the industry when mitigations plan need to be taken due to its versatility to switch from different electron acceptors. As it has been informed, nitrate treatment can be performed in the pipelines favouring the growth of these bacteria group.

Furthermore, two bacteria genera described in the table below are spore formers firmicutes (*Clostridium and Thermoanaerobacter*). The capability to form spores makes these bacteria very resistant and able to be in a wide variety of environments. However, with the studies performed in this project, there is no certainty about their development and viability in the pipelines. When dealing with habitat questions, one has to keep in mind that the only presence of a corresponding 16S rRNA gene sequence does not indicate that the isolates or the corresponding bacteria grew or were able to grow and multiply in that environment [Wiegel *et al.,* 2006]. Saying this, it would explain the fact of having found these obligately anaerobes in aerobic enrichment media. Although many species belonging to the family Clostridiaceae are able to reduce sulphur or thiosulfate, *C. caminithermale,* the main species of this family detected in the enrichments, is not able to reduce these compounds [Brisbarre *et al.,* 2003].

On the other hand, it is important to highlight the lack of detection of methanogens, iron reducers and iron oxidizers. These types of bacteria are also

relevant for corrosion of metals as previously mentioned. For instance, methanogens, which normally use molecular hydrogen and carbon dioxide to produce methane, use either pure elemental iron ($Fe^0$) or iron in mild steel as a source of electrons in the reduction of $CO_2$ to $CH_4$ [Daniels et al., 1987]. A great part of these microorganisms are not bacteria but archea and unfortunately due to time limits, archea primers were not used during the molecular tests performed in this project. Nevertheless, there is a certainty of their presence due to detection of methane in the different enrichment media used. Moreover, extensive works performed by other members of the BIOCOR network using 16S RNA archea primers and pyrosiquencing, have made evident the presence of further microorganisms in the pigging debris which include methane producers archea and IRB belonging to the genera *Geobacter* and *Shewenella* [Cote *et al.*, 2013; Sztyler *et al.*, 2012].

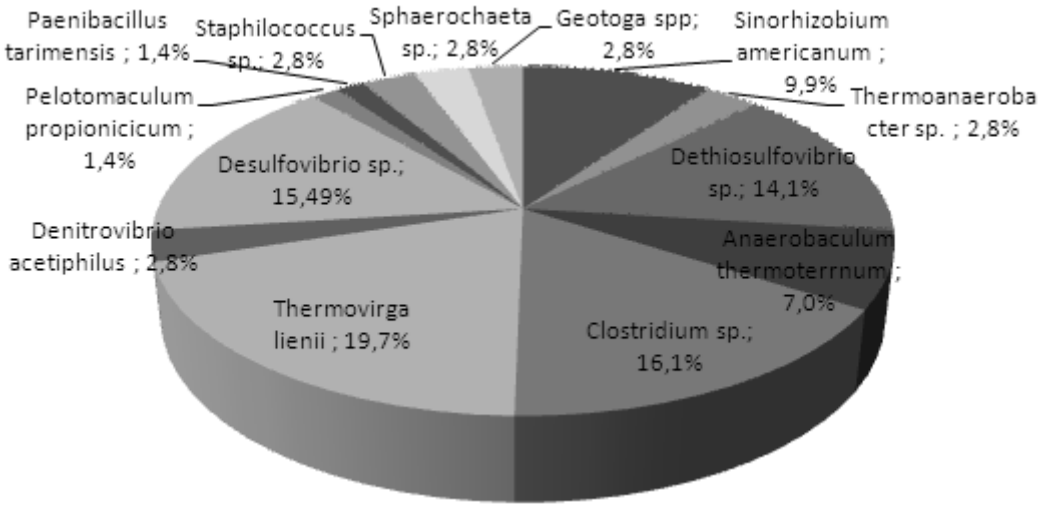


Fig. IV.8. Abundance of microbial strains in the installation "A" based on signal intensity of probes for C-cytochrome detection.

In conclusion, our results suggest that DGGE analysis performed in the enrichments did not allow detecting the complete diversity communities of microorganisms inherent of the water injection system. However, results suggest that there is indeed presence of a large biodiversity of microorganisms that can be related to corrosion in the water injection pipelines thus, implying that SRB are the main responsible for corrosion in the systems of this oil company might be an overstated mistake which could lead to errors in the monitoring and mitigations decisions taken when biocorrosion is observed.

| Bacteria genera | Phyla | Metabolism | Description |
|---|---|---|---|
| *Clostridium* | Firmicutes | Fermentative bacteria, $H_2S$, $CO_2$ lactate, butyric acid and acetate producers. This family include species that are able to reduce Fe (III) | Clostridium is a genus of Gram-positive bacteria, belonging to the Firmicutes. They are obligate anaerobes capable of producing endospores |
| *Thermoanaerobacter* | Firmicutes | The fermentable substrates included glucose, fructose, galactose, among others. The products of fermentation of glucose were lactate, acetate, ethanol, $H_2$, and $CO_2$. Thiosulfate and sulphur reduction to $H_2S$ | A strictly anaerobic, thermophilic, gram-positive, spore-forming cubacterium |
| *Thermovirga* | Synergistes | fermentative type of metabolism and utilized proteinous substrates, some single amino acids and a limited number of organic acids, but not sugars, fatty acids or alcohols. Cystine, elemental sulfur reduction to sulphide. Production of acetate, propionate, $H_2$, $CO_2$ | An anaerobic, moderately thermophilic bacterium |
| *Dethiosulfovibrio* | Synergistes | Fermentative type of metabolism and utilized proteins, peptides, amino acids and some organic acids, but not sugars, fatty acids or alcohols. Production of acetate, $CO_2$ and $H_2$ Reduces thiosulfate and sulphur to $H_2S$ when fermenting organic compounds | A mesophilic, strictly anaerobic, slightly halophilic bacterium, non-spore-forming, motile, gram negative bacteria |
| Anaerobaculum | Synergistes | peptide-fermenting bacterium. Carbohydrates and organic acids were converted to acetate, $H_2$ and $CO_2$. Thiosulfate, sulfur and cysteine reducing bacteria to sulphide | A novel anaerobic, moderately thermophilic strain, gram-negative, motile straight rods |
| *Desulfovibrio* | Proteobacte-ria | SRB, $H_2S$ producer, can use either nitrate, nitrite, sulphur or sulphate as final electron acceptor | Anaerobic facultative, non-spore forming, gram negative bacteria |
| *Geotoga* | Thermotogae | Fermentative and capable of reducing elemental sulfur to $H_2S$ | moderately thermophilic bacteria rod-shaped cells with a sheath-like outer structure, obligately anaerobic. |

Table IV.8. Description of detected bacteria from enrichments

### IV.5.2. Electrochemical and weight loss results

The main electrochemical results obtained from this second part of the project, have been collected and displayed in article 3. Moreover, some weight loss results are also displayed in this article but more extensive tests were performed. These tests are presented here as supplementary results right after presenting the article. Together with the supplementary weight loss results, XPS results and analysis from coupons extracted from the electrochemical experiments presented in article 3, are displayed.

#### *IV.5.2.1. Article 3*

Article 3 titled **"Corrosion of Low Carbon Steel by Microorganisms from the 'Pigging' Operations Debris in Water Injection Pipelines"** consist mainly in an electrochemical analysis of two systems: ASW system (biotic and abiotic) and MIXED water system (biotic and abiotic). Both systems were inoculated with pigging debris (pig 1) extracted from the water injection system, installation A.

The work carried out aimed to perform a comparison of the electrochemical response between these two systems. For this, electrochemical tests such as EIS and OCP monitoring and weight loss tests were performed. Moreover, a 16S rRNA gene sequencing for identification of bacteria was performed using two sources of samples: 1) the pigging debris extracted from the water injection system and 2) the inoculated media used for the electrochemical experiments. A community diversity comparison between these two sources was performed in order to acknowledge the differences in the community profiles detected regarding the source of DNA extraction.

“Corrosion of Low Carbon Steel by Microorganisms from the 'Pigging' Operations Debris in Water Injection Pipelines”

*Article submitted to Bioelectrochemistry Journal*

# Corrosion of Low Carbon Steel by Microorganisms from the 'Pigging' Operations Debris in Water Injection Pipelines

Claudia Cote[a,*], Omar Rosas[a], Magdalena Sztyler[b], Jemimah Doma[b], Iwona Beech[b] Régine Basseguy[a]

[a]*Laboratoire de Génie Chimique, CNRS, Université de Toulouse, 4 Allée Emile Monso, 31432, Toulouse, France*
[b]*School of Pharmacy and Biomedical Sciences, University of Portsmouth, St. Michael's Building, White Swan Road, PO1 2DT Portsmouth, UK*
**e-mail: ccotecoy@ensiacet.fr, telephone: +33 (0)5 34 32 36 26*

## Abstract

Water injection systems in the oil and gas industry show a tremendous complexity regarding corrosion issues due to the wide variety of environments developed in aqueous media. Present in all environments, microorganisms develop biofilms adjacent to the metallic structures creating corrosion conditions which may cause production failures that are of great economic impact to the industry. The most common practice in the oil and gas industry to annihilate these biofilms is the mechanical cleaning known as „pigging"". In the present work, microorganisms from the "pigging" operation debris are tested biologically and electrochemically to analyse their effect on the corrosion of carbon steel. Results in presence of bacteria display the formation of black corrosion products allegedly FeS, the corrosion potential (OCP) showed a sudden increase of more than 400 mV vs. Ag/AgCl and the shape of the impedance signal describe mass transport and/or charge transfer mechanisms depending on the media used. Denaturing Gradient Gel Electrophoresis (DGGE) results proved that bacterial diversity decreased when cultivating the debris in the media used and suggested that the bacteria involved in the whole set of results are mainly sulphate reducing bacteria (SRB) and some other bacteria that make part of the taxonomic order *Clostridiales.*

*Keywords:* Low Carbon Steel; EIS; Pigging debris; Anaerobic biocorrosion; DGGE

***** Corresponding author. Tel.: +33 5 34 32 36 17; fax: +33 5 34 32
E-mail address: regine.basseguy@ensiacet.fr (R. Basseguy).

## 1. Introduction

Microbial development occurs in almost all environments throughout biofilm formation and may be responsible for microbial influenced corrosion (MIC), also known as microbial corrosion or biocorrosion which can be defined as the enhancement or acceleration of corrosion by the presence of bacteria [1]. MIC is not a new corrosion mechanism but it integrates the role of microorganisms in corrosion processes. Thus, an inherently abiotic process can be influenced by biological effects [2].

Corrosion represents a considerable economic stake projected between 1 and 4% of the gross national product (GNP) of developed countries [3]. Fleming *et al.* [4] estimate that 20% of corrosion problems are linked to the presence of microorganisms and more over Jack *et al.* [5] estimated that 34% of the corrosion damage experienced by oil companies was related to MIC.

Oil and gas industries battles MIC problems and its potential damages in pipelines by different methods such as the use of biocides, coatings, corrosion inhibitors and different chemicals that could reduce or control bacterial growth and/or reduce corrosion rates but probably the best way to avoid microbial influenced corrosion is an appropriate design and operation to keep the systems clean combined with regular mechanical cleaning [6].

Mechanical cleaning involves any method capable of the physical removal of deposits formed on the surface. It includes brushing, pigging and the use of cleaning spheres or water jet, etc., and is applied to remove sludge, scale, and encrustations as well as the biomass associated with these deposits [7]. Mechanical cleaning is mainly performed in water injection and production pipeline systems of oil and gas industries by the use of mechanical pigs.

Pipeline operators now describe any device made to pass through a pipeline for cleaning and other purposes with the word pig. The process of driving the pig through a pipeline by fluid is called a pigging operation [8]. Operators need to run cleaning pigs to dewax and descale the inside surface of the pipe and remove debris (corrosion products and biofilm), which help improve pipeline performance [9]. This debris collected in the receivers of the pipelines may be used to analyse not only corrosion products, organic matter, oil and water residues but also biofilm and bacterial presence.

Depending on the operating system, oil and gas companies combine different methods for the prevention and/or protection of corrosion of their pipelines. For instance, pigging operations are combined with biocide treatments and/or corrosion inhibitors treatments in order to reduce bacteria development. However, it is known that bacteria can adapt to drastic conditions posed by these treatments and resist rough environmental conditions still causing a threat for the materials. For example sulphate reducing bacteria (SRB) show considerable adaptability to extreme conditions making it possible to isolate active cultures from sites where bacteria are exposed to $O_2$ regardless the anaerobic nature of this group [10-12].

One of bacteria‟s defensive mechanisms against corrosion treatments is precisely the secretion of slime or extracellular polymer substances (EPS) that leads to the

formation of biofilms forming a gel matrix on the metal surface that not only may enhance corrosion rates but also protects bacteria from biocides [12]. It also may aid to the entrapment of corrosion inhibitors such as aliphatic amines and nitrites to be later degraded by microorganisms. Biofilms also reduce the effectiveness of corrosion inhibitors by creating a diffusion barrier between the metal surface and the inhibitor in the bulk solution [12-16].

Due to biofilm formation in diverse environments such as pipelines, microorganisms can coexist in naturally occurring biofilms with a wide bacterial community including fermentative bacteria, often forming synergistic communities (consortia) that are capable of affecting electrochemical processes through co-operative metabolisms [1, 17]. Nevertheless, most of the research on anaerobic microbially influenced corrosion has focused on SRB primarily for the hydrogen sulphide generation and the fact that there is injection of sulphate-containing seawater into the reservoirs during the secondary recovery of oil which favours the proliferation of these bacteria [18,19]. However, recent studies suggest that SRB need not to be present in abundance in the microbial communities responsible for MIC [20] and that other types of bacteria could be involved, such as metal reducing-bacteria and methanogens [1,19, 21,22]. Thus, studies with other bacterial groups or consortia must be enhanced.

This study has as objective to explore the influence of a consortium of microorganisms present in a sample of pigging debris on the corrosion of low carbon steel and determine its corrosive activity. For this, samples of pigging debris extracted from a water injection system of an oil and gas company located in Norway were used. Electrochemical experiments were performed, simulating some of the field conditions, comparing two different electrolytes as medium: artificial sea water (ASW) and a mixture of water from the field used to irrigate the water injection pipelines (MIXED). Furthermore, microbial diversity present in the debris and in the water used for the electrochemical experiments was characterised by Denaturing Gradient Gel Electrophoresis (DGGE) analysis of the Polymerase Chain Reaction (PCR) products for bacterial 16S rRNA genes (550bp) aiming to comprehend the influence of bacterial consortia involved in corrosion.

## 2. Experimental procedure

### *2.1. Sample collection*

Pigging debris samples were collected from a water injection pipeline “A” located in the installation “A” of an Oil and gas company located in Norway between November 2010 and June 2011. The pipeline consists in 10-15 km long pipe made of low carbon steel with an average operating temperature of 35°C. Pig 1 was used for the electrochemical experiments and Pig 1 and 5 were used for the weight loss experiments. Pig 1 corresponds to the first debris collected after the first pigging operation and Pig 5 corresponds to the fifth debris collected after the fifth pigging operation. Samples were transported to the lab in Schott bottles, flash with an inert gas and sealed.

Water passing through the water injection system is a mixture of 50% aquifer water plus 50% produced water recycled from the production pipelines. This water is re-injected into the oil-bearing formations to maintain pressure and facilitate oil

recovery. The mixture of these waters is used for the electrochemical and weight loss experiments and will be called MIXED throughout this paper. Corrosion inhibitor KI-3804, imidazoline type, is added regularly in the production lines. Thus, 4 ppm of corrosion inhibitor is expected to be in the water injection pipelines according to the information provided by this company.

*2.2 Inoculum and medium*

Two different mediums were tested for the electrochemical experiments: Artificial Sea water (ASW) and mixed water from the field (MIXED) previously mentioned. ASW consist of: NaCl 408 mM, $Na_2SO_4$ 28 mM, KCl 9.3 mM, $NaHCO_3$ 24 mM, KBr 839 µM, $H_3Br$ 36 µM, $MgCl_2*6H_2O$ 53 mM, $CaCl_2*2H_2O$ 10 mM and it was supplemented with 10 mM of sodium acetate and 25 mM of sodium fumarate. MIXED water was supplemented with 24 mM of $NaHCO_3$ and generally after 300 hours of running with 10 mM of sodium acetate and 25 mM of sodium fumarate when indicated.

The supplementation with acetate and fumarate is done to enhance a faster growth of heterotrophic species contained in the consortia. $CO_2$ added as part of the injected gas and inorganic substances such as iron (metal coupon) and sulphate were also present for the growth of autotrophic and lithotrophic species that may be present in the consortia.

Approximately 10 g of pigging debris were used to inoculate the electrochemical reactors and 3 g for the anaerobic vials used for the weight loss experiments. Inoculation was performed after de-aerating the medium with $N_2/CO_2$. An approximate number of planktonic cells were evaluated by bacteria counting in a Thoma counting chamber after performing serial dilutions.

*2.3. Electrochemical measurements*

Anaerobic reactors of 0.5 L were used adjusting the liquid level to 400 mL of total volume. The anaerobic conditions were obtained by bubbling $N_2/CO_2$ 80:20 into the reactors for no less than 45 min before inserting the metal coupons. The flow of $N_2/CO_2$ was maintained during the whole experiment. Reactors were kept at 35°C during experiments. pH was measured for all the experiments at initial time (h=0) and final time (h≥700 h).

The working electrodes (WE) were 2 cm diameter cylinders of carbon steel S235 JR. The nominal chemical composition for the steel S235 JR is shown in table 1. The WE was covered by a polymeric coating (thermo-contractible polyolefin, ATUM ®) leaving uncovered a flat disk surface with a total exposed area of 3.14 $cm^2$. Connections were made through titanium wire protected with the same polymeric coating. The electrodes were ground with SiC paper using P120-P600 until achieving a 600 grit surface followed by a cleaning with ethanol (70%) and throughout rinsing with sterile deionised water.

For all the experiments, electrochemical measurements were performed using a multipotentiostat (VMP-Bio-Logic) with a platinum grid (Pt, Ir 10%) used as counter electrode (CE) and a silver wire coated with silver chloride (Ag/AgCl 0.5M) was used as reference electrode (RE).

The Open circuit potential (OCP) was measured in function of time for all the experiments. Electrochemical Impedance Spectroscopy (EIS) was used to obtain information on the interface, using a frequency from 100 kHz to 10 mHz and amplitude of 10 mV.

Table 1.
Chemical composition of AISI S235 JR (wt %)

| *Alloy* | *C* | *Mn* | *Cu* | *S* | *P* | *N* |
|---|---|---|---|---|---|---|
| S235 | 0.17 | 1.40 | 0.55 | 0.03 | 0.03 | 0.01 |

*2.4. Surface analysis*

Scanning Electron Microscopy (SEM) pictures were taken using a TM3000 Hitachi Analytical Table Top Microscope at 7000x magnification working at 15 kV acceleration voltages, immediately after removing the coupons from the solution. The coupons were washed with distilled water and dried with the gas mixture $N_2/CO_2$ 80:20. Energy dispersive x-ray spectroscopy (EDX) was used for elemental analysis of the coupons.

*2.5. Weight loss tests*

Weight loss tests were performed following the American Society for Testing and Materials (ASTM) standards D26811 during 3 months. Rectangular sheets with dimensions of 20 mm x 10 mm x 1 mm were used. The sheets were immersed in ASW and MIXED water from the field both supplemented with 10 mM sodium acetate, 25 mM sodium fumarate and 2g/L of sodium bicarbonate as added buffer to a total volume of 100 mL per test. Fishing thread was used to suspend the coupons into the water mediums served in 150 mL glass anaerobic vials hermetically closed with butyl rubber septums. ASW and MIXED water were flashed with $N_2/CO_2$ during 1 hour previous to the inoculation and 30 minutes after inoculation.

At the end of the experiment, coupons were cleaned introducing the coupon in a solution of 50% vol HCl concentrated and 2.5 g/L of EDTA ($C_{10}H_{16}N_2O_8$) during 30 seconds. Weight loss was calculated after the cleaning procedure using the following equation:

Corrosion rate (mmpy): $$\frac{0.465\ X}{tA} \quad (1)$$

where:
0.465: is a factor accounting for the dimensional analysis and the density of the steel.
X: is the difference between “initial weight” and “weight after cleaning” in milligrams
t: is exposure time in days
A: is total area of the coupon in cm².

*2.6. Molecular identification of bacteria*

Pigging debris from the water injection pipeline "A" and bacterial pellets from the bacterial growth resulting from the electrochemical experiments previously described were analysed in the Microbiology Research Laboratory of the University of Portsmouth (UoP), UK, aiming identification and possible quantification of microorganisms which may be involved in corroding the systems. The samples were analysed using techniques which include, Polymerase Chain Reaction (PCR), Denaturing Gradient Gel Electrophoresis (DGGE), and examination through sequencing.

DNA was extracted using NucleoSpin® (Machery-Nagel) following the manufacturer's instructions. A NanoDrop ND-1000 spectrophotometer (Thermo Scientific, USA) was used to establish the concentration of extracted and purified DNA.

PCR was performed on DNA extracted from samples in order to probe the presence of gene 16SrRNA. The targeted gene was amplified using the primers 341F+GC: 5`-CGCC CGCCGCGCGCGGGCGGGGCGGGGGCACGGGGGGCCTACGGGAGGCAGCAG-3` and 907R: 5`-CCGTCA ATTCMTTTGAGTTT-3`[23] (purchased from Life Technologies, UK). Reactions contained 10x GoTaq® Green Master Mix (12.5 µL, Promega); primers 341F+GC and 907R (each 1µL, 10 pmol/µL). Reactions were initially denatured at 94°C for 4 minutes, followed by a touchdown PCR: 20 cycles of 94°C for 1 minute, 63-54°C for 1 minute and 72°C for 1 minute followed by 15 cycles of 94 °C for 1 minute, 53°C for 1 minute and 72°C for 1 minute plus an additional 10 minutes cycle at 72°C. Reactions were performed in 25 µL reaction mixtures.

Agarose gel electrophoresis was performed after PCR to determine the size of the PCR products by running beside a DNA marker (1kb Ladder, Promega). PCR products were run on 0.9% of agarose gel on 150V for 30 minutes to 1 hour to enable proper separation. Agarose gel was stained with SYBR® Safe DNA gel stain (Invitrogen Corp., USA) and viewed under UV transillumination (Alpha Innotech Corporation, USA) and Digital Camera (Olympus C-4000 Zoom) to ensure that the correct size fragment was amplified.

To separate the PCR-amplified products for bacterial 16S rRNA genes (550 bp), 40µL of PCR-amplified products was used in an Ingeny Gel Apparatus (Ingeny, Netherlands), at a constant voltage of 90 V for 18 hours and a constant temperature of 60°C, after an initial 15 minutes at 200V. The standard gradient was formed of 6% polyacrylamide in 0.5x TAE buffer with between 30% and 90% denaturant (7M urea and 40% formamide defined as 100% denaturant). After electrophoresis, the gel was stained with SYBR® Safe DNA gel stain (Invitrogen Corp.), viewed under UV transillumination, and a permanent image captured by the Alpha Innotech Gel Documentation System (Alpha Innotech Corporation, USA).

All visible bands were cut from the gel using a sterile scalpel blade and transferred into sterile 1.5 mL microcentrifuge tubes containing 30 µL of ultra-pure water to extract the DNA. Samples were then centrifuged at 13 000 x g for 1 minute (Heraeus Fresco 21, Thermo Scientific, UK) and 5 µL aliquots of supernatants were used for

PCR re-amplification as described above. PCR products were purified using the NucleoSpin® Extract II PCR purification kit (Macherey-Nagel, UK) and sent to the GATC Biotech UK DNA sequencing service.

## 3. Results and Discussion

### *3.1. Open circuit potential results and observations*

Low carbon steel coupons were immersed in ASW and MIXED water from the field during at least 600 hours. The metallic coupons were immersed in the reactors medium 24 h before inoculation. The systems were kept under continuous $N_2/CO_2$ (80/20) flow during all the time of the experiments. At hour 24, the reactors were inoculated with approximately 10 g of pigging debris obtained from the water injection pipeline, under a continuous inert gas flow. In the cases of the control reactors, the pigging debris was sterilised by autoclaving it previously to introducing it to the reactor. In this way both systems, control and inoculated, were identical to one another and the only variant element was the presence of microorganisms. The electrochemical behaviour of the system was tested recording OCP in function of time.

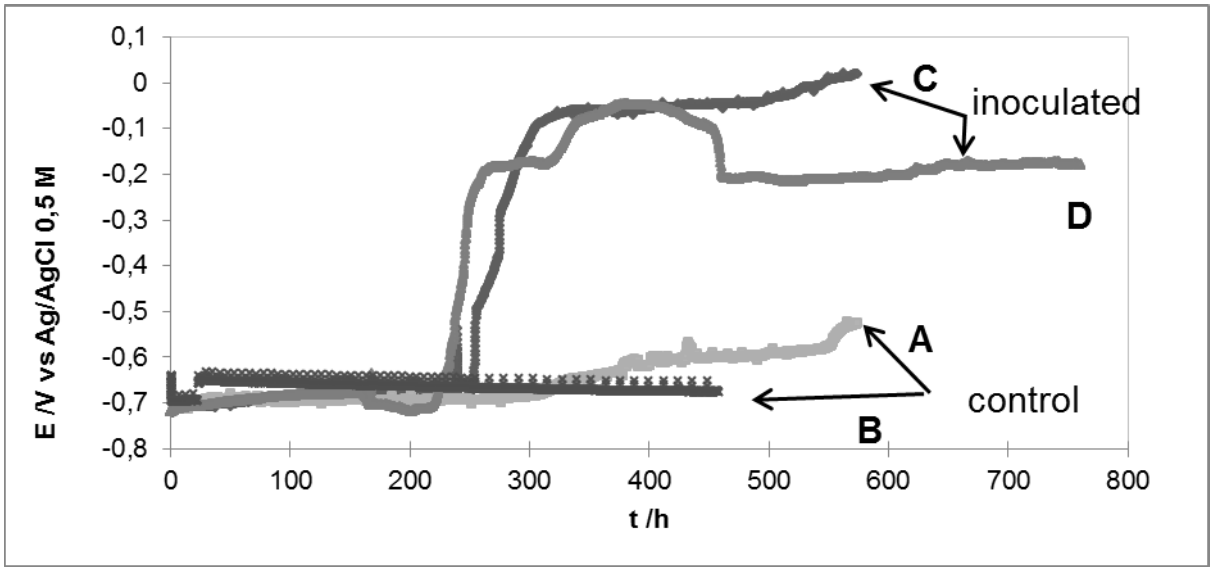


Fig.1. Variation of OCP of low carbon steel S235JR in presence of approximately 10 g of pigging debris in artificial sea water. The ASW contains a supplement of 10 mM of sodium acetate (electron donor) and 25 mM of sodium fumarate (electron acceptor). A and B: control system with pigging debris autoclaved; C and D: inoculated system with pigging debris.

### *3.1.1 Open circuit potential results with ASW*

Fig. 1 describes the OCP behaviour of low carbon steel submerged in ASW supplemented with acetate and fumarate, of 4 different experiments running in parallel: two control systems (curves A and B) and two systems with microorganisms (curves C and D). OCP remained stable along the time in the control reactors having an average increment of no more than 150 mV vs. Ag/AgCl during the whole experiment. In contrast, it was observed a potential increment of over 500 mV vs. Ag/AgCl in the inoculated reactors (curves C, D) after hour 200.

Note that the results of the experiments stated in this paper were carried out 4 times for the systems with bacteria and 3 times for the control system finding high reproducibility amongst them. In all the cases, it was observed increment of the OCP on the inoculated systems whereas none or very little increment was observed in the control systems. The increments on OCP observed in the systems with bacteria were observed between hour 200 and 300 of the experiment (See table 2).

The increment in OCP or corrosion potential indicates that there is higher corrosion risk with an incremented probability for pitting and crevice corrosion [22,24,25] which in this case has been enhanced by the presence of microorganisms in the system. The absence of such an increment in the control reactors leads to think that the absence of bacteria posed conditions less aggressive than in presence of microorganisms.

Table 2.
Initial and final potential of S235 JR steel, pH and planktonic cells concentration at the beginning and at the end of the experiments using ASW and MIXED water from the field. (A) Inoculated systems, (B) control systems.

| **A** | **Planktonic CFU $mL^{-1}$** | **pH Initial** | **pH final** | **Initial OCP (V vs. Ag/AgCl)** | **Final OCP (V vs. Ag/AgCl)** |
|---|---|---|---|---|---|
| **ASW Inoculated** | 60,5 X $10^6$ | 6.8 | 7.2 | -0.67 | -0.25 |
| | 30 X $10^6$ | 6.6 | 7.1 | -0.72 | -0.18 |
| | 55 X $10^6$ | 6.7 | 7.1 | -0.72 | -0.09 |
| **MIXED inoculated** | 4 X $10^6$ | 6.5 | 7.0 | -0.72 | -0.23 |
| | 4,2 X$10^6$ | 6.5 | 6.9 | -0.75 | -0.21 |
| | 3,5 X $10^5$ | 6.8 | 7.1 | -0.70 | -0.43 |
| | 5,7 X $10^5$ | 6.6 | 6.7 | -0.71 | -0.14 |

| **B** | **pH Initial** | **pH final** | **Initial OCP (V vs. Ag/AgCl)** | **Final OCP (V vs. Ag/AgCl)** |
|---|---|---|---|---|
| **ASW control** | 5.9 | 5.8 | -0.73 | -0.67 |
| | 6.1 | 5.8 | -0.69 | -0.68 |
| | 6 | 6.5 | -0.73 | -0.65 |
| **MIXED control** | 6.8 | 7.1 | -0.72 | -0.60 |
| | 6.4 | 6.6 | -0.72 | -0.59 |
| | 6.7 | 6.8 | -0.72 | -0.53 |
| | 6.5 | 6.8 | -0.71 | -0.67 |

Precipitates macroscopically observed in the abiotic systems reveal that are mainly yellow rust looking - iron oxides (Fig. 2B). Whereas the black precipitates and high turbidity observed in the inoculated systems suggest a high quantity formation of iron sulphide, FeS (Fig. 2A). These observations were corroborated when observing the metal coupons using SEM microscopy. Figure 3A shows deposits formed on the surface of the metal in presence of microorganisms whereas Fig. 3B shows no

deposits on the surface of the metal of the control system and it is observed only a general corrosion pattern.

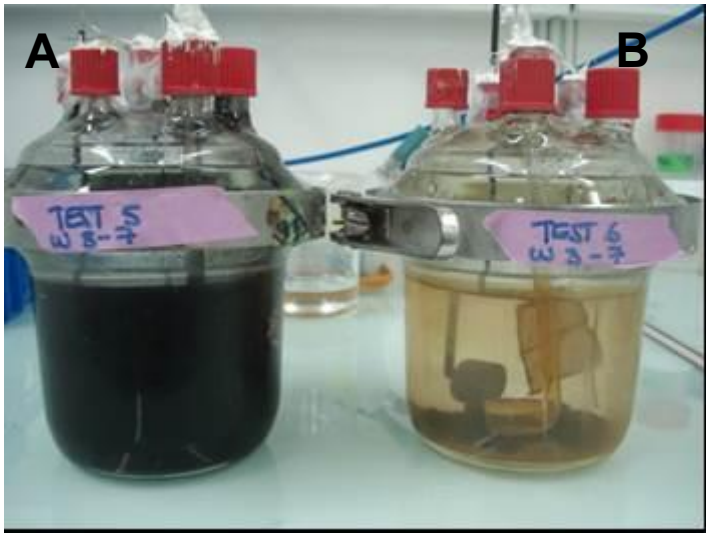


Fig 2. Photographs of reactors after approximately 600 hours of experiment under a $N_2/CO_2$ atmosphere in ASW. Reactors in presence of pigging debris from a water injection system. (A): Reactor in presence of bacteria that grew from the pigging debris inoculum and (B): Reactor in absence of bacteria after adding pigging debris autoclaved.

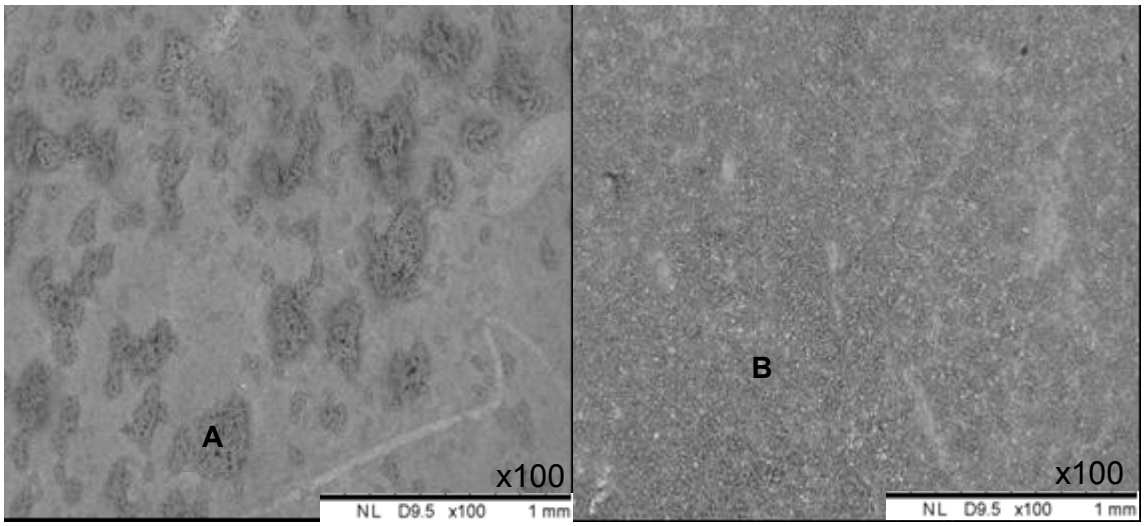


Fig.3. Micro photographs of coupons after 600 hours of immersion in ASW: (A) SEM image of layer formed in the coupon with bacteria. (B) SEM image of control coupon.

Surface analysis using energy dispersive x-ray spectroscopy (EDX) (Table 3A) confirmed that the deposits formed on the surface of the coupon in presence of microorganisms contained high quantity of sulphur and iron (1:1 %) , backing up the argument made after macroscopic observations suggesting that the deposits formed are mainly FeS. Table 3B shows the presence of mainly Fe, O and C suggesting, together with the SEM micrographs, that the type of corrosion of the control system is dominated by general corrosion in absence of oxygen.

Coupons were also observed after performing chemical cleaning aiming to observe pitting corrosion (see section 2.6) using a 100X lens magnifier (Fig. 4). In figure 4A (inoculated system) it is observed a general corrosion attack with numerous small pits. In contrast, figure 4B (control system) shows less general corrosion compared to the inoculated system, to the point that after removing the iron oxide layer, grinding lines may still be observed.

Table 3
EDX analysis of coupons surface after 600 hours of immersion in ASW (see Fig. 3). (A): coupon with bacteria; (B): control coupon

**A**

| Element | Weight % | Atomic % |
|---|---|---|
| O | 15.8 | 31.0 |
| Na | 12.5 | 17.1 |
| Mg | 1.7 | 2.2 |
| S | 24.2 | 23.7 |
| Ca | 0.8 | 0.6 |
| Fe | 45.1 | 25.4 |

**B**

| Element | Weight % | Atomic % |
|---|---|---|
| C | 22.2 | 42.3 |
| O | 21.4 | 30.6 |
| Na | 5.4 | 5.4 |
| S | 2.8 | 2.0 |
| Fe | 48.2 | 19.8 |

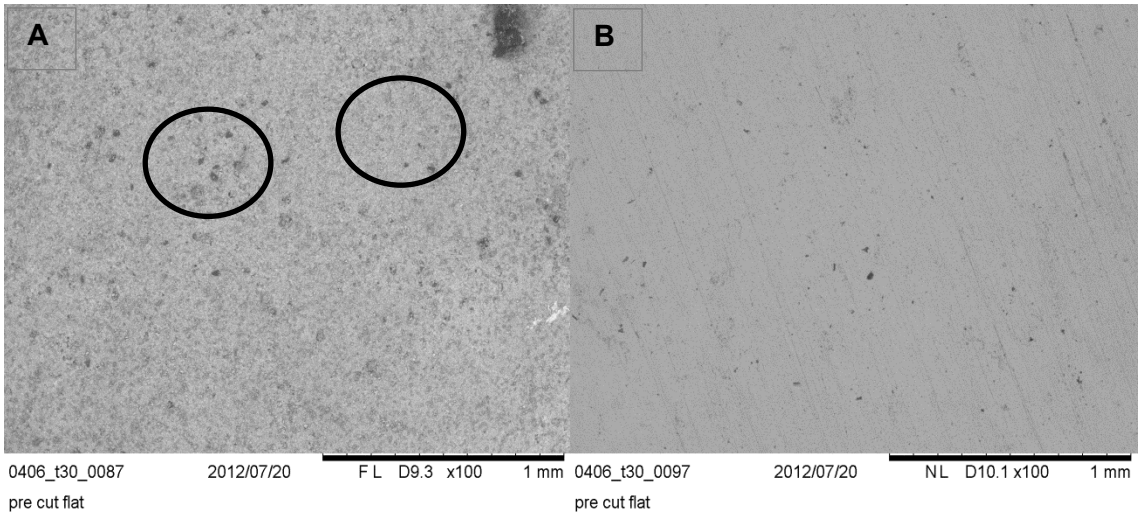


Fig.4. Micro photographs of coupons after 600 hours of immersion in ASW after cleaning treatment with HCl + EDTA: (A) SEM image of the coupon with bacteria (circles point out zones of pitting corrosion). (B) SEM image of control coupon.

Corrosion enhanced by the formation of FeS in conditions lacking oxygen has been widely studied. For instance, Mc Neal *et. al.,* [26] proposed a thermodynamic model about the susceptibility of metal substrata changed by microbiologically produced sulphides in order to explain ennoblement. This model for predicting SRB-influenced corrosion is based on the likelihood that a metal would react with microbiologically produced sulphide which will attack the oxide layer on the metal (or the metal itself) destabilising it and making it act as a source of metal ions. If the reaction to convert

the metal oxide to a metal sulphide has a positive Gibbs free energy under surface conditions, the sulphide will not strip the protective oxide and no corrosion will take place. If the free Gibss energy for the reaction is negative, the reaction will proceed, sulphide microcrystals will redissolve and precipitate as larger, more sulphur rich crystals, ultimately altering the sulphide minerals stable under biofilm conditions.

In our paper, the ennoblement of OCP is attributed to the acceleration of the rate of the cathodic reaction which is the evolution of $H_2$ catalysed by the presence of sulphide formed by the microorganisms present in the pigging debris of the water injection system. Indeed, it is acknowledge that other mechanisms (change on the localised pH, cathodic depolarisation, increase of the partial pressure by biofilm formation, thermodynamics, among others [24-27]) may play a role along with the described one, in the acceleration of corrosion of carbon steel.

*3.1.2 Open circuit potential results with MIXED water from the field*

Fig. 5 describes the OCP behaviour of low carbon steel submerged in MIXED water from the field of 4 different experiments running in parallel: two control systems (curves A and B) and two systems with microorganisms (curves C and D). MIXED water from the field has a high quantity of long chain hydrocarbon contaminants due to the water recycling process performed from the production pipelines. These hydrocarbons may be used by microorganisms as carbon source to enhance growth rates but is a time consuming process [28] whereas short chain volatile fatty acids (VFAs) are consumed in a much shorter period of time. These VFAs are not present in high quantities in this water (see table 4) thus, acetate was added in order to accelerate bacterial growth to both systems (inoculated and control).

Table 4. Average values of chemical analysis performed on the water injected in the water injection system “A” between 2001 and 2009. Analysis performed and provided by the Oil and gas Industry which provided the pigging samples analysed in this paper.

| Conductivity (mS/cm) | pH | $H_2S$ (mg/L) | Total Organic C (mM) | $SO^{2-}_4$ (mM) | $NO_3^-$ (mM) | $PO^3_4$ (mM) | $NH_4^+$ (mM) | Formic acid (mM) | Acetic acid (mM) | Propanoic acid (mM) | Butyric acid (mM) | Pentanoic acid (mM) |
|---|---|---|---|---|---|---|---|---|---|---|---|---|
| 38.75 | 7.45 | 0.77 | 3.74 | 0.42 | 0.03 | 0.03 | 1.33 | 0.09 | 0.96 | 0.08 | <0.02 | <0.02 |

In this MIXED water system, OCP also remained stable along the time in the control reactors having an average increment of no more than 100 mV vs. Ag/AgCl during the whole experiment. In contrast, it was observed a preliminary corrosion potential increment of 150 mV vs. Ag/AgCl in the inoculated reactors (curves C, D) between hours 180 and 280 followed by a larger increment of 350 mV around hour 500, after addition of an oxygen free solution of sodium acetate and sodium fumarate between hours 250 and 350. This bigger increment on the corrosion potential is consequently due to a faster development of microorganisms that increased corrosive conditions once in presence of these short chain carbohydrates (acetate and fumarate).

Deposits macroscopically observed in the abiotic systems (control) with MIXED water reveal that there are also yellow rust looking - iron oxides (Fig. 6B), whereas in the inoculated ones (with microorganisms) (Fig. 6B) it can be observed a slight turbidity and a light greyish colour deposits in the medium that due to its organoleptic properties, it can be inferred that there is a small quantity of FeS. Nevertheless, the colour observed in this system is not as dark as the one observed in ASW. These macroscopic differences between ASW and MIXED water suggest that the corrosion inhibitor and or the presence of hydrocarbon species may be not only inhibiting corrosion but also bacterial growth and/or sulphide production.

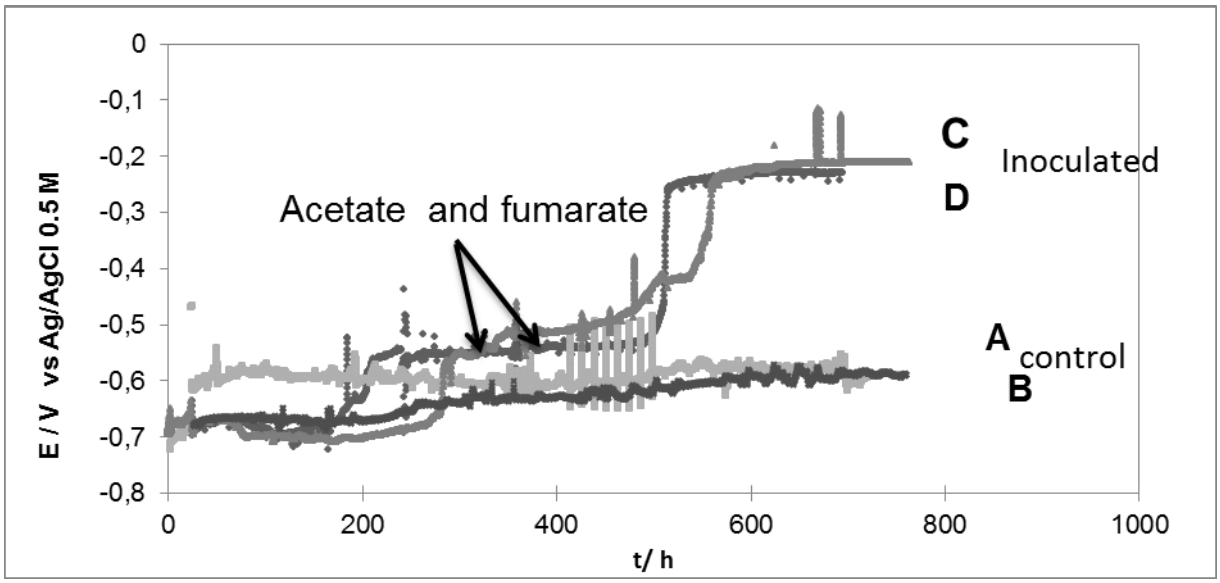


Fig. 5. Variation of OCP of low carbon steel S235 JR in presence of approximately 10 g of pigging debris in MIXED water medium. A supplement of 10 mM of sodium acetate (electron donor) and 25 mM of sodium fumarate (electron acceptor) was added. A and B: control system with autoclaved pigging debris; C and D: inoculated system with pigging debris.

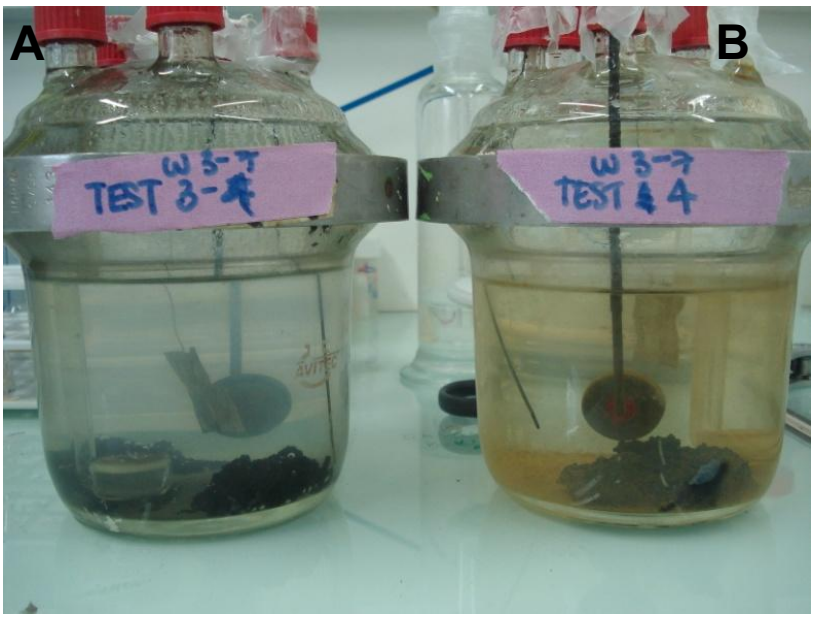


Fig. 6. Photographs of reactors with MIXED water after approximately 600 hours of experiment under a $N_2/CO_2$ atmosphere. Reactors in presence of pigging debris from a water injection system. (A): Reactor in presence of bacteria that grew from the pigging debris inoculum and (B): Reactor in absence of bacteria after adding pigging debris autoclaved.

Table 2 resumes total bacterial counting in ASW and MIXED water systems at the end of the experiments. It can be observed a lower concentration of bacteria in MIXED water compared to ASW concentration despite the acetate addition. The low bacterial counting at the end of the experiments of MIXED water compared to the counting performed in ASW, backs up the argument about bacterial inhibition by the corrosion inhibitor used by the company. Due to confidential policies of the company not much information has been provided about the inhibitor.

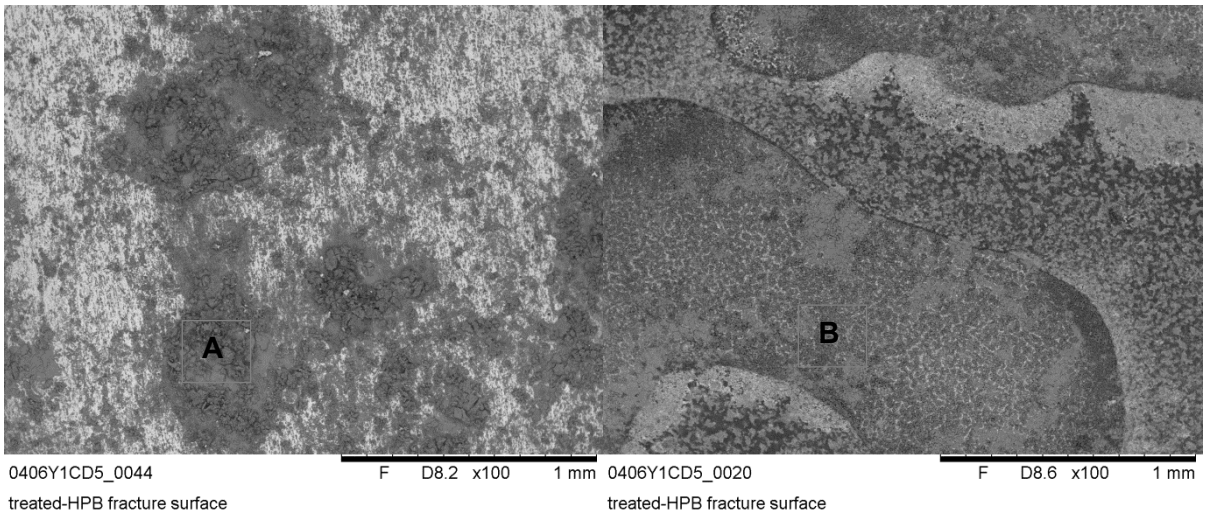


Fig.7. Micro photographs of coupons after 600 hours of immersion in MIXED water: (A) SEM image of layer formed in the coupon with bacteria. (B) SEM image of control coupon.

When observing the metal coupons using SEM microscopy (Fig. 7) it is evident the less aggressive corrosion attack compared with ASW. Figure 7A shows deposits formed on the surface of the metal in presence of microorganisms whereas Fig. 7B shows no deposits on the surface of the metal but what it seems to be only iron oxide.

Surface analysis using energy dispersive x-ray spectroscopy (EDX) (Table 5A) confirmed that the deposits formed on the surface of the coupon in presence of microorganisms contained low quantity of sulphur (0.7 % of the total atomic weight) but high quantities of oxygen (68.6% of the total atomic weight) and Fe (14.5% of the total atomic weight) suggesting that only a small quantity of the deposits precipitated as FeS and instead there is a high quantity of iron oxides. Table 5B shows the presence of mainly Fe, O and C suggesting, together with the SEM micrographs, that the type of corrosion of the control system is dominated by general anaerobic corrosion in absence of microorganisms.

Surface observations on the clean coupons were also performed aiming to observe pitting corrosion (see section 2.6) using a 100X lens magnifier (Fig. 8). In figure 8A (inoculated system) it is observed a general corrosion attack with several irregular pits. Pits seem to be of irregular form but slightly bigger in diameter compared to the ones found in ASW. The reason why these pits seem bigger in diameter might be due to the corrosion inhibitor which has inhibited further general corrosion highlighting pitting zones. In contrast, figure 8B (control system) shows a general corrosion attack that is considerably less strong to the one observed in the inoculated system and to the one observed in ASW. Grinding lines are more evident on the

control coupon from MIXED water compared to the control coupon submerged in ASW; once again, it may be due to the presence of the corrosion inhibitor present in the MIXED water from the field.

Table 5.
EDX analysis of coupons surface after 600 hours of immersion in MIXED water (see Fig. 8). (A): coupon with bacteria; (B): control coupon.

**A**

| Element | Weight % | Atomic % |
|---|---|---|
| **C** | 8.6 | 15.2 |
| **O** | 50.1 | 68.6 |
| **Na** | 1.0 | 0.9 |
| **Fe** | 37.1 | 14.5 |
| **S** | 3.5 | 0.7 |

**B**

| Element | Weight % | Atomic % |
|---|---|---|
| **C** | 5.4 | 9.9 |
| **O** | 54.3 | 74.8 |
| **Na** | 4.0 | 3.8 |
| **S** | 0.3 | 0.2 |
| **Cl** | 0.6 | 0.4 |
| **Fe** | 18.8 | 7.4 |

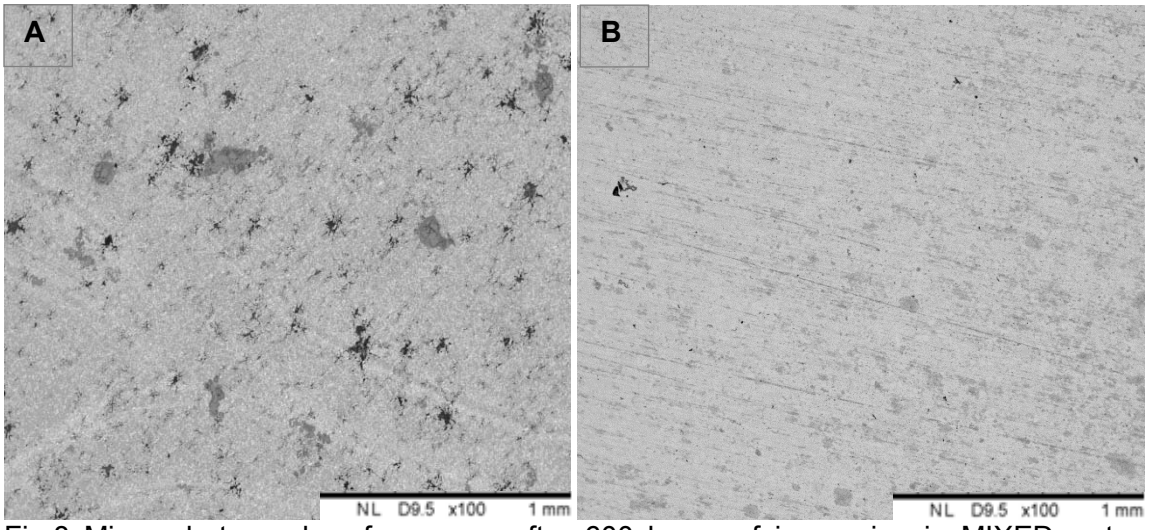

Fig.8 Micro photographs of coupons after 600 hours of immersion in MIXED water after cleaning treatment with HCl + EDTA: (A) SEM image of the coupon with bacteria. (B) SEM image of control coupon.

*3.2. Electrochemical impedance measurements*

Electrochemical Impedance Spectroscopy measurements were performed in order to complement OCP results and surface observations to elucidate the effect of the microorganisms consortium present in the pigging debris on the corrosion of carbon steel. Two different media were used ASW and MIXED water, each of them has a control system without microorganisms.

*3.2.1. EIS results with ASW*

Fig. 9 shows the impedance response for carbon steel exposed to ASW medium and its evolution with time for the abiotic control system. In the Nyquist diagram, the shape of one semi-circle is observed at all times during the whole experiment, except for times 280 and 360 where a linear shape is observed at low frequencies (LF). The depressed semi-circles and its fluctuating diameters are represented in terms of resistance polarisation ($R_p$) in table 6A. $R_p$ corresponds to the real impedance part which crosses the axis at LF. Initially, an increasing tendency of $R_p$ (increase of the semi-circle diameter) is observed between hours 0 and 216 (220 to 5650 Ω cm², respectively). For times 288 and 360 the phenomena seem to be more complex and $R_p$ cannot be calculated. Beyond hour 360 the tendency shifts displaying decreasing $R_p$ values along time.

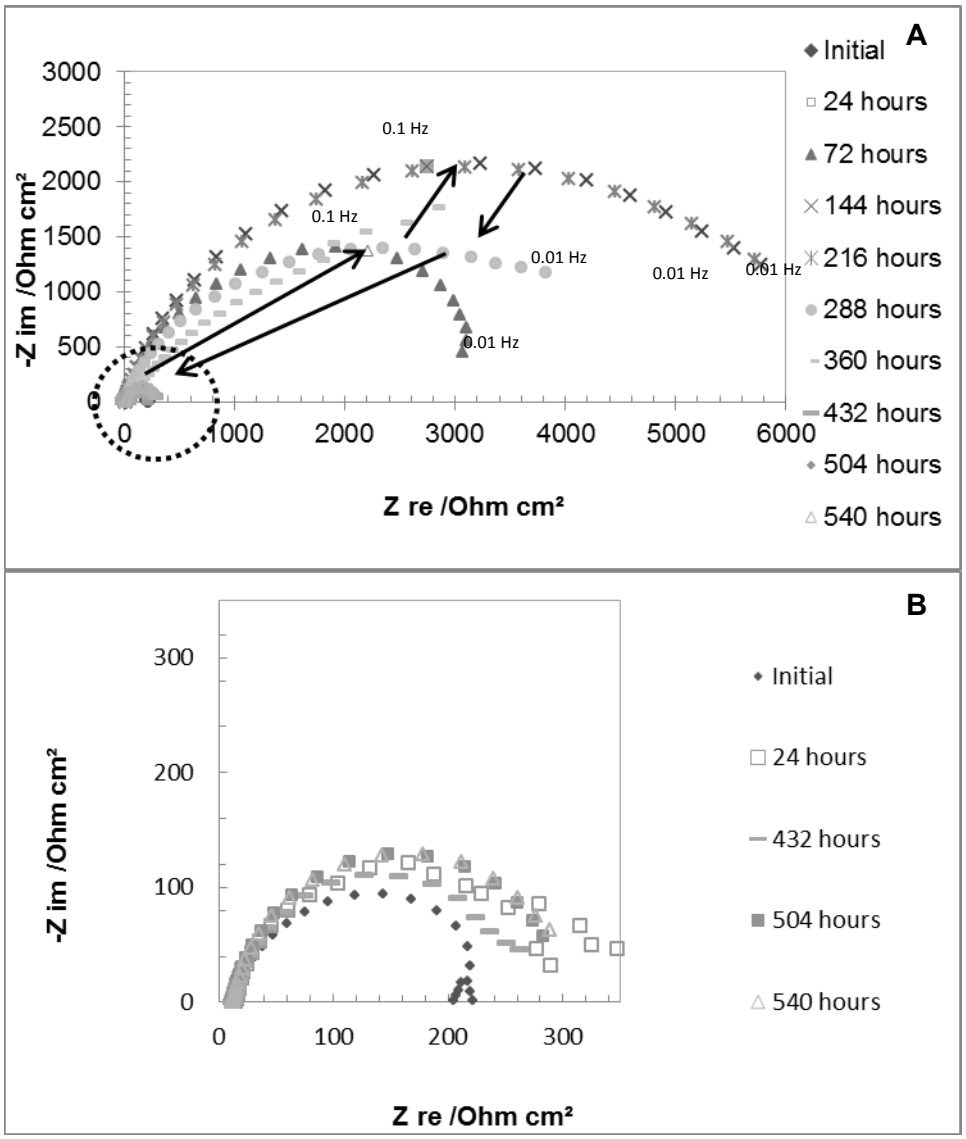


Fig.9 Impedance spectra of carbon steel S235JR during 600 hours of immersion in ASW medium. Control (abiotic) system with pigging debris autoclaved kept in anaerobic conditions. Supplemented with 10 mM acetate and 25 mM of fumarate.. (A) Nyquist, (B) Zoom-up Nyquist diagram of highlighted zone by a dashed circle.

Table 6. Evolution in time for experimental data of $R_{s,}$ and $R_p$ of the control and inoculated systems in ASW supplemented with 10 mM of acetate and 25 mM of fumarate in presence of a coupon of S235 JR. Systems kept in anaerobic conditions. (A) control system; (B) inoculated system with pigging debris. NA: Not applicable due to linear shape at LF.

**A**

| Time (h) | $R_S$ (Ω cm²) | $R_p$(Ω cm²) |
|---|---|---|
| Initial | 13 | 220 |
| 24 h | 13 | 314 |
| 72 h | 15 | 3500 |
| 144 h | 15 | 5650 |
| 216 h | 14 | 5650 |
| 288 h | 14 | NA |
| 360 h | 13 | NA |
| 432 h | 12 | 270 |
| 504 h | 12 | 285 |
| 540 h | 12 | 300 |

**B**

| Time (h) | $R_s$ (Ω cm²) | $R_P$ (Ω cm²) |
|---|---|---|
| Initial | 9 | 270 |
| 24 h | 10 | 220 |
| 72 h | 10 | 282 |
| 144 h | 10 | 452 |
| 216 h | 8 | NA |
| 288 h | 11 | NA |
| 360 h | 10 | NA |
| 432 h | 9 | NA |
| 504 h | 9 | NA |
| 540 h | 9 | NA |

Fig. 10 shows the impedance response for carbon steel exposed to the microorganisms present in the pigging debris in ASW medium and its evolution with time. For the initial times (hours 0 to 144), the presence of a depressed semi-circle is observed in the Nyquist diagram, and an increasing diameter is observed during time which, in terms of $R_p$ corresponds to an increase in the corrosion protection ($R_p$ from 220 to 452 Ω cm², table 6B), therefore a decrease on the corrosion rate. From hour 216 the Nyquist diagram shows straight lines at LF preceded by a semi-circle shape at HF for hours 216 and 288 (Fig. 10B). The linear shapes observed at HF can be linked to mass transfer phenomenon which appears after inoculation with biotic pigging debris when the OCP jumped and the medium turned black.

Due to the so varied impedance shapes and responses exposed by these systems (control and inoculated), in time, a sole model does not achieve to represent the different mechanisms observed. Thus, these systems were now analysed qualitatively, only making allusion to $R_p$ values (that provide us an estimation on the corrosion protection) and/or mass transfer phenomenon.

First, the two systems (control and biotic) exposed the same behaviour between hour 24 and 144, i.e. an increase of $R_p$ suggesting the formation of a protective layer. However, it is important to indicate that the magnitudes for $R_p$ in the biotic system are 12 times smaller than in the control abiotic system, showing that the layer in presence of microorganisms is less protective than the one in absence of them. The expected growth of bacteria certainly catalysed the formation of FeS, whereas in the control, the formation of an oxide layer is presumed. For the two cases, the following mechanisms are proposed, sustained by macroscopic and surface observations and EDX results.

For the control system case:

$$2H_2O + 2e^- \longrightarrow H_2 + 2OH^- \quad (2)$$

$$Fe^0 \longrightarrow Fe^{2+} + 2e^- \quad (3)$$

$$Fe^{2+} + 2OH \longrightarrow Fe(OH)_2 \quad (4)$$

Where (2) is the cathodic reaction for neutral conditions; (3) is the anodic reaction in neutral conditions and (4) is the final corrosion product that precipitated as a yellow rusting looking product mentioned in 3.1.1.

For the inoculated system case:

$$CH_3COOH + SO_4^{2-} \longrightarrow 2HCO_3^- + H_2S \quad (5)$$

$$Fe^{2+} + H_2S \longrightarrow FeS + 2H^+ \quad (6)$$

Where (5) and (6) are reactions catalysed by the presence of sulphate reducing microorganisms (SRM). Reaction (6) is faster mediated by microorganisms than in water and also promotes the so-called hydrogen embrittlement of the metal [30]

For times beyond 216, both systems suffer a switch on the impedance behaviour. For the case of the control system, the drastic decrease of $R_p$ observed can be attributed to the decrease of the protection and to a subsequent higher dissolution of the metal. For the case of the biotic system, a mass transfer phenomenon appears, when it is presumed that the rate of the proton consumption increased on the FeS deposit concomitantly with a faster dissolution of iron (anodic reaction) and then a bigger production of FeS is induced: FeS is then found not only on the coupon surface but also as a precipitate in the reactor.

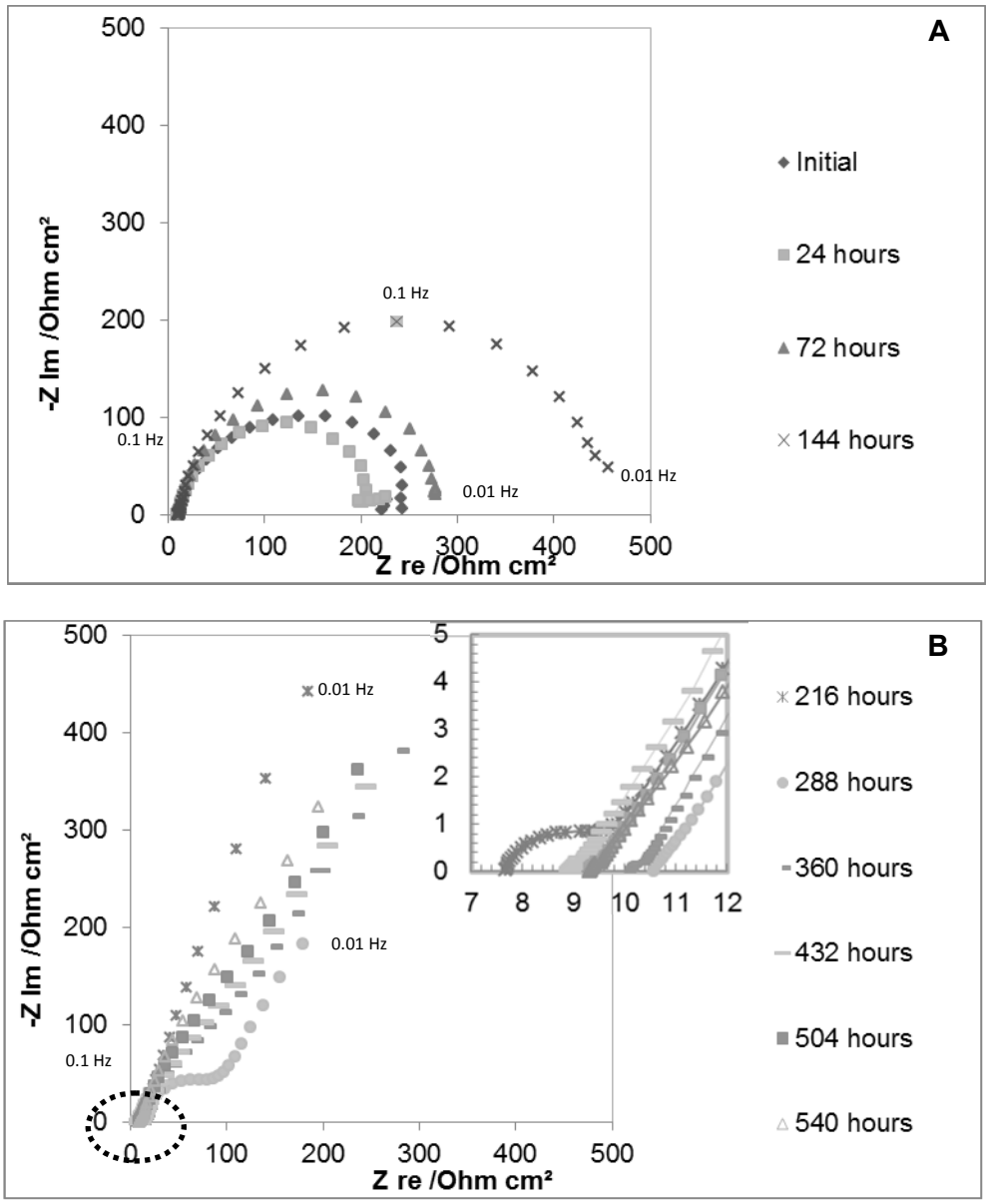


Fig.10 Impedance spectra of carbon steel S235JR during 600 hours of immersion in ASW medium Inoculated (biotic) system kept in anaerobic conditions. Supplemented with 10 mM acetate and 25 mM of fumarate. (A) Nyquist, (B) Zoom-up Nyquist diagram of highlighted zone by a dashed circle.

*3.2.2. EIS results with MIXED water from the field*

Fig. 11 (A,B and C) shows the impedance response for carbon steel exposed to abiotic MIXED water medium with autoclaved pigging debris (control system) and its evolution with time. The Nyquist diagram (A) displays the presence of one depressed semi-circle all along the different times of measurement with fluctuating diameters. Fig. 12 displays the impedance response for carbon steel in presence of microorganisms from the pigging debris and its evolution with time. One capacitive loop is observed at all the times tested, exposing depressed semi-circles which grow in size until reaching steady state from around hour 144.

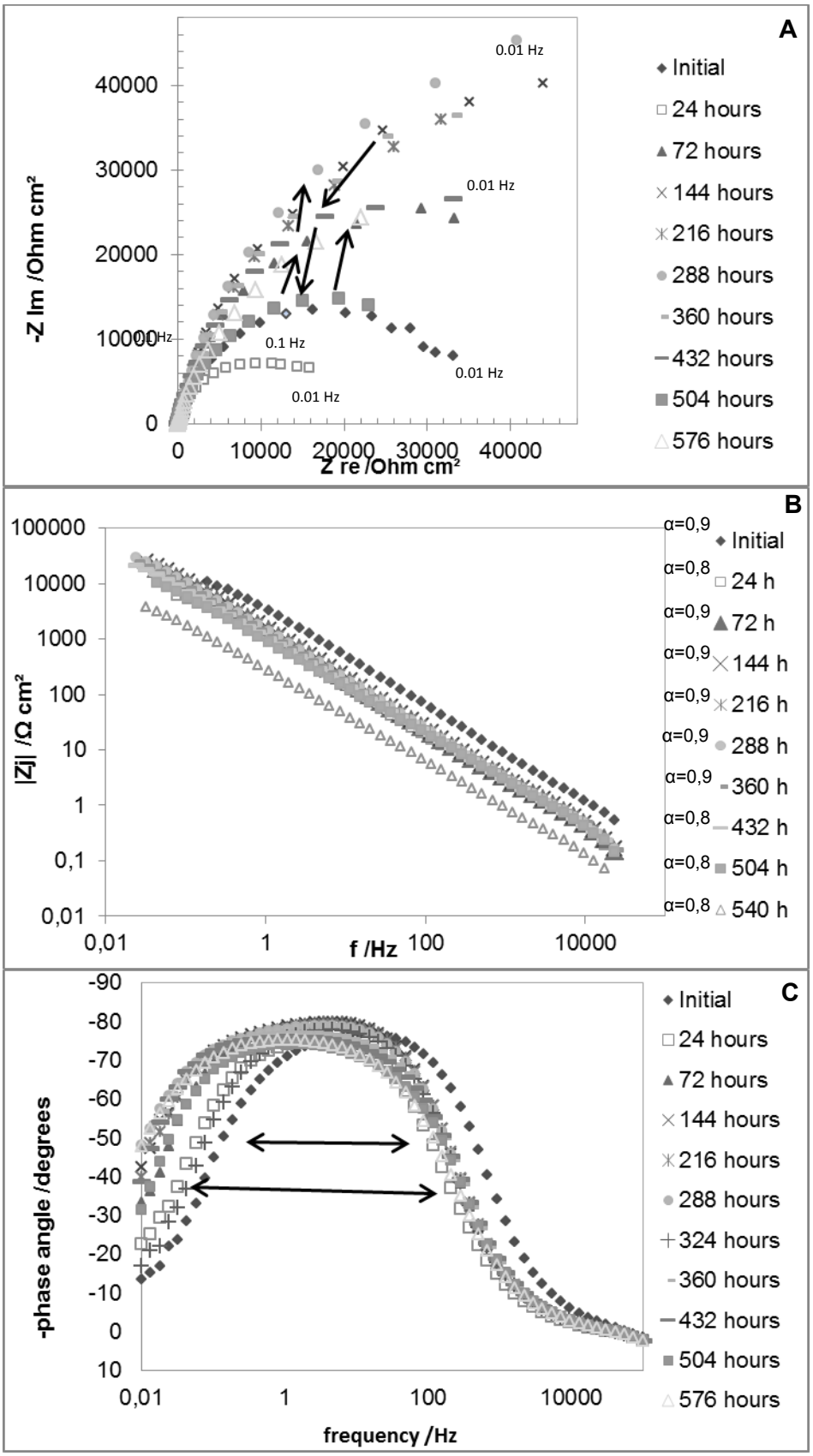


Fig.11 Impedance spectra of carbon steel S235JR during 600 hours of immersion in MIXED water medium. Control (abiotic) system with pigging debris autoclaved kept in anaerobic conditions. Supplemented with 10 mM acetate and 25 mM of fumarate. (A) Nyquist, (B) Bode plot of imaginary part of the impedance as function of frequency and (C) Bode plot phase angle vs. frequency.

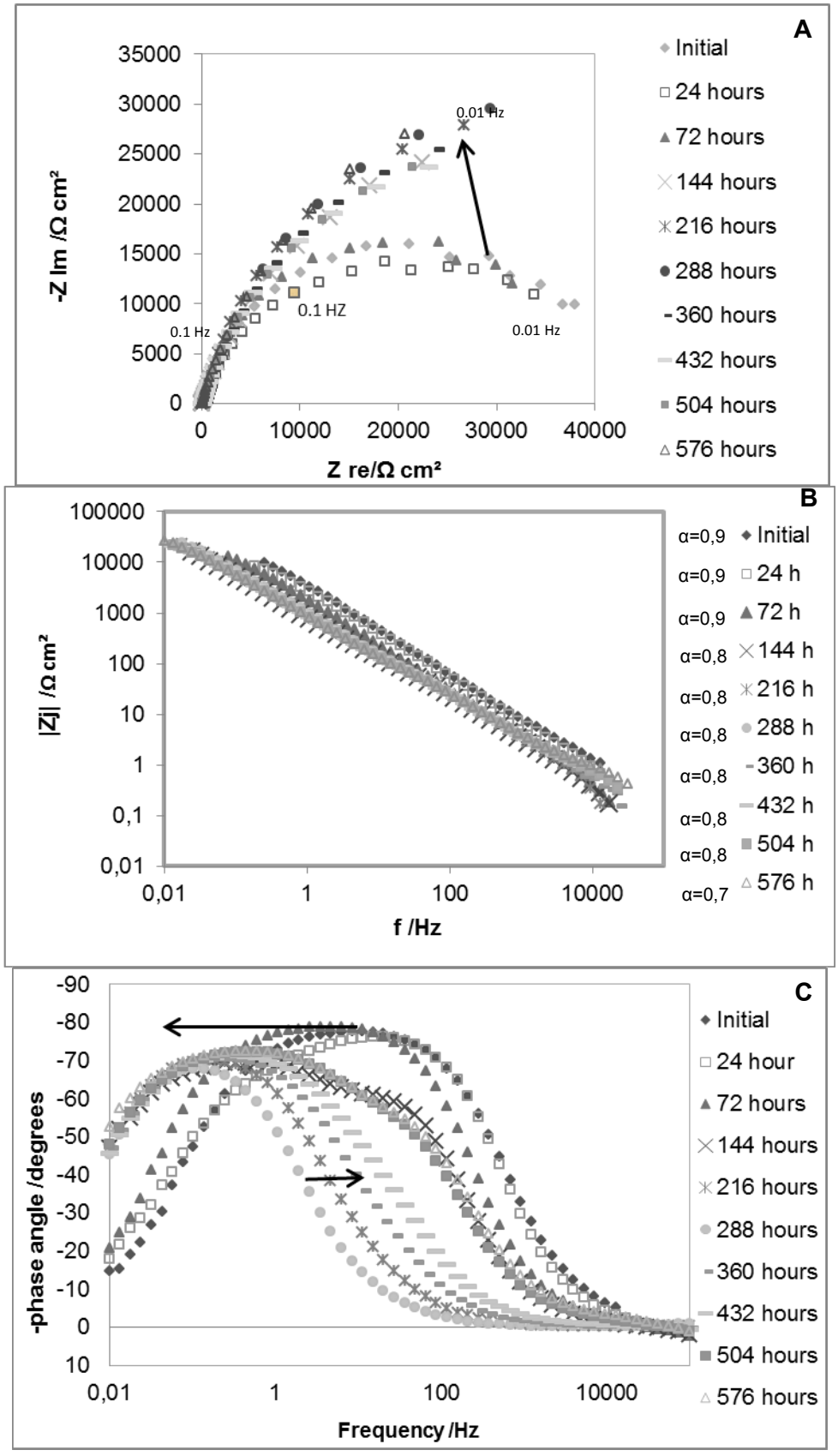


Fig.12 Impedance spectra of carbon steel S235JR after 600 hours of immersion in MIXED water medium. Inoculated (biotic) system kept in anaerobic conditions. Supplemented .with 10 mM acetate and 25 mM of fumarate.. (A) Nyquist, (B) Bode plot of imaginary part of the impedance as function of frequency and (C) Bode plot phase angle vs. frequency.

Thanks to the apparent simplicity of the MIX water systems (compared to ASW) the analysis of the response was treated using the approach reported by Orazem *et. al.* [31] plotting the modulus of the imaginary component of the impedance in function of the frequency in logarithmic coordinates, withdrawing the drawbacks of the influence of the electrolyte resistance on the estimation of time constants (Fig 11B and 12B). The slope values of the linear parts at high frequencies (HF) were used for the calculation of alpha (α) values to determine whereas the system followed a constant phase element (CPE) behaviour or a pure capacitive behaviour [31]. For both systems, the α values found and displayed in table 7 were lower than 1 confirming a CPE behaviour. i.e. the system exposed a heterogeneous distribution of time constants: The impedance of a CPE can be described by (7) [31, 32]:

$$Z_{CPE} = 1/Q(\omega)^{\alpha} \times [\cos(\alpha\pi/2) - j \sin(\alpha\pi/2)] \quad (7)$$

where the coefficient Q was calculated by using the imaginary part of the impedance ($Z_j$) with:

$$Q = - 1/[Z_j(f)(2\pi f)^{\alpha}] \times \sin(\alpha\pi/2) \quad (8)$$

and

$$\omega = 2\pi f \quad (9)$$

Table 7 also exposes the Q values ($Q_{eff}$) corresponding to the experimental parameters of the CPE impedance. The capacitance values were calculated applying the equation derived by Brug *et. al.* [31-33] after assuming that the distribution of time constants was all along the surface:

$$C_{dl} = Q^{1/\alpha} (R_s^{-1} + R_{ct}^{-1})^{(\alpha-1)/\alpha} \quad (10)$$

For both systems, the $C_{dl}$ values obtained (between 20 and 75 μF cm²) correspond to typical values for a double layer capacitance [32]. The depressed semi-circle observed is attributed to a resistance to the charge transfer ($R_{ct}$) that fluctuates along the time (table 7). These fluctuations provide us an initial estimation on corrosion rates.

For the control system, it is observed that capacitance values do not evolve much along the time but $R_{ct}$ values increase over time until hour 360. Beyond this time, $R_{ct}$ values fluctuate between 37 kΩ cm² and 100 kΩ cm² perhaps reflecting some fluctuations on the activation of the interface. In contrast, for the biotic system a slightly bigger fluctuation is observed on the capacitance values but a lower fluctuation in the $R_{ct}$ values (between 80 kΩ cm² and 110 kΩ cm² for hour 114 to 576, respectively) suggesting that a more stable layer has been formed on the interface. However, the magnitudes for the real impedance are equivalent in both MIXED water systems suggesting that there is probably not much difference in terms of corrosion rate regardless the presence of microorganisms. Moreover, phase angle plot (Fig. 12C) shows a fluctuating displacement of the phase angle peak between low and middle frequencies, suggesting a continuous fluctuation of the capacitance of the interface with time. These observations are in accordance with capacitance values described in table 7B.

Table 7. Evolution in time for experimental data of $R_{s,}$ $R_{ct}$, α, $Q_{eff}$ and $C_{dl}$ of the control and inoculated systems in MIX water supplemented with 10 mM of acetate and 25 mM of fumarate in presence of a coupon of S235 JR. Systems kept in anaerobic conditions. (A) control system; (B) inoculated system with pigging debris.

**A**

| Time (h) | $R_s$ (Ω cm²) | $R_{ct}$ (Ω cm²) | α | $Q_{eff}$($\Omega^{-1}cm^{-2}s^{\alpha}$) | $C_{dl}$ µFcm$^{-2}$ |
|---|---|---|---|---|---|
| Initial | 11 | 32300 | 0,86 | 6,0E-05 | 18,4 |
| 24 h | 10 | 17900 | 0,84 | 2,4E-04 | 74,7 |
| 72 h | 9 | 60000 | 0,88 | 1,3E-04 | 57,0 |
| 144 h | 9 | 100500 | 0,89 | 1,3E-04 | 56,6 |
| 216 h | 9 | 100000 | 0,88 | 1,4E-04 | 55,9 |
| 288 h | 9 | 118400 | 0,87 | 1,4E-04 | 55,6 |
| 360 h | 9 | 100100 | 0,86 | 1,7E-04 | 60,3 |
| 432 h | 8 | 36800 | 0,84 | 2,0E-04 | 59,8 |
| 504 h | 8 | 37000 | 0,83 | 2,4E-04 | 65,6 |
| 576 h | 8 | 72200 | 0,82 | 2,7E-04 | 69,6 |

**B**

| Time (h) | $R_s$ (Ω cm²) | $R_{ct}$ (Ω cm²) | α | $Q_{eff}$($\Omega^{-1}cm^{-2}s^{\alpha}$) | $C_{dl}$ µFcm$^{-2}$ |
|---|---|---|---|---|---|
| Initial | 12 | 41000 | 0,86 | 5,9E-05 | 18,2 |
| 24 h | 12 | 34700 | 0,87 | 7,1E-05 | 24,5 |
| 72 h | 12 | 41000 | 0,89 | 1,1E-04 | 49,9 |
| 144 h | 16 | 817000 | 0,81 | 2,6E-04 | 71,7 |
| 216 h | 17 | 107000 | 0,82 | 2,1E-04 | 61,9 |
| 288 h | 18 | 109000 | 0,80 | 2,2E-04 | 53,2 |
| 360 h | 18 | 87000 | 0,81 | 2,4E-04 | 65,4 |
| 432 h | 19 | 85000 | 0,78 | 2,5E-04 | 55,8 |
| 504 h | 19 | 84000 | 0,77 | 2,7E-04 | 55,0 |
| 576 h | 15 | 110000 | 0,75 | 2,8E-04 | 44,8 |

Furthermore, when the two MIXED water systems are compared, it can be inferred that even though the $C_{dl}$ and $R_{ct}$ values are similar, the phenomena occurring at the interface might be different. System with bacteria achieves a steady state after hour 144 whereas control system $R_{ct}$ fluctuates along time. This divergence might reflect the differences in the interface on which the double layer developed. As suggested by micro and macroscopic observations, the layer formed on the coupon surface in the control system is a combination of iron oxides (in the form of magnetite ($FeO*Fe_2O_3$)).whereas the layer formed in the system with bacteria may content some deposits of iron sulphide which affected the charge transfer phenomena ($R_{ct}$, $C_{dl}$). Moreover, pit areas can be observed on the coupon of the biotic system confirming the idea of this FeS layer formation. Pits formation induced by SRM have been widely studied in the frame of microbial corrosion and its mechanisms have been elucidated by different authors [1,5,10]. Here it can be claimed that even if the bacterial growth was reduced due to the presence of the corrosion inhibitor (previously stated in 3.1.2), SRM concentration was sufficient to induce FeS formation and consequently pitting pattern.

On the other hand, a comparison of the impedance magnitudes in the abiotic systems of the two mediums tested show that they are smaller in ASW than in MIXED water. The magnitudes of the real part of the impedance in MIXED water are about 200 times higher than in ASW at initial time (hour zero). The high resistivity observed in MIXED water medium must be due to the presence of corrosion inhibitor and organic acids in the production pipeline water. Thus, this medium could be claimed to be far less corrosive for the carbon steel than ASW. Indeed, the EDX results and macroscopic observations suggest that there was little corrosion in the MIXED water system and only few corrosion products compared to ASW results.

*3.3 Weight loss results*

Weight loss tests for carbon steel were performed in ASW and MIXED water media using as inoculum two samples of pigging debris (pig 1 and 5) collected from the water injection pipeline of system A. Pig 1 corresponds to the first debris collected after the first pigging operation and Pig 5 corresponds to the debris collected after the fifth consecutive pigging operation. Control and blank were run in parallel for the two systems (ASW and MIXED water). The blank consisted on the metal coupon immersed in the respective medium of the system; the control consisted on the previous items plus the addition of autoclaved pig. The mass lost was measured after 3 months of immersion for duplicated coupons. The results obtained from these tests are representative of the complete set of experimental results (Fig. 13 and 14).

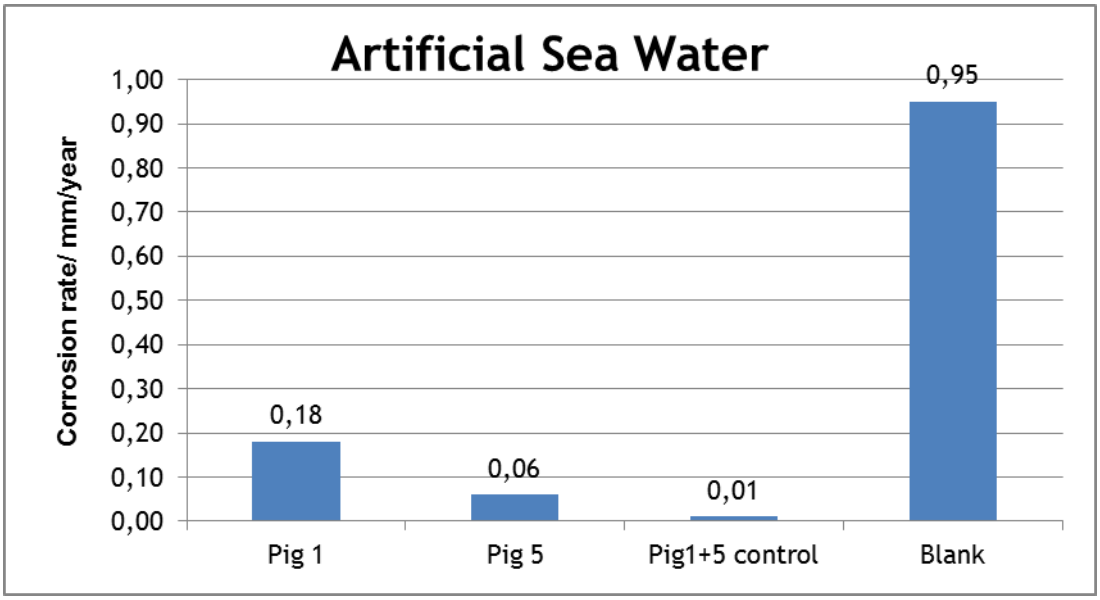


Fig. 13 Weight loss diagram in mm/year for carbon steel S235JR after 3 months of immersion in ASW with 10 mM acetate, 25 mM fumarate

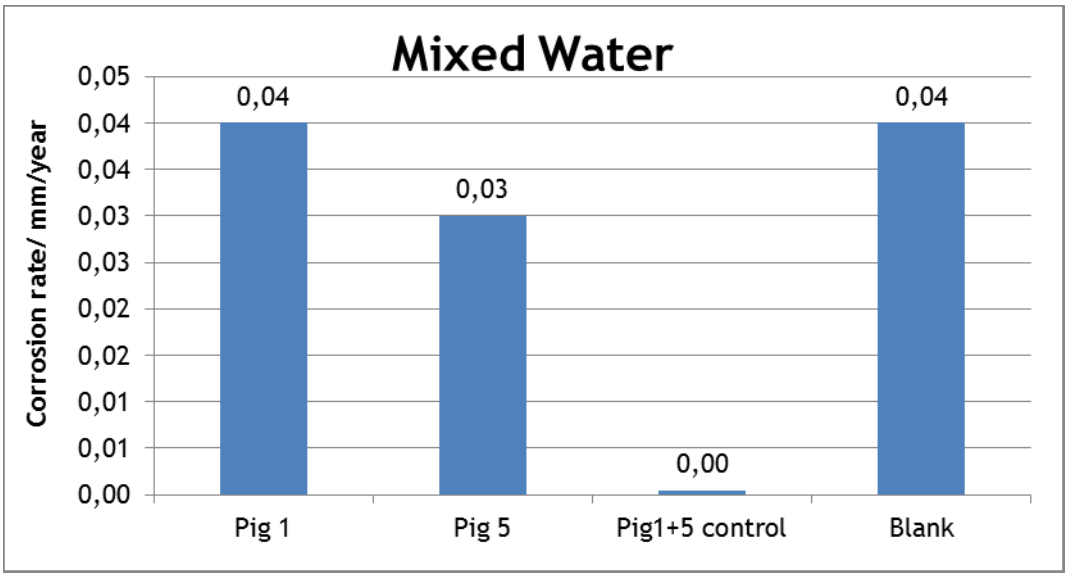


Fig. 14 Weight loss diagram in mm/year for carbon steel S235JR after 3 months of immersion in MIXED water with 10 mM acetate, 25 mM fumarate

In ASW system, the highest corrosion rate observed was in the blank whereas the lowest one observed was in the control system. The corrosion rate of the blank was 90 times higher than in the control system. It is believed that this drastic difference of corrosion rate between the blank and the control systems are due to the organics (in the form of hydrocarbons) and traces of corrosion inhibitor that are attached and released by the debris. Furthermore, when comparing the biotic systems (pig 1 and pig 5) it was observed a higher corrosion rate in pig 1 (0,18 mm/year) than in pig 5 (0,06 mm/year).

In MIXED water the results showed that the corrosion rate observed in the blank was 40 times higher than the one observed in the control system. In this case, this difference is mainly attributed to the presence of organics attached to the debris since the amount of residual corrosion inhibitor is the same in the control and the blank of MIXED water. On the other hand, gravimetric measurements of the carbon steel samples indicated that after 3 months of immersion in either ASW or MIXED water, more mass is lost when the carbon steel is immersed in presence of biotic pig1 than biotic pig5. However, the relation of mass loss for pig 1 and 5 in ASW is (3:1) whereas in MIXED water is (1.45:1). The explanation for this difference is the higher concentration of corrosion inhibitor in the MIXED water which affects the development of bacteria.

Therefore, the most corrosive media which induced higher mass loss for all the conditions tested was ASW in which a high quantity of corrosion deposits precipitated as biologically induced FeS (Fig. 15) and planktonic bacteria concentration was greater.

For each condition tested (biotic pig, control autoclaved pig and blank) it was concluded that all of them followed the same trend in both media. The blank was the condition that showed the highest mass loss for both media. This condition did not have inoculated pigging debris, therefore did not have any trace of hydrocarbons. The control for pig 1 and 5 which was inoculated with sterile debris was the condition

that showed the least mass loss in both media and the pigging debris that induced higher corrosion rates was Pig 1.

Thus, it can be resumed that ASW is the most corrosive system for the immersion of low carbon steel. Furthermore, MIXED water was the least corrosion system for carbon steel and this might be due to the presence of corrosion inhibitor present in this water. The presence of biotic pig 1 induced the highest corrosion rates for the biotic systems and the presence of autoclaved pigging debris used for the control systems induced the least corrosion rates, probably due to the following reasons:

(1) The absence of microorganisms and more over of sulphide producers
(2) The presence of organic acids (in the form of hydrocarbons) attached to the debris
(3) The presence of corrosion inhibitor traces attached to the debris

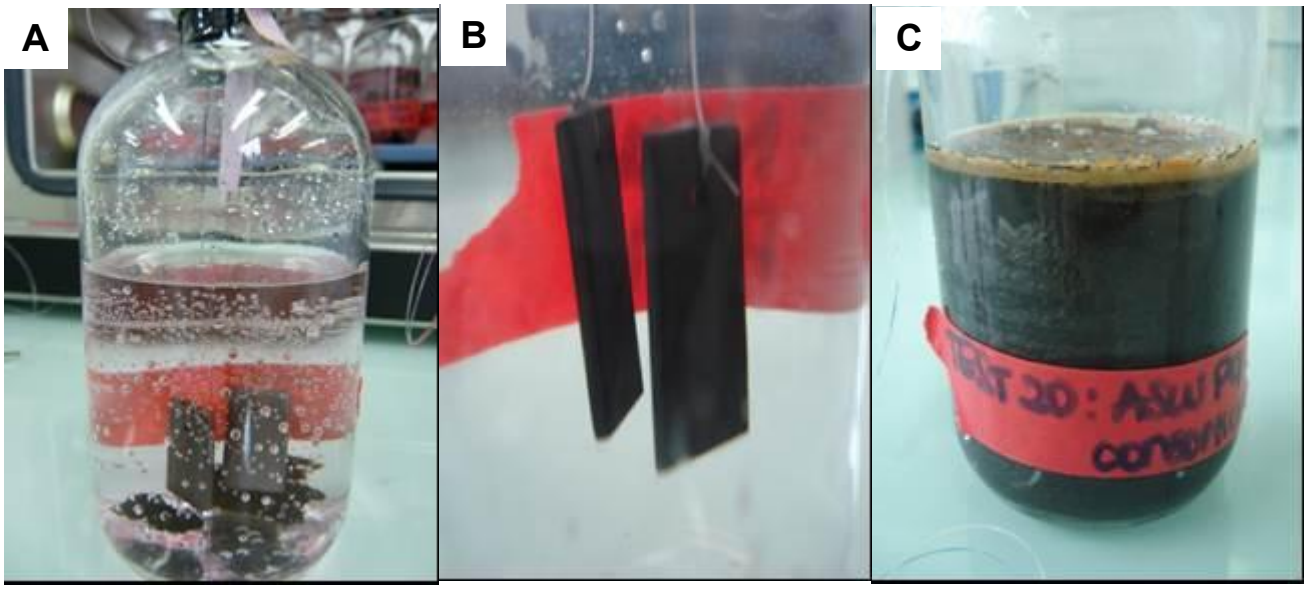


Fig. 15 Weight loss experiment photos for carbon steel S235JR at time zero and after 3 months of immersion (A): MIXED water with 10 mM acetate, 25 mM fumarate in presence of pigging debris at time 0; (B): MIXED water with 10 mM acetate, 25 mM fumarate in presence of pigging debris after 3 months; (C): ASW with 10 mM acetate, 25 mM fumarate in presence of pigging debris after 3 months

*3.4. Bacteria identification*

DGGE analysis allows the separation of PCR products of similar size based on the difference of their GC-content in the sequence [19]. DGGE has been applied to the study of microbial community complexity in which the PCR products are variable regions of the 16S rRNA gene, to infer the composition of microbial communities [23].

The DGGE gels in Fig.16 illustrate the variety of 16S rRNA gene fragments amplified from two sources: 1) from the pigging debris of the water injection system (Fig. 16A) and 2) from the inoculated media used for the electrochemical experiments once these lasts stop (Fig. 16B). Each column in the DGGE gels represents one sample and the number of individual bands obtained is related to the number of bacterial species in the tested samples.

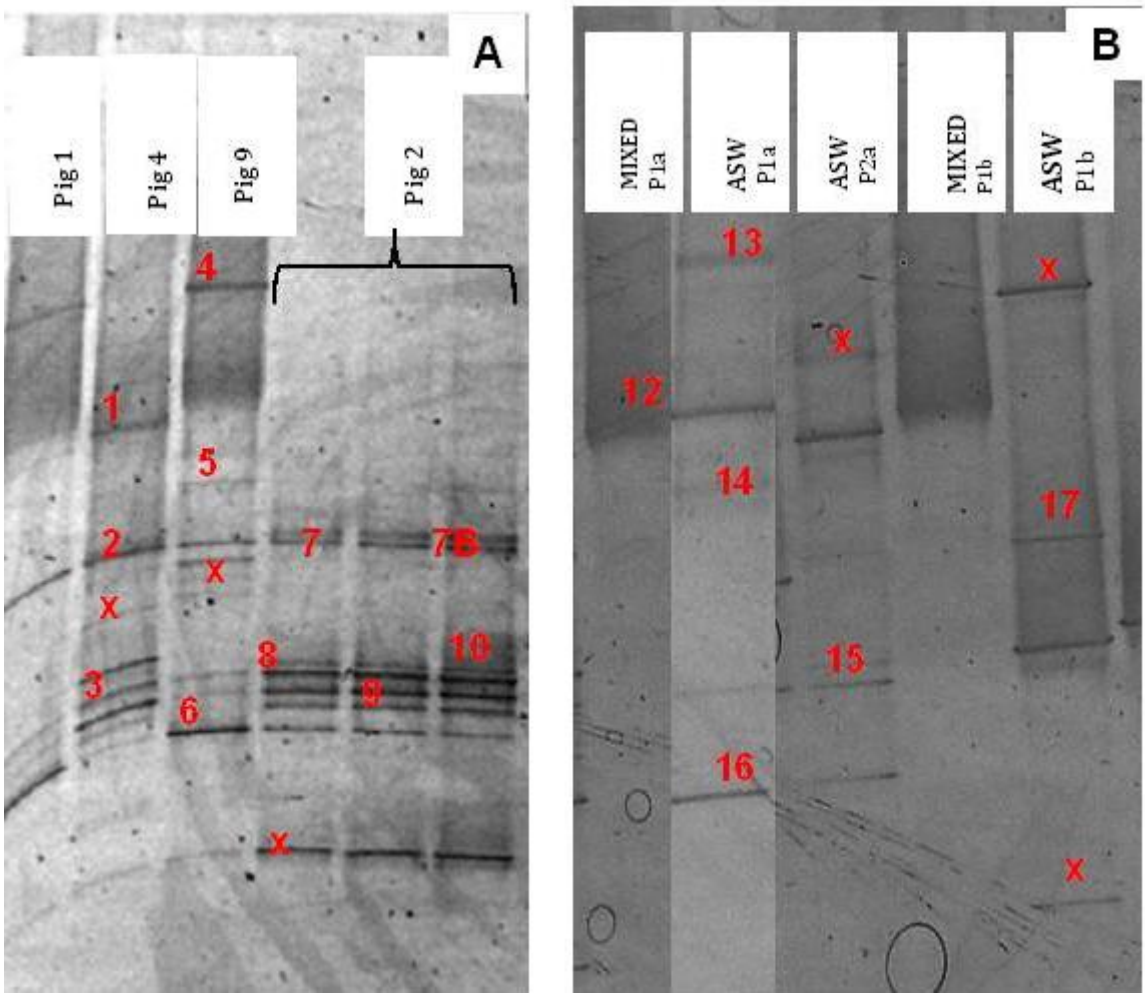


Fig. 16 DGGE gel profile demonstrating diversity of bacterial populations based on PCR products of 550 bp of Bacterial 16S rRNA.. (A) Profile obtained using directly the pigging debris as samples (pig 2 in triplicate) (sequenced bands were labeled 1-11; not yield results were labeled "x"), (B) Profile obtained of cultivable bacteria that grew in ASW supplemented ad MIXED water supplemented used to perform the electrochemical experiments (bands sequenced labelled 12-30)

More specifically, Fig. 16 A shows the DGGE community fingerprint of a consortium living in the pigging debris. Out of the 4 samples, it was found a total of 30 strong bands; pig 2 was the sample that exposes the highest quantity of bands (9 bands). However, only 13 bands were taken into account for sequencing assuming that bands that fell in the same or close-by position in the gel of the different columns were the same repeated DNA sequence or a close polymorphism. Bands marked with "X" (Fig. 16A) did not yield ideal results when sequencing. Likewise, Fig. 16B shows the DGGE community fingerprint of the consortium which developed in the second source (media used for the electrochemical experiments). Out of the 5 samples tested, it was found a total of 16 strong bands being; ASW was the sample that exposes the highest quantity of bands (6 bands). However, only 9 bands out of the 16 were taken into account for sequencing assuming the same premises mentioned for the previous gel.

Table 8A summarises the bacterial diversity found in the pigging debris extracted from 4 pigging operations performed in the water installation after matching each sequencing result with the most closely related sequence found in the database of

the National Centre for Biotechnology Information (NCBI). The obtained sequences were at least 95% identical to already deposited sequences of the GenBank database. Table 8B summarises the species identified that developed in the 2 different mediums used for performing the electrochemical and weight loss experiments after inoculation with pigging debris from the same installation.
A comparison between the bacterial diversity present in the debris and the bacterial diversity that developed in the mediums used for the electrochemical tests was attempted in order to determinate the actual bacteria species that may be involved in the electrochemical and weight loss results in terms of corrosion.
The average of bands found in the gel when amplifying DNA directly from the pigging debris was 7.5 bands. In contrast, the quantity of bands found in the gels containing PCR samples extracted from the media used for the electrochemical tests was 3.2. Moreover, it was observed that only 1 band was found in the 2 samples of MIXED water run in the gel suggesting that bacteria do not develop well in MIXED water and the population diversity gets decreased severely. However, the population diversity does not get as reduced in ASW, finding in average 5 bands. Overall, it can be said that the quantity of bands detected in the pigging debris were reduced by 33,4% when inoculating the pigging debris in ASW and by 86,7% when inoculating the pigging debris in MIXED water. Thus, the number of bacterial species was reduced when performing the electrochemical and weight loss experiments. These results are in accord with the results obtained with the electrochemical and weight loss experiments.

Table 8. Bacterial 16S rRNA sequences results obtained from: (A) pigging debris; (B) developed bacteria in mediums used for electrochemical experiments. Refer to Fig. 16

**A**

| ID | Identity (%) | Result |
|---|---|---|
| 1 | 95 | *Desulfobacter halotolerans* DSM 11383 |
| 2 | 97 | *Clostridium halophilum* DSM 5387 |
| 3 | 99 | Uncultured Synergistetes bacterium clone NRB29 |
| 4 | 97 | *Marinifilum* sp. KYW 585 |
| 5 | 97 | *Desulfovibrio* sp. AND1 |
| 6 | 100 | *Dethiosulfovibrio russensis* strain WS 100; DSM 12537 |
| 7 | 99 | Uncultured *Caminicella* sp. clone TCB261x |
| 7B | 99 | Uncultured *Caminicella* sp. clone TCB207x |
| 8 | 100 | Uncultured *Thermovirga* sp. clone TCB168x |
| 9 | 99 | Uncultured Synergistetes bacterium clone D010011F15 |
| 10 | 98 | Uncultured *Thermovirga* sp. clone TCB8y |

**B**

| ID | Identity (%) | Result |
|---|---|---|
| 12 | 97 | *Desulfovibrio dechloracetivorans* strain SF3 |
| 13 | 99 | *Desulfovibrio* sp. Z1 16S ribosomal RNA gene |
| 14 | 99 | Uncultured bacterium 16S rRNA gene, clone Dan_Bac88 |
| 15 | 95 | Uncultured *Spirochaetes* bacterium clone D010012E07 |
| 16 | 99 | *Dethiosulfovibrio russensis* strain WS 100; DSM 12537 |
| 17 | 100 | *Arthrobacter* sp. MDB1-56 16S |

Among the 11 species identified in table 8A, 18% of them fall among the SRB group (*D. halotolerans* and *Desulfovibrio* sp.). Furthermore, 36% of them are able to produce sulphide as a metabolic product (*Clostridium halophilum, Thermovirga* sp. and the 2 SRB). It was also found that only *D. russensis* is able to reduce elemental

sulphur and thiosulphate. Moreover, *Clostridium halophilum, Thermovirga* sp and *D. russensis* share the same taxonomic order; *Clostridiales*. Furthermore, most of the detected bacteria are fermentative bacteria that produce as metabolic products a large variety of organic acids such as butyric, lactic and acetic acids that may affect the local pH accelerating corrosion. SRBs have been widely studied and it is known the danger these bacteria represent to corrosion of metals due to the production of $H_2S$ and FeS catalysed by this group. Thus, the presence of these bacteria in pipelines represents the most potential danger in terms of corrosion.

On the other hand, among the 6 bands that yielded acceptable sequences in table 8B, 3 of them coincided with species found in the pigging debris and 3 with bacteria species that were not detected in the analysis performed to the pigging debris. More precisely, 2 bands resulted to be sequences of bacteria belonging to the SRB group; 1 band belonged to the taxonomic order *Clostridiales* (*D. russensis*), 1 band which sequence corresponds to the typical soil bacteria *Arthrobacter* sp. and 2 bands corresponding to sequences of uncultured bacteria. On the other hand, the detection of the only band in MIXED water yielded the sequence corresponding to the SRB, *Desulfovibrio dechloracetivorans*

Thus, it has been confirmed what it was suspected and previously discussed. The corrosion observed in carbon steel S235 JR is enhanced by the presence of SRB and sulphide producers in the 2 media tested. However, the effect of these bacteria is more evident when using ASW due to the better development of bacteria in this medium. The poor development of bacteria in MIXED water medium is attributed to the presence of corrosion inhibitor which reduced the growth of bacteria by nearly 87%.

## 4. Conclusions

The influence of a consortium of microorganisms present in a sample of pigging debris on the corrosion of carbon steel S235 JR was studied in supplemented ASW and MIXED water media by combining electrochemical measurements, surface analyses and weight loss tests. The bacterial diversity composition of the debris and the resulting growth in the media used was assessed by DGGE analysis of the PCR products for bacterial 16S rRNA genes.

The corrosion potential (OCP) measured in function of time showed a sudden increase of more than 400 mV vs Ag/AgCl in both media tested when the system was exposed to the biotic pigging debris whereas little (less than 100 mV) or none increase was observed in the control systems where the debris was autoclaved. However, it was noticed that this ennoblement occurred later in terms of time and lower in terms of potential increment when using MIXED water as electrolyte instead of ASW. The increment in OCP or corrosion potential indicates that there is higher corrosion risk with an incremented probability for pitting and crevice corrosion [22,24,25] which in this case has been enhanced by the presence of microorganisms in the system.

In agreement with previous results, EIS measurements show higher impedance magnitudes in MIXED water than in ASW suggesting that MIXED water system is the least corrosive of the two. The high resistivity observed in MIXED water medium

must be due to the presence of corrosion inhibitor and organic acids (hydrocarbons) present in the production pipeline where this water has been recycled from. In the presence of microorganisms is the FeS which gives the characteristics of the interface (both, when is governed by mass transfer in ASW and when is governed by charge transfer in MIXED). In the case of the control systems, it is rather the iron oxides of the type $Fe(OH)_2$ or $FeO*Fe_2O_3$ characterising the interface with variations in the quality of protection.

From weight loss tests it can be concluded that results are representative of the whole set of experiments finding higher corrosion rates in ASW than in MIXED water. Moreover, DGGE results proved that bacterial diversity gets decreased when harvesting de debris in the media used and suggested that the bacteria involved in the whole set of results are mainly sulphate reducing bacteria (SRB) and some other bacteria part of the taxonomic order *Clostridiales.*

The combination of electrochemical measurements, surface analyses, weight loss and DGGE tests allow us to conclude that:

- ASW system was more corrosive than MIXED water system.
- Bacteria from the pigging debris grow better in ASW than in MIXED water.
- Bacterial consortium found in the pigging debris altered the electrochemical response of the ASW systems tests inducing an increase in the OCP and a decrease in $R_p$ ; this compared to the control abiotic systems. In MIXED water, the presence of microorganisms altered the electrochemical response of the system inducing less fluctuation in $R_{ct}$ along time.
- The bacterial diversity gets reduced when introducing and growing the pigging debris into the 2 water media tested. Thus, it cannot be said that the only bacteria found in the media of the electrochemical tests are representative of the bacteria found in the field. Thus, it cannot be said that only SRB are the responsible for the corrosion of carbon steel in the field.

**Acknowledgments**

The research leading to these results has received funding from the European Community's Seventh Framework Programme (FP7/2007-2013) under grant agreement n° 238579. Project website: www.biocor.eu/ip2. The author would like to thank Dr. Turid Liengen from Statoil and Ing. Øystein Birketveit from M-I-Swaco for the helpful discussions about the field samples and special thanks to Dr. Isabelle Frateur for the support and fruitful discussions concerning impedance results

## References


[1] I. Beech, C. Gaylarde, Recent advances in the study of biocorrosión: an overview, Revista de Microbiología, 30 (1999). 177-190, ISSN 0001-3714.

[2] I. Beech, A. Bergel, A. Mollica, H-C. Flemming, V. Scotto, W. Sand. Simple methods for the investigation of the role of biofilms in corrosion. *On-line:* Brite-Euram III Thematic Network No. ERB BRRT-CT98-5084 (2000)

[3] M. Mehana, Mécanismes de transfert direct en corrosion microbienne des aciers: Application à *Geobacter sulfurreducens* et à l'ħdrogénase de *Clostridium acetobutylicum*, Thesis Université de Toulouse (2009)

[4] H. C. Flemming, Biofuling and Microbilogically Influenced Corrosion (MIC) an Economical and Technical Overview. E. Heitz, H-C Flemming, W. Sand (Eds.), Springer, Heidelberg

[5] R. F. Jack, D.B. Ringelberg, D.C White, Differential corrosion rates of carbon steel by combinations of *Bacillus* sp., *Hafnia alvei,* and *Desulfovibrio gigas* established by phospholipid analysis of electrode biofilm. Corr. Sci., 33 (1992) 1843-1853

[6] M. Sparr and M. Linder, Avoidance of corrosion problems in cooling water . Swerea KIMAB, Stockholm (2010), ISBN: 978-91-633-6852-3

[7] H. A. Videla, Prevention and control of biocorrosion, Int. Biodeter. & Biodegrad. 49(2002) 259-270

[8] B. Guo, S. Song, J Chacko, A. Ghalmbur, Offshore pipelines, Elsevier Inc (2005) 215-233

[9] B. Bubar, Pipeline pigging and inspection, in: E. S. Menon, Pipeline planning and construction field, Elsevier Inc, (2011): 313-339

[10] W. A. Hamilton, Sulphate reducing bacteria and anaerobic corrosion, Ann. Rev. Microbiol. 39(1985): 195-217

[11] C. Marshall, P. Frenzel, H. Cypionka, Influence of oxygen on sulphate reduction and growth of sulphate reducing bacteria, Arch. Microbial. 159(1993): 168-173

[12] I. B. Beech, J. Sunner, Biocorrosion: towards understanding interactions between biofilms and metals, Curr. Opinion in Biothech. 15(2004): 181-186

[13] B. Little, P. Wagner, F. Mansfeld, Microbiologically influenced corrosion of metals and alloys, Int. Mater. Rev. 36(1991): 253-272

[14] D. H. Pope, Microbial corrosion in fossil-fired power plants –a study of microbiologically influenced corrosion and a practical guide for its treatment and prevention-, Electric Power Research Instiute, Palo Alto, CA, (1987)

[15] J. P. Kirkpatrick, L. V McIntire , W. G. Characklis, Mass and heat transfer in a circular tube with biofouling Water Res., 14(1980)117-127

[16] E. Korenblum, G. V. Sebastian, M. M. Paiva, C. M. L. M. Coutinho, F. C. M. Magalhaes, B. M. Peyton, L. Seldin, Action of antimicrobial substances produced by different oil reservoir *Bacillus* strains against biofilm formation, App. Microb. Cell Physiol. 79(2008): 97-103

[17] C. A. Gonzalez-Rodriguez, F. J. Rodriguez-Gomez, J. Genesca-Llongueras, The influence of *Desulfovibrio vulgaris* on the efficiency of imidazoline as a corrosion inhibitor on low carbon steel in seawater, Electrochem. Acta. 54(2008): 86-90

[18] A. Rajasekar, S. Maruthamuthu, N. Palaniswamy, A. Rajendran, Biodegradation of corrosion inhibitors and their influence on petroleum product pipeline, Micrbiolog. Resear. 2007(162) 355-368

[19] J. Jan-Roblero, J. M. Romero, M. Amaya, S. Le Borgne, Phylogenetic characterization of a corrosive consortium isolated from a sour gas pipeline, App. Microbiol. Biotechnol., 64(2004):862-867

[20] X. Y. Zhu, J. Lubeck, J. J. Kilbane, Characterisation of microbial communities in gas industry pipelines, App. Environ. Microbiol, 69(2003): 5354-5363

[21] C. Cote, O. Rosas-Camacho, R. Basseguy, *Geobacter sulfurreducens:* An Iron Reducing Bacterium that Can Protect Carbon Steel Against Corrosion?,"Unpublished results": Manuscript submitted for publication, (2012)

[22] R. Javaherdashti, Microbially Influenced Corrosion – An Engeneering ensight-, Springer (Eds), (2008), London

[23] G. Muyzer, E. De Wall, A. G. Uitierlinden, Profiling of Complex Microbial Populations by Denaturing Gradient Gel Electrophoresis Analysis of Polymerase chain Reaction-Amplified Genes Coding for 16S rRNA, Appl. Environ. Microbiol. 59(1993): 695-700

[24] F. Mansfeld, The interaction of bacteria in methal surfaces, Electroch. Acta.52(2007):7670-7680

[25] B. J. Little, J. S. Lee, R. I. Ray, The influence of marine biofilms on corrosion: A consice review, Electroch. Acta. 54(2008):2-7

[26] M. B. McNeal, A. L. Odom, Microbiologically Influenced Corrosion Testing in: J. R. Kearns and B. Little (Eds), ASTM STP 1232, American society for testing and materials, Philadelphia, PA (1994):173

[27] C. von Wolzogen Kuehr, Water and gas 7(1923):277

[28] I. A. Davidova, J. Suflita, Enrichment and Isolation of Anaerobic Hydrocarbon-Degrading Bacteria in: J. R. Leadbetter (Eds), Methods in Enzymology, Elsevier Inc, 397 (2005): 17-34

[29] Z. Keresztes, I. Felhosi, E. Kalman, Role of Redox Properties of Biofilm in corrosion processes, Electrochim. Acta., 46(2001): 3841-3849

[30] H. Din, J. Kuever, M. Mubmann, A. W. Hassel, M. Stradman, F. Widdel, Iron corrosion by novel anaerobic microorganisms, Nature., 427(2004) 829-832

[31] M. E. Orazem, N. Pébère, B. Tribollet, Enhanced Graphical Representation of Electrochemical Impedance Data, J. Electrochem. Soc., 153(2006) B129-B136

[32] M. E. Orazem, B. Tribollet, Electrochemical Impedance Spectroscopy, John Wiley & Sons publications, NJ, USA

[33] G.J. Brug, A.L.G. van den Eeden, M. Sluyters-Rehbach, J.H. Sluyters, The analysis of electrode impedances complicated by the presence of a constant phase element, J. Electroanal. Chem. 176 (1984) 275–295

*IV.5.2.2. Supplementary results*

Several weight loss tests were performed immersing during 3 months the metal sheets C1015 in ASW and MIXED water from the field, both supplemented with different compounds regarding the test (table IV.9). These compounds are described in the table IV.9 and were added to supplement the different bacterial growth requirements. Different types of bacteria inoculum were used: pigging debris 1 and 5, consortium (pre-grown pigging debris in supplemented ASW) and enriched IOB/NRB and IRB. Control abiotic systems were performed for each of the conditions tested. Control systems consisted on injecting a filtrate of the grown bacteria culture medium (5%) into the reactor for the cases of: IOB/NRB and IRB. For the cases of systems with pigging debris, it consisted on the autoclaved debris (about 10 g). For the case of the consortium, they were compared to a blank system which is a system that does not have either bacteria or bacteria metabolites (it consists on the electrolyte plus the steel only). This is because we didn't want to add a source of sulphide found in the consortium cultures.

These set of gravimetric experiments were performed using two coupons for each of the conditions tested. Table IV.9 resumes the experimental matrix designed for the mass loss experiments. Conditions were kept anaerobic during the whole experiment by first taking out dissolved oxygen after injection of $N_2/CO_2$ (80:20) during 45 minutes into the anaerobic vials and then placing them into a nitrogen chamber.

Fig.IV.9 shows the results of weight loss in millimetres per year (mmpy) for carbon steel C1015 immersed in ASW and MIXED water media during 3 months: test 15-26. The figure displays the blue bars referring to MIXED water systems and the red bars referring to the ASW systems.

Results show that in all the conditions tested, it was found less mass loss when using MIXED water medium than when using ASW, including the control abiotic systems. These results were expected since knowing that the MIXED water medium contain a maximum of 4 ppm of corrosion inhibitor which was added to the water injection system where this water come from; this is in accordance with results described in article 3. In what it concerns the biotic systems, it was found that the highest corrosion rate was observed in systems inoculated with the consortium inoculum compared to with the pigging debris. It is presumed that the high mass loss observed in the systems inoculated with consortium, was due to the concentration of corrosive bacteria when pre- culturing the debris in the ASW medium. In terms of pigging number, it was found higher corrosion rates in systems inoculated with pig 1, either consortium or pigging debris themselves. Thus, it can be concluded that the bacterial diversity contained in the first sample taken from the water injection system (pig 1) exert the biggest influence on corrosion, in accordance with molecular analysis. In general, the highest corrosion rate observed was the one of the ASW system –blank condition-, depicting 90 times more corrosion than the control systems. It is presumed that this drastic difference of corrosion rate is due to the presence of organics (in the form of hydrocarbons) and traces of corrosion inhibitor that are attached and released by the sterile debris present in the controls and not in the blanks.

| Test No. | Medium | Medium modifications | Bacteria source |
|---|---|---|---|
| **15** | ASW | Same as reactor medium | Blank |
| **16** | Mixed | Same as reactor medium | Blank |
| **17** | Mixed | Same as reactor medium | Pig 1 |
| **18** | ASW | Same as reactor medium | Pig 1 |
| **19** | Mixed | Same as reactor medium | Pig 5 |
| **20** | ASW | Same as reactor medium | Pig 5 |
| **21** | Mixed | Same as reactor medium | Pig 1 + 5 control |
| **22** | ASW | Same as reactor medium | Pig 1 + 5 control |
| **23** | Mixed | Same as reactor medium | Consortium Pig 1 |
| **24** | ASW | Same as reactor medium | Consortium Pig 1 |
| **25** | Mixed | Same as reactor medium | Consortium Pig 5 |
| **26** | ASW | Same as reactor medium | Consortium Pig 5 |
| **27** | Mixed | Reactor medium supplemented with (g/L): 0.3 g $NH_4Cl$, 4 mM $NaNO_3$ | IOB/NRB 5 % |
| **28** | ASW | Reactor medium supplemented with (g/L): 0.3 g $NH_4Cl$, 4 mM $NaNO_3$ | IOB/NRB 5% |
| **29** | Mixed | Reactor medium* supplemented with (g/L): 0.3 g $NH_4Cl$, 4 mM $NaNO_3$ | IOB/NRB (CONTROL) |
| **30** | ASW | Reactor medium* supplemented with (g/L): 0.3 g $NH_4Cl$, 4 mM $NaNO_3$ | IOB/NRB (CONTROL) |
| **31** | Mixed | Reactor medium supplemented with (g/L): 1.5 g $NH_4Cl$ | IRB 5% |
| **32** | ASW | Reactor medium supplemented with (g/L): 1.5 g $NH_4Cl$ | IRB 5% |
| **33** | Mixed | Reactor medium supplemented with (g/L): 1.5 g $NH_4Cl$ | IRB (CONTROL) |
| **34** | ASW | Reactor medium supplemented with (g/L): 1.5 g $NH_4Cl$ | IRB (CONTROL) |

Table IV.9. Matrix of different conditions tested on weight loss experiments in presence and absence of bacteria from the water injection pigging debris using carbon steel 1015 immersed in ASW and Mixed water media (mediums marked with (*) were not supplemented with acetate or fumarate)

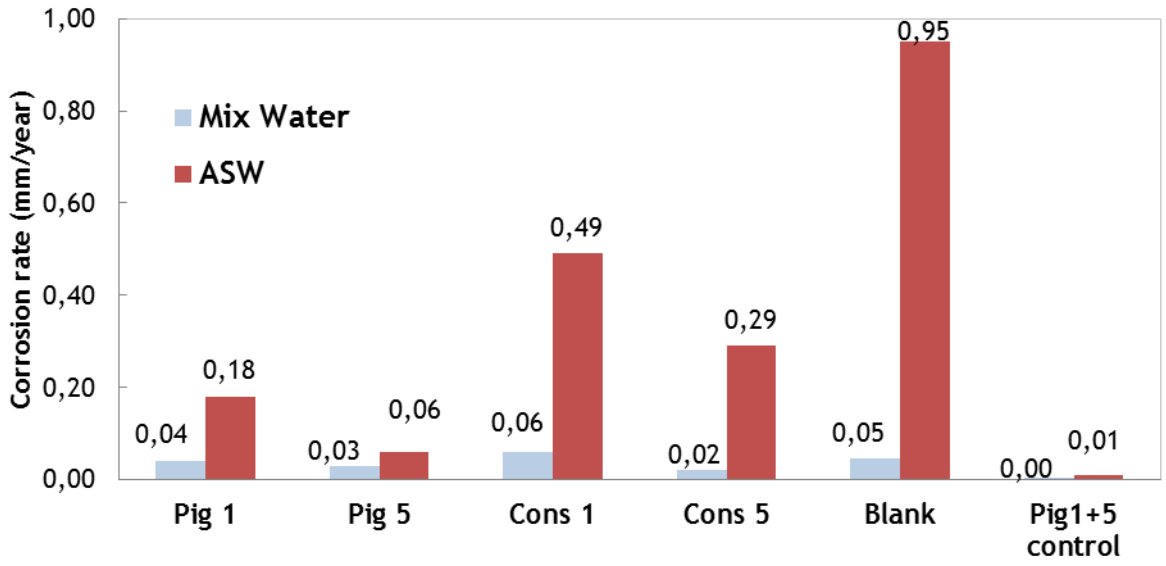


Fig. IV.9. Weight loss diagram in mm/year for carbon steel C1015 after 3 months of immersion in ASW and MIXED water medium: tests 15-26.

Fig.IV.10 shows the results of weight loss in millimetres per year (mmpy) for carbon steel C1015 immersed in ASW and MIXED water supplemented media during 3 months: test 27-34 –IRB and IOB/NRB bacteria from enrichments-. The figure displays the blue bars referring to MIXED water systems and the red bars referring to ASW systems.

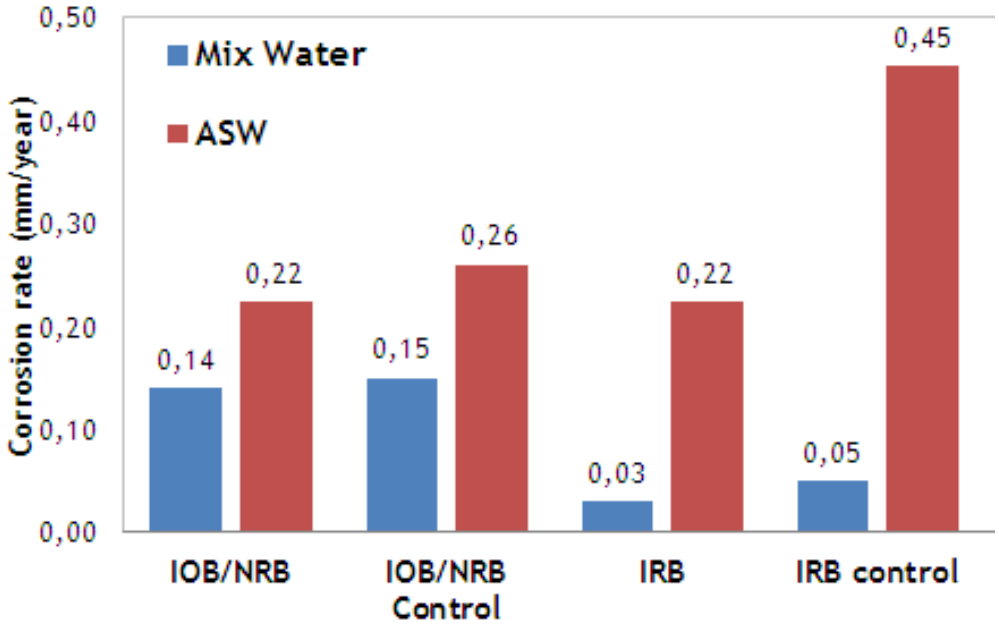


Fig. IV.10. Weight loss diagram in mm/year for carbon steel C1015 after 3 months of immersion in ASW and MIXED water medium: tests 27-36.

Once again with these tests it was observed less mass loss in all the systems with MIXED water medium than with ASW medium. The corrosion inhibitor used by the industrial partner seems to considerably reduce corrosion compare to ASW systems which do not have this inhibitor. Furthermore, it was observed higher corrosion rates in the control abiotic systems than in systems with bacteria. Corrosion rates in the control abiotic systems for IOB/NRB displayed similar rates regardless the medium. In contrast, there was a large difference on corrosion rates for IRB control systems with ASW, depicting 9 times more corrosion than with MIXED water. The corrosion difference of this last, is justified by the presence of the corrosion inhibitor in the MIXED water. By contrary, the fact of not finding this difference on corrosion rate between the IOB/NRB control systems is due to the presence of sodium nitrate added to the media which acted also as a corrosion inhibitor for the ASW control system.

The mechanisms that would explain why there is less corrosion in the biotic systems with presence of IRB and IOB/NRB enriched bacteria than in the control abiotic systems are still not well understood. Thus, further analysis would be needed in order to totally comprehend it. Nevertheless, these results with IRB can be partially related to results obtained in the first part of the project where it was also found generally lower corrosion rates in systems where the IRB *Geobacter sulfurreducens* was present.

On the other hand, in order to complete the results presented in article 3 and in supplementary results, XPS analysis were performed for some coupons (coupons from tests 17, 18, 21 and 22) extracted from weight loss experiments. For this, surface analyses were performed once the corrosion products and the biofilm that might have formed on the surface were cleaned off in order to observe the differences on the inner oxide layer.

Table IV.10 shows the peak parameters of all the chemical species for different elements used in this study: (A) test 17, (B) test 21, (C) test 18 and (D) test 22. Moreover, table IV.11 shows the composition (as relative percentages) of the two main elements of interest, Fe and S, found on the surface layer for each of the samples.

XPS results show that in both ASW and Mixed water biotic systems, the carbon (C $2p_{3/2}$) core level spectrum exhibits 3 peaks (Fig. IV.10 (A and C)tables) : One located at 285.08 eV attributed to C-C, another one with a binding energy located at 286.9 eV attributed to C-O and a last peak at 288.8 eV attributed to C=O. In contrast, differences are found in the oxygen and sulfur peaks between ASW and MIXED water systems (O $2p_{3/2}$ and S $2p_{3/2,}$ respectively)$_;$ these differences are: for the oxygen core level, one peak out of the three found in the two systems is depicted at a different binding energy (532.19 eV). For MIXED water the peak was attributed to $SO_4^{2-}$ and for ASW the peak at 533.4 eV was attributed to $(C=O)/H_2O$. For the case of the sulphur core level: two peaks are depicted in the Mixed water system whereas three peaks are depicted for the ASW system. The extra peak found in ASW and not found in Mixed water system is located at 164.07 and is attributed to $S^\circ$.

Additionally, results suggest that due to the absence of a peak indicating the detection of $Fe^{\circ}$(metal iron), the oxide layer formed on the surface of all the coupons have a thickness superior to 10 nm thick. Furthermore, these results confirm that there is formation of higher quantities of sulphide in ASW: there is nearly 15 times more sulphide in biotic ASW than in biotic Mixed water (table IV.11).

Regarding the iron, it is found higher quantities of iron compounds in the surface of the biotic Mixed water coupon than in the rest of the coupons (table IV. 11), suggesting higher formation of iron oxides/hydroxides which remain at the surface and not precipitate into the reactor. This is probably due to lower vulnerability to dissolution of iron oxides/hydroxides on the surface of these coupons which remain on the surface protecting it against further corrosion whereas it is presumed that in coupons immersed in ASW there is higher dissolution of the oxide layer which precipitates as corrosion products in the bulk medium or it was easily removed by cleaning. These suggestions will support weight loss findings which indicate lower corrosion rates in Mixed water systems. At the same time, iron/oxygen ratios from table IV.10 suggest that there is higher concentration of iron oxides in the surface of the coupon immersed in the biotic MIXED water than in the rest of the coupons which are presumed to have instead higher concentrations of iron hydroxides. Moreover, iron only in the form of Fe (III) was found on the surface of all the coupons. It is believed that the process of removing the biofilm and corrosion products (by HCl + EDTA), oxidized all the iron of the surface layer. However, the iron peak found in the control coupon from ASW system (table IV.11, D) was depicted at a binding energy of 708 eV instead of 711 eV as all the others, suggesting the presence of $Fe_3C$ (cementite) instead of the iron oxide/hydroxides.

**A**

| Element (photo electron core level) | | Peak position[a] | Assignment | FWHM eV | At. % |
|---|---|---|---|---|---|
| Biotic Pig 1 MIXED | C1s | 285.08 | C-C | 1.56 | 23.1 |
| | C1s A | 286.90 | C-O | 1.56 | 4.8 |
| | C1s B | 288.80 | C=O | 1.3 | 4.6 |
| | Cl2p | 198.48 | | 0.56 | 0.2 |
| | O1s | 530.22 | $CaO/Fe_2O_3$ | 1.25 | 23.3 |
| | O1s A | 531.46 | $[CO_3]^{2-}/FeO(OH)$ | 1.25 | 11.8 |
| | O1s B | 532.19 | $SO_4^{2-}$ | 1.25 | 7.3 |
| | Fe2p | 711.24 | $Fe_2O_3/FeOOH$ | 3.44 | 22.7 |
| | N1s | 400.44 | | 1.36 | 2.0 |
| | S2p | 163.09 | FeS | 3.5 | 0.4 |
| | S2p A | 168.64 | $SO_4^{2-}$ | 3.5 | 0.3 |

**B**

| Element (photo electron core level) | | Peak position[a] | Assignment | FWHM eV | At. % |
|---|---|---|---|---|---|
| Control Pig 1 MIXED | C1s | 285.33 | C-C | 1.55 | 21.2 |
| | C1s A | 287.01 | C=O | 1.62 | 4.4 |
| | C1s B | 289.28 | O-C=O | 1.4 | 3.3 |
| | C1s C | 288.36 | C=O | 0.48 | 0.4 |
| | C1s D | 283.16 | $Fe_3C$ | 0.44 | 0.2 |
| | Cl2p | 198.76 | | 1.14 | 0.8 |
| | Fe2p | 711.14 | $Fe_2O_3/FeOOH$ | 3.28 | 9.2 |
| | N1s | 400.45 | | 2.27 | 1.6 |
| | O1s | 530.37 | $CaO/Fe_2O_3$ | 1.23 | 30.5 |
| | O1s A | 531.86 | $[CO_3]^{2-}/FeO(OH)$ | 1.48 | 24.7 |
| | O1s B | 533.22 | $(C=O)/H_2O$ | 1.3 | 2.5 |
| | S2p | 163.23 | FeS | 3.5 | 0.5 |
| | S2p A | 169.40 | $SO_4^{2-}$ | 3.5 | 0.6 |

**C**

| | Element (photo electron core level) | Peak position[a] | Assignment | FWHM eV | At. % |
|---|---|---|---|---|---|
| Biotic Pig 1 ASW | C1s | 285.29 | C-C | 1.46 | 20.9 |
| | C1s A | 286.73 | C-O | 1.46 | 10.3 |
| | C1s B | 288.65 | C=O | 1.46 | 8.2 |
| | Cl2p | 198.66 | | 0 | 0.2 |
| | Fe2p | 711.21 | $Fe_2O_3$/FeOOH | 3.65 | 10.6 |
| | N1s | 400.51 | | 1.39 | 6.6 |
| | O1s | 531.85 | $[CO_3]^{2-}$/FeO(OH) | 1.68 | 22.8 |
| | O1s A | 530.24 | $CaO/Fe_2O_3$ | 1.23 | 13.8 |
| | O1s B | 533.4 | $(C=O)/H_2O$ | 1.58 | 2.6 |
| | S2p | 164.07 | S° | 2.06 | 1.8 |
| | S2p A | 162.12 | FeS | 2.06 | 1.5 |
| | S2p B | 168.58 | $SO_4^{2-}$ | 2.06 | 0.8 |

**D**

| | Element (photo electron core level) | Peak position[a] | Assignment | FWHM eV | At. % |
|---|---|---|---|---|---|
| Control Pig 1 ASW | C1s | 282.49 | Ca2C | 1.57 | 24.3 |
| | C1s A | 284.22 | $Fe_3C$ | 1.57 | 5.3 |
| | C1s B | 286.23 | C-O | 1.57 | 4.1 |
| | Cl2p | 195.92 | | 1.02 | 0.6 |
| | Fe2p | 708.35 | $Fe_3C$ | 3.53 | 10.0 |
| | O1s | 527.48 | | 1.32 | 29.4 |
| | O1s A | 528.94 | FeO | 1.34 | 22.3 |
| | O1s B | 530.24 | $CaO/Fe_2O_3$ | 1.14 | 2.3 |
| | N1s | 397.35 | | 1.38 | 0.9 |
| | S2p | 160.37 | FeS | 3.5 | 0.4 |
| | S2p A | 166.34 | $SO_2^{3-}$ | 3.5 | 0.4 |

Table IV.10. The peak parameters of chemical species for different elements used in this study: (A) test 17, (B) test 21, (C) test 18 and (D) test 22. [a]binding energy.

| Sample | Test | Fe total (%) | S/Fe total (%) | $S^{=}$/Fe (total) (%) | $SO_X$/Fe (total) (%) | $SO_4^{2-}$/Fe (total) (%) | Fe (III) (%) | Fe (II) (%) |
|---|---|---|---|---|---|---|---|---|
| Biotic Pig1 Mix | 17 | 22,7 | 2,2 | 1,1 | 0 | 1,4 | 100 | 0 |
| Control Pig1 Mix | 21 | 9,2 | 12,0 | 5,9 | 0 | 6,1 | 100 | 0 |
| Biotic Pig1 ASW | 18 | 10,6 | 32,2 | 17,4 | 14,0 | 7,8 | 100 | 0 |
| Control Pig1 ASW | 22 | 10,0 | 8,8 | 4,5 | 0 | 4,3 | 100 | 0 |

Table IV.11. Relative elemental composition of the surface layer

## IV.6. Conclusions

The main conclusions that can be extracted from this part of the project are: firstly, ASW is the most aggressive system of the two tested. This suggestion is supported by the higher corrosion rates found in the weight loss tests and by the big resistances observed for Mixed water in the EIS results, displayed in article 3. The high resistance observed in MIXED water medium must be due to the presence of corrosion inhibitor and organic acids (hydrocarbons) present in the production pipeline where this water has been recycled from. This was evident in weight loss tests when observing little or non-corrosion especially in the control abiotic Mixed water systems.

In what it concerns the bacterial diversity of the pigging samples, it can be said that thanks to the enrichments grow results, pig 1 is the debris sample which has the larger bacterial diversity obtaining more positive growths detected in the different enrichment media. These results are reflected in the weight loss results where it was found that this bacterial source was the most aggressive one of the 3 tested for the corrosion of carbon steel; this is presumed since knowing that most of the 16 S rRNA gene sequences identified corresponded to sulphide producers bacteria which due to the sulphide production are considered to be a threat to the corrosion of carbon steel. Moreover when pig 1 was pre-grown in ASW supplemented with acetate and fumarate, it was found the highest corrosion rate out of the 6 bacterial sources tested. It is believed that this pre-grown culture had concentrated sulfidogenic bacteria which accelerated the corrosion of carbon steel in the weight loss tests. At the same time, XPS results confirmed that there is formation of a higher quantity of sulphide in biotic ASW system than in biotic Mixed water system, confirming that the corrosion inhibitor added to the water injection system and present in the Mixed water, inhibits the growth of sulfidogenic bacteria.

On the other hand, 16S rRNA gene diversity results exposed in article 3 suggested that bacterial diversity gets decreased when culturing the debris in the media used for the electrochemical tests, especially in Mixed water medium. Sequencing genes detected implied that the only bacteria growing in these media and influencing the electrochemical results are: sulfidogenic bacteria such as SRB and bacteria from the genus *Clostridium* for the case of ASW and only SRB for the case of Mixed water.

Finally, concerning the results with the enriched IRB and IOB/NRB it can be concluded that these bacterial group do not exert much influence on the corrosion of carbon steel after observing higher corrosion rates in the control abiotic systems than when these bacteria was present. However, the mechanisms that would explain why there is less corrosion in the biotic systems with presence of IRB and IOB/NRB enriched bacteria than in the control abiotic systems are still not well understood. Yet, these results with IRB can be partially related to results obtained in the first part of the project where it was also found generally lower corrosion rates in systems where the IRB *Geobacter sulfurreducens* was present.

# *Chapter V-General conclusions & recommendations*

**General Conclusion**

Nowadays, it is more and more recognised the involvement of other bacterial groups different to SRB, playing a key role in corrosion. Few studies, including this one, provide an insight on anaerobic corrosion of carbon steel caused by other mechanisms different to those described with SRB. The main objective of this thesis was to develop new experimental models that may reproduce biocorrosion "in lab" on carbon steel using samples and environmental conditions found in pipelines of water injection systems of the oil and gas industry. The new experimental models applied during this study aimed to obtain new insights to understand biocorrosion mechanisms that could be extrapolated to the field mechanisms. To achieve this, the study has been divided into two approaches; the first approach consisted on investigating the involvement of a model iron reducing bacterium using *an electroactive strain, G. sulfurreducens* in order to assess its influence on the corrosion of carbon steel. The second approach *consisted* on using biofilm from the field to study its influence on the anaerobic corrosion of carbon steel under laboratory conditions but simulating some of those found in the field. This second part of the project aimed to assess the corrosivity of field biofilm and to confirm whether only SRB bacteria are involved in the corrosion process or if by contrary, other bacterial groups such as IRB might be involved.

Concerning the experimental works performed towards the first approach, they have brought insights to the study about the influence of *G. sulfurreducens* on the anaerobic corrosion of carbon steel using a medium with different compounds composition, assessing: acetate (electron donor), fumarate (electron acceptor), phosphate and ammonium. The most important conclusion that was obtained is that corrosion and the influence of the IRB *Geobacter sulfurreducens* are highly dependent on the medium composition. However, it seems that for most of the different conditions tested, *G. sulfurreducens* tends to protect the metal or to not accelerate the corrosion process by, for example, inducing the formation of a protective vivianite layer or by restraining corrosion rate in cases of accelerated corrosion as observed in the example of weak acids ($NH_4^+$).
Concretely, the presence of *Geobacter sulfurreducens* in phosphate medium induces the formation of a compact layer of iron (II) phosphate (vivianite) on the surface of carbon steel C1145 immersed in a medium containing 1 mM of acetate, 10 mM of fumarate and 5 mM of sodium phosphate. The hypothesis of the protection to corrosion thanks to the vivianite layer catalysed by the bacteria presence was supported by impedance, Rp and weight loss measurements results which showed that in presence of bacteria the corrosion resistance increases along time (in terms of $R_p$, $R_{ct}$ and corrosion rate, respectively). Moreover, this layer maintains the stability of the open circuit potential even after air is allowed to enter into the system so that, it prevents an acceleration of the cathodic reaction rate. In contrast, the iron phosphate layer was not formed in the control systems in absence of bacteria which allowed an increment of the open circuit potential of 400-450 mV once oxygen entered.

Furthermore, it can be concluded that presence and/or absence of the electron donor and acceptor play also a key role in the corrosion of carbon steel. For instance, the acetate (electron donor) concentration influences corrosion of carbon steel. When the acetate concentration increases it is observed higher anodic

currents in the voltammetry experiments, therefore higher corrosion. Additionally, experiments in absence of fumarate (electron acceptor) led us to understand that the formation of a vivianite layer was possible also in abiotic conditions but with longer immersion times. These experiments were performed for more than 200 hours which was about 50 hours longer than experiments described in article 1. Oxidation of iron in anaerobic conditions is a slow process which derives in the formation of Fe III and Fe II species which in presence of phosphate will end up to bond forming vivianite. In contrast, IRB induces a faster and higher concentration of Fe (II) ions which bond to phosphate consequently forming in shorter time vivianite, as described in article 1. However the main difference between vivianite layers found in absence of fumarate and the one described in article 1 is that, in the system without fumarate the vivianite layer is thicker and damaged, possibly inducing a cell galvanic effect. This may be explained by the fact that in absence of fumarate, the bacteria start reducing the iron (III) sooner and with a higher reaction rate than when a soluble electron acceptor is present.

In contrast, when performing experiments in absence of phosphate, it became evident the influence of $NH_4^+$ which was present in the medium, as a weak acid. Impedance and weight loss measurements suggested that when phosphate is not present into the medium, the charge transfer reactions and the corrosion rate, respectively, are much higher than when phosphate is present, suggesting that the $NH_4^+$ accelerates corrosion due to its behaviour as weak acid which will undergo a reversible mechanism of electrochemical deprotonation that may be accelerated by hydrogen removal, inducing an acceleration of the cathodic reaction and thus of the corrosion. Additionally, when comparing the abiotic and biotic systems without phosphate, it was found lower corrosion when bacteria were present. For instance, dissolved iron was in average 4.6 times higher in absence of bacteria than in presence of it. These results together with the whole set of results suggest that the IRB *Geobacter sulfurreducens* reduces corrosion in medium without phosphate, even though a vivanite protective layer was not formed as shown in article 1. However, the mechanisms linked to the corrosion limitation effects of the bacteria are still uncertain but a cathodic protection thanks to the electroactivity of the bacteria can be suggested.

On the other hand, concerning the experimental works performed towards the second approach, the influence of different media, either ASW or MIXED water from the field on the corrosion of carbon steel was studied. Additionally, it was observed the 16S rRNA gene sequencing and identification of the biofilm community contained in the pigging debris and the influence of these bacteria on the corrosion of carbon steel. Finally, insights on the influence of bacteria groups such as IRB and IOB/NRB enriched from the pigging debris, on the corrosion of carbon steel were acknowledged.

The first conclusion highlighted from the study, was that the ASW medium is the most aggressive of the two media tested in terms of corrosion. This asseveration is supported by the impedance and weight loss measurements which showed that the Mixed water system displays higher resistances (120 times higher $R_p$ in Mixed water than in ASW) and lower corrosion rates than ASW. The high resistances observed in MIXED water medium must be due to the presence of corrosion inhibitor and organic acids (hydrocarbons) in the production pipeline where this water has been

recycled from. At the same time, XPS results confirmed that there is formation of a higher quantity of sulphide in biotic ASW system than in biotic Mixed water system, confirming that the corrosion inhibitor added to the water injection system and present in the Mixed water, inhibits the growth of sulfidogenic bacteria.
Furthermore, with respect to the influence on corrosion of the bacterial consortium contained in the pigging debris, it was concluded that its presence accelerated corrosion in both systems: ASW and Mixed water systems. The corrosion potential (OCP) measured in function of time showed a sudden increase of more than +400 mV vs Ag/AgCl in both media tested when the system was exposed to the biotic pigging debris whereas no jump was observed in the control abiotic systems where the debris was autoclaved. The increment in OCP or corrosion potential indicates that there is higher corrosion risk with an incremented probability for pitting and crevice corrosion which in this case has been enhanced by the presence of microorganisms in the system. Furthermore, EIS results show that in presence of microorganisms, FeS is the species that governs the characteristics of the interface (both, when is governed by mass transfer in ASW and when is governed by charge transfer in MIXED). By contrary, in the cases of the control systems, it is rather the iron oxides of the type $Fe(OH)_2$ or $FeO*Fe_2O_3$ characterising the interface with variations in the quality of the iron oxides/hydroxides protection.

On the other hand, for what it concerns the DGGE analysis performed in the enrichments the most abundant 16S rRNA gene sequence detected in the enrichments analysed (20%) was that similar to *Thermovirga lienii*. After this last, sequences similar to those of bacteria from the genera *Clostridium* was the most frequently detected, finding it 16% of the times of the total bacteria identified. Moreover, sequences similar to the genera *Desulfovibrio* and the genera *Dethiosulfovibrio* were also abundantly detected, finding them in around 15% each of the total bacteria detected. Thus, it can be concluded that most of the 16S rRNA gene sequences identified corresponded to sequences of sulfidogenic bacteria which due to the sulphide production are considered to be a threat to the corrosion of carbon steel. However, these sulfidogenic bacteria, in its majority, do not belong to the widely studied SRB group, thus, implying that SRB are the main responsible for corrosion in the systems of this oil company might be an overstated mistake which could lead to errors in the monitoring and mitigations decisions taken when biocorrosion is observed. Additionally, it can be concluded that these analyses did not allow detecting the complete diversity communities of microorganisms inherent of the water injection system. Moreover, it has been concluded that bacterial diversity gets decreased when culturing the debris in the media used for the electrochemical tests. Sequencing genes detected implied that the only bacteria growing in these media and influencing the electrochemical results are: sulfidogenic bacteria such as SRB and bacteria from the genus *Clostridium* for the case of ASW and only SRB for the case of Mixed water.

Finally, concerning the results with the enriched IRB and IOB/NRB it can be concluded that these bacterial group do not exert much influence on the corrosion of carbon steel after observing higher corrosion rates in the control abiotic systems than when these bacteria was present. However, the mechanisms that would explain why there is less corrosion in the biotic systems with presence of IRB and IOB/NRB enriched bacteria than in the control abiotic systems are still not well

understood. Yet, these results with IRB can be partially related to results obtained in the first part of the project where it was also found generally lower corrosion rates in systems where the IRB *Geobacter sulfurreducens* was present.

**Recommendations**

As time limitations did not allow producing further results that could lead to further and deeper conclusions during this thesis, few experiment recommendations have been formulated which could lead to complement and/or better conclude the set of results presented here. The following recommendations are:

- It is recommended to perform more extensive experiments about the influence of other weak acids that are likely produced by microorganisms found in the water injection system.

- It is recommended to perform XPS analysis for experiments from the first approach to more accurately relate the EIS results to corration rate.

- It is recommended to perform electrochemical and corrosion experiments with ASW but adding also the corrosion inhibitor utilised by the industry in order to have larger parameters of comparison.

- It is recommended to perform analysis that will clarify the microbial sulphate reduction activity of the community found in the water injection pipeline bearing in mind that the sulphide production is not led by SRB. This might be of vital importance during the decision making process of the industrial partners.

- It is recommended to the industry to adopt more standardise ways of sampling due to the importance of this step for future studies.

- It is recommended to contunie experimenting with IRB in more accuraltely field conditions and higher scale to elucidate whether in these conditions IRB is still able to protect the steel.

# *Bibliographic references*

*A*

H. Abdollahi, J.W.T. Wimpenny, **Effects of oxygen on the growth of *Desulfovibrio desulfuricans***. *J. Gen. Microbiol.*, 136(1990): 1025-1030

L. Abildgaard, M. B. Nielsen, K. U. Kjeldsen, K. Ingvorsen, **Desulfovibrio alkalitolerans sp. nov., a novel alkalitolerant, sulphate reducing bacterium isolated from heating district water**, *Int. J. Syst. Evol. Microbiol.*, 56(2006): 1019-1024

A. Al-Hashem, J. Carew, A. Al-Borno, **Screening test for six dual biocides regimes against planktonic and sessile population of bacteria**, *Nace Int. Corros.* (2004), Paper No. 04748

J. W. Arnold, G. W. Bailey, **Surface Finishes on Stainless Steel Reduce Bacterial Attachment and Early Biofilm Formation: Scanning Electron and Atomic Force Microscopy Study**, *Poultry Sci.*, 79(2000):1839-1845

*B*

F. Back, H. A. Cypionka, **Novel type of energy metabolism involving fermentation of inorganic sulfur compounds**. *Nature*, 326(1987): 891-892

A. J. Bard, L. R. Faulkner, **Electrochemical methods: Fundamentals and applications**, John Wiley and Sons, Inc. Eds., second edition, In *Introduction and overview of electrode processes*, Chapter 1, (2001).

L. L. Barton, W. A. Hamilton, **Sulfate-Reducing Bacteria**, Larry L. Barton and W. Allan Hamilton Eds., In *Environmental and Engineered systems*, Cambridge University Press, 2007

I. B. Beech, V. Zinkevich, R. Tapper, R. Gubner, **Direct involvement of an extracellular complex produced by a marine sulphate-reducing bacterium in deterioration of steel**, *Geomicrobiol. J.*, 15 (1998):119-132

I. Beech, C. C. Gaylarde, **Recent advances in the study of biocorrosión: an overview**, *Revista de Microbiología*, 30 (1999). 177-190, ISSN 0001-3714.

I. Beech, A. Bergel, A. Mollica, H-C. Flemming, V. Scotto, W. Sand, **Simple methods for the investigation of the role of biofilms in corrosion**. *On-line:* Brite-Euram III Thematic Network No. ERB BRRT-CT98-5084 (2000)

I. B. Beech, *Sulfate reducing bacteria in biofilms on metallic materials and corrosion*, *Microbiolog. Today.*, 30(2003): 115-117

I. B. Beech, J. A. sunner, **Biocorrosion: towards understanding interactions between biofilms and metals**. *Curr. Opinion Biotechnol.* 15(2004):181-186

I. B. Beech, J. A. Sunner, K. Hiraoaka, **Microbe–surface interactions in biofouling and biocorrosion processes**, *Intern. Microbiol.*, 8(2005): 157-168

D.R. Bond, D.R. Lovley, **Electricity production by *Geobacter sulfurreducens* attached to electrodes**, *Appl. Environ. Microbiol*. 69 (2003) 1548–1555.

B. Bubar, **Pipeline pigging and inspection**, in: E. S. Menon, *Pipeline planning and construction field*, Elsevier Inc, (2011): 313-339

J. P. Busalmen, M. Vázquez, S. R.de Sánchez, **New evidences on the catalase mechanism of microbial corrosion**. *Electrochim Acta,* 47(2002):1857-1865

J. P. Busalmen, M. Vázquez, S. R.de Sánchez, **Electrochemical Polarization-Induced Changes in the Growth of Individual Cells and Biofilms of *Pseudomonas fluorescens* (ATCC 17552)**, *App. Environ. Microbiol.*, 71(2005):6235-6240

N. Brisbarre, M-L. Fardeau, V. Cueff, J-L. Cayol, G. Barbier, V. Cilia, G. Ravot, P. Thomas, J-L. Garcia, B. Ollivier, **Clostridium caminithermale sp. nov., a slightly halophilic and moderately thermophilic bacterium isolated from an Atlantic deep-sea hydrothermal chimney**, *Int. J. Syst. Evol. Microbiol.,* 53(2003):1043–1049

G.J. Brug, A.L.G. van den Eeden, M. Sluyters-Rehbach, J.H. Sluyters, **The analysis of electrode impedances complicated by the presence of a constant phase element**, *J. Electroanal. Chem*. 176 (1984) 275–295
H. G. Byars, **Corrosion Control in Petroleum Production**, Chapter 2, TPC Publications 5, second edition, *NACE int. Corros.* (1999)

*C*

F. Caccavo, D. J. Lonergan, D. R. Lovley, M. Davis, J. F. Stolz, and M. J. Mclnerney, ***Geobacter sulfurreducens* sp. nov., a hydrogen- and acetate-oxidizing dissimilatory metal-reducing microorganism**. *Appl. Environ. Microbiol.*, 60(1994): 3752-3759.

X.Campaignolle, **Etude des facteurs de risque de la corrosion bactérienne des aciers au carbone induite par les bactéries anaérobies sulfurogènes**, *PhD Thesis,* Institut National Polytechnique de Toulouse (1996).

J. L . Cayol, B. Ollivier, B. K. Patel, G. Ravot, M. Magot, E. Ageron, P. A. Grimont, J. L. Garcia, **Description of *Thermoanaerobacter brockii* subsp. lactiethylicus subsp. nov., isolated from a deep subsurface French oil well, a proposal to reclassify *Thermoanaerobacter finnii* as *Thermoanaerobacter brockii* subsp. finnii comb. nov., and an emended description of *Thermoanaerobacter brockii***., *Int. J. Syst. Bacteriol.*, 45,4(1995):783-9.

I. G. Chamritski, G. R. Burns, B. J. Webster, N. J. Laycock, **Effect of iron-oxidizing bacteria on pitting of stainless steels**. *CORROS.* 60(2004) (7)

B. E. Christensen, W. G. Characklis, **Physical properties of biofilms**. In *Biofilms*. W. G. Characklis & K. C. Marshall Eds. New York. (1990):93-*130*

S. E. Coester, T. E. Cloete, **Biofouling and Biocorrosion in Industrial Water Systems**, *Critical Rev. Microbiol.*, 31(2005):213-232

C. Cote, O. Rosas-Camacho, R. Basseguy, ***Geobacter sulfurreducens:* An Iron Reducing Bacterium that Can Protect Carbon Steel Against Corrosion**?, "*Unpublished results*": Manuscript submitted for publication, (2013)

C. Cote, O. Rosas-Camacho, M. Sztyler, J. Doma, I. Beech, R. Basseguy, **Corrosion of Low Carbon Steel by Microorganisms from the 'Pigging' Operations Debris in Water Injection Pipelines**, *Unpublished results*: article submitted in December 2012 to Bioelectrochemistry Journal (revision in process)

J.-L. Crolet, and M.F. Magot, **Non-SRB sulfidogenic bacteria in oilfield production facilities**, *Mater. Perform.* 35 (1996) 60-64.

M. Critchley, R. Javaherdashti, **Materials, micro-organisms and microbial corrosion -A review**. *Corrosion and Materials* 30(3) (2005):8–11

S. Chongdar, G. Gunasekaran, P. Kummar, **Corrosion inhibition of mild steel by aerobic biofilm**, *Electrochem. Acta.* 50(2005) 4655-4665.

*D*

L. Daniels, N. Belay, B. Rajagopal, P. Weimer, **Bacterial Methanogenesis and Growth from $CO_2$ with elemental iron as the sole source of electrons,** *Science,* 237(1987):509-511

S. Da Silva, R. Basseguy, A. Bergel, **The role of hydrogenases in the anaerobic microbiologically influenced corrosion of steels**, *Bioelectrochem.*, 56(2002):77-79

S. Da Silva, R. Basseguy, A. Bergel, **Hydrogenase-catalysed deposition of vivianite on mild steel**, *Electrochem. Acta.* 49 (2004) 2097-2103

H. Dahle, N-K. Birkeland, ***Thermovirga lienii* gen. nov., sp. nov., a novel moderately thermophilic, anaerobic, amino-acid-degrading bacterium isolated from a North Sea oil well**, *Int. J. Sys. Evol. Microbiol.* 56 (2006): 1539–1545

M. Davey, W. A. Wood, R. Key, K. Nakamura, D. A. Stahl, **Isolation of Three Species of *Geotoga* and *Petrotoga*: Two New Genera, Representing a New Lineage in the Bacterial Line of Descent Distantly Related to the "*Thermotogales*"**, *Syst. Appl. Microbiol.*, 16(1993): 191–200

L. De Silva Munoz, **Des aspects positifs issus des recherches en biocorrosion : de la production d'hydrogène aux biopiles à combustible**, *PhD Thesis*, Ecole Mécanique, Energétique, Génie civil & Procédés, Université de Toulouse, (2007).

L. De Silva Munoz, Alain Bergel, Regine Basseguy, **Role of the reversible electrochemical deprotonation of phosphate species in anaerobic biocorrosion of steels**, *Corr. Sci*. 49(2007): 3988-4004

L. De Silva Munoz, Alain Bergel,Demien Ferron, Regine Basseguy, **Hydrogen production by electrolysis of a phosphate solution on a stainless steel cathode**, Int. J. Hydrogen Energ., (2010):8561-8568

L. De Silva Munoz, C. Cote, O. Rosas, A. Bergel, Regine Basseguy, **Weak acids as catalysts of the cathodic reaction in anaerobic biocorrosion of steels**, accepted *abstract Eurocorr* 2011.

Deutsche Sammlung von Mikroorganismen und Zellkulturen DSMZ GmbH, Microorganisms, 826. Geobacter medium, 2007

H. Dinh, J. Kuever, M. Mubmann, A. W. Hassel, M. Stradman, F. Widdel, **Iron corrosion by novel anaerobic microorganisms**, *Nature*., 427(2004) 829-832

Y.-H.R. Ding, K.K. Hixson, C.S. Giometti, A. Stanley, A. Esteve-Nunez, T. Khare, S.L. Tollaksen, W. Zhu, J.N. Adkins, M.S. Lipton, R.D. Smith, T. Mester, D.R. Lovley, **The proteome of dissimilatory metal-reducing microorganism *Geobacter sulfurreducens* under various growth conditions**, *Biochim. Biophys. Acta* 1764 (2006) 1198–1206

X. Dominguez Benetton, **Biocomplexity and electrochemical influence of biofilms in carbon steel deterioration in gasoline-containing environments**, *PhD Thesis*, Instituto Mexicano del Petroleo (2007), D.F., Mexico.

J. Duan, S. Wu, X. Zhang, G. Huang, M. Du, B. Hou, **Corrosion of carbon steel influenced by anaerobic biofilm in natural seawater**, *Electrochem. Acta*, 54(2008) 22-28

M. Dubiel, C. H. Hsu, C. C. Chien, F. Mansfeld, D. K. Newman, **Microbial iron respiration can protect steel from corrosion**, *Appl. Environ. Microbiol*. 68(2002) 1440-1445

C. Dumas, **Catalyse électro-microbienne dans les piles à combustible**, *Thèse de doctorat*. Laboratoire de Génie Chimique, 2007. Toulouse, France.

C. Dumas, R. Basseguy, A. Bergel, **DSA to grow electrochemically active biofilms of *Geobacter sulfurreducens***, *Electrochim. Acta* 53 (2008a) 3200–3209.

C. Dumas, R. Basseguy, A. Bergel, **Electrochemical activity of *Geobacter sulfurreducens* biofilms on stainless steel anodes**, *Electrochim. Acta* 53 (2008b) 5235–5241.

K. Duncan, L. Gieg, V. Parisi, R. Tanner, T. S. Green, J. Bristow, J. Suflita, **Biocorrosive thermophilic microbial communities in Alaskan North Slope Oil facilities**, *Environ. Sci. Technology*, 43(2009): 7977-7984

*E*

EC-Lab Software: Techniques and Applications, Version 9.4x, Bio-logic (2007), France

R. G. J. Edyvean, J. Benson, C.J. Thomas, I. B. Beech, H. Videla, **Biological influences on hydrogen effects in steel in seawater**. *Mat. Perform.*, 37: 40-44, 1998

B. Elsener, **Corrosion rate of steel in concrete-Measurements beyond the Tafel law**, *Corr. Sci.* 47 (2005):3019-3033

D. Emerson, V. J. Weiss, J. P. Megonigal, **Iron Oxidizing bacteria are associates with ferric hydroxide precipitates (Fe-Plaques) on the roots of wetland plants**, *Appl. Environ. Microbiol.*, 65(1999):2758-2761

M. Eashwar, S. Maruthamuthu, **Mechanism of biologically produced ennoblement -Ecological perspectives and a hypothetical model**, *Biofouling* 8(1995): 303-312

M. Eashwar, S. Maruthamuthu, S. Sathiyanarayanan, S. Balarkrishnan, **The ennoblement of stainless alloys by marine biofilms -The neutral pH and passivity enhancement model**-, *Corr. Scienc.* 37(1995):1169-1176

L. Esnault**, Réactivité géomicrobiologique des matériaux et minéraux ferrifères : impact sur la sureté d'un stockage de déchets radioactifs en milieux argileux,** *Thesis Université de Nancy,* 2010

L. V. Evans, **Recent Advances in their Study and Control,** in *Biofilms*. CRC Press Eds., ISBN 90-5823-093-7, (2000):1-57.

*F*

H. C. Flemming, **Biofuling and Microbilogically Influenced Corrosion (MIC) an Economical and Technical Overview**. E. Heitz, H-C Flemming, W. Sand (Eds.), Springer, Heidelberg (1996)

H-C Flemming, U. Szewzyk, T. Griebe, **Investigative methods & applications** in *Biofilms*, 2000

I. Frateur, H. Perrot, V. Vivier, B. Tribollet, P. Rousseau, F. Huet, **Mesure d'impedance appliquée à l'electrochimie** Niveau 2, Electrochemical Impedance cours, *LISE-UPMC*, Sorbonne Universités, Paris, France (2012)

*G*

C. Gabrielli, **Identification of electrochemical processes by frequency response analysis**, *Solartron*, Technical report number 004/83. (1998).

Y. Gourbeyre, E. Guilminot, F. Dalard, **Study of the corrosion layer on iron obtained in solutions of water-polyethilene glycol (PEG400)- Sodium phosphate**, *J. Mater. Sci.* 38 (2003)1307-1313

C. A. Gonzalez-Rodriguez, F. J. Rodriguez-Gomez, J. Genesca-Llongueras, **The influence of *Desulfovibrio vulgaris* on the efficiency of imidazoline as a corrosion inhibitor on low carbon steel in seawater**, *Electrochem. Acta.* 54(2008): 86-90

B. Guo, S. Song, J Chacko, A. Ghalmbur, *Offshore pipelines*, Elsevier Inc (2005) 215-233

J. Goldstein, *Scanning Electron-Microscopy and X-ray Microanalysis*, Springer, ISBN 978-0-306-47292-3, London 2003

*H*

W. A. Hamilton, **Sulphate reducing bacteria and anaerobic corrosion**, *Ann. Rev. Microbiol.* 39(1985): 195-217

W. A. Hamilton, **Microbially influenced corrosion as a model system for the study of metal microbe interactions: a unifying electron transfer hypothesis**. *Biofouling*, 19(2003):65-76

D. T. Hang, **Microbiological study of the anaerobic corrosion of iron**, *PhD. Thesis,* Universität Bremen vorgelegt von, Bremen, Germany, 2003

D. C. Hansen, A. Alfantazi, V. J. Gelling, **Corrosion** (General), 217th *ECS Meeting,* ECS transactions, 28(2010):77-94

P. A. Jr. Harrison, **The acidophilic *Thiobacilli* and other acidophilic bacteria that share their habitat**, *Ann. Rev.Microbiol.* 38 (1984) 265-292

J. J. Harrison, R. Turner, L. L. Marques, H. Ceri, **Biofilms, A new understanding of these microbial communities is driving a revolution that may transform the science of microbiology**, *American Scientist*, 93(2005):508.

H. M. Herro, R. D. Port, *Nalco Guide to Cooling Water System Failure Analysis*; McGraw-Hill, Inc.: New York. (1993)

B. Hirschorn, M. E. Orazem, B, Tribollet, V. Vivier, I. Frateur, M. Musiani, **Constant-Phase element behavior caused by resistivity distribution in films**, *J. Electrochem. Soc.* 157(2010):C458-C463

L. K. Herrera, H. Videla, **Role of iron-reducing bacteria in corrosion and protection of carbon steel**, *Intern. Biodeterior. Biodegrad.* 63(2009) 891-895

*I*

W.P. Iverson, G.J. Olson, L.F. Herverly, **The role of phosphorus and hydrogen**

**sulphide in the anaerobic corrosion of iron and the possible detection of this corrosion by an electrochemical noise technique.** In *Biologically Induced Corrosion*. S.C. Dexter (Eds.) Houston, USA(1985).

F. S. Islam, R. L. Pederick, A. G. Gault, L. K. Adams, D. A. Polya, J. M. Charnock, J. R. Lloyd, **Interactions between the Fe (III)-Reducing bacterium *Geobacter sulfurreduscens* and Arsenate, and capture of the metalloid by biogenic Fe(II)**, *Appl. Environ. Microbio.* 71 (2005) 8642-8648

*J*

R. F. Jack, D.B. Ringelberg, D.C White, **Differential corrosion rates of carbon steel by combinations of *Bacillus* sp., *Hafnia alvei*, and *Desulfovibrio gigas* established by phospholipid analysis of electrode biofilm**. *Corr. Sci.*, 33 (1992) 1843-1853

J. Jana, A. K. Jain, S. K. Sahota, H. C. Dhawan, **Failure analysis of oil pipelines**, *Bull. Electrochem.*, 15(1999):262-265

J. Jan-Roblero, J. M. Romero, M. Amaya, S. Le Borgne, **Phylogenetic characterization of a corrosive consortium isolated from a sour gas pipeline**, *App. Microbiol. Biotechnol.*, 64(2004):862-867

R. Javaherdashti, *Microbially Influenced Corrosion – An Engineering insight-*, Springer (Eds), (2008), London

D. A. Jones, P. S. Amy, **A thermodynamic interpretation of microbiologically influenced,** *Corrosion*, 58(2002):638-645

J-B. Jorcin, M. E. Orazem, N. Pébère, B. Tribollet, **CPE analysis by local electrochemical impedance spectroscopy**, *Electrochem. Acta*, 51(2006):1473-1479

*K*

J. P. Kirkpatrick, L. V McIntire , W. G. Characklis, **Mass and heat transfer in a circular tube with biofouling**, *Water Res.*, 14(1980)117-127

G. Kobrin, **Corrosion by microbiological organisms in natural waters**. *Mat. Perform.*, 15(1976): 38-43

J.H. Koch, M.P.H. Brongers, N.G. Thompson, Y.P. Virmani, J.H. Payer. 2002. **Corrosion Cost and Preventive Strategies in the United States**. Federal Highway Administration, Washington, D.C. Report no. FHWA-RD-01-156.

L. J. Korb, *Metals handbook*, Ninth edition, Volume 13 (ASM Handbook), 1987

E. Korenblum, G. V. Sebastian, M. M. Paiva, C. M. L. M. Coutinho, F. C. M. Magalhaes, B. M. Peyton, L. Seldin, **Action of antimicrobial substances produced by different oil reservoir *Bacillus* strains against biofilm formation**, *App. Microb. Cell Physiol.* 79(2008): 97-103

*L*

J. S. Lee, R. I. Ray, E. J. Lemieux, A. U. Falster, B. J. Little, **An evaluation of carbon steel corrosion under stagnant seawater conditions**. *Biofouling* 20(2004):237-247

W. Lee, Z. Lewandowski, P. H. Nielsen, W. A. Hamilton, **Role of sulfate-reducing bacteria in corrosion of mild steel: A review.** *Biofouling*, 8(1995): 165-194.

M. Libert, O. Bildstein, L. Esnault, M. Jullien, R. Sellier, **Molecular hydrogen: An abundant energy source for bacterial activity in nuclear waste repositories,** *Physics and Chemistry of the earth,* 36 (2011) 1616–1623

B. Little, P. Wagner, F. Mansfeld, **Microbiollogically influenced corrosion of metals and alloys**, *Int. Materials Rev.* 36(1991):253-271

J. B. Little, R. Ray, **A perspective of corrosion inhibition by biofilms**, *Corrosion*, 58(2002): 424-428

J. B. Little, S. J. Lee, I. R. Ray, **The influence of marine biofilms on corrosion: A concise review**, *Electrochem. Acta,* 54(2008):2 – 7

Y. Londer, P. Pokkuluri, V. Orshonsky, N. Duke, and M. Schiffer, **Studies of multi-heme cytochromes from *Geobacter sulfurreducens***, *POSTER*, Biosciences Division, Argonne National Laboratory, Argonne, IL 60439 (2007)

M. A. Lopez, F. J. Zavala Diaz de la Serna, J. Jan-Roblero, J. M. Romero, C. Hernandez-Rodriguez, **Phylogenetic anaysis of a biofilm bacterial population in a water pipeline in the gulf of Mexico**, *FEMS Microbiol Ecol.* 58(2006):145-154

R. D. Lovely, J. P. E. Phillips, **Organic matter mineralization with the reduction of ferric iron in anaerobic sediments**, *Appl. Environ. Microbiol.*, 51(1986):683-689

R. D. Lovley, J. F. Stolz, G. L. Jr. Nord, and J. P. E. **Anaerobic production of magnetite by a dissimilatory iron-reducing microorganism**, *Nature*, 330(1987):252-254

R. D. Lovley, J. P. E. Phillips, **Competitive mechanisms for inhibition of sulfate reduction and methane production in the zone of ferric iron reduction in sediments**, *Appl. Environ. Microbiol.* 53(1987):2636-2641

R. D. Lovley, J. P. E. Phillips, **Novel mode of microbial energy metabolism: Organic carbon oxidation coupled to dissimilatory reduction of iron or manganese**, *Appl. Environ. Microbiol.*, 54(1988):1472-1480

R. D. Lovley, F. H. Chapelle, J. C. Woodward, **Use of dissolved $H_2$ concentrations to determine distribution of microbially catalized redox reactions in anoxic groundwater**, *Envrion. Sci. Technol.* 28(1994):1205-1210

D. Lovley, **Dissimilatory Fe (III) and Mn (IV) reducing prokaryotes**, *The Prokariotes,* Chapter 1.21(2006) 2:635-658

*M*

D. D. Macdonald, **Application of electrochemical impedance spectroscopy in electrochemistry and corrosion science**, *in Techniques for characterization of electrodes and electrochemical processes*, R. Varma and J. R. Selman (Eds.), John Wiley and Sons Inc., Chapter 11 (1991):515-580, ISBN 0-471-82499-2.

D. D. Macdonald, *Transient techniques in electrochemistry*, Plenum Publishing Corporation, ISBN: 0306310104 (1977).

M. Mackintosh, **Nitrogen fixation by *Thiobacillus ferrooxidants***, *J. Gener. Microbiol*. 105(1978):215-218

E. Malard, D. Kervadec, O. Gil, Y. Lefevre, S. Malard, **Interactions between stainless steel and sulphide producing bacteria –Corrosion or carbon steels and low-alloy steels in natural sea water-**,*Electrochem. Acta*, 54(2008):8-13

F. Mansfeld, B. Little, **A technical review of electrochemical techniques applied to Microbiologically Influenced Corrosion**, *Corr. Sci*, 32(1991):247-272

F. Mansfeld H. Hsu, D. Ornek, T. K. Wood, **Corrosion control using regenerative biofilms on Aluminium 2024 Brass in different media**, *J. Electrochem. Soc.* 149(2002) B130-B138

F. Mansfeld, **The interaction of bacteria in metal surfaces**, *Electrochem. Acta* 52 (2007) 7670-7680

F. Mars, *Corrosion Engineering*, McGraw-Hill Book Company 3a. Ed 1987

C. Marshall, P. Frenzel, H. Cypionka, **Influence of oxygen on sulphate reduction and growth of sulphate reducing bacteria**, *Arch. Microbial*. 159(1993): 168-173

M. W. Maune, R. S. Tanner, **Description of *Anaerobaculum hydrogeniformans* sp. nov., an anaerobe that produces hydrogen from glucose, and emended description of the genus Anaerobaculum**., *Int. J. Syst. Evol. Microbiol*. 2012 Apr;62(Pt 4):832-8

M. Mehanna, R. Basseguy, M-L Delia, L. Girbal, M. Demuez, A. Bergel, **New hypotheses for hydrogenase implication in the corrosion of mild steel**, *Electrochem. Acta*, 54(2008):140-147

M. Mehanna, **Mécanismes de transfert direct en corrosion microbienne des aciers: Application à *Geobacter sulfurreducens* et à l'hydrogénase de *Clostridium acetobutylicum***, *PhD Thesis*, Ecole Mécanique, Energétique, Génie civil & Procédés, Université de Toulouse, (2009)

M. Mehanna, R. Basseguy, M-L. Délia, A. Bergel, ***Geobacter sulfurreducens* can protect 304L stainless steel against pitting in conditions of low electron acceptor concentrations**. *Electroche. communications*, 12(2010):724-728

J. D. A. Miller, **Metals** *In Economic Micribiology,* A. H. Rose Eds., Academic Press, 6(1981): 150-202

M. N. Monfort, **Corrosion localisée des aciers au carbone induite par des bactéries sulfatoréductrices: développement d'un capteur spécifique**, *Thèse de Doctorat,* Université Paris VI, Spécialité: Electrochimie(2001).

M. Magot , G. Ravot , X. Campaignolle , B. Ollivier , B.K. Patel , M.L. Fardeau , P. Thomas , J.L. Crolet, J.L. Garcia, ***Dethiosulfovibrio peptidovorans* gen. nov., sp. nov., a new anaerobic, slightly halophilic, thiosulfate-reducing bacterium from corroding offshore oil wells**, *Int. J Syst. Bacteriol.* 47 (1997) 818-24.

G. Muyzer, E. De Wall, A. G. Uitierlinden, **Profiling of Complex Microbial Populations by Denaturing Gradient Gel Electrophoresis Analysis of Polymerase chain Reaction-Amplified Genes Coding for 16S rRNA**, *Appl. Environ. Microbiol.* 59(1993): 695-700

*N*

H. K. Nealson, **The manganese-oxidizing Bacteria**. *The Prokariotes,* Chapter 3 (2006) 5:222-231

H. C. Neu, **The crisis in antibiotic resistance**, *Science*, 257(1992):1064-1073

*O*

M. E. Orazem, N. Pébère, B. Tribollet, **Enhanced graphical representation of electrochemical impedance data**, *J. Electrochem. Soc.* 153(2006):B129-136

M. E. Orazem, B. Tribollet, **Electrochemical impedance spectroscopy**, *The electrochemical society series*, John Wiley & sons, Inc., publication, (2008)

M. E. Orazem, B. Tribollet, P. Pintauro, **Tutorials in electrochemical technology: Impedance spectroscopy**, *the electrochemical society*, 13(2008)

V.J. Orphan, L.T. Taylor, D. Hafenbradl, E.F. Delong, **Culture-dependent and culture-independent characterization of microbial assemblages associated with high-temperature petroleum reservoirs**, *Appl. Environ. Microbiol.* 66 (2000) 700-11.

C. O. Obuekwe, D. W. S. Westlake, J. A. Plambeck, F. D. Cook, **Corrosion of mild steel in cultures of ferric iron bacterium isolated from crude oil**, 37(1981):461-637

*P*

F.N. Ponnamperuma, **The chemistry of submerged soils,** *advances in agronomy*, 24(1972):29-88

D. H. Pope, **Microbial corrosion in fossil-fired power plants** –a study of microbiologically influenced corrosion and a practical guide for its treatment and prevention-, Electric Power Research Instiute, Palo Alto, CA, (1987)

*Q*

X. Qian, **Investigation of fe (III) reduction in geobacter sulfurreducens characterization of outer surface associated electron transfer components**, *PhD thesis*, University of Massachussets, (2009). Open Access Dissertations. Paper 116. http://scholarworks.umass.edu/open_access_dissertations/116

*R*

B. S. Rajagopal, J. LeGall, **Utilization of cathodic hydrogen by hydrogen-oxidizing bacteria**, *Appl. Microbiol. Biotech.*, 31(1989): 406-412

A. Rajasekar, S. Maruthamuthu, N. Palaniswamy, A. Rajendran, **Biodegradation of corrosion inhibitors and their influence on petroleum product pipeline**, *Micrbiolog. Resear*. 2007(162) 355-368

A. Rajasekar, A. Balakrishnan, M. Sundaram, T. Yen-Peng, K. Pattanathu, **Characterization of corrosive bacterial consortia isolated from petroleum-product-transporting pipelines**, *Appl. Environ. Microbiol*. 85(2010): 1175-1188

P. R. Roberge, *Handbook of corrosion Engineering*, McGraw-Hill companies Ed., 2000

E. E. Roden, D. R. Lovley, **Dissimilatory Fe (III) reduction by marine microorganism *Desulfuromonas acetooxidans***. *Appl. Environ. Microbiol.*, 59(1993): 734-742

*S*

P. F. Sanders, P. J. Sturman, **Biofouling in the Oil Industry**, in *Petroleum Microbiology*, Olivier B. and Magot M. (eds.), ASM Press, Washington, DC, pp. 171-198, (2005).

P. A. Schweitzer, *Corrosion Engineering handbook*, second edition, Marcel Dekker, Inc., Ed. CRC press, 1996

J.H. Scofield, **subshell photoionization cross-sections,** *J. Electron Spectrosc. Relat. Phenom.*, 8 (1976)129-137

M. Sparr, M. Linder, *Avoidance of corrosion problems in cooling water*, Swerea KIMAB, Stockholm (2010), ISBN: 978-91-633-6852-3

E. E. Stansbury, R. A. Buchanan, *Fundamentals of electrochemical corrosion*, ASM International, Ohio, USA, 2000

A. Stefánsson, I. Gunnarsson, N. Giroud. "**New methods for the direct determination of dissolved inorganic, organic and total carbon in natural waters by Reagent-Free Ion Chromatography and inductively coupled plasma atomic emission spectrometry**". *Anal. Chim. Acta* **582** (2007): 69–74.

B. S. Stevenson, H. S. Drilling, P. A. Lawson, K. E. Duncan, J. Suflita, **Microbial communities in bulk fluids and biofilms of an oil facility have similar composition but different structure,** *Environ Microbiol*. 13(2011):1078-90

J.G. Stoecker, **A practical Manual in Microbiologically Influenced Corrosion**, Volume 2, J. Stoecker Eds., *NACE international*, 2001

*L. K. Straubk, E. B. Buchholz-Cleven,* ***Enumeration and detection of anaerobic ferrous iron oxidizing, nitrate-reducing bacteria from diverse European sediments****, Appl. Environ. Microbiol., 64(1998):4846-4856*

*A. V. Surkov, G. A. Dubinina , A. M. Lysenko , F. O. Glöckner , J. Kuever ,* ***Dethiosulfovibrio russensis sp. nov., Dethosulfovibrio marinus sp. nov. and Dethosulfovibrio acidaminovorans*** **sp. nov., novel anaerobic, thiosulfate- and sulfur-reducing bacteria isolated from 'Thiodendron' sulfur mats in different saline environments**., *Int J Syst Evol Microbiol*. 51(2001):327-37.

M. Sztyler, I. B. Beech, J. Mitchell, S. Thresh, V. Zinkevich, **Oligonucleotide probes for detection of microbial genes implicated in biocorrosion of carbon steel in oil field environments**, "*unpublished results*": Article submitted to Bioelectrochemistry Journal, January 2013 (revision in process)

*T*

S. Tanuma, C.J. Powell, D.R. Penn, **Calculations of electron inelastic mean free paths.**, *Surf. Interf. Anal.*, (1994) 165-176

Tatnall, R. **Fundamentals of bacterial induced corrosion**. *Mat. Perform.*, 20(1981): 32-38

R. J. Thomas, **Biological Corrosion Failures**, *ASM Handbook*, NOVA Chemicals Ltd. 11(2002):881–898.

*U*

H.H. Uhlig, *Corrosion and Corrosion Control*, Wiley 4th Ed, 2008

*V*

H. Videla, *Manual of Biocorrosion*, CRC-Press; first ed., USA, 1997

H. A. Videla, **Prevention and control of biocorrosion**, *Int. Biodeter. & Biodegrad.* 49(2002) 259-270

H. A. Videla, L. K. Herrera, **Microbiologically influenced corrosion: looking to the future**, *Int. Microbiol.*, 8(2005):169-180

H. Videla, L. K. Herrera, **Understanding microbial inhibition of corrosion. A comprehensive overview**, *Intern. Biodeterior. Biodegrad.* 63(2009) 869-900

H-P. Volkland, H. Harms, B. Müller, G. Repphun, O. Wanner, A. J. B. Zehnder, **Bacterial phosphating of mild (unalloyed) steel**, *Appl. Environ. Microbiol* 66 (2000) 4389-4395.

H-P. Volkland, H. Harms, A. J. B. Zehnder, **Corrosion protection by anaerobiosis**, *Water Sci. technolo.* 44 (2001a) 103-106.

H-P. Volkland, H. Harms, K. Kauffman, O. Wanner, A. J. B. Zehnder, **Repair of damaged vivianite coatings on mild steel using bacteria**, *Corr. Sci.* 43 (2001b) 2135-2146.

E. Vrignaud, La deteriorations des canalisation, *Le monde enterré des canalisations publiques. Mém. D.U. "Eau et Environnement"*, D.E.P., univ. Picardie, Amiens, 53 p. + annexes, (1988).

C. Von Wolzogen Kuehr, *Water and gas* 7(1923):277

*W*

D. Wallinder, J. Pan, C. Leygraf, A. Delblanc-Bauer. **Electrochemical investigation of pickled and polished 304L stainless steel tubes**. *Corr. Sci.*, 42(2000): 1457-1469.

D. White, *The physiology and biochemistry of prokaryotes*. Oxford University press New York, (2000).

B. W. Whitman, T. L. Bowen, D. Boone, **The methanogenic bacteria**, *The Prokariotes,* Chapter 9 (2006) 3:165-207

J. Wiegel, R. Tanner, F. Rainey, **An introduction to the family Clostridiaceae**, *The Prokaryotes*, Chapter 1.2.20, 4(2006):654-678

*X*

Y. Xue, Y Xu, Y. Liu, Y. Ma, P. Zhou, ***Thermoanaerobacter* sp. Nov., a novel anaerobic, saccharolytic , thermophilum bacterium isolated from a hot spring in Tengcon, China,** *Int. J. Sys. Evol. Microbiol.*, 51(2001): 1335-1341

*Y*

L. Young, *Trans. Farad. Soc*. 51(1955):1250
L. Young, *Anodic oxide films*, Academic press, New York (1961)

*Z*

X. Y. Zhu, J. Lubeck, J. J. Kilbane, **Characterisation of microbial communities in gas industry pipelines**, App. Environ. Microbiol, 69(2003): 5354-5363
R. Zuo, **Biofilms: strategies for metal corrosion inhibition employing microorganisms**, *Appl. Environ. Microbiol*. 76 (2007) 1245-1253

2012

**University of Portsmouth**
**(BIOCOR)**

**Doma Jemimah**

# IDENTIFICATION REPORT FOR ENRICHMENTS FROM LGC-CNRS TOULOUSE, FRANCE

# INTRODUCTION

BIOCOR is a Marie Curie Initial Training Network (ITN), funded by the European Union (EU) Seventh Framework "People" Programme. The collaborative network expands through Europe with partners in Norway, Germany, France, Italy, Hungary, Sweden and the UK.

Field samples from the production line of the water injection systems where microbial induced corrosion (MIC) was detected were collected from the associated partners in Norway. These samples were sent to the network partners in France to be analysed. Analysis techniques performed include checking electrochemical activity, material surface science, and molecular biology techniques. The analysed samples were then sent to the University of Portsmouth (UoP), either as pigging debris, brage, coupons, pellets, or enriched growing cultures for identification by the BIOCOR partners present here at University of Portsmouth.

In the Oseberg south (OSS) water injection system K and J structures belonging to the production lines, from an oilfield in Norway, a corrosion problem in whereby iron sulphide (FeS) was detected and reported as a corrosion product. Pigging debris from the system were sent to the BIOCOR partner laboratory in Toulouse, France for analysis. The samples were inoculated in media enriched with race elements to help identify the presence of different possible micro organisms. Enrichment cultures for bacteria included Non selective bacteria, Iron reducing bacteria, Iron oxidizing bacteria, Acid producing bacteria and sulphate reducing bacteria.

After growth, pellets from the enrichment were sent to the UoP BIOCOR partner for identification and possible quantification of microorganism which may be involved in corroding the systems. The samples were analysed using techniques which include DNA extraction from the samples, Polymerase Chain Reaction (PCR), agarose gel electrophoresis, Denaturing gradient Gel electrophoresis (DGGE), and examination through cloning and sequencing.

# MATERIALS AND METHODS

Reagent-grade chemicals were obtained from different companies including Fisher scientific, England, UK; Sigma-Aldrich, UK and Invitrogen, Life technologies, USA. Primers were obtained from Sigma company and life sciences (Invitrogen), the master mix used (Green go-Taq) was purchased from Promega, USA while the SYBR safe stain used in electrophoresis was supplied by invitrogen. Kits used for DNA extraction was acquired from QIAGEN and Nucleospin from FISHER scientific. Extraction and other processes were executed under sterile and aseptic conditions where applicable to reduce risk of contaminating samples.

## SAMPLE SOURCE

Pigging debris from Oseberg south K and J water injection systems were sampled from three pigs (1, 4 and 9) and sent to CNRS Laboratoire de Génie Chimique, Toulouse. These were enriched for Sulfate Reducing Bacteria SRB, IRB, IOB, APB and Non selective microorganisms. Pellets were made by centrifuging grown cultures in eppendorf tubes, theses were neatly packed posted without precise temperatures (since pellets are stable) to the University of Portsmouth for identification.

Enrichments after growth and culture sent to the University of Portsmouth BIOCOR team as pellets are labelled as below:

**Table 1: showing list of samples from CNRS Toulouse**

| NUMBER OF SAMPLE | NAME OF SAMPLE | PIGS |
|---|---|---|
| 1. | Non selective pre-enrichment | Pig 1 |
| 2. | Non selective pre-enrichment | |
| 3. | IOB | |
| 4. | IRB | |
| 5. | SRB | |
| 6. | SRB | |
| 7. | APB | |
| 8. | APB | |
| 9. | SRB | |
| 10. | Non selective pre-enrichment | Pig 4 |
| 11. | IOB | |
| 12. | APB | |
| 13. | APB | |
| 14. | IRB | |
| 15. | Non selective pre-enrichment | Pig 9 |
| 16. | Non selective pre-enrichment | |
| 17. | APB | |
| 18. | APB | |
| 19. | IOB | |

IOB: Medium for selective enrichment of Iron Oxidizing Bacteria
IRB: Medium for selective enrichment of Iron Reducing Bacteria
SRB: Medium for selective enrichment of Sulfate Reducing Bacteria
APB: Medium for selective enrichment of Acid Producer Bacteria

# MOLECULAR BIOLOGY TECHNIQUES

## DNA EXTRACTION

DNA was extracted using the QIAGEN DNeasy Blood and Tissue Kit and extraction was performed as explained in the manufacturer's handbook (DNeasy Blood and Tissue Handbook 07/2006 pp. 45, 46 and 30 respectively).

A NanoDrop ND-1000 spectrophotometer was used to establish the concentration of extracted and purified DNA.

## POLYMERASE-CHAIN REACTION (PCR)

PCR was performed on DNA extracted from samples sent from CNRS Toulouse in order to probe possibly available gene such as 16S rRNA, *aprA*, *dsrAB*, genes specific for *Shewanella* sp. The conditions for PCRs performed are detailed below:

**a. Bacterial 16S rRNA**

The bacterial 16S rRNA 233bp was amplified using the primers F3+GC-5'CGCCCGCCGCGCGCGGCGGGCGGGGCGGGGGCACGGGGGGCCTACGGGAGGCAGCAG 3' and Rev- 5'ATTACCGCGGCTGCTGG 3' (Muyzer G, 1993). Reactions contained Gotaq green master mix Buffer (12.5µl, promega); primers F3+GC and Rev (each 0.5µl). Reactions for 16S rRNA were initially denatured at 95°C for 5 minutes, followed by 35 cycles of 94°C for 1 minute, 60°C for 1 minute and 70°C for 1 minute followed by a final extension step at 72°C for 5 minutes.

**b. *dsrAB***

Amplification of *dsrAB* amplicons was performed using the primers set DSR 1F: 5`-ACSCAYTGGAAR CACG-3`and DSR 4R: 5`-GTGTARCAGTTDCCRCA-3` (Klein et al., 2001). Reactions contained Gotaq green master mix Buffer (12.5µl, Promega); primers DSR 1F and DSR 4R, (each 0.5µl). Reactions were initially denatured at 94°C for 4 minutes; followed by 35 cycles of 94°C for 1 minute, 54°C for 1 minute and 72°C for 2 minutes and a final extension for 10 minutes at 72°C.

**c. *aprA***

*aprA* amplification carried out by using the primer set P1F9: 5`-CCAGGGCCTGTCCGC CATCAATAC-3` and P1R10: 5`-CCGGGCCGTAACCGTCCTTGAA-3`(Zinkevich & Beech, 2000). Reactions contained GoTaq green master mix Buffer (12.5µl, Promega); primers P1F9 and P1R10 (each 0.50µl) and 5µl of DNA to be checked. The reaction mixtures were initially denatured at

95°C for 5 minutes; followed by 35 cycles of 95°C for 1 minute, 62°C for 1 minute and 72°C for 1 minute followed by a final extension step at 72°C for 10 minutes.

**d. Bacterial 16S rRNA (550bp) for cloning**

The bacterial 16S rRNA 550bp to be used for cloning was amplified using the primers 341F+GC: 5`-CGCCCGCCGCGCGCGGGCGGGGCGGGGGCACGGGGGGCCTACGGGAGGCAGCAG-3` and 907R: 5`-CCGTCAATTCMTTTGAGTTT-3` (Muyzer *et al*., 1998). Reactions contained Gotaq green master mix Buffer (12.5µl, Promega); primers 341F+GC and 907R (each 0.5µl). Reactions for bacterial 16SrRNA 550bp was initially denatured at 94°C for 4 minutes; followed by a touchdown PCR: 20 cycles of 94°C for 1 minute, 63-54°C for 1 minute and 72°C for 1 minute followed by 15 cycles of 94°C for 1 minute, 53°C for 1 minute and 72°C for 1 minute and finally elongated for 10 minutes at 72°C.

**e. PCR for *Shewanella spp* 16S rRNA**

PCR for *Shewanella* specific gene was performed using the primers She211F:5`-CGCGATTGGATGAACCTAG-3` and She1259R: 5`- GGCTTTGCAACCCTCTGTA-3` Todorova and Costello, 2006). Reactions for *Shewanella* 16SrRNA contained buffer (5µl), jumpstart REDtaq (1µl), dNTPs (0.4µl), and primers She211F and She1259R (each 1.0µl). The reaction mixtures were initially denatured at 94°C for 1.5 minutes; followed by 24 cycles of 92°C for 1 minute, 53°C for 1.5 minutes and 72°C for 1 minute followed by a final extension step at 72°C for 5 minutes.

## AGAROSE GEL ELECTROPHORESIS

Agarose gel electrophoresis was performed after PCR to determine the size of the PCR product by running beside a DNA marker (1kb Ladder, Promega). PCR products were run on 0.9% of agarose gel on 150V for 30 minutes to 1 hour to enable proper separation.

## DENATURING GRADIENT GEL ELECTROPHORESIS (DGGE)

To separate the PCR-amplified products for bacterial 16S rRNA genes (233bp), 40µl of PCR-amplified products was used in an Ingeny Gel Apparatus (Ingeny, Netherlands), at a constant voltage of 90 V for 18 hours and a constant temperature of 60°C, after an initial 15 minutes at 200V. The standard gradient was formed of 6% polyacrylamide in TAE buffer with between 30% and 90% denaturant (7M urea and 40% formamide defined as 100% denaturant). After electrophoresis, the gel

was stained with SYBR® Safe DNA gel stain (Invitrogen Corp.), viewed under UV transillumination, and a permanent image captured by the NucleoCam Digital Image Documentation System™ (NucleoTech Corp.).

## EXAMINATION OF MICROBIAL DIVERSITY BY CLONING AND SEQUENCING

The PCR products 16S rRNA (550bp) were cloned into the pGEM®-T vector (Promega, USA) according to the manufacturer's instructions.

Using sterile toothpicks, clones were transferred in 50µl falcon tubes which contained 5ml of media with ampicillin and grown overnight at 37°C. Plasmids were extracted using the nucleospin Plasmid kit and sent for sequencing at GATC BIOTECH, London.

Sequences from GATC Biotech Company were checked in NCBI BLAST.

# RESULTS AND DISCUSSION

## DNA EXTRACTION

To ascertain that DNA was extracted from the enrichments sent into the Laboratory from Toulouse, the DNA a was checked on a NanoDrop ND-1000 spectrophotometer

**Table 2: showing concentration of DNA extracted from enrichments from CNRS Toulouse**

| Sample ID | Sample name | ng/ul | Quantity (ul) | 260/280 absorbance ratio |
|---|---|---|---|---|
| **1** | Non selective pre-enrichment | 11.1 | 200 | 0.16 |
| **2** | Non selective pre-enrichment | 30.7 | 200 | 1.07 |
| **3** | IOB | 34.6 | 200 | 1.43 |
| **4** | IRB | 84.1 | 200 | 1.41 |
| **5** | SRB | 8.6 | 200 | 1.62 |
| **6** | SRB | 10.2 | 200 | 1.35 |
| **7** | APB | 2.5 | 200 | 1.23 |
| **8** | APB | 2.8 | 200 | 1.53 |
| **9** | SRB | 7.0 | 200 | 1.98 |
| **10** | Non selective pre-enrichment | 2.5 | 200 | 1.33 |
| **11** | IOB | 39.4 | 200 | 1.42 |
| **12** | APB | 2.1 | 200 | 1.84 |
| **13** | APB | 2.4 | 100 | 1.35 |
| **14** | IRB | 167.1 | 100 | 1.34 |
| **15** | Non selective pre-enrichment | 0.7 | 100 | 1.75 |
| **16** | Non selective pre-enrichment | 1.0 | 100 | 2.66 |
| **17** | APB | 1.0 | 100 | -0.90 |
| **18** | APB | 0.5 | 100 | -4.10 |
| **19** | IOB | 114.8 | 100 | 1.12 |

## POLYMERASE-CHAIN REACTION (PCR)

Bacterial 16SrRNA PCR was performed on DNA which was extracted from samples to indicate presence of bacteria in enrichment.

### PCR Results

**Table 3: Showing PCR results of samples from CNRS Toulouse**

| Sample ID | Sample name | Bacteria 16SrRNA | *aprA* | *dsrAB* | Shewanella spp 16SrRNA | Archaea 16S rRNA |
|---|---|---|---|---|---|---|
| 1 | Non selective pre-enrichment | + | + | - | - | + |
| 2 | Non selective pre-enrichment | + | + | + | - | + |
| 3 | IOB | Weak band | - | - | - | - |
| 4 | IRB | Weak band | - | - | - | - |
| 5 | SRB | + | + | + | - | + |
| 6 | SRB | + | + | + | - | + |
| 7 | APB | + | - | - | - | + |
| 8 | APB | + | - | - | - | - |
| 9 | SRB | + | + | - | - | - |
| 10 | Non selective pre-enrichment | + | - | - | - | - |
| 11 | IOB | - | - | - | - | - |
| 12 | APB | + | - | - | - | - |
| 13 | APB | + | - | - | - | - |
| 14 | IRB | Weak band | - | - | - | - |
| 15 | Non selective pre-enrichment | + | - | v/w | - | - |
| 16 | Non selective pre-enrichment | + | - | v/w | - | - |
| 17 | APB | + | - | - | - | - |
| 18 | APB | + | - | - | - | - |
| 19 | IOB | Weak band | - | - | - | - |

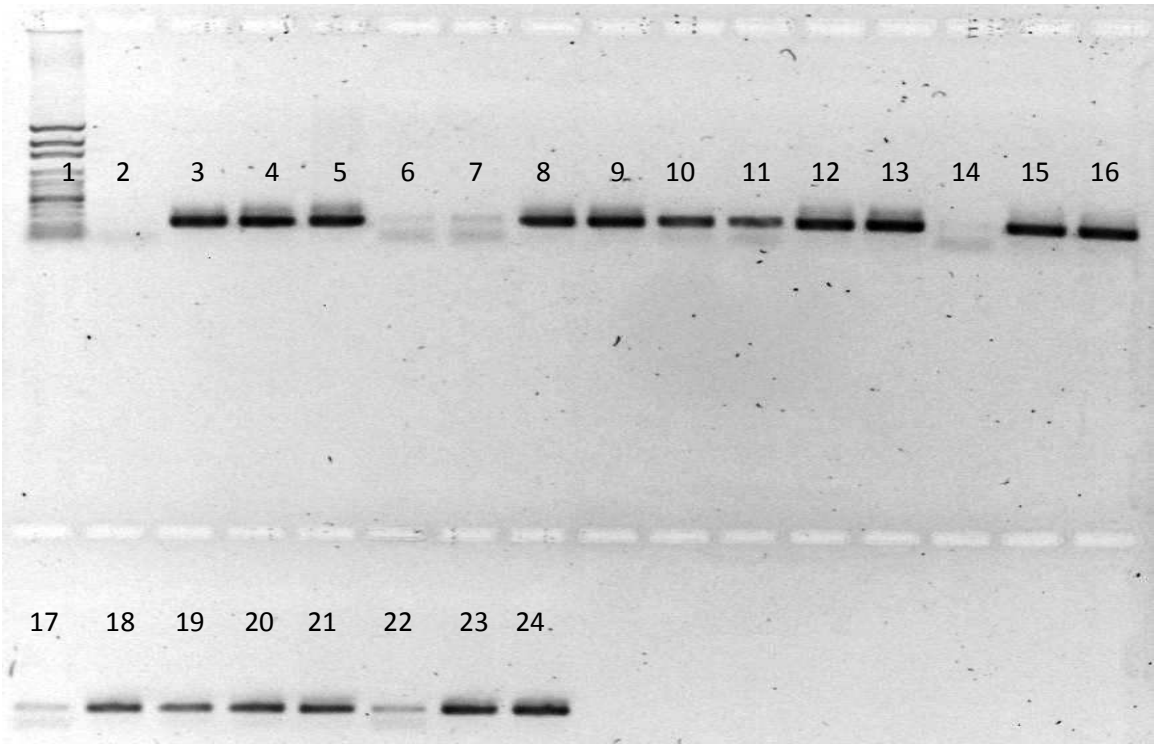


Figure 1: Picture of 0.9% agarose gel showing result of Bacteria 16S rRNA from enrichments from Toulouse Enrichment samples Lanes: 1: 1 kb DNA Ladder, 2: negative control, 3: positive control, 4: Non selective pre-enrichment, 5: Non selective pre-enrichment, 6:IOB, 7:IRB, 8:SRB, 9:SRB, 10:APB, 11:APB, 12:SRB, 13: Non selective pre-enrichment, 14:IOB, 15:APB, 16:APB, 17:IRB, 18: Non selective pre-enrichment, 19: Non selective pre-enrichment, 20:APB, 21:APB, 22:IOB, 23:*D. alaskensis*, 24:*D. alaskensis*

Careful observation of the agarose gel electrophoresis performed on PCR products amplified from DNA extracted, indicated that bacteria were present in enrichment as shown in figure 1 above. It was also observed that while some enrichment revealed strong dark bands indicating a high concentration of amplified PCR products, it was observed that other samples (lanes 17 and 22 ) showed low bands while PCR products in lanes 6, 7 and 14 presented very weak bands. The weak bands observed in lanes 17 could have been as a result of one of two cases: (i) it could have come from concentration of bacteria cells from enrichment which could have produced not enough cells for enough DNA to be extracted and (ii) it could have been as a result of the pigging process, since the sample is stated to have been enriched from pig 9, therefore, producing less growth in enrichments as a result of low diversity from sample.

Considering lanes 6, 7 and 14, although these samples came from pig 1, the low bands or absence of a band observed could be attributed to improper growth of the bacterial enriched. .

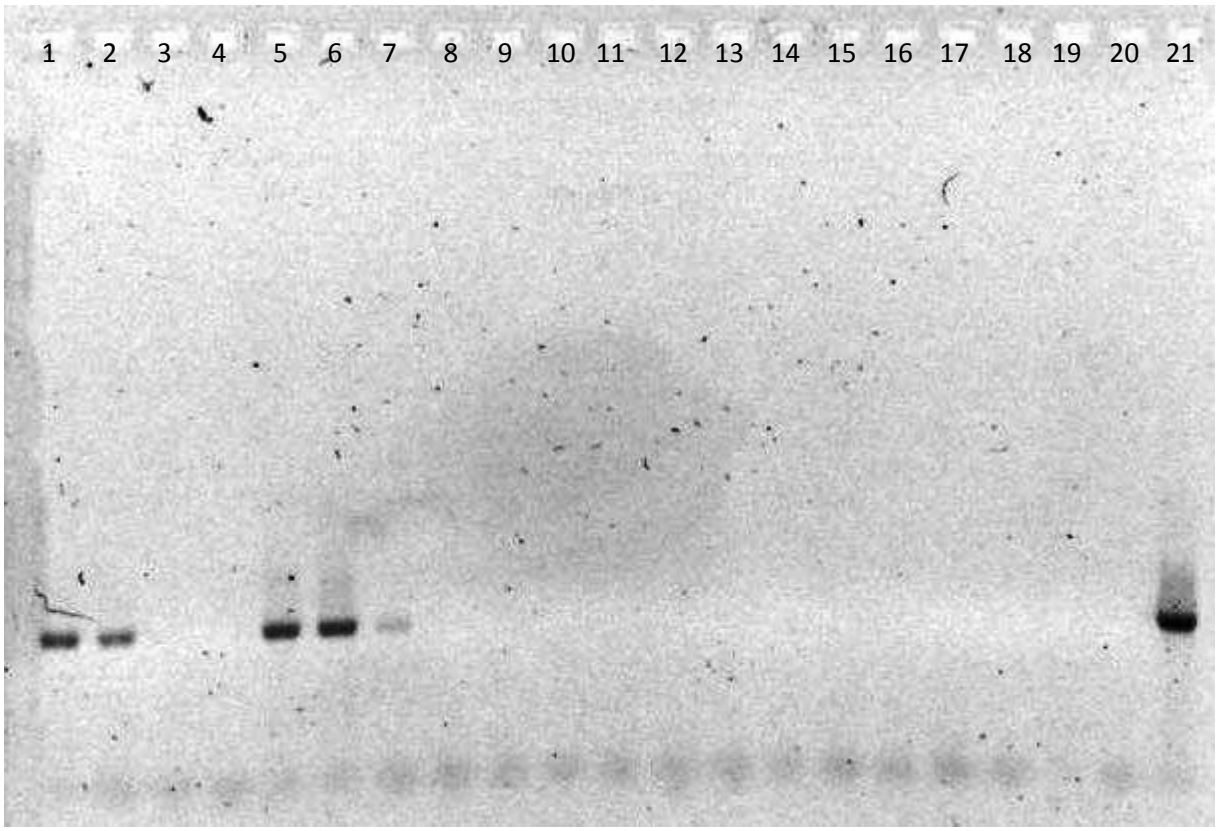


Figure 2: Picture of 0.9% agarose gel showing result of Archaea 16S rRNA from enrichments from Toulouse Enrichment samples Lanes: 1:Non selective pre-enrichment, 2: Non selective pre-enrichment, 3:IOB, 4:IRB, 5:SRB, 6:SRB, 7:APB, 8:APB, 9:SRB, 10: Non selective pre-enrichment, 11:IOB, 12:APB, 13:APB, 14:IRB, 15: Non selective pre-enrichment, 16: Non selective pre-enrichment, 17:APB, 18:APB, 19:IOB, 20:negative control, 21: positive control (*D. alaskensis* DNA)

DNA extracted from enrichments were further analysed with functional gene primers. This was performed to test whether the organisms enriched for were present in the culture by checking for functional genes involved in corrosion.

Similarly performed for bacteria 16S rRNA, all PCR products extracted were analysed for Archaea 16S rRNA. However, only five samples in lanes 1, 2, 5, 6 and 7 indicated the presence of Archaea in the enrichments. It should be noted that these samples were obtained from the same pig *i.e.* Pig 1.

Subsequently, samples that tested positive will be analysed for methanogens, *Archaeoglobus spp* and for hydrogenaseA (hydA) genes as characteristic of Archaea.

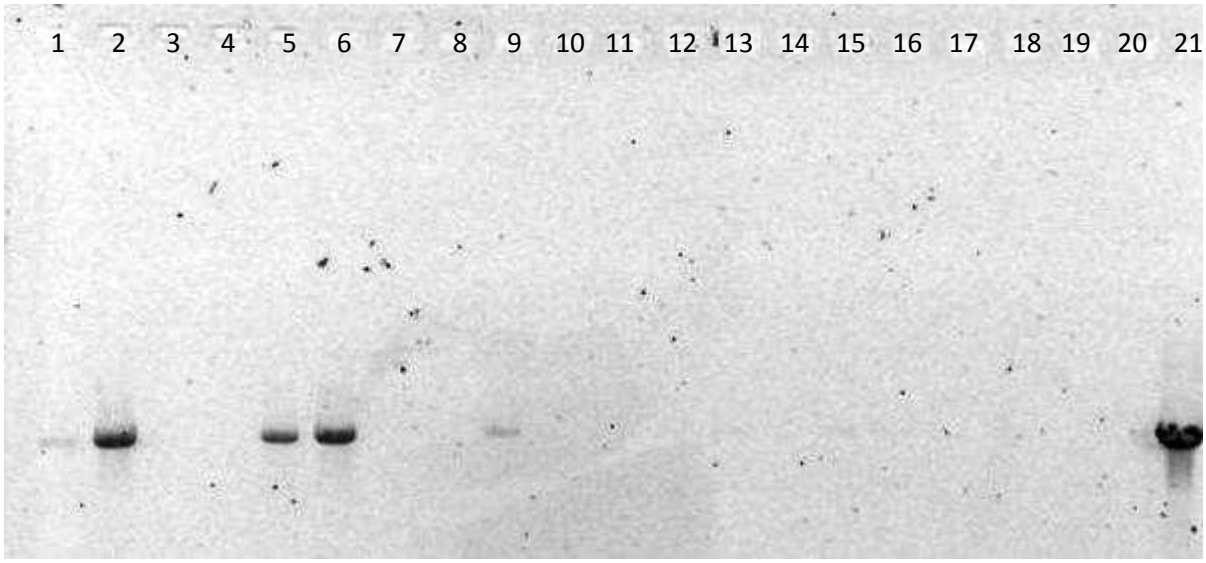


Figure 3: Picture of 0.9% agarose gel showing result of *dsrAB* gene from enrichments from Toulouse

Lanes: 1:Non selective pre-enrichment, 2: Non selective pre-enrichment, 3:IOB, 4:IRB, 5:SRB, 6:SRB, 7:APB, 8:APB, 9:SRB, 10: Non selective pre-enrichment, 11:IOB, 12:APB, 13:APB, 14:IRB, 15: Non selective pre-enrichment, 16: Non selective pre-enrichment, 17:APB, 18:APB, 19:IOB, 20:negative control, 21: positive control

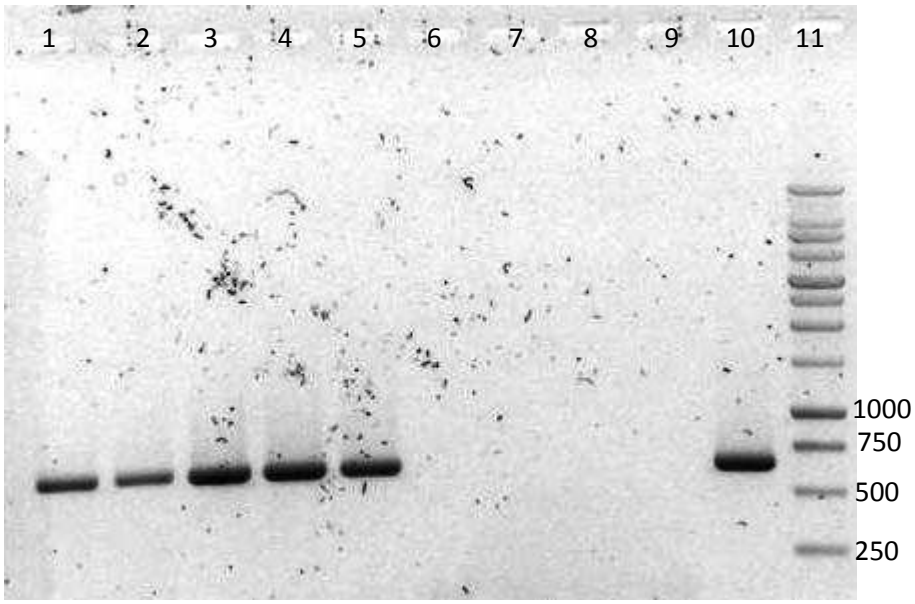


Figure 4: Picture of 0.9% agarose gel showing result of *aprA* gene from enrichments from Toulouse. Enrichment samples Lanes: 1: Non selective pre-enrichment (1), 2: Non selective pre-enrichment (2), 3: SRB (5), 4: SRB (6), 5: SRB (9), 6: Non selective pre-enrichment (10), 7: Non selective pre-enrichment (15), 8: Non selective pre-enrichment (16), 9: negative control, 10: positive control, 11: 1 kb DNA Ladder

Since pigging samples were enriched for SRB, it was essential to test for the presence of SRB. Therefore, SRB specific functional genes were tested for; these include dissimilatory sulphur reductaseAB (*dsrAB)* gene and alkaline proteaseA (*aprA*) genes.

From figure 3 and 4 above, it was observed that samples enriched for SRB presented a positive result as seen in lanes 1, 2, 5, 6 and 9 in figure 3 while in figure 4 the same enrichments represented in lanes 1, 2, 3, 4, and 5 as the PCR products tested positive for both *dsrAB* and *aprA* genes. However, it should not be ignored that on the agarose gel in Figure 3 positive signs in lanes 1 and 9 were weak.

The samples enriched for IRB and IOB had PCR performed on them with primers for *Shewanella spp* 16S rRNA but a negative observed as no bands were visible but control was intact and positive.

## DENATURING GRADIENT GEL ELECTROPHORESIS

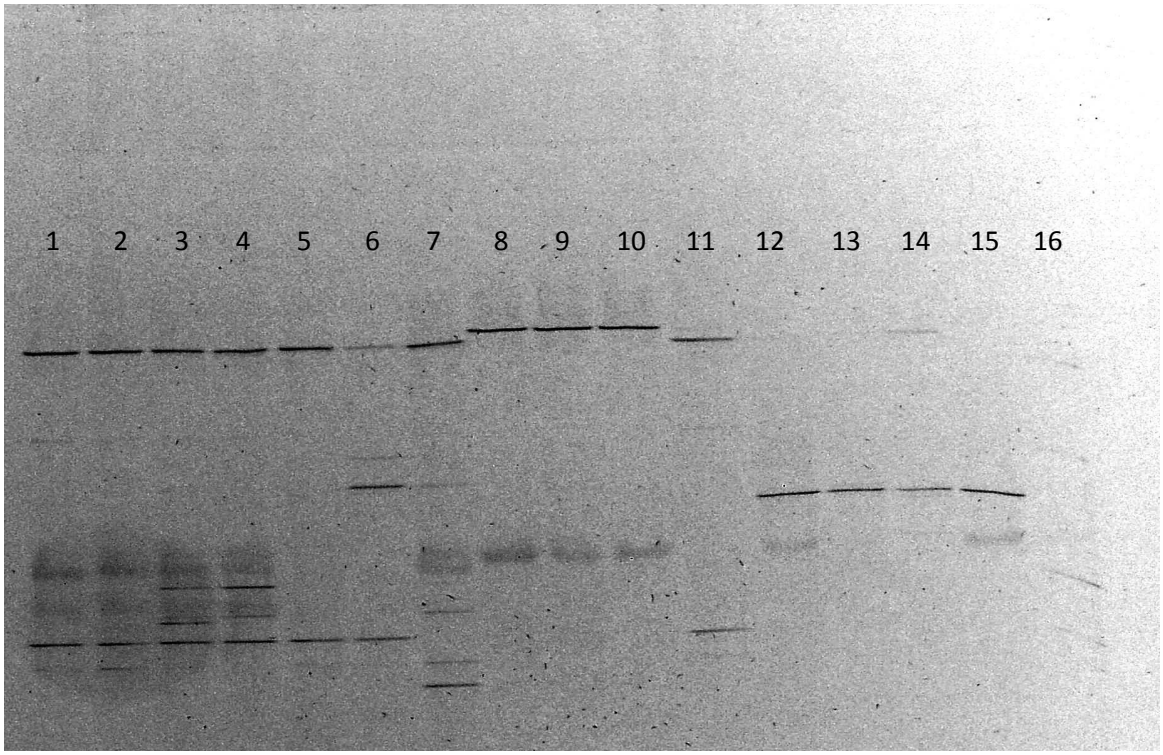


Figure 5: Picture of 9% polyacrylamide DGGE gel showing biodiversity from enrichments from Toulouse

Enrichment samples Lanes: 1: Non selective pre-enrichment, 2: Non selective pre-enrichment, 3: SRB, 4: SRB, 5: APB, 6: APB, 7: SRB, 8: Non selective pre-enrichment, 9: APB, 10: APB, 11: IRB, 12: Non selective pre-enrichment, 13: Non selective pre-enrichment, 14: APB, 15: APB, 16: Ladder

DGGE was performed for 15 of the 19 enrichments received from CNRS Toulouse, this was as a result of little or no PCR product present in samples numbered 3, 4, 11 and 19. PCR products amplified did not produce enough amplicons to be used on DGGE gel.

Of the 15 enrichments received approximately 44 visible bands were observed, with samples in lanes 1, 2, 3, 4, 5 and 6 showing a similar pattern in the first, second, third and fourth regions on the gel. Samples in lanes 1 and 2 were observed to be more similar to each other as were samples in lanes 3 and 4.. The sample in lane 5 was slightly different with just two visible bands while sample 6 was also slightly different with two visible bands not in the same regions as compared to samples in lanes 1 to 5. Although samples in lanes 1 to 7 were enriched in different media even but from the same pig (Pig 1), a marked difference was observed in the sample in lane 7, though it was enriched for SRB with samples in lanes 3 and 4. Nevertheless, a similarity in the visible band in the first region of the sample in lane 7 tallied with samples in lanes 1 to 6. Furthermore, the sample in lanes 7 had more biodiversity than samples in lanes 1 to 6 being that they were enriched from the same pig. However, it remains that

the samples were enriched for different bacteria including non-selective pre-enrichments, APB and SRB.

From Figure 5 above, it can be observed that samples in lanes 8, 9, and 10 showed marked similarities despite coming from different enrichments which include APB, IRB and non-selective pre-enrichment. Thus, it could be suggested that a similar organism could have grown in the enrichments from the same pig (Pig 4). The sample in lane 11 though enriched for IRB, is also from the same pig as samples in lanes 8, 9 and 10. A marked difference was seen with two visible bands which do not conform with visible band as samples from same pig.

In lanes 12 to 15 the samples exhibited high similarity with almost a single visible band though samples in lanes 12, 14 and 15 indicate very weak bands.

Finally, a trend observed in the biodiversity shown in the DGGE gel above shows a decline in the number of bands in the samples. This could probably indicate that as the cleaning pigs are sent down the systems sequentially, the quantity of MIC causing organisms could be reducing. Thus, to state on a side note, that pigging exercise performed could be effective in getting rid of some MIC causing organisms from the systems.

# CLONING AND SEQUENCING

Sequencing results from cloning of Bacteria 16S rRNA from enrichments from CNRS Toulouse, France.

**Table 4: Showing results from cloning and sequencing of enrichments from CNRS Toulouse**

| Sample name | | Result | Identity |
|---|---|---|---|
| **Non selective pre-enrichment** | 1.1a | *Dethiosulfovibrio spp* | 99-96% |
| | | Uncultured SRB in environmental sample | 99-98% |
| | 1.1b | Uncultured bacterium in environmental samples | 100-91% |
| | | *Geotoga spp* | 100-91% |
| | | *Thermotoga spp* | 99-91% |
| | 1.1c | Uncultured bacterium in environmental samples | 100-91% |
| | | *Geotoga spp* | 100-91% |
| | | *Thermotoga spp* | 99-91% |
| | 1.1d | Uncultured bacterium in environmental samples | 100-91% |
| | | *Geotoga spp* | 100-91% |
| | | *Thermotoga spp* | 99-91% |
| | 1.1e | Uncultured bacterium in environmental samples | 100-91% |
| | | *Geotoga spp* | 100-91% |
| | | *Thermotoga spp* | 99-91% |
| | 1.1f | *Dethiosulfovibrio spp* | 99-96% |
| | | Uncultured SRB in environmental sample | 99-98% |
| | 1.1g | Uncultured bacterium in environmental samples | 96-89% |
| | | *Geotoga spp* | 96-89% |
| | | *Thermotoga spp* | 96-89% |
| | 1.1h | *Dethiosulfovibrio spp* | 99-98% |
| | | Uncultured SRB in environmental sample | 99-98% |
| | 1.1i | Uncultured bacterium in environmental samples | 91-86% |
| | | *Geotoga spp* | 91% |
| | | Thermotogales bacterium | 90% |
| | | *Thermopallium natronophilum* | 86% |
| | 1.1j | *Dethiosulfovibrio spp* | 99-98% |
| | | Uncultured SRB in environmental sample | 99-98% |
| **Non selective pre-enrichment** | 2.2a | Uncultured Spirochaetes | 100-99% |
| | | Uncultured SRB in environmental sample | 100-99% |
| | 2.2b | Uncultured Spirochaetes | 100-99% |
| | | Uncultured SRB in environmental sample | 100-99% |
| | 2.2c | Uncultured Spirochaetes | 100-99% |
| | | Uncultured SRB in environmental sample | 100-99% |
| | 2.2d | *Dethiosulfovibrio spp* | 99-96% |
| | | Uncultured SRB in environmental sample | 99-98% |
| | 2.2e | *Dethiosulfovibrio spp* | 100-96% |
| | | Uncultured bacteria in environmental sample | 99-98% |
| | 2.2f | Uncultured bacterium in environmental samples | 100-91% |
| | | *Geotoga spp* | 100-91% |
| | | *Thermotoga spp* | 99-91% |
| | 2.2g | Uncultured bacterium in environmental samples | 100-91% |
| | | *Geotoga spp* | 100-91% |
| | | *Thermotoga spp* | 98-91% |
| | 2.2h | Uncultured bacterium in environmental samples | 100-91% |
| | | *Geotoga spp* | 100-91% |
| | | *Thermotoga spp* | 98-91% |
| | 2.2i | *Dethiosulfovibrio spp* | 99-96% |
| | | Uncultured SRB in environmental sample | 99-98% |
| | 2.2j | Uncultured bacterium in environmental samples | 100-91% |
| | | *Geotoga spp* | 100-91% |
| | | *Thermotoga spp* | 98-91% |
| **SRB** | 3.5a | *Dethiosulfovibrio spp* | 99-98% |
| | | Uncultured SRB in environmental sample | 99-98% |
| | 3.5b | *Dethiosulfovibrio spp* | 99-96% |

| | | | |
|---|---|---|---|
| | | Uncultured SRB in environmental sample | 99-97% |
| | 3.5c | *Dethiosulfovibrio spp* | 99-96% |
| | | Uncultured SRB in environmental sample | 99-98% |
| | 3.5d | Uncultured bacterium in environmental samples | 99-91% |
| | | *Geotoga spp* | 99-91% |
| | | *Thermotoga spp* | 99-91% |
| | 3.5e | Contaminated | |
| | 3.5f | Uncultured bacterium in environmental samples | 99-91% |
| | | *Geotoga spp* | 99-91% |
| | | *Thermotoga spp* | 98-91% |
| | 3.5g | *Desulfovibrio sp* | 98-97% |
| | | Uncultured desulfovibrio | 97% |
| | 3.5h | *Dethiosulfovibrio spp* | 99-96% |
| | | Uncultured SRB in environmental sample | 99-98% |
| | 3.5i | *Dethiosulfovibrio spp* | 99-98% |
| | | Uncultured SRB in environmental sample | 99-98% |
| | 3.5j | Contaminated | |
| **SRB** | 4.6a | Uncultured Bacteroidetes bacterium | 94% |
| | | Uncultured bacterium | 93% |
| | 4.6b | *Dethiosulfovibrio spp* | 99-96% |
| | | Uncultured SRB in environmental sample | 99-97% |
| | 4.6c | *Dethiosulfovibrio spp* | 99-98% |
| | | Uncultured SRB in environmental sample | 99-98% |
| | 4.6d | Uncultured bacterium in environmental samples | 100-91% |
| | | *Geotoga spp* | 100-91% |
| | | *Thermotoga spp* | 99-91% |
| | 4.6e | Uncultured bacterium in environmental samples | 99-91% |
| | | *Geotoga spp* | 99-91% |
| | | *Thermotoga spp* | 98-91% |
| | 4.6f | *Dethiosulfovibrio spp* | 99-98% |
| | | Uncultured SRB in environmental sample | 99-98% |
| | 4.6g | Uncultured bacterium in environmental samples | 99-91% |
| | | *Geotoga spp* | 99-91% |
| | | *Thermotoga spp* | 98-91% |
| | 4.6h | *Dethiosulfovibrio spp* | 99-96% |
| | | Uncultured SRB in environmental sample | 99% |
| | 4.6i | *Desulfovibrio sp* | 99-98% |
| | 4.6j | Uncultured bacterium in environmental samples | 99-91% |
| | | *Geotoga spp* | 99-91% |
| | | *Thermotoga spp* | 98-91% |
| **APB** | 5.7a | Uncultured bacterium in environmental samples | 100-91% |
| | | *Geotoga spp* | 99-91% |
| | | *Thermotoga spp* | 99-91% |
| | 5.7b | *Dethiosulfovibrio spp* | 99-97% |
| | | Uncultured SRB in environmental sample | 99-97% |
| | 5.7c | Uncultured bacterium in environmental samples | 100-91% |
| | | *Geotoga spp* | 100-91% |
| | | *Thermotoga spp* | 99-91% |
| | 5.7d | Uncultured bacterium in environmental samples | 100-91% |
| | | *Geotoga spp* | 100-91% |
| | | *Thermotoga spp* | 99-91% |
| | 5.7e | *Dethiosulfovibrio spp* | 97% |
| | | Uncultured SRB in environmental sample | 98-95% |
| | 5.7f | *Dethiosulfovibrio spp* | 99-98% |
| | | Uncultured SRB in environmental sample | 99% |
| | 5.7g | *Dethiosulfovibrio spp* | 99-96% |

| | | | |
|---|---|---|---|
| | | Uncultured SRB in environmental sample | 99-98% |
| | 5.7h | Uncultured bacterium in environmental samples | 100-91% |
| | | *Geotoga spp* | 100-91% |
| | | *Thermotoga spp* | 99-91% |
| | 5.7i | *Burkholderia fungorum* | 100% |
| | | Bacterium AH1BSX+8aut | 100% |
| | | Bacterium E1R14aut | 100% |
| | | Uncultured bacterium in environmental samples | 100% |
| | | Bacterium E3B8aut | 100% |
| | 5.7j | Uncultured bacterium in environmental samples | 99-91% |
| | | *Geotoga spp* | 99-91% |
| | | *Thermotoga spp* | 98-91% |
| **APB** | 6.8a | *Serratia spp.* | 100-99% |
| | | Uncultured bacterium | 100-99% |
| | 6.8b | *Dethiosulfovibrio spp* | 99-96% |
| | | Uncultured SRB in environmental sample | 99-98% |
| | 6.8c | *Dethiosulfovibrio spp* | 99-98% |
| | | Uncultured SRB in environmental sample | 99-98% |
| | 6.8d | *Burkholderia spp* | 100% |
| | 6.8e | *Dethiosulfovibrio spp* | 99-96% |
| | | Uncultured SRB in environmental sample | 99-97% |
| | 6.8f | *Serratia spp.* | 99% |
| | | Uncultured bacterium | 99% |
| | 6.8g | *Serratia spp.* | 99% |
| | | Uncultured bacterium | 99% |
| | 6.8h | *Dethiosulfovibrio spp* | 99-98% |
| | | Uncultured SRB in environmental sample | 99-98% |
| | 6.8i | *Dethiosulfovibrio spp* | 99-96% |
| | | Uncultured SRB in environmental sample | 99-97% |
| | 6.8j | *Serratia spp.* | 100% |
| | | Uncultured bacterium | 100% |

Table 4 above details results obtained from sequencing of cloned DNA enrichments. From these results, the trend of sequences observed were *Desulfovibrio spp*, *Dethiosulfovibrio spp*, *Geotoga spp*, *Thermatoga spp* and some uncultured sulphur reducing bacteria clones in most of the samples. In sample 2 (non- selective pre-enrichments), uncultured spirochetes were identified, while in sample 7(APB enriched) species of *Burkholderia spp*, *Bacterium* AH1BSX+8aut and *Bacterium* E3B8aut were identified alongside *Dethiosulfovibrio spp*, *Geotoga spp*, *Thermatoga spp*. However, in sample 8 (APB enriched) *Serratia spp* 99-100%, *Burkholderia spp* 100%, were observed alongside uncultured bacteria clones and *Dethiosulfovibrio spp.*

However, it is observed from the table 4 above that in samples 5 (SRB enriched) clones 3.5e and 3.5j were contaminated as there was no meaningful sequence.

# CONCLUSION

This report has revealed a step by step process used in the analysis of enrichment samples received from partners from CNRS in Toulouse. Samples have been identified using molecular biology techniques. Media enriched for specific microorganisms including SRB, IRB, APB, IOB and non-selective Bacteria were inoculated and cultured in the laboratory at CNRS Toulouse, France. Cells were concentrated by centrifuging cultures in eppendorf tubes and supernatant discarded to obtain pellets of bacteria cells obtained at the end of the eppendorf tubes. These eppendorf tubes with pellets were sent to the University of Portsmouth Laboratory to be identified using molecular biology techniques.

DNA was extracted from pellets and several molecular techniques including PCR, DGGE, cloning and sequencing were performed on the enriched samples.

From the results shown above, it was observed that bacteria were present in the enrichment as shown by agarose gel picture (see figure 1) of PCR product of bacteria 16S rRNA, though weak bands were observed in few samples. Moreso, it was observed that some enrichment contained SRB as depicted by the agarose gels which showed PCR products with the primers for *dsrAB* and *apsA*. Though enriched for IRB and IOB, the primers for *Shewanella spp* 16S rRNA did not detect any *Shewanella spp* in the samples.

Nonetheless, DGGE profile of the enriched pellets with good PCR product (detected strength of band on agarose gel) expressed the presence of approximately 44 visible bands with similarities and difference among the enriched samples. Likewise, from the DGGE gel, it was noticed that there was a decline in biodiversity among samples which could have been as a result of sequential pigs sent in to the systems from whence the sample were collected.

Furthermore, cloning and sequencing disclosed the incidence of *Desulfovibrio spp, Dethiosulfovibrio spp, Geotoga spp, Thermatoga spp* and some uncultured sulphur reducing bacteria clones in most of the samples and the occurrence of bacteria which include uncultured Spirochetes, *Serratia spp* 99-100%, *Burkholderia spp* and Bacteroides spp in the samples.

With reference to this report, we could correctly conclude that *Desulfovibrio spp, Dethiosulfovibrio spp, Geotoga spp, Thermatoga spp* and some uncultured sulphur reducing bacteria clones trending in the samples and the occurrence of bacteria including uncultured Spirochetes, *Serratia spp, Burkholderia spp* and Bacteroides spp in the samples have been identified as microorganisms involved in MIC in the reported systems.

Nevertheless, it is important to note that identification continues on these samples as techniques have not been exhausted. Conditions are still been optimised for using more analytical techniques which include cloning the Archaea 16S rRNA gene in order to sequence and identify the Archaea species indicated by the Archaea 16S rRNA result (see figure 2). In addition, enhancing conditions for detecting IOB, IRB and APB are also in progress.